STATUS OF THESIS

Title of thesis	PATH ANALYSIS FOR THE RETROFIT OF HEAT EXCHANGER NETWORKS AND THE UTILITY SYSTEM

I ABDELBAGI OSMAN ELSIDDIG MUSTAFA,

hereby allow my thesis to be placed at the information Resource Center (IRC) of Universiti Teknologi PETRONAS (UTP) with the following conditions:

1. The thesis becomes the property of UTP
2. The IRC of UTP may make copies of the thesis for academic purposes only.
3. This thesis is classified as

☐ Confidential

☑ Non-confidential

If the thesis is confidential, please state the reason:

____

____

____

The contents of the thesis will remain confidential for ____________years.

Remarks on disclosure:

____

____

____

Endorsed by

Signature of Author

Signature of Supervisor

Permanent address:
Dept. of Applied Chemistry
and Chemical Technology,
Faculty of Eng. and
Technology,
University of Gezira,
P.O. Box 20 - Wad Medani,
Sudan.

Date: 24 JAN 2011

Assoc. Prof. Dr. Mohamed Ibrahim Abdul Mutalib

Date: 24 JAN 2011

UNIVERSITI TEKNOLOGI PETRONAS

PATH ANALYSIS FOR THE RETROFIT OF HEAT EXCHANGER NETWORKS AND THE UTILITY SYSTEM

By

ABDELBAGI OSMAN ELSIDDIG

The undersigned certify that they have read, and recommend to the Postgraduate Studies Programme for acceptance this thesis for the fulfillment of the requirements for the degree stated.

Signature:

Main Supervisor: Assoc. Prof. Dr. Mohamed Ibrahim Abdul Mutalib

Signature:

Co-Supervisor: Assoc. Prof. Dr. Shuhaimi Bn Mahadzir

Signature:

Head of Department: Assoc. Prof. Dr. Shuhaimi Bn Mahadzir

Date: 24/1/11

Dr. Shuhaimi Mahadzir
Associate Professor & Head
Chemical Engineering Department
Universiti Teknologi PETRONAS

PATH ANALYSIS FOR THE RETROFIT OF HEAT EXCHANGER NETWORKS AND THE UTILITY SYSTEM

By

ABDELBAGI OSMAN ELSIDDIG

A Thesis

Submitted to the Postgraduate Studies Programme
as a Requirement for the Degree of

DOCTOR OF PHILOSOPHY

CHEMICAL ENGINEERING DEPARTMENT

UNIVERSITI TEKNOLOGI PETRONAS

BANDAR SRI ISKANDAR

PERAK

JANUARY 2011

DECLARATION OF THESIS

Title of thesis	PATH ANALYSIS FOR THE RETROFIT OF HEAT EXCHANGER NETWORKS AND THE UTILITY SYSTEM

I ABDELBAGI OSMAN ELSIDDIG MUSTAFA,

hereby declare that the thesis is based on my original work except for quotations and citations which have been duly acknowledged. I also declare that it has not been previously or concurrently submitted for any other degree at UTP or other institutions.

Signature of Author

Permanent address:
Dept. of Applied Chemistry and
Chemical Technology,
Faculty of Eng. and Technology,
University of Gezira,
P.O. Box 20 - Wad Medani,
Sudan.

Date: 24 · Jan. 2011

Witnessed by

Signature of supervisor

Name of supervisor:

Assoc. Prof. Dr. Mohamed
Ibrahim Abdul Mutalib

Date: 24 · Jan. 2011

ABSTRACT

This study introduced a new approach for HEN retrofit that featuring area addition to the existing exchangers without massive topology changes in HEN. The approach has developed based on a combinatorial method to combine the available utility paths in HEN systematically to generate several alternatives for increasing the process-to-process heat recovery. To ensure feasible heat transfer between hot and cold streams, the Heat Recovery Approach Temperature (HRAT) is maintained while increasing the heat recovery. The available exchangers' pressure drop is considered in calculating the film heat transfer coefficients. A demonstrative example showed several retrofit options where the energy savings ranged from \$150K/yr to \$450K/yr with payback of less than 2 years to refund the investment rose from the mandatory area addition. The developed approach is termed as '*Paths Combination Approach for HEN Retrofit*'. Moreover, a concept of varying the process stream temperature has been established to further increase the heat recovery and make the infeasible solutions more competitive. This concept mainly depends on the process streams' flexibility to changing the inlet and outlet temperature; and termed as the Temperature Flexibility concept (TF concept). Implementation alternatives are generated and integrated into the paths combination approach. Given that major changes in process conditions are rarely desired, the temperature changes has been kept within a small magnitude regardless of the usual process temperature oscillations. A user friendly computer programme has been developed for performing the approach in view of the significant number of iterations required. Most of the infeasible retrofit solutions have changed to the feasible zone where higher savings are featured along the temperature flexibility range. The energy savings derived from HEN retrofit have been further investigated to study the impact on the utility system. Through a case study integrating HEN retrofit and utility system, the most efficient way was found to redistribute the steam surplus among the utility system devices while considering the turbines flow constraints. Accordingly, the power production in the utility system has increased

using one of the retrofit options from 4.1% to 10.5% when applying the full range of the TF in HEN.

ABSTRAK

Kajian ini memperkenalkan pendekatan baru pengubahsuaian rangkaian penukar haba (HEN) menerusi penambahan luas permukaan pemindah haba tanpa melibatkan perubahan topologi rangkaian yang ketara. Pembangunan pendekatan di buat berdasarkan kepada kaedah kombinatorial yang menggabungkan kesemua laluan utiliti secara sistematik untuk menghasilkan alternatif penyelesaian bagi peningkatan prestasi pemuliharaan haba. Untuk memastikan pemindahan haba dari aliran panas ke aliran sejuk, perbezaan suhu di kedua penghujung alat penukar haba (HRAT) di kekalkan sementara perbezaan tekanan di ambil kira di dalam pengiraan pekali pemindah haba yang di gunakan dalam pendekatan ini. Contoh demonstrasi menunjukkan terdapat beberapa pilihan yang boleh di aplikasikan dengan menghasilkan penjimatan tenaga sekitar $150K ke $450K setahun dan pembayaran balik kurang dari 2 tahun bagi menampung kos pelaburan. Pendekatan ini dikenali sebagai "Pendekatan Kombinasi Laluan bagi Pengubahsuaian Rangkaian Pemindah Haba". Kaedah yang di bentuk bagi pendekatan ini di perkasakan lagi dengan konsep perubahan suhu aliran proses yang di perkenalkan untuk menambah lagi prestasi pemulihan haba seterusnya menjadikan alternatif penyelesaian lebih kompetitif. Konsep ini berdasarkan kepada kefleksibelan perubahan suhu ke atas aliran proses yang masuk atau keluar dari alat penukar haba dan di termakan sebagai Konsep Suhu Fleksibel (Konsep TF). Alternatif penyelesaian di bentuk menggunakan konsep ini dan di integrasikan bersama pendekatan kombinasi laluan bagi mencari penyelesaian terbaik. Memandangkan pengubahan ketara ke atas kondisi proses jarang sekali di praktikkan di industri, julat perubahan suhu di tetapkan dalam nilai yang kecil. Hasilnya banyak alternatif penyelesaian yang pada mula nya tidak kompetitif berubah sebaliknya setelah perubahan suhu aliran di buat mengikut julat yang ditentukan. Disebabkan oleh bilangan iterasi pengiraan yang banyak, satu perisian mesra pengguna telah di bangunkan. Penyelesaian yang di pilih menggunakan kaedah di atas

seterusnya di kaji lagi bagi melihat kesan ke atas sistem utiliti. Menerusi satu kajian kes yang di buat, penyelesaian paling efisien adalah dengan mengagih semula lebiha stim yang terhasil daripada aplikasi penjimatan tenaga kepada peralatan sistem utiliti dengan mengambilkira kekangan aliran turbin. Sementara penghasilan kuasa dari sistem utiliti pula dapat ditambah sekitar 4.1 ke 10.5 peratus apabila konsep TF di guna pakai.

ACKNOWLEDGEMENTS

This thesis arose in part out of years of research that has been done since I came to Universiti Teknologi PETRONAS (UTP) in Malaysia. By that time, I have worked with a great number of people whose contribution in assorted ways to the research and the making of the thesis deserved special mention. It is a pleasure to convey my gratitude to them all in my humble acknowledgment.

In the first place I would like to record my gratitude to my supervisor AP. Dr. Mohamed Ibrahim Abdul Mutalib for his supervision, advice, and guidance from the very early stage of this research as well as giving me extraordinary experiences throughout the work. Above all and the most needed, he provided me unflinching encouragement and support in various ways. His truly scientist intuition has made him as a constant oasis of ideas and passions in science, which exceptionally inspire and enrich my growth as a student, a researcher and a scientist want to be. I am indebted to him more than he knows.

I gratefully acknowledge my co-supervisor AP. Dr. Shuhaimi Bn Mahadzir for his advice, supervision, and crucial contribution, which made him a backbone of this research and so to this thesis. His involvement with his originality has triggered and nourished my intellectual maturity that I will benefit from, for a long time to come. AP. Dr. Shuhaimi, I am grateful in every possible way and hope to keep up our collaboration in the future.

Many thanks go in particular to AP. Dr. Kamarul Ariffin Aminuddin. I am much indebted to AP. Dr. Kamarul for his early valuable advice in science discussion, supervision. I have also benefited by advice and guidance from AP. Dr. Kamarul who also always kindly grants me his time even for answering some of my unintelligent questions about HENs retrofit and Path analysis.

I would also acknowledge the financial support provided by PETRONAS-Sudan, Ministry of Higher Education-Sudan, and University of Gezira-Sudan. Without their support I would have been lost to seek the financial and living expenses in Malaysia.

I also benefited by the outstanding work from Mohamed Elshiekh Elobied who helped me with his particular skill in handling the programming part in this work in several sessions. I gratefully thank Maysara Eissa and Mohamed Ayoub for their constructive comments on this thesis. It is a pleasure to pay tribute also to the sample collaborators such as Mohamed Osman Hussien, Abu Bakr Kidir, Omer Essa and Gassan Eltaj.

Where would I be without my family? My Father, Osman Elsiddig who passed away in 1998, in the first place is the person who put the fundament my learning character, showing me the joy of intellectual pursuit ever since I was a child. My Mother, Haram Omer, who also passed away in 2002, is the one who sincerely raised me with her caring and gently love. My brothers and sisters deserve special mention for being supportive and caring siblings.

Words fail me to express my appreciation to my wife Sara whose dedication, love and persistent confidence in me, has taken the load off my shoulder. I owe her for being unselfishly let her intelligence, passions, and ambitions collide with mine. Therefore, I would also thank Sara's family for letting me take her hand in marriage, and accepting me as a member of the family, warmly.

Finally, I would like to thank everybody who was important to the successful realization of the thesis, as well as expressing my apology that I could not mention personally one by one.

DEDICATION

To The Souls of My Parents

To My Wife　　　*To My Daughters*

TABLE OF CONTENTS

LIST OF FIGURES

LIST OF TABLES

LIST OF ABBREVIATIONS

BFW	Boiler Feed Water
C	Combination, Cooler
CCC	Cold Composite Curve
Crnt	Current
CU	Cold Utility
CW	Cooling Water
DP	Double Pipe
E	Energy, Exchanger
EIA	Energy Information Administration
EMAT	Exchanger Minimum Approach Temperature
F	Fuel
GCC	Grand Composite Curve
H	Heater
HCC	Hot Composite Curve
HEN	Heat Exchanger Network
HP	High Pressure steam
HRAT	Heat Recovery Approach Temperature
HU	Hot Utility
inv	Investment
Ld	Let down valve
LMTD	Logarithmic Mean Temperature Difference
LP	Low Pressure steam
MILP	Mixed Integer Linear Programming
MINLP	Mixed Integer Non Linear Programming
Mn	Minimum
MP	Medium Pressure steam
Mx	Maximum
NLP	Non Linear Programming

Opt	option
P	Power
PB	Payback
sav	Saving
SGCC	Site grand Composite Curve
ST	Shell and Tube
T	Temperature, Turbine
TF	Temperature Flexibility
VHP	Very High Pressure steam
WPA	Water Pinch Analysis

NOMENCLATURE

Symbol	*Definition*
A	Exchanger heat transfer area (m^2).
A_C	Exchanger shell side cross-sectional area (m^2)
A_{ex} , A_{exist} , $A_{ex.HEN}$	Total area of the existing HEN before heat shifting (m^2).
$A_{new.HEN}$	Total area of the new HEN after heat shifting (m^2).
A_{before}, A_{after}	Exchanger heat transfer area before and after heat shifting, respectively (m^2).
a, b, c	Cost coefficients of the exchanger area.
av_{shell}	Average Size of exchangers shell.
A, B	Coefficients depend on the pressure drop and saturation temperature across the turbine.
b_0, b_1, b_2,b_3	Regression parameters depend on the steam turbine power and turbine configuration.
B_C	Baffle cut (to direct the stream fluid across the tubes).
c	Constant in the tube side pressure drop relation.
CP	Stream heat capacity flow rate (kW/^{o}C).
C_P	Specific heat capacity (kJ/kg.^{o}C).
$C_{P,water}$	Specific heat capacity of the water (kJ/kg.^{o}C).
$CU_{ex.cost}$, $CU_{new.cost}$	Existing and new (after heat shifting) cold utility cost ($)
$C(n,r)$	Number of combinations.
CU_{price}	Cold utility price. ($/kW)
D_s	Shell diameter (m)
d_o	Outside tube diameter (m)
d_I	Inside tube diameter (m)
E_{exist}	Existing energy consumption in HEN (kW)
F_I, F_o	Exchanger tube and shell sides flow rate, respectively (m^3/s)
F_{price}	Fuel price ($/kW)

F_T	LMTD correction factor.
F_{hn}, F_{hw}, F_{hb}, F_{hL}, F_{Pb}, F_{PL}	Correction factors in the shell side pressure drop equation.
$F_{cost,\ surp}$	Cost of fuel to generate surplus steam.
$HU_{ex.cost}$, $HU_{new.cost}$	Existing and new (after heat shifting) hot utility cost ($)
HU_{price},	Hot utility price ($/kW).
H	Film heat transfer coefficient (kW/m^2.°C).
h_{BFW}	Specific enthalpy of the boiler feed water (kJ/kg).
$h_{H,out}$	Specific enthalpy of the outlet steam from HEN's heater.
h_T, h_S	Tube and shell side heat transfer coefficients, respectively (kW/m^2.°C).
$h_{T,in}$	Turbine inlet specific enthalpy (kJ/kg).
$h_{T,is,out}$	Turbine outlet isentropic enthalpy (kJ/kg).
$h_{T1,out}$, $h_{T2,out}$, $h_{T3,out}$, $h_{T4,out}$:	Outlet enthalpy from turbine 1, 2, 3 and 4 (KJ/kg), respectively in the utility case study.
$HP_{stm,sav}$:	High pressure steam saving (t/h).
h_{VHP}, h_{HP}, h_{MP}, h_{LP}	Specific enthalpies for very high, high, medium and low pressure steam headers, respectively and any outlet from them (kJ/kg)
h_{header}	Specific enthalpy of steam in steam header (kJ/kg)
$h_{header,\ in}$, $h_{header,\ out}$	Inlet and outlet specific enthalpy of steam to and from the header, respectively (kJ/kg).
i	Matrix row
j	Matrix column
K	1000 units, Kelvin.
k	Thermal conductivity (W/m.°C), / dimensional constant in pressure drop relations, (Polley et al, 1990).
KP_{T1}, KP_{T2}, K_{S1}, K_{S2}, K_{S3}, K_{hT}, K_{hS}, K_{PS1}, K_{PS2}, K_{PS3}, K_{PS4}	Dimensional constants in the exchanger tube and shell sides pressure drop equation. They basically depend on the geometrical configuration and the fluid physical properties.
L	Intercept ratio in the Willian's line equation.
L_B	Distance between Baffles (m).

m, m_{min}, m_{max}	Current, minimum, and maximum steam flow through steam turbine, respectively (t/h).
$m_{heder,in}$, $m_{header,out}$	Steam inlet and outlet to and from steam header, respectively in the utility system (t/h).
$m_{p,\ HP,\ ex}$, $m_{p,\ MP,\ ex}$	Existing HP and MP steam mass flow to process, respectively (t/h).
$m_{p,VHP}$, $m_{p,HP}$ $m_{p,MP}$, $m_{p,LP}$	Very high, high, medium and low pressure steam mass flow to processes heating demand respectively (t/h).
m_{B1}, m_{B2}	Steam mass flows from boiler (1) and (2), respectively in the utility case study (t/h).
m_{T1}, m_{T2}, m_{T3}, m_{T4}, m_{T5}	Steam mass flow through steam turbine 1, 2, 3, 4 and 5, respectively in the utility case study (t/h).
$m_{Ld,1}$, $m_{Ld,2}$, $m_{Ld,3}$	Steam mass flow through let down valve 1, 2 and 3, respectively in the utility case study (t/h).
m_{vnt}	Steam mass flow through venting valve (t/h).
$m_{p,HP,ex}$, $m_{p,HP}$	Steam mass flow rate from HP header to process HEN before (existing) and after saving scheme (t/h).
$MP_{stm,sav}$	Medium pressure steam saving (t/h).
$m_{p,MP,ex}$, $m_{p,MP}$	Steam mass flow rate from MP header to process HEN before (existing) and after saving scheme (t/h).
N_{shell}	Number of shells.
N_T, N_{TP}	Number of tubes and number of tube passes, respectively.
n	Slope of Willian's line equation/exponential power in the pressure drop relations (Polley et al, 1990)/ Size of the set from which elements are combined, (number of available paths in HEN).
P_C	Pitch configuration factor.
$P_{cost,\ surp}$	Cost of power generated by the surplus steam.
P_{price}	Power price ($/kW).
P_T	Exchanger's tube pitch (centre to centre distance between adjacent tubes).
Pr	Prandtl number

Q	Exchanger heat load (heat quantity) [kW]
Q_{CUmin}, Q_{Cmin}, Q_{CU}	Minimum cold utility requirements in HEN (kW).
Q_{HUmin}, Q_{Hmin}, Q_{HU}	Minimum hot utility requirements in HEN (kW).
$Q_{ex.C}$, $Q_{new.C}$	Existing and new (after heat shifting) cold utility load (kW).
$Q_{ex.H}$, $Q_{new.H}$	Existing and new (after heat shifting) hot utility load (kW).
Q_{before}, Q_{after}	Exchanger heat load before and after heat shifting (kW).
R	Matrix name of temperature flexibility ranges.
r	Size of combination (number of paths to be combined).
r_{ij}	Any element in the matrix of temperature flexibility ranges.
T_1, T_2	Exchanger input and output temperature, respectively for either hot or cold stream (°C).
$T_{C,in}$, $T_{C,out}$	Exchanger's cold stream inlet and outlet temperatures, respectively (°C).
T_{BFW}	Inlet temperature of the boiler feed water (°C)
TF	Temperature flexibility (°C).
$T_{H,in}$, $T_{H,out}$	Exchanger's hot stream inlet and outlet temperatures, respectively (°C).
$T_{sat,in}$, $T_{sat,out}$	Turbine inlet and outlet saturation temperature, respectively (°C).
t^{+}_{hst}	Incremental increase of temperature (to hot streams) (°C).
t^{-}_{cst}	Incremental decrease of temperature (from cold streams) (°C).
U	Overall heat transfer coefficient (kW/m^2.°C).
W	Shaft work generated by steam turbine (MW).
W_{INT}, W_{int}	Intercept of Willian's line equation.
W_{min}, W_{max}	Minimum and maximum shaft work generated by the turbine, respectively (MW).
x	Shifted heat load through the utility path in HEN (kW)

ΔA, $add.A_{HEN}$, ΔA_{HEN}	Required additional area to HEN (m^2).
ΔH, H	Enthalpy (kW).
Δh_{is}	Isentropic enthalpy difference along the turbine (kJ/kg).
Δh_{gen}	Steam generation enthalpy difference (kJ/kg).
Δh_{H}	Process steam enthalpy difference along the heater of HEN (kJ/kg).
ΔN	Number of required additional shells.
ΔP	Pressure drop (kPa).
ΔP_T	Tube side pressure drop (kPa).
ΔP_S	Shell side pressure drop (kPa).
ΔT	Temperature difference (°C).
$\Delta T1$, $\Delta T1$	Exchanger's hot side and cold side temperature difference, respectively (°C).
ΔT_{min}	Minimum Temperature difference between hot and cold streams of HEN (grass-root design) °C.
ΔT_{sat}	Saturation temperature difference (°C).
ΔT_{small}	Smallest temperature difference between hot and cold streams of an existing HEN equivalent to HRAT.
ΔW_T	Turbine shaft work difference (before and after steam saving).
Greeks	
ρ	Density (kg/m^3).
η_{boiler}	Boiler efficiency.
$\eta_{crnt,}$	Current heat flow path efficiency
η_{gen}	Power generation path efficiency
η_{imp}	Power import efficiency.
η_{loss}	Steam distribution loss.
η_{ST}	Steam turbine efficiency.
μ	Viscosity (cps).
v	Velocity (m/s).

CHAPTER 1

INTRODUCTION

1.1 Importance of energy conservation projects

Industry is currently considering energy conservation projects more favorably as a result of increasing pressure from current economic uncertainties and tighter environmental regulations. The significant hike in oil and gas prices, according to the data taken from the Energy Information Administration (EIA) [1] as plotted in Fig 1.1, has impacted the energy price tremendously. This increasing price trend is expected to continue over the long run as the oil and gas supply depletes with time. Accordingly, energy conservation projects featuring small capital investment and quick economic returns are particularly thought of as attractive for industries to adopt.

A recent report by Campbell [2] highlighted that most oil and gas producing countries have attained peak production and the decline is forecasted to be at 2-3% a year as shown in Fig 1.2. The new oil discoveries made were insufficient to cope with the shortfall of supply. Additionally, the situation is made worse by the population growth and massive industrialization effort by China and India [3]. Even though the current economic recession has led to a significant drop in oil and gas prices, it is expected to be only temporary. Therefore, projects leading to improved heat recovery in chemical processes will be expected to continue receiving support from the industry.

Apart from industry demand, OPEC [4] has reported that the population growth and improvement of living standards in the developing countries have rapidly increased the overall energy consumption as shown in Fig 1.3. According to the U.S energy information administration (EIA) [5], the world's total oil production between 2006 and 2008 has mostly failed to fulfill the demand as illustrated by Fig 1.5.

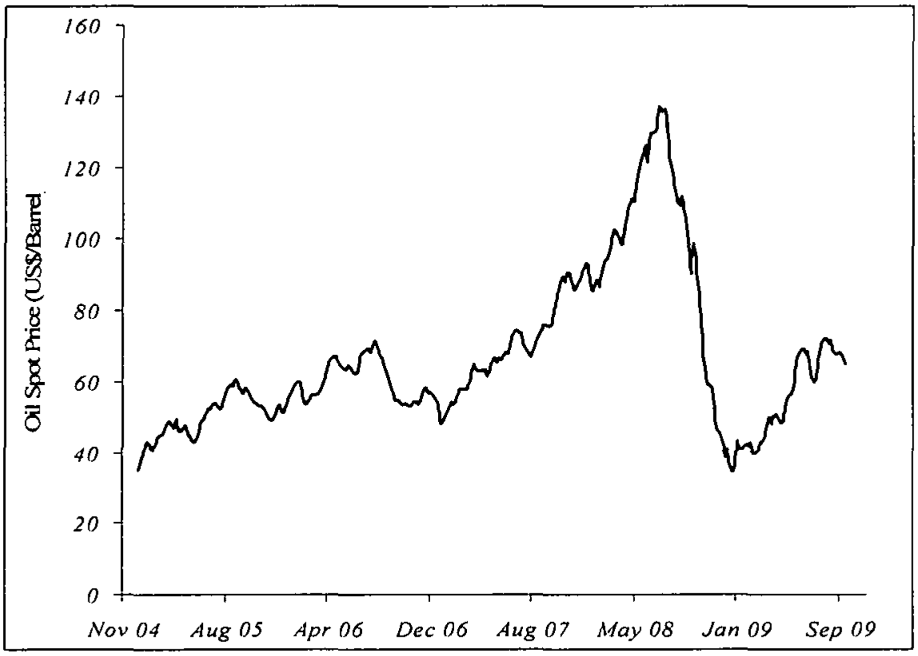

Fig 1.1: World Oil Price; Estimated Export (2004 - 2009)
(Source: Integrated energy statistics; EIA, 2009)

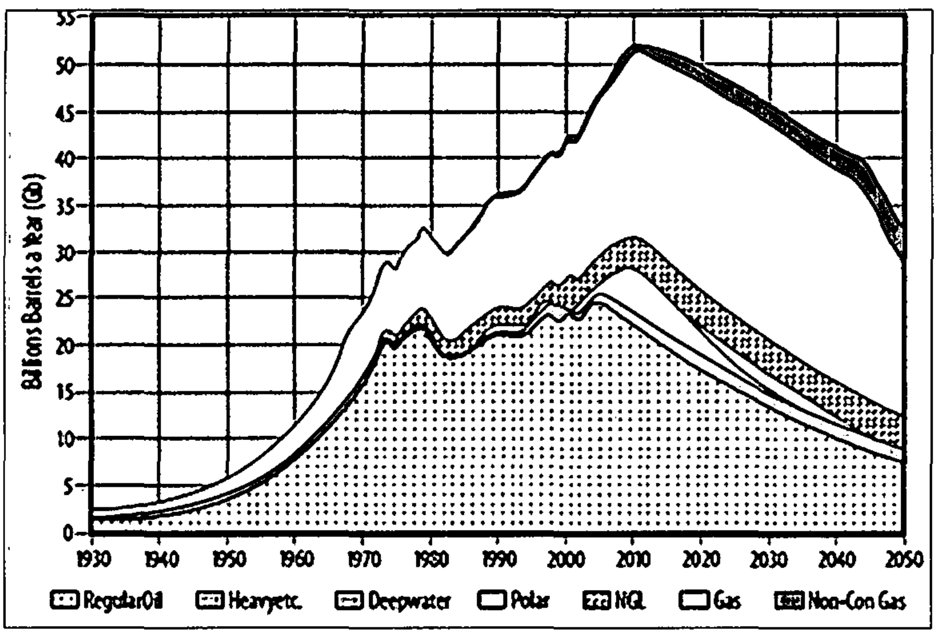

Fig 1.2: Worldwide Oil and Gas Production Profile – 2006 Base Case
(Source: Cambpell, 2006)

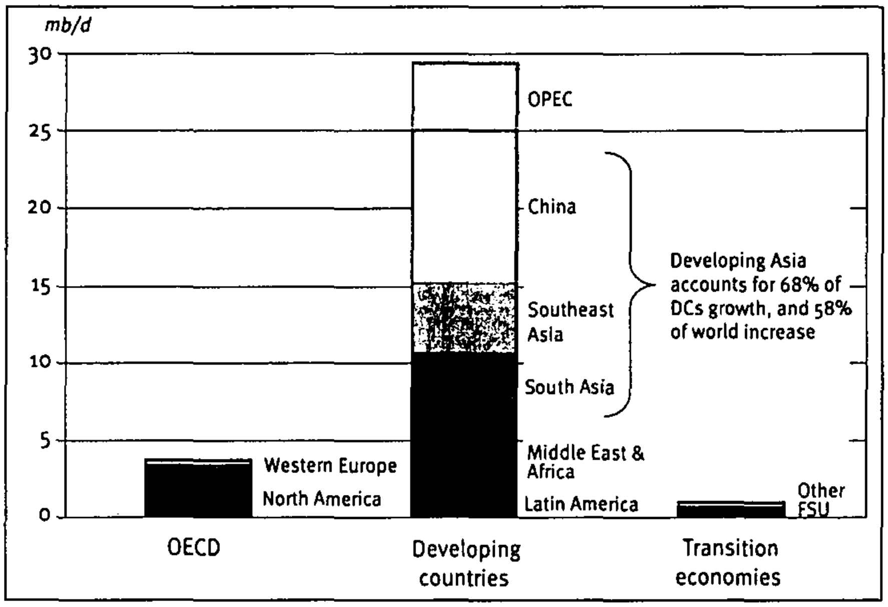

Fig 1.3: Annual growth of oil demand (million barrels per day) 2005 -2030
(Source: OPEC, 2007)

Besides the energy crisis, stricter environmental regulations relating to atmospheric discharge have become another prime driver for energy conservation projects. Process plants contribute to the level of CO_2 emissions through their central utility system which mostly fires fuel to generate heat and power. Data over the past 150 years have shown an increase in the level of Greenhouse Gases emissions [6]. The levels of several main greenhouse gases have increased by about 40% since the large-scale industrialization began around 150 years ago as shown in Fig 1.4 below:

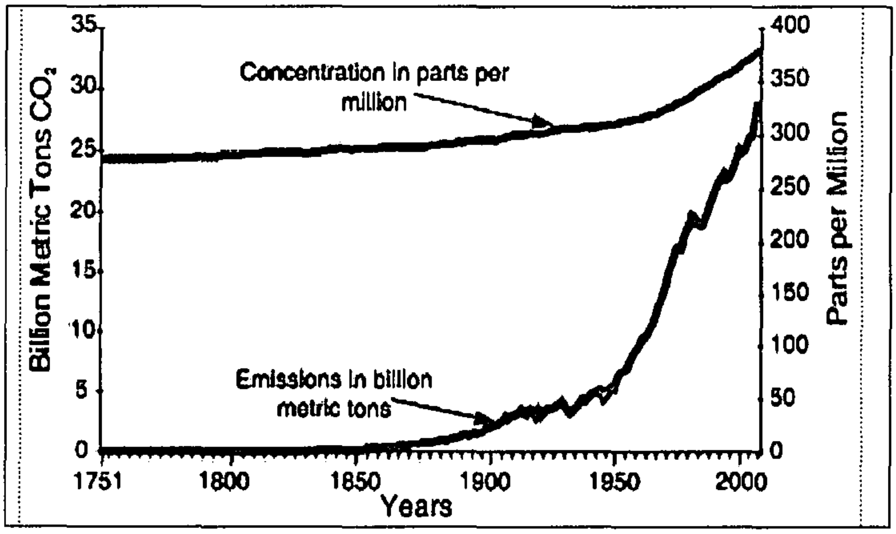

Fig 1.4: CO_2 emission and concentration (1751- 2000)
(Source: Oak Ridge National Laboratory; EIA, 2009)

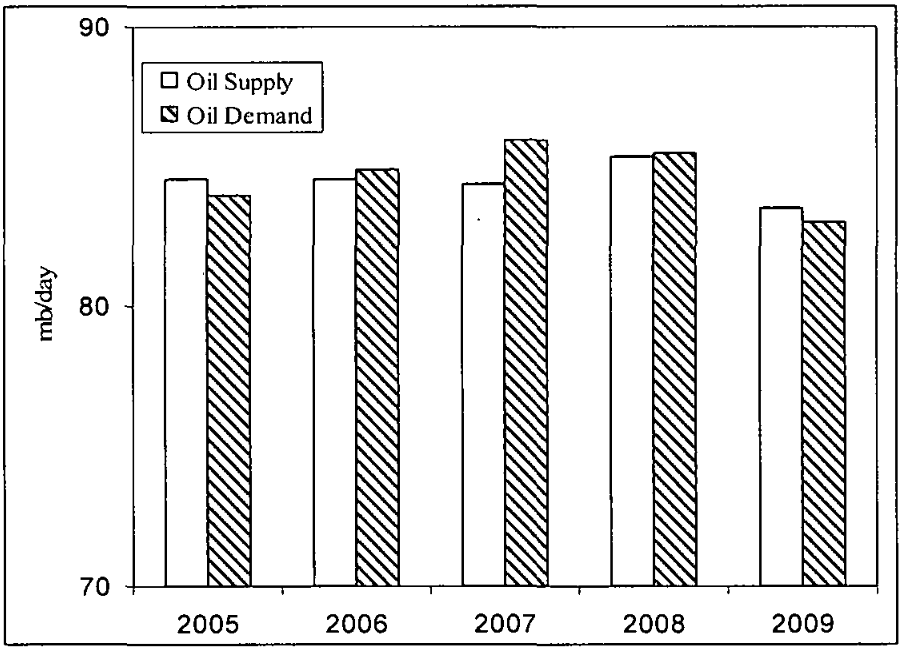

Fig 1.5: World oil supply and demand (million barrels per day); (2005-2009)
(Source: Official energy statistics; EIA, 2009)

1.2 Heat recovery in process plant

Heating and cooling of plant process streams are common features in chemical processes. Hot and cold process streams are subjected to heat exchange matching using heat exchanger devices to recover as much process heat as possible. The potential of energy transfer between such streams depends on several factors. These factors are the streams' fluid flow rates, heat exchanger area, heat transfer coefficient, temperature gradient between the exchange streams and several others. After the process to process heat recovery is established, the remaining heating and cooling demands have to be supplemented with external utilities. The heat recovery system that enables heat exchange between hot and cold streams is called the 'Heat Exchanger Network (HEN)' which is essential for energy conservation within a plant [7]. The grass-root design of the heat exchanger network has been significantly improved through the use of the Pinch Technology [8-10], which could also be applied for the HEN retrofit.

Based on the Pinch Technology, the grass-root design of the HEN involves several steps beginning with setting a target for energy and capital cost. ΔT_{min} is used as the only parameter for optimizing the HEN design. The design engineer is then provided with a target for what could be achieved ahead of design implementation [11]. For instance, target could be set for lower energy consumption and the respective capital cost required for a particular HEN design before implementing the project.

On the other hand, the retrofit of the HEN is more complicated than the grass-root design since the designer is bounded by the constraints of the existing HEN. Moreover, the available capital to spend for the retrofit might not be sufficient and/or must be regained within a specified and relatively short span of time. Similar steps as conducted for the grass-root design could be followed for the retrofit of the HEN but with some variations in the specific methods adopted to consider the existing network structure.

Although the Pinch Technology is highly useful for both the HEN grass-root design and retrofit where the user is involved right from the start point, it is time-consuming for the whole design cycle to be executed. An alternative approach for the HEN design was developed based on a Mathematical Programming method. However, the designer involvement is very minimal during the design stage. A breakthrough was made by combining the Pinch Technology approach and the mathematical programming method to harness the strength of both for the HEN retrofit [12].

1.2.1 Retrofit of heat exchanger networks

It is economically not feasible for the industry to build new processes for improving the heat recovery system for an existing plant. Instead, retrofitting the current system with a lower investment is an alternative energy conservation choice, especially in the light of uncertain economic situations. It has been reported that 70% of the projects conducted in the industry involved process retrofits [13].The setting up of the retrofit targets using the Pinch Technology has been developed since 1980s [7].

The HEN retrofit scenario is more complicated than the grass-root design since the existing infrastructure has to be considered. Each system and subsystem in the process plant has to be well understood when addressing the energy system modification. Consequently, the interaction between the plant processes (HEN and utility system, mainly) could be handled properly.

1.3 The Impact of Energy Conservation in HENs on the Utility System

The chemical process units usually extract the required power from a central utility system within the total site. For instance, the heating utilities required by HENs are often supplied in the form of steam at certain pressure levels such as VHP, HP, MP, and/or LP steam. Therefore, the interaction between the two systems should be well addressed and analyzed to explore the economic impact. Retrofit of HENs mostly results in reduction of heating requirements. Consequently, the surplus steam from the utility system has to be reviewed accordingly to ensure its usage is channeled to the best option. Such surplus could either be utilized for generating more power from the turbines in the utility system or eliminated by reducing the fuel consumption in the boiler house.

1.4 Problem Statement

Since the 1970s, systematic techniques have been developed for designing HENs to reduce energy consumption in the process plants. Currently, industries are not undertaking new HENs' design for the existing plants, and even not willing to invest heavily on large scale retrofit projects due to economic uncertainties.

Generally, the retrofit of heat exchanger networks could be classified either as a major or minor retrofit. The major HEN retrofit typically incorporates topological modification of the network where new device(s), re-sequencing, stream splitting and/or re-piping are considered. The minor retrofit projects may only involve installation of additional area to the existing HEN devices. It is found that most of the conducted research in HEN retrofit concentrated on reconstruction and topological changes in order to justify acceptable economic returns. The massive topological changes always require high capital investment and massive plant changes which is risky in the light of current economic situations. Several points have been neglected by the previous researchers when conducting HEN retrofit with structural modifications as pointed out below:

- The topology changes might not be applicable due to safety zone constraints.
- The cost of the civil work to implement the structural changes.
- The availability of the platform in the plant location for the required modifications.

Therefore, minor retrofit projects with only area addition to the existing HEN matches are more suitable (advisable) as they are cheap and require less structural adaptation and civil work.

The previous HEN design and retrofit methods were basically depending on the structured techniques of the Pinch Technology and/or mathematical programming techniques. However, these techniques have considered the HEN retrofit problem as a pseudo new HEN design where the entire steps of the grass-root design were followed [14]. In fact, the retrofit treats an existing HEN where the existing constraints are to be dealt with and hence becomes more complicated than the grass-root design. Furthermore, Pinch Technology does not automatically provide or generate retrofit options in a wider range either with or without structural changes in HEN. On the other hand, the mathematical techniques are complicated lacking user interaction. Accordingly, a comprehensive mathematical and computational knowledge is required to address the energy problem through the HEN retrofit. However, the time factor associated with the current economic uncertainties is very precious and hence the energy solutions should be obtained and decided quickly.

Most of the previous studies in the field of HEN design and retrofit have considered fixed operating conditions. Only few researchers were taken the advantages of changing the process conditions for better heat recovery such as Linnhoff and Parker [15], Linnhoff and Kotjabasakis [16] and later Zhang and Zhu [17]. However, they did not develop or use specific procedure to handle the process conditions changes systematically.

Furthermore, most of the past researches in the field of process heat recovery, have taken the HEN retrofit as a standalone problem. Nevertheless, external heating and cooling are always needed for some streams in the HEN which is often supplied from a central utility system. This interaction between the HEN and the utility system imply that any energy alteration in one of the two systems would have an impact on the other.

The essential contribution of the current work is the development of HEN retrofit approach using a simple combinatorial method for combining the available utility paths in HEN to generate several energy saving alternatives. The retrofit solutions are obtained at the expense of minor changes in the HEN. Moreover, the retrofit solutions are made more competitive by developing a systematic procedure for handling the process streams' temperature changes. Further contribution is achieved by developing a user friendly computer programme for implementing the overall approach.

The developed approach is further extended to study the impact of energy saving derived from the HEN retrofit on the utility system as a key concept for the total site energy improvement.

1.5 Objectives of Research

The overall objectives of the current research are pointed out as follows:

1. To develop a new HENs retrofit approach based on a simple combinatorial method for generating several energy saving options without major changes in the existing structure of the HEN.

2. To establish a systematic procedure for maneuvering the process streams' temperature flexibility for exploring additional energy saving to make the HEN retrofit options more competitive.

3. To develop a user friendly *JAVA* programme for implementing the proposed HEN retrofit approach along with the concept of temperature flexibility.

4. To apply the proposed approach of HEN retrofit on the utility system to explore the effect of energy saving on the power generation in the utility system.

1.6 Scope of Research

The current research work focuses on developing a structured method for reducing energy usage in the existing heat exchanger networks (HENs) while increasing the heat recovery within the network. The method uses a combinatorial concept to combine the available utility paths in the HEN in different alternatives for screening wider options for shifting the heat loads from the HEN utilities. The heat recovery approach temperature (HRAT) as opposed to ΔT_{min} of the existing network is used as a control parameter for the heat load shifting. HRAT is also kept at the minimum possible to ensure the operability of the HEN in terms of the heat transfer process between the heat exchange streams while shifting the heat loads.

Generating several alternatives for the retrofit of the HEN would allow the process engineer to choose the best solution within the affordability of the capital investment. The selection depends on the economic criterion embedded in the method, i.e., amount of savings gained, capital cost to be invested and the payback period to refund the investment.

The process streams' temperature flexibility (TF) is integrated within the developed method to enable further assessment to be made on the selected solutions by allowing for temperature changes on the operation of some of the equipment. It is worth mentioning that temperature changes related to the process sensitivity and the TF alternatives provided in this work are based on a ceiling of $\pm 5^{o}C$ of the streams.

Generating several options of energy savings together with integrating the streams' temperature flexibility in the HEN, causes iterations where looping is required. Therefore, a user friendly computer interface programme is developed to overcome the calculation complexity.

In the light of the expected interaction between HEN and the utility system, energy savings derived from the HEN retrofit will affect the steam balance within the utility system. Therefore, top-down analysis in the utility system has been used to investigate the effect.

The application of the approach developed is demonstrated using selected case studies of the HEN and the utility system from the literature.

1.7 Overall thesis organization

Chapter 1 is mainly an introduction where the general features, research incentives, problem statements, objectives and scope of the current work are covered.

Chapter 2 generally highlights the literature review covering the various aspects of the process integration and the development of Pinch Technology for energy conservation in the process plant. The approaches developed for HENs retrofit based on the Pinch Technology, Mathematical Programming or a combination of both during the last three decades are explained in detail. More elaboration is given to the retrofit methods that depend on the path analysis idea and the approaches account for the pressure drop constraints. Moreover, the association of the process condition changes with the retrofit approaches is also described. Finally, the approaches considering the total site and utility system management are highlighted.

Chapter 3 describes the overall methodology followed for path combination along with the idea of temperature flexibility for the HEN retrofit. The discussion starts with highlighting the theoretical background of the concepts related to the current study. The overall steps of the Pinch Technology for the HEN design are briefly described where emphasis is given to the use of loops and paths for HEN optimization. Then, the plus/minus principle is discussed in detail since the temperature flexibility suggested in the current work is based on the same idea. Besides the theoretical aspects, the developed approach of paths combination for the HEN retrofit is comprehensively explained in this chapter. The consideration of pressure drop for calculating the exchangers' heat transfer coefficients is also elaborated. Based on the theory of plus/minus principle, the association of the proposed idea of temperature flexibility with the developed approach of path combination is also described. Finally, a case study of the HEN with detailed data to validate the approach is presented in this chapter with comprehensive analysis.

Chapter 4 describes in detail the interaction between the HEN and the utility system. Firstly, the reasons to study such interaction are briefly highlighted. To understand the correct handling of material and energy balance, the configuration of the steam and utility system is clearly described. Then, the power generation opportunities and steam turbine model are explained. The steam savings derived from selected HEN retrofit options are presented in this chapter to study the HEN-Utility interaction. To explore the HEN-Utility interaction, the method of top-level and path analysis to distribute the steam savings wisely among the utility system components is described in this chapter. A demonstration example of the utility system to be integrated with the HEN is presented and analyzed based on the top-level analysis.

Chapter 5 mainly discusses the outcomes of the developed approach where results and analysis are presented for both a standalone HEN and the HEN-Utility system.

In Chapter 6, the overall work and results are concluded. Based on the obtained results, some future work and suggestions are pointed out in this chapter.

CHAPTER 2

LITERATURE REVIEW

2.1 Introduction

A comprehensive survey for most of the research works in the process plant dealing with energy conservation is presented in this section of the thesis. A particular description is given to the common approaches and methodologies developed during the last three decades for the retrofit of heat exchanger networks (HENs). The HENs' retrofits based on the techniques of the Pinch Technology and/or Mathematical Programming are comprehensively discussed. The approaches using path analysis, considering the pressure drop constraints and dealing with process condition changes are given more emphasis. Some of the work on energy management in the utility system and total site are briefly touched on.

2.2 Process integration highlights

Dunn and El-Halwagi [18] states that process integration can be considered as a holistic approach to process design attempting at uniting a chemical process. The chemical process integration could best be represented by the onion diagram shown in Fig 2.1[19]. Several methodologies and tools have been developed over the past two decades emphasizing on this understanding. The essential target is to improve the overall plant in terms of productivity enhancement, energy conservation and environmental protection. In the past, process design was given more emphasis where many new plants need to be designed and constructed. However, the need to retrofit existing plants becomes growingly important. The essentiality of retrofit arises from the realization that the invested capital in building the plants could be exploited further for better performance to maintain the operation in a competitive manner.

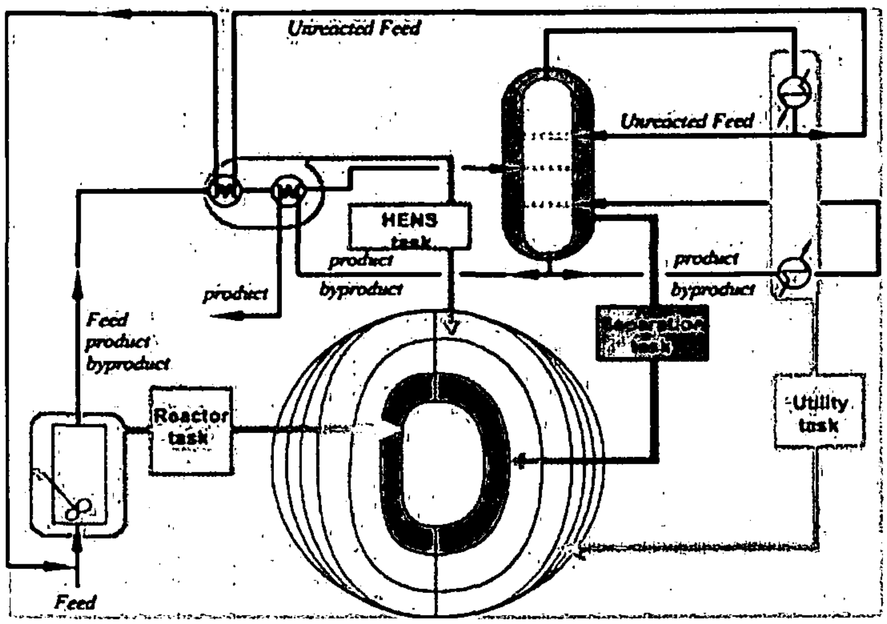

Fig 2.1: The onion diagram represinting the unity of chemical processes
(Rašković and Stoiljković, 2009)

Nevertheless, undertaking any modification towards any process unit requires a full consideration and understanding of the interaction between the processes.

Process integration is broadly categorized into energy integration and mass integration[18]. The energy integration generally deals with energy generation and recovery throughout the process[20], [21]. According to the review made by Dunn and El-Halwagi [18], some of the energy forms considered are:

- Heating energy
- Cooling energy
- Power generation
- Power consumption
- Fuel

Several methodologies have been developed for energy conservation due to the increasing demand for expensive utilities in chemical process industries. Mainly, the development has been oriented towards increasing heat recovery using a heat exchange system which is simply represented in Fig 2.2 and later termed as the Heat Exchanger Network (HEN).

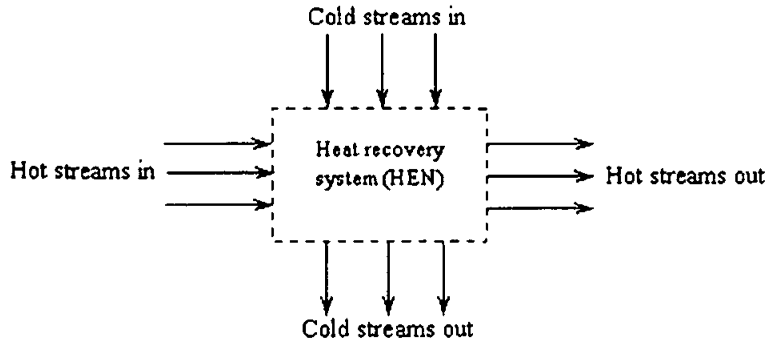

Fig 2.2: Simple representaion of heat recovery system

Researchers have developed several methods for the synthesis of the HEN system as a response to the call for energy conservation in chemical process industries. A comprehensive review for most of these methods have been presented by Shenoy [20], Linnhoff [21], Douglas [22] and Gundersen and Naess [23].

2.3 Energy Conservation Importance and Startup

Besides its mandatory need by industry, energy is an essential concern to modern life and recently became a controversial problem of the century. Several ways to manage the energy problems are highlighted in the literature mainly aiming at introducing the best approaches for minimizing energy consumption. The essential energy issues are typically the cost and efficiency which are often considered to be the major elements in process economics.

Efforts in energy conservation in process industries are primarily targeted at reducing the amount of energy consumption through efficient energy usage while achieving a similar throughput and thus maximizing profit. The useful utilization of energy in chemical processes is essential to maintain the plants' productivity and profitability. Besides the monetary incentives, the wise utilization of energy must be persistent due to uncertainties associated with the future of energy in addition to the growing challenge for a clean environment.

Energy conservation within industry has received remarkable attention since the first oil crisis struck the world in 1973. Since then, effort has been geared towards understanding and managing the use of energy right from the point of designing the plant and later its operation. This principle is also carried forward into the maintenance stage as discussed by Linnhoff [24]. The premier interest is to improve the process equipment and utilities usage all over the process site.

Process integration begins with process heat recovery which was later expanded to cover other process areas in the late 1980's. The structured heat recovery process design started with the introduction of the Pinch Technology which had later been modified for other designs. For instance, the process heat recovery pinch has been developed for mass transfer operations, particularly in water management. The use of the Pinch Technology for process heat recovery is widely explained by Linnhoff *et al* [10], Smith [25] and Klemes *et al* [26]. Besides the process heat recovery within the HEN grass-root and retrofit design, the Pinch Technology was also used for the total site improvement as introduced by Klemes *et al* [27].

2.3.1 Pinch Technology as a breakthrough for energy conservation

The prime objective of the Pinch Analysis is to achieve financial savings in the process industries by optimizing the ways in which process utilities are applied for a wide variety of purposes. The Heat Recovery Pinch was first discovered by Hohmann [28] when he designed the first optimum networks for the heat exchange system. It was then developed for the purpose of an energy-efficient and cost effective heat-exchange system in the late 1970s and the early 1980s. The incentive was to reduce the impact of the oil crisis and the rapid hike of energy prices in 1973.

Umeda *et al* [29], introduced and discussed the significance of the pinch point when they presented a synthesis strategy for heat exchange systems as a project for energy conservation in a petroleum refinery. Within the same time, Linnhoff and Flower [30], [31] presented a thermodynamically orientated method used to synthesize a four-stream heat exchanger network (HEN). Linnhoff and Hindmarsh [32] later formalized the full conception of the Pinch Technology for the grass-root design of the HEN.

Since then, the Pinch Technology techniques have been widely utilized for designing new plants or a total site level improvement. Furthermore, it has been generalized for other areas rather than just 'heat recovery pinch'. For instance, El-halwagi and Manousiouthakis [33] have developed the Mass Pinch in order to handle the mass exchange between the number of process units in the plant. The Mass Pinch relays on the driving force of concentration difference rather than temperature difference which was for the heat recovery pinch. A further development of the Mass Pinch is the introduction of Water Pinch Analysis (WPA) by Wang and Smith [34] to handle the wastewater minimization in the process industries through reuse and regeneration. Later, WPA had been applied for urban/domestic buildings as introduced by Manan *et al* [35].

Based on a full understanding of thermodynamic insight in the Pinch Technology, Hui [36] has examined the subject of heat integration between identifiable regions of the process plant. He proposed a systematic procedure for designing minimum energy networks which feature few interconnections between the areas of integrity aiming at reducing the additional capital expenditure. For both the grass-root design and the retrofit cases, the tradeoff between energy and capital costs has been examined to find near optimum schemes. Since the developed procedure was based on the concept of the Pinch Technology, it allows the design engineer's inputs to be imposed during the targeting and design stages in order to generate more practical results.

2.3.2 The Retrofit of Heat Exchanger Networks

Most of the methods developed for the heat recovery target are related to the grass-root design of process HENs. However, and as mentioned earlier industry does not build new plants for the same product unnecessarily since the existing ones could still be improved for better performance. Accordingly, HENs' retrofit is the alternative used to improve the heat recovery system of the existing plants. Nonetheless, in view of expected modifications in the retrofit projects, targeting is much more difficult and complicated than that for the grass-root design of the HEN. Currently, the developed HEN retrofit design approaches are using either:

1. Thermodynamically based methods such as Pinch Technology [7, 37-38], or
2. Mathematical Programming methods such as genetic algorithm and transshipment models [39-40], [41-42] or

3. Hybrid methods combining the Pinch Technology and the Mathematical Approaches [12, 43-45].

2.3.2.1 State of the art for HENs retrofit approaches

Retrofit of heat exchanger networks could be classified either as a major or a minor retrofit. The major one incorporates topological modification of the HEN where new device(s), re-sequencing and/or re-piping are considered. However, the minor retrofit projects only involve adding heat transfer area to the existing HEN. Most of the HEN retrofit studies undertaken so far featured reconstruction and topological changes mainly.

The setting up of retrofit targets using the Pinch Technology approach was first developed by Tjoe [7]. He states that for the grass-root design of the HEN, the principle is mainly to target what could be achieved ahead of the detailed design as shown in Fig 2.3 below:

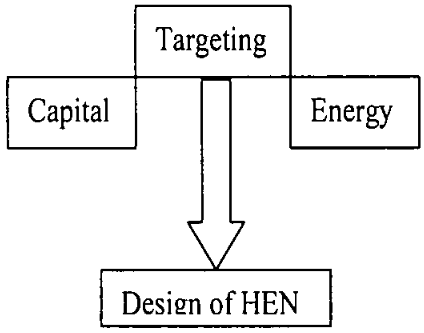

Fig 2.3: Simple idea of Pinch Technolgy for the grass-root design

Using the same principles (i.e. targeting and thermodynamic insights of Pinch Technology), Tjoe improved the idea by introducing a developed method to undertake the HEN retrofit problem. The targeting approach involved trade-off between energy savings, investment cost and the project payback as summarized in Fig 2.4 below:

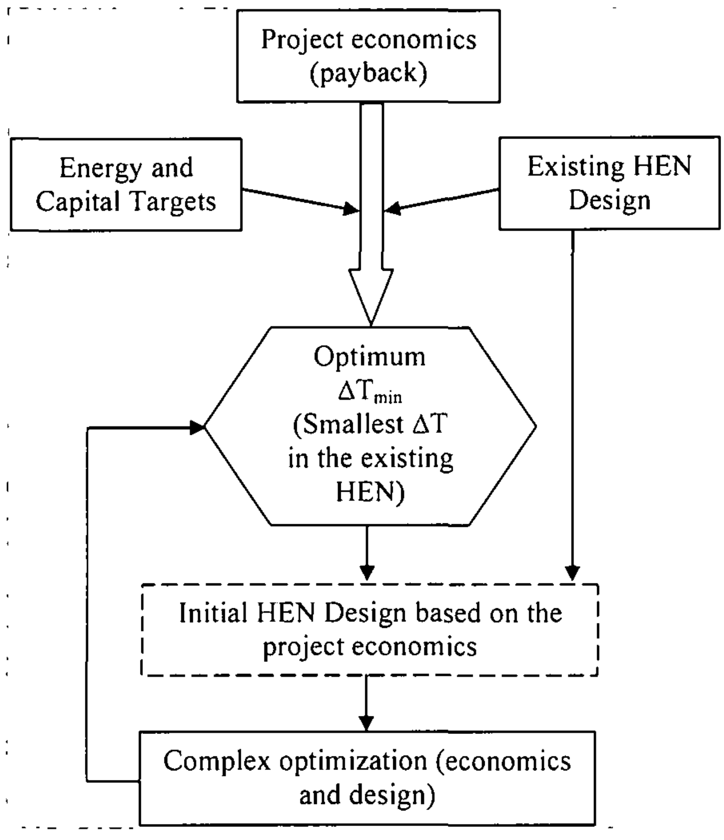

Fig 2.4: HEN retrofit procedure of Tjoe
(Tjoe, PhD thesis, 1986)

This method aimed at exploiting the existing HEN efficiently as a starting point to predict and design a better network. The retrofit curve which is a plot of a retrofit target on a graph of exchanger area against utility requirement has been proposed to provide a graphical representation of capital-energy trade-off for retrofit project. This graphical representation is shown in Fig 2.5. Another form of graphical representation for the retrofit economics was also proposed to relate the energy savings ($/year) to the investment cost ($) and project payback time (year) as shown in Fig 2.6. The approach was considered as a pseudo grass-root design which has been criticized by many researchers.

The HEN retrofit method proposed by Tjoe determined the overall additional area required for the HEN. However, it does not provide any guide for distributing the additional area within the HEN.

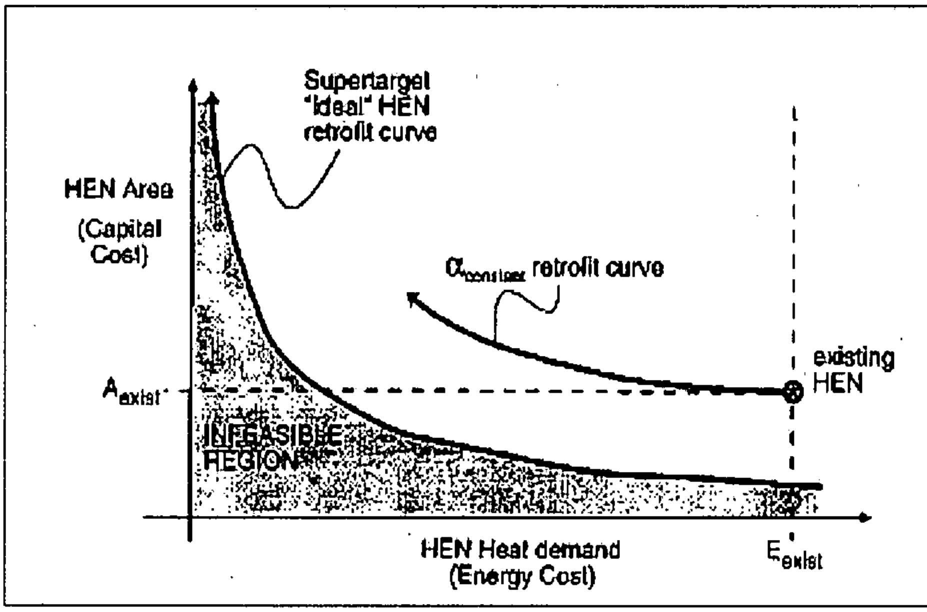

Fig 2.5: Retrofit curves
(Tjoe and Linnhoff, Chem. E. J, 1986)

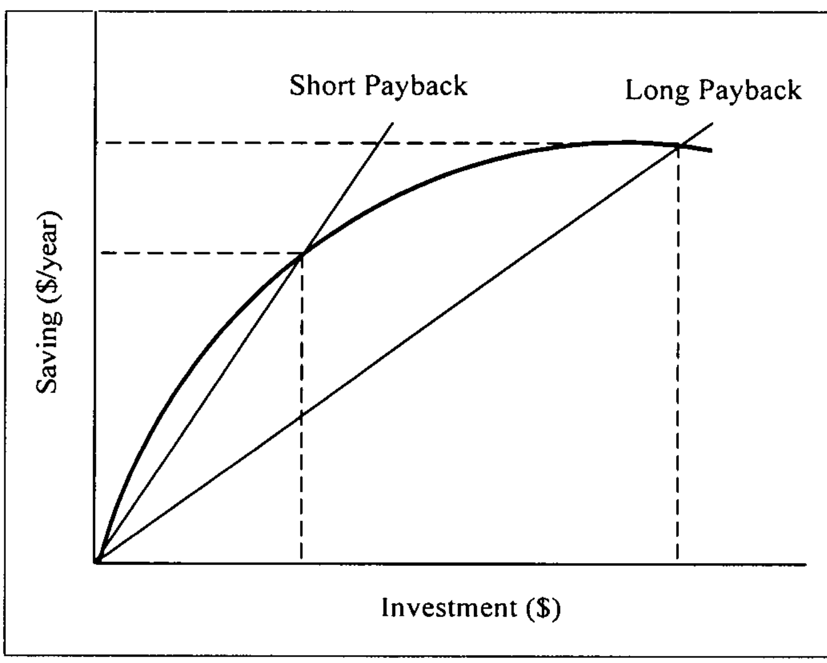

Fig 2.6: Energy savings against capital investment
(Tjoe, PhD thesis, 1986)

Later, the above limitation had been addressed and overcome by Shokoya [46] by introducing the area matrix which accounts for the actual distribution of the heat transfer area between the streams. The area matrix method minimized the mismatch between the existing exchangers' area and the targeted area using linear programming techniques. Using the technique, it was shown that some exchangers in the HEN do require additional new area (+ve retrofit trend) for improvement while others showed excess area available more than the required (-ve retrofit trend). The positive and negative deviations were balanced by redistributing the area over the network matches and sometimes adding new exchangers. Compared to the Tjoe's retrofit method, the Shokoya's technique is characterized by the simplification of the retrofit task and producing many design alternatives. Nonetheless, the method did not consider additional pressure drop resulting from the additional heat transfer area. Therefore, the cost when implementing the project would be higher than expected during the targeting stage. The additional cost is normally associated with the pumping system which needs to be altered to cope with the additional pressure drop.

Later, an approach using cost matrix was introduced by Carlsson *et al* [47] for the HEN retrofit. In addition to the cost of topology changes, the matrix method includes the pumping and maintenance cost associated with each exchanger. The consideration of pumping cost was given to the HEN sections above and below the pinch point separately. The cost matrix method of Carlsson *et al* [47] performed the capital/energy trade-off based on different levels of heat recovery regardless of the thermodynamic principles of the Pinch Technology.

Recently, a graphical method for the HEN retrofit has been introduced by Nordman and Berntsson [48]. Their method is considered as a screening tool to identify different targets for heat recovery while rearranging the HEN units. The units considered for the rearrangement are mainly the heaters and coolers. Accordingly, the method concluded that the closer the heater(s) and cooler(s) position to the pinch in an existing HEN the higher the potentials for a cost effective HEN retrofit.

Besides the approach discussed above, Gadalla [49] has proposed an application retrofit model for the process heat exchanger networks. His model was a part of the retrofit design of heat-integrated crude oil distillation systems aimed at enhancing the overall heat recovery system. The retrofit approach was an optimization-based approach which considered the existing distillation process simultaneously with the associated heat recovery system. Existing equipment limitations, such as exchanger network pressure drop and bottlenecked exchangers, were considered for any proposed changes made. The approach encountered several structural modification options resulting in significant benefits. Several objectives were considered, such as reducing energy consumption and overall cost, increasing capacity, improving profit and reducing CO_2 emissions.

A HEN modification hierarchy was introduced by Makwana [50] for a total site study. In his work he studied the impact of modifying the steam flow within the utility system on the overall capital cost and HEN operability. His suggestion was made as a result of a top level analysis where steam saving in the utility system has a direct influence on HEN operability. Minimum capital investment could be achieved by only switching the external heating media of the HEN from HP to MP steam while maintaining the HEN operability. The structural modifications featured could only be for the utility exchangers (heaters) in order to deal with steam level switching. The MINLP model was proposed to select the optimal selection of steam level switching. The steam switching hierarchy consisted of three options as shown in Fig 2.7. It is either by changing HP steam to MP steam, decreasing HP steam while increasing MP steam, or decreasing HP steam at the expense of increasing heat recovery by adding new exchanger(s) to the existing network.

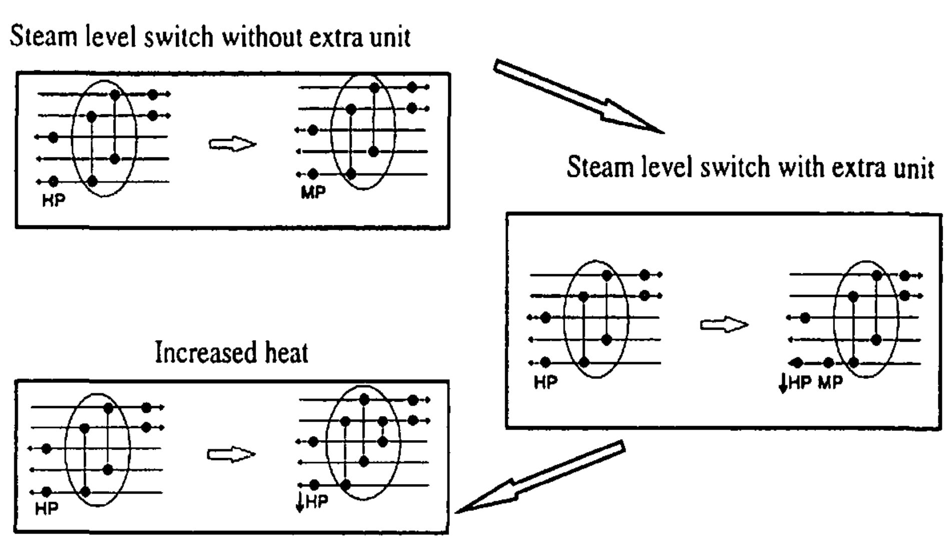

Fig 2.7: Options of hierarchy for HEN retrofit
(Zhu and Vaideeswaran, Applied Thermal Engineering, 2000)

2.3.2.2 Path Analysis for HEN retrofit

Varbanov and Klemes [51] presented the rule of path construction for the HEN retrofit based on the techniques developed by Linnhoff and Tjoe [38]. They also extended the methodology of the Network Pinch which has been explored by Asante and Zhu [12, 45]. In certain HEN systems, if there is no available utility path to increase the heat recovery or, the potential of existing paths is exhausted to handle more heat recovery the Network Pinch could not be established [51]. Based on this fact, the rule for path construction was developed and used for the HEN retrofit when the Network Pinch could not be identified. Similar to Asante and Zhu, Varbanov and Klemes have proposed an ordered topology changes for this special case of the HEN retrofit. Five Topological changes were suggested, consisting of:

1. Match relocation.
2. Match addition.
3. Match removal.
4. Splits addition.
5. Splits removal.

Other procedure based on the path analysis for the HEN retrofit was introduced by Van Reisen *et al* [52]. The method is also a prescreening approach to analyze an existing HEN system for energy saving purposes. From the existing HEN, the approach initially identified all the possible sub-networks that contain at least one heat shifting path. Then, energy conservation using the identified path was established for each sub-network and analyzed economically. The outcomes of each sub-network were compared graphically in a savings/investment trade-off plot as shown in Fig 2.8. Based on such a trade-off, the most efficient sub-network is selected for retrofit irrespective of the remaining sub-networks. The number of the possibilities to find more sub-networks increases with the number of streams, number of exchangers, and number of heaters and coolers. Within the Path Analysis approach, two important rules must be met while decomposing the HEN:

- All the sub-networks should be heat balanced.
- At least, a heater and a cooler connection within one path should be included in each sub-network.

Increasing the heat recovery using the identified path(s) would save energy at the expense of adding new area to the existing exchanger on the existing path, or adding new matches which create new paths. Adding area is preferred due to the minor impact on the existing exchangers during the implementation.

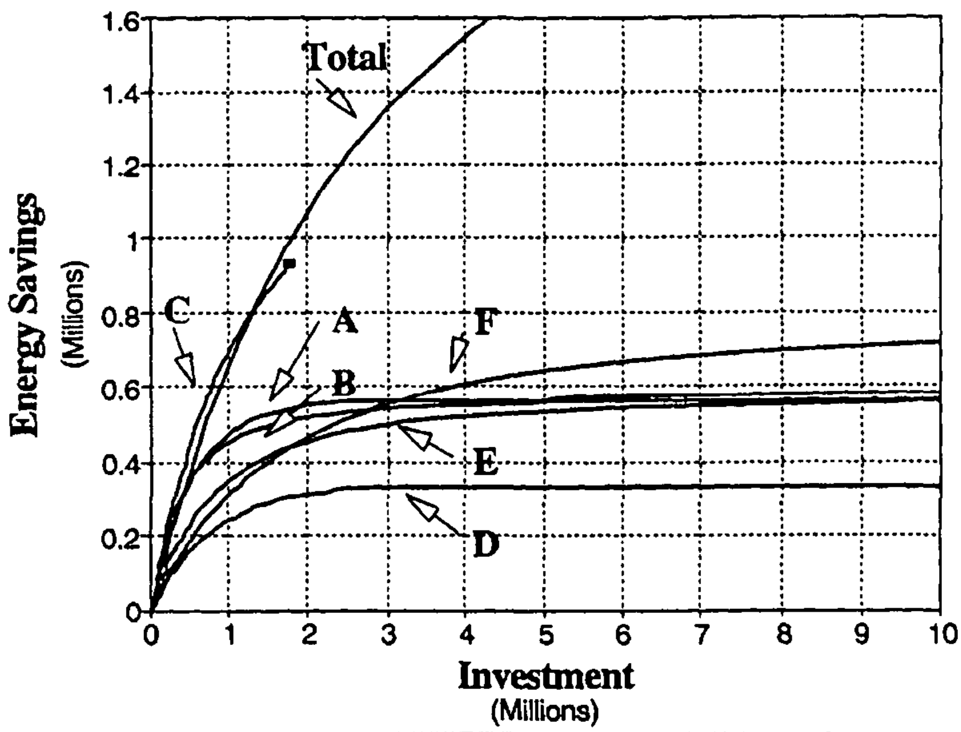

Fig 2.8: Savings on Investment plot for the case study used by Van Reisen *et al*
A, B, C, D, E, F: represent the sub-networks
(Van Reisen et al, Computer and Chemical Engineering, 1995)

The path analysis method was later extended by Van Reisen *et al* [53], where they incorporated the structural targeting methodology for the HEN retrofit that best fit the large network aiming at reducing the retrofit design effort. Besides the energy savings and area investment, this method gives a target for structural modifications where the location of the topology changes is essentially considered. Also, the HEN layout, functionality and operability have been taken into account but ignored the effect of the matches and streams' pressure drops which are considered as crucial parameters that could affects the design cost. Since the method is based on the path analysis approach, it identifies part of the network with high energy savings to investment potentials. The overall steps of the path analysis and structural targeting method according to Van Reisen *et al* [53] is shown in Fig 2.9 below:

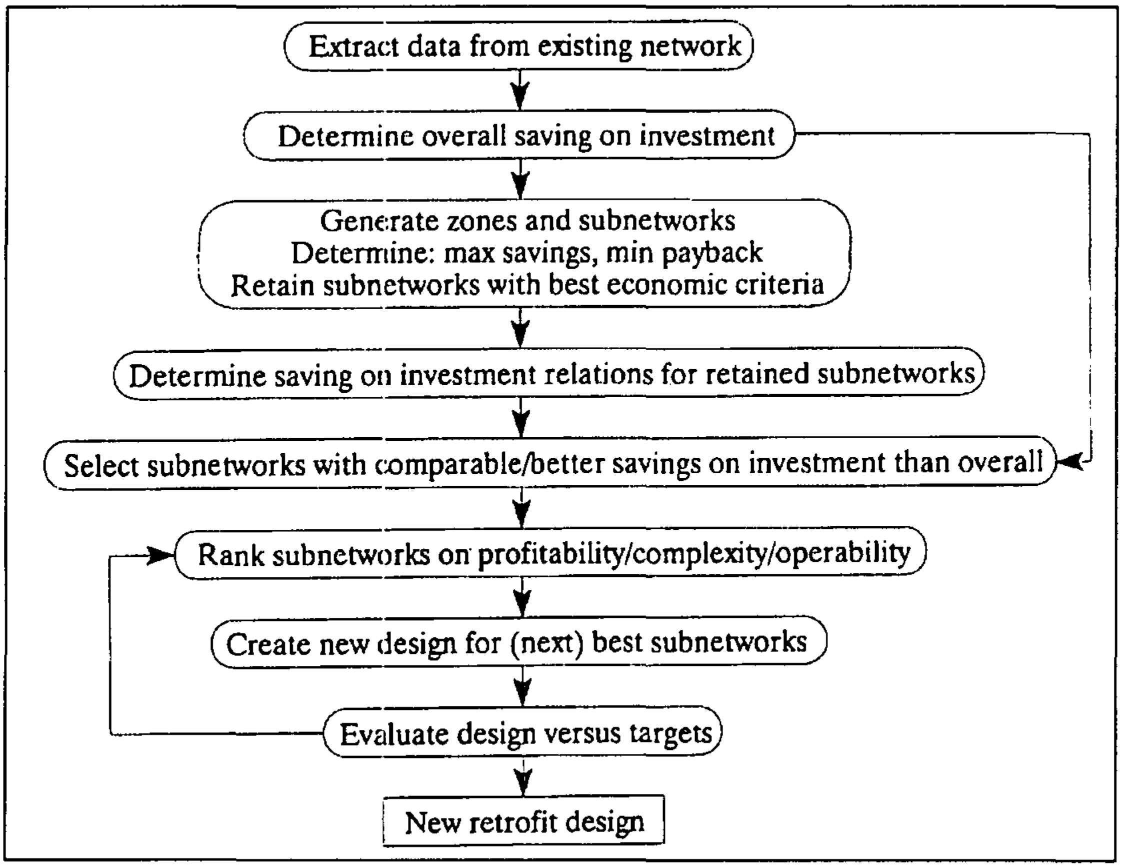

Fig 2.9: Flow chart for path analysis and structural targeting for the HEN retrofit
(Van Reisen et al, Applied Thermal Engineering, 1998)

2.3.2.3 Pressure drop constraints and HEN retrofit

Retrofit approaches were extended to account for the actual layout of existing exchangers [7], [51]. Nevertheless, those approaches have neglected the pressure drop of the existing exchangers and the new added ones for the retrofit. Moreover, the methods were restricted to constant heat transfer coefficients. Recently, it was discovered that heat transfer rate and pressure drop are dependent parameters which affect the capital and operational cost of any heat exchanger network [54].

Most of the developed technologies for the HEN design and retrofit gave significant attention to the thermal aspects while neglecting the hydraulic aspects which mainly disturbed by the pressure drops changes. For the HEN design and retrofit, most researchers considered the effect of the HEN reconstruction on the flow system after the design stage. More precisely, the pressure drop aspect has been ignored for the HEN retrofit although the flow system is usually disturbed when altering the existing HEN configuration [55]. The retrofit targeting procedure of Tjoe

[7] serves as the foundation for the HEN retrofit from which most of the retrofit approaches were developed. However, when the approach was applied for a real retrofit project, the predicted cost was short by £1 million mainly due to the pumping installation as a result of neglecting the pressure drop [55].

The previous established HEN retrofit targeting methods have featured two main limitations as pointed out below:

The methods were considering fixed heat transfer coefficients throughout the stream of the HEN. However, the stream flow system is definitely different inside the exchanger due to the pressure drop disturbance and exchanger geometrical configuration. Therefore, each exchanger should have tube and shell film heat transfer coefficients based on the allowable pressure drop on the stream and the geometrical configuration of the exchanger itself.

The methods considered the pressure drop as a fixed parameter together with fixed heat transfer coefficients which is considered to be too optimistic.

The above limitations were highlighted by Jegede [56] where the stream film coefficient and pressure drop could both be shown to be affected by the fluid velocity of the stream. From this point, Polley *et al* [55] pointed out that it is possible to relate the pressure drop and the exchanger contact area to the film heat transfer coefficient of the fluid. They pointed out that increasing the contact area of the exchanger during the retrofit would decrease the film heat transfer coefficient at a fixed pressure drop. The area-energy targeting plot for a fixed pressure drop shows that a higher add on area for the retrofit is required compared to the target when ignoring the pressure drop as demonstrated in Fig 2.10. Based on this argument, two relationships have been derived by Polley to consider the pressure drop in both sides of the exchanger (shell and tube) which are shown in equations (2.1) and (2.2) for the tube and shell side respectively.

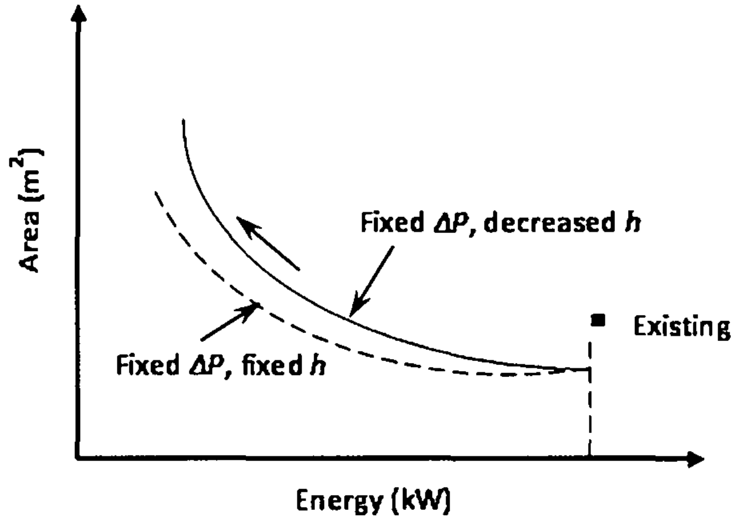

Fig 2.10: Area-energy target plot for the HEN retrofit at a fixed pressure drop
(Polley et al, Trans. IChemE, 1990)

$$\Delta P = \left(\frac{k_2 k_3}{k_1^{3.5}}\right) A.h^{3.5} \tag{2.1}$$

$$\Delta P = \left(\frac{k_2 k_3}{k_1^{5.1}}\right) A.h^{5.1} \tag{2.2}$$

The inclusion of the pressure drop correlations in the HEN retrofit was indeed a significant breakthrough. However Polley *et al* [55] have assumed identical film coefficients for all the exchangers located on the same stream in the HEN. In fact, the HEN retrofit would definitely change the flow and geometrical system of some exchangers in the HEN and hence the film coefficients should vary from one exchanger to another according to the changes made.

A wider study on pressure drop consideration in heat exchanger network was conducted in 1992 by Panjeh-Shahi [57]. He managed to incorporate the allowable pressure drop of any process stream during the targeting stage of the design. Accordingly, he developed a retrofit targeting procedure to account for the existing flow system of the HEN. The procedure then was ensured the consistency of the final obtained results with the targeted ones.

Marcone *et al* [58] combined the pressure drop approach of Polley and the area matrix approach of Shokoya in developing a retrofit targeting of a pressure drop constrained HEN. The approach attempted to overcome the drawbacks of the previous retrofit approaches by proposing a superstructure network where an additional exchanger was placed near to an existing one in parallel as shown in Fig 2.11. The retrofit procedure was conducted in three simultaneous steps:

1. Optimizing the first exchanger of each pair in the superstructure network (in terms of heat load) till the closest match to the existing exchangers is to be achieved in order to use the actual heat transfer coefficient.

2. Distributing the remaining heat load through the second exchanger in each pair to minimize the additional area.

3. Making full use of the available streams pressure drop where the new heat transfer coefficient is calculated.

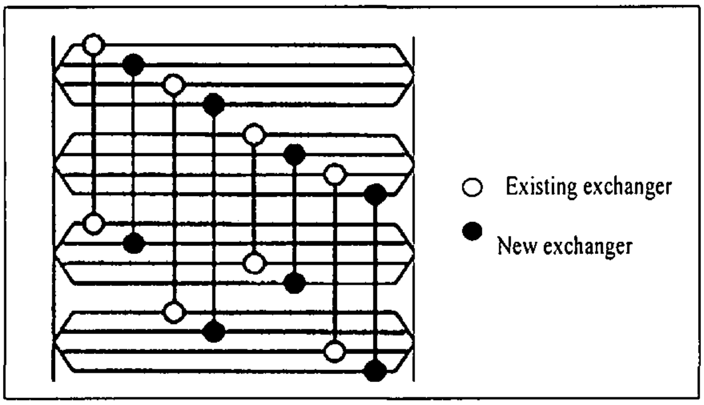

Fig 2.11: Spaghetti network (parallel arrangement)
(Marcone et al, Applied Thermal Engineering, 2000)

Nie and Zhu [59] have developed new correlations for considering the pressure drop in the HEN retrofit more rigorously as described in the following equations for the tube side and the shell side respectively.

$$\Delta P_T = K_{PT1}.A.h_T^{\ 3.5} + K_{PT2}.h_T^{\ 2.5} \tag{2.3}$$

$$\Delta P_S = K_{S1}.h_S^{2.86} + K_{S2}.A.h_S^{4.42} + K_{S3}.A.h_S^{4.69} \tag{2.4}$$

The constant parameters in the relationship depend on the fluids physical properties and exchanger geometrical data. They derived these correlations while developing a decomposition strategy for the HEN retrofit considering the pressure drop and the heat transfer enhancement. Initially, they developed a unit based model to identify which exchanger in the HEN required additional heat transfer area. Based on this model, several options were suggested for the required additional area for the designated unit(s) as shown below:

- Area distribution.
- Shell arrangement.
- Heat transfer enhancement.

These alternatives were optimized for the unit(s) of required additional area in the HEN. However, altering the arrangement of any unit in the HEN will affect the pressure drop for all the remaining units. Therefore, even the units with a zero additional area were modeled and optimized in a different way to accurately calculate the pressure drop. Eventually and as a result of their optimization, they came up with the most attractive option within the suggested alternatives to be the heat transfer enhancement for the HEN retrofit. In addition to reducing the additional area, the heat transfer enhancement reduces the required topology changes. A complete picture to describe the Nie and Zhu optimization approach is shown in Fig 2.12 below:

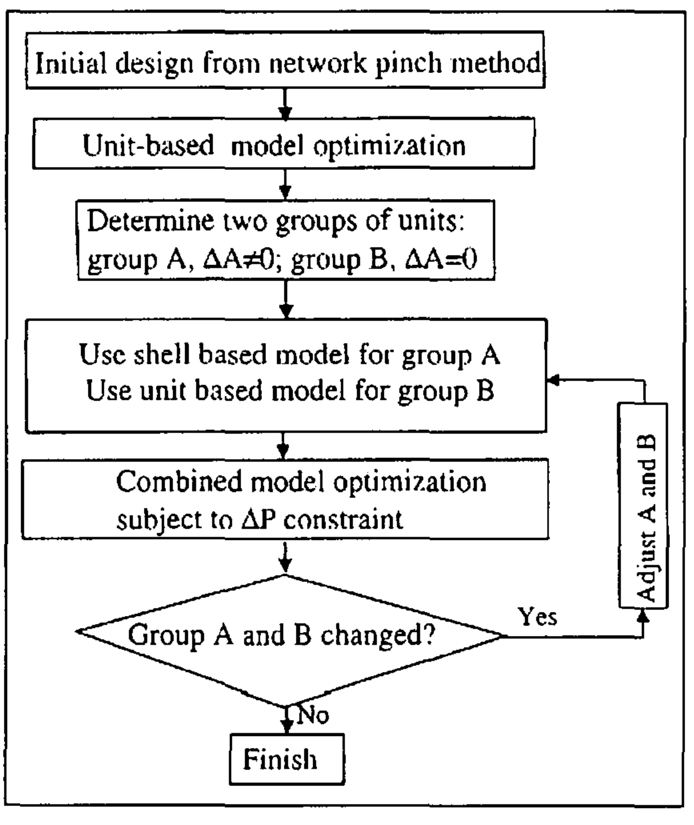

Fig 2.12: Nie and Zhu optimization procedure for the HEN retrofit
(Nie and Zhu, AIChE J, 1999)

The pressure drop optimization has been investigated for the grass root design of HENs by Panjeshah and Fallahi which later extended for the retrofit design [60], [61]. The same optimization approach has been extended recently by Panjeshahi and Tahouni [62] for HEN debottlenecking. Their concept was to study the association of pumps' and compressors' cost together with the required additional area and operational cost. The overall optimization was targeted at increasing the plant throughput.

2.3.2.4 Process conditions changes

The influence of temperature and flow rate variation was considered by Duran and Grossmann [63] when they introduced an optimization model for flow sheets in a process synthesis. Their main goal was to ensure minimum utility targets for the process HEN. Within their model, the pinch location was allowed to vary for each set of process flow rate and temperature. This procedure was later improved by Lang *et al* using an infeasible path optimization model to account for process changes in addition to maximum heat integration of process streams [64].

Samanta and Jobson [65] presented a heat integration model for the case of a variable process stream temperature and flow rate. It uses a disjunctive logic to quantify the feasible heat transfer between hot and cold streams in the HEN.

Kotjabasakis and Linnhoff [66] introduced the sensitivity table approach for the changeable operating conditions in the heat recovery system of the process plant. Their approach was to figure out which exchanger in the system of the HEN would be subjected to additional heat transfer area aiming at a sufficient flexible design. Consequently, optimal decision could be made based on the trade-off between the capital investment and the design flexibility.

The idea of adopting process changes with the HEN retrofit has been introduced by Zhang and Zhu [17]. They have developed a systematic method to investigate the impact of process temperatures and flow-rates changes while undertaking the HEN retrofit. Likewise the plus-minus principle, Zhang and Zhu have represented their insight in a *T-H* diagram to show how energy consumption reduces by managing the process conditions changes. The interaction between process changes and HEN retrofit was explored based on the retrofit model of topology modification which was proposed by Asante and Zhu [12]. Accordingly, their finding has revealed a significant cost savings. However, the streams' and exchangers' pressure drop have not been considered despite their great impact on the network units operation as well as operational cost especially when the stream's flow rate varies.

For improving HEN operability in the light of the changeable operating conditions of process streams, Aspen Technology [67] has presented an approach to assist in analyzing existing HEN. Using this approach, the design engineer could easily interfere during the process operation and maintenance. The developed approach has been illustrated and applied to an industrial case study of the HEN system for the crude pre-heat train.

2.3.2.5 Mathematical Programming for the HEN retrofit

Similar to the case of the Pinch design methods, the early mathematical programming methods developed for describing the HEN were started with the grass-root design [59]. The retrofit of the HEN that associates topological modifications was later conducted by improving these methods.

The first mathematical programming method for solving the problem of the retrofit projects was reported in 1989 by Ciric and Floudas where they proposed a two stage approach [39]. The first stage involved a match selection to determine the needed modification followed by a cost-wise optimization stage. The match selection stage was performed by a transshipment model as a mixed integer linear programme (MILP), while the optimization stage performed nonlinearly (NLP). The Optimization was mainly for exchanger order and flow configuration in the HEN within an affixed heat recovery level.

Later, Ciric and Floudas [40] united the two-stage approach into a single approach by formulating the HEN retrofit problem as a mixed integer nonlinear programme (MINLP) with the capability to optimize the overall HEN optimization.

Apart from the two-stage approach discussed above, Yee and Grossmann have introduced another two-stage approach for the HEN retrofit [41]. The first stage involved a prescreening step to determine a feasible heat recovery level in the HEN. Then some matches are chosen to be adapted for that heat recovery based on economical assessment. The second stage is mainly an optimization stage using an MINLP model where the suggested heat recovery level in the first stage is allowed to vary for selecting the best retrofit solution.

Soršak and Kravanja [68] developed a multi-type MINLP model for the HEN retrofit based on a HEN grass-root design model (step-wise superstructure MINLP optimization model) which was proposed by Yee and Grossmann [42]. According to the multi-type model, each exchanger in the superstructure approach was replaced by a new match comprising a double pipe (DP), shell and tube (ST), and plate and frame (PF) exchanger. A special model for each type of exchanger was formulated to make the approach operable and flexible.

For complex integrated chemical process systems, Jeżowski *et al* [69] introduced a new method for the heat recovery calculation. Their developed method aimed at extending the heat recovery calculation to cover complicated cases of multiple utilities with wide temperature spans and disturbed flow rates of HEN streams. The method ensures global optimality where it could be solved based on a linear optimization model based on the transshipment model of Papoulias and Grossmann [70].

2.3.2.6 Combined Pinch and Mathematical Techniques for HENs Retrofit

Tackling the heat recovery problem for complex systems could prove to be very slow using the Pinch Technology alone. Instead, integrating the useful insights provided by the Pinch Analysis with the Mathematical Programming techniques provides an attractive approach to solve the heat recovery problems. Thus, the complex calculations will be executed swiftly and the optimum solutions could be determined faster.

A systematic design and optimization method using the combined approach for HENs retrofit was proposed by Briones and Kokossis [44]. The targeting procedure of the Pinch Analysis was embedded within the Mathematical Programming models employed. Three steps were used in implementing the method. Area targeting was firstly addressed to select solutions which give minimum area and the least number of modifications to the existing HEN. Then the selected structural solutions were optimized using an MILP model. Both additional area and the recommended modifications for the existing HEN were optimized simultaneously. Eventually, the final network structure was optimized further to reduce the capital cost.

A systematic procedure that combined mathematical and thermodynamic insight of the Pinch Technology was also introduced by Asante and Zhu for industrial HENs retrofit [12]. Their approach was characterized by the involvement of a meaningful user interaction together with mathematical techniques. However, during the series of enhancements proposed for improving heat recovery, a pinching match ($\Delta T = 0^oC$) was encountered and this set the limit for improvement within the fixed topology. The required topology modifications were first identified before any further improvement. Several topology solutions were suggested based on such an approach and then optimized using an NLP model to produce the best solution.

2.3.3 Total site Analysis Approaches

The methodology for total site integration was first developed by Dhole and Linnhoff where the main target was to investigate the total site cogeneration potentials and further reducing the fuel and CO_2 emissions [71]. Recently, the method was extended by Bandyopadhyay *et al* for analyzing and estimating energy saving potentials among several processes [72]. They observed several opportunities for additional heat transfer aiming at further improving the integration between the processes. The approach is characterized to be simple and features a thorough energy balance for all the steam headers in the utility system. However, they revealed that the approach may not possibly lead to major energy savings. Accordingly, they proposed an overall economic evaluation and optimization of the approach for any particular project.

2.3.3.1 Top-down philosophy approach

For the total site system, a top-level analysis technique has been presented by Makwana [50] for energy retrofit and debottlenecking. The top-level-analysis begins with the analysis of the utility system first before analyzing the energy demand units such as the HEN in order to identify the best solution. In doing so, a target for the retrofit of HEN could be established. Using this technique, the interactions between the process heat exchanger networks (HENs) and the utility system could be analyzed. The utility system analysis might result in excess steam beyond the required amount which must be managed properly. The excess steam could be treated using one of these options:

1. Cutting down the fuel consumption in the boiler house which results in a power shortage and hence power import is required to replace the deficit.

2. Redistributing the excess steam in the utility system to increase the power generation, and this applies only for the sites of in-house power generation.

A trade-off between the above two options was made by Makwana where he suggested a graphical tool called the '*power efficiency curve*'. Beside the efficiencies of the current generated power in the utility system, this tool is useful to differentiate between the power import, and the power export options. For the case used by Makwana, the '*power efficiency curves*' is shown graphically in Fig 2.13. The curves could be used as a guide for HEN retrofit since they define the financial output associated with the operational changes in the utility system. Accordingly, two stages of the HEN retrofit have been carried out, i.e. retrofit that incorporates topology changes and that of only adapting the utility exchangers in case of switching the utility media from one steam level to another. By contrast to the top-level analysis, the bottom-up analysis begins with analyzing the site processes such as energy recovery in the HEN and then proceeds to investigate and manage the impact of energy savings on the steam flow in the utility system.

More recently, a combination of top-down and bottom-up approaches has been introduced by Muller *et al* [73] to analyze and manage energy saving opportunities in the food industry. They use the top-down analysis to correlate between the measured and actual energy consumption in order to set the appropriate energy saving actions. Meanwhile, they defined the consumer energy needs using the bottom-up analysis according to the thermodynamics of process operations.

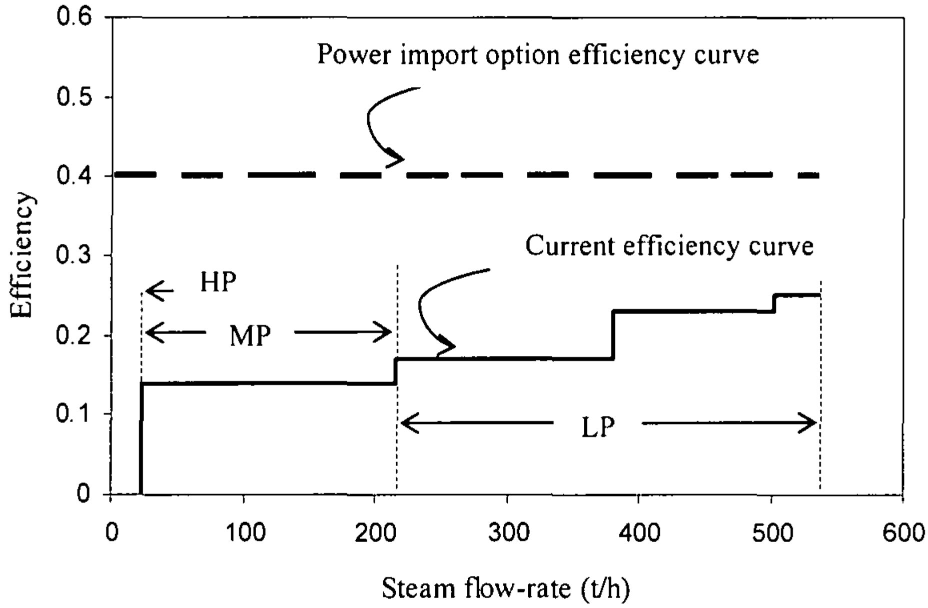

Fig 2.13: Power efficiency curves for the case used by *Makwana (Makwana et al, Computers Chemical Engineering, 1998)*

2.3.3.2 Utility System analysis

The utility network design and operation affects the overall efficiency of the process and the cogeneration potential of the plant. The design for such a system involves the selection of steam levels and the determination of suitable operating units. This basically requires a model for the operating units to convert the power potentials of the steam into a useful shaft work. Mavromatis and Kokossis [74], have introduced a turbine hardware model with procedures to analyze existing design options ahead of the detailed design. Their model was proposed to study the performance of the turbine efficiency as a function of turbine size, turbine load, and variable operating conditions. The essential feature of the model is the ability to set real targets for shaft work at the startup of the design stages.

Based on the targeting model discussed above, Mavromatis and Kokossis [75] have also proposed an optimization approach for the utility networks. The approach introduced a decomposition scheme for the utility system comprising simple and complex units. The approach principles are further exploited to set up a network superstructure where the units are developed to consider the operational variations. The optimization effort is simply facilitated by an MILP formulation.

Mavromatis and Kokossis [76-77], have also proposed a conceptual tool for industrial steam turbine networks to analyze and optimize the design and operation of the utility network. The tools termed as '*Hardware Composites*' which involves a graphical construction which is presented to provide optimum operation mode for the network. The *Hardware Composites* were also used as a road-map to select the best operation while process demands vary and further to evaluate and assess the utility network flexibility. Moreover, the *Hardware Composites* were used to manage the required maintenance with less disruption for the turbine network operation optimality.

The conceptual tool introduced in the form of *Hardware Composites* discussed above was later extended by Strouvalis *et al.* [78]. They utilized the tool to cover more realistic and complicated utility networks which involve multiple levels, friction losses, allocated turbines and letdown valves.

Later, a complete modeling and optimization of the utility system had been presented by Varbanov *et al* [79]. In their approach, new models for the steam and gas turbines were developed where they have studied the part load performance for these turbines. They also presented a top-level analysis of an industrial site utility system to determine the true value of steam savings based on the approach developed by Makwana [50]. Consequently they identified the required improvement for such case.

As an application approach for the utility system development, Hirata *et al* [80] have introduced a *Site-model* optimization tool to overcome the complexity problem of a utility supplier in Japan. The developed tool is a linear mathematical programming model that considered wide range information of the utility system which enables the model to be adapted for future development plans.

2.4 Summary

The state of the art works reviewed in this chapter mostly dealt with the approaches and methodologies developed in the last few decades to tackle the HENs retrofit problem for energy conservation in the process plant. It also highlighted the techniques used for energy management in the total site and utility system in particular. The HENs retrofit approaches and methods are generally incorporating topology changes in the HEN. Those approaches are summarized in the following points:

1. Pinch Technology approach for heat recovery which was first designated for the HEN grass-root design and further developed (with some drawbacks) to handle the retrofit design in 1986 by Tjoe[7].

2. Area Matrix approach represented by Shokoya [46] in 1992 to handle the drawbacks of the Pinch Technology for the HEN retrofit and debottlenecking. The area matrix has further developed to include pumping and maintenance cost by Carlsson [47] in 1993.

3. Methodologies based on the Path Analysis in the HEN such as those developed by Van Reisen *et al* [52] in 1995, Zhu and Asante [43] in 1999, Varbanov and Makwana [51] in 2000.

4. HENs Retrofit studies considering the constraints of the pressure drop in the HEN is first considered in 1990 by Polley *et al* [55]. A wide study considering the pressure drop was conducted by Panjeh-Shahi [57] in 1992 and then in 2000 by Marcone *et al* [58]. Also Gadalla [49] has considered the pressure drop in the retrofit study in 2003, and more recently Panjeshahi and Tahouni [62] for the HEN debottlenecking in 2008.

5. Retrofit studies dealing with process changes were introduced in 1986 by Duran and Grossmann [63], followed later by Lang *et al* [64] in 1988 and in 2001 by Samanta and Jobson [65]. In 1984 the Plus-Minus principle was first proposed by Linnhoff and Parker [15] for process modifications which had been carried forward later in 2000 by Zhang and Zhu [17].

6. Retrofit studies based on Mathematical Programming were conducted in 1989 and 1990 by Cirirc and Floudas [39], [40] and later in 1991 by Yee and Grossmann [41]. Recently, in 2004 Sorsak and Kravanja [68] presented an MINLP model for retrofitting HENs of different exchanger types.

7. A combination of the Pinch Technology and Mathematical Programming techniques had been presented in 1996 as an optimization method for the HEN retrofit by Briones and Kokossis [44]. Later in 1997, an automated and interactive approach was presented by Asante and Zhu [12] for the HEN retrofit.

8. For the total site improvement, integration methodologies were presented by Dhole and Linnhoff [71] in 1993. Makwana [50] had first introduced the top-down analysis for the total site improvement in 1997. A combination of top-down and bottom-up approaches had been presented in 2007 by Muller *et al* [73]. More recently in 2010, Bandyopadhyay *et al* [72] presented an approach to analyze energy saving potentials among several processes besides the utility system.

9. For the utility system of operational variation, Mavromatis and Kokossis [74-78, 81] developed models optimization methods in 1998. Later in 2004, Varbanov *et al*, also presented a utility system optimization which incorporated new models for the steam and gas turbines, and then a top-level analysis for the utility system [79, 82-83].

The drawbacks of the previous works conducted for the HENs retrofit could be concluded in the following points:

- The topological changes for the HEN retrofit have been considered by most of the researchers require additional space (platform) in the plant which might be available or/and restricted for safety consideration. Moreover, the topological changes always associated with civil work which has not been mentioned in the previous works.

- The HEN retrofit techniques which based on the Pinch Technology do not automatically generate retrofit options in a wider range either with or without topology changes. On the other hand, the techniques of Mathematical Programming are rather complicated which require a comprehensive mathematical and computational knowledge.

- Only few works have addressed the operational changes towards improving the process-to-process heat recovery. However, they did not use a specific procedure to handle the operational changes systematically.
- The HEN retrofit was considered as a standalone problem and the interaction between the HEN and the utility system was not considerably highlighted.

CHAPTER 3

DEVELOPMENT OF PATHS COMBINATION APPROACH FOR HEN RETROFIT

The Pinch Technology [10], considered the utility paths in the HEN as a useful tool to increase the heat recovery between hot and cold streams during the optimization stage of the HEN design. Accordingly, the utility consumption in an existing HEN could be decreased even without changing the topology of the network. Based on the understanding of HEN optimization using utility paths, the method of developing the *Paths Combination Approach* as a backbone of the thesis is comprehensively described in this chapter. The method is typically a combinatorial procedure to combine the available utility paths in the HEN systematically for generating several options to shift the heat load from the HEN utilities. The approach aims at screening wider alternatives for enhancing the process-to-process heat recovery while maintaining the HEN topology and considering the constraints, but at the expense of adding new heat transfer area. Within the approach, a trade-off between the capital investment and energy savings is established to economically assess and select the best retrofit option(s). Based on the plus/minus principle [15, 17], a proposed concept of streams' *Temperature Flexibility* in the HEN is also described to be integrated with the *Paths' Combination Approach* to allow for further heat recovery. An appropriate case study from the literature with detailed information is introduced to demonstrate and clarify the overall approach.

In view of the significant iterations required in the calculation involving various potential options, the entire method is implemented on a developed computer programme based on a Neatbeans platform created as a user-friendly JAVA interface. To demonstrate the data input and output procedure, the overall programming interface is presented in appendix A.

3.1 Heat recovery Pinch

While this study is focusing on enhancing the heat recovery, more details regarding the process heat recovery pinch should be clarified. Raskavic and Stoiljkovic [19] have clearly explained the concept of the Pinch Technology for the process heat recovery as stated below:

Within the scope of heat recovery, the Pinch Technology is an interactive and quantitative method that belongs to the group of thermodynamic methods of process integration. It is mainly based on the first law of thermodynamics (in terms of energy conservation constraints), and the second law of thermodynamics (in terms of positive temperature difference between the hot streams and the cold streams).

The concepts of the Pinch Technology for the HEN could be explained by considering a simple heat exchange as earlier shown in Fig 2.2 where the change of thermodynamic parameters of hot and cold streams passes through the exchanger(s). To verify the minimum external utility duties required for the entire system, a temperature versus enthalpy plot called a *pinch diagram* provides the outlines for the creation of a feasible heat-exchange network as shown in Fig 3.1 below:

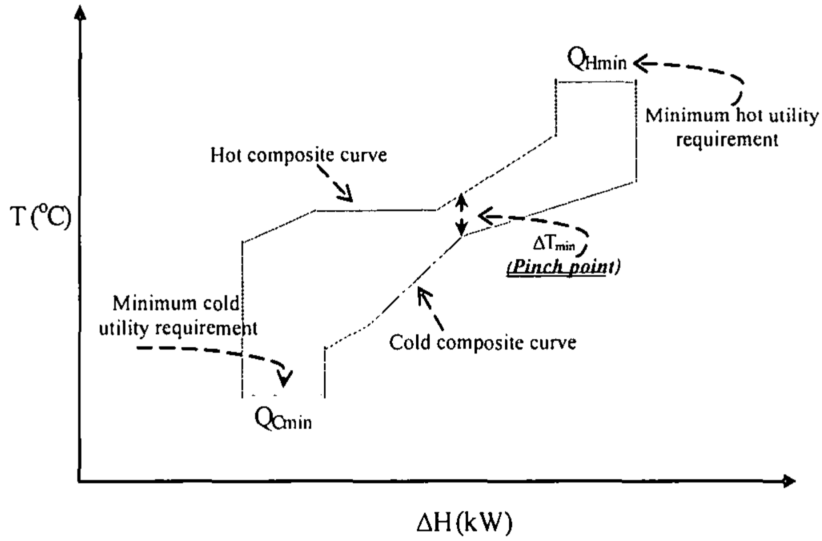

Fig 3.1: Heat recovery pinch diagram (composite curves)

Such a diagram and as detailed in the user guide of process integration [10], is primarily constructed by combining the process hot streams together for creating the Hot Composite Curve (HCC); and the cold ones for creating the Cold Composite Curve (CCC). Hot and cold composite curves are plotted together in a temperature-enthalpy axis to produce the so called pinch diagram. The HCC and CCC are adjusted according to the hot and cold utility targets or to a given minimum heat transfer driving force between the two curves. This driving force is termed as ΔT_{min} which represents the pinch point for heat recovery. Recalling, the number of pinches might be more than one. Two different approach temperatures are used in the terminology of the Pinch Technology; namely:

- Heat Recovery Approach Temperature (HRAT), which is defined as the smallest vertical distance (temperature difference) between HCC and CCC.
- Exchanger Minimum Approach Temperature (EMAT), which is defined as the minimum allowable temperature difference for the individual heat exchangers.

In this study, the minimum approach temperature, ΔT_{min}, is related to the HRAT and sometimes called ΔT_{small}.

For instance, given the value of ΔT_{min}, the size of the overlapping zone between the HCC and the CCC in the pinch diagram represents the process-to-process heat recovery where the cost of the exchange area is the capital to be invested. The non-overlapping zone should be supplemented by the minimum external heating duties (Q_{HUmin}) above the pinch point, and the minimum external cooling duties (Q_{CUmin}) below the pinch point [28]. The cost of the external heating and cooling represents the operating cost of the HEN.

Moving the HCC and CCC vertically towards each other by $\Delta T_{min}/2$, the pinch diagram comes to a position called shifted position (presented by the dashed line in Fig 3.2a). In the shifted position, the composite curves touch each other in a point called the 'Thermal Pinch Point'. Another graphical tool in the Pinch Technology is created by using the enthalpy horizontal differences based on the shifted composite curves (HCC and CCC). This graphical tool is termed as the 'Grand Composite Curve

(GCC)' [10] as shown in Fig 3.2b. The GCC allows the selection of appropriate utilities.

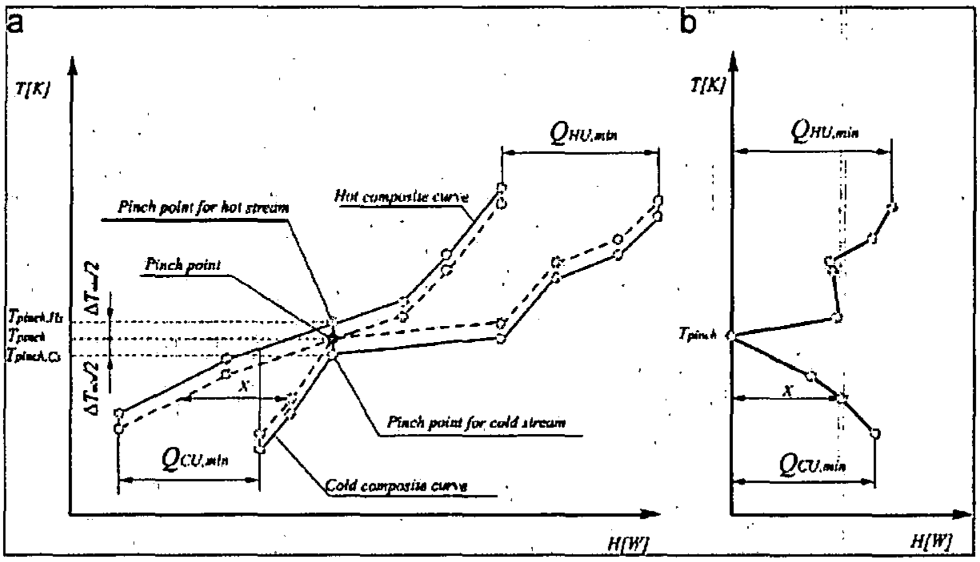

Fig 3.2:Pinch diagram and grand composite curve
(Source: Rašković and Stoiljković, 2009)

3.1.1 Overall Pinch Technology steps for the HEN design

The grass-root design of the HEN using the Pinch Technology is to be achieved through four steps starting with data extraction going through targeting and design stages and finally the optimization step. These steps are described as follows:

3.1.1.1 Data extraction phase

Data extraction is a very essential stage in the Pinch Technology for either a new design or a retrofit design of the HEN. The process streams and utilities should be well identified from the plant flow sheeting with all required physical properties and thermodynamic data. Misunderstanding or inappropriate data extraction typically leads to upsetting the overall mass and energy balances and consequently miss-identifying the energy saving opportunities.

3.1.1.2 Targeting phase

After extracting the required data, a target must be set prior to the design stage of the HEN. It is possible to identify targets for minimum utility usage, minimum number of exchangers in the HEN, and minimum heat exchange area. This stage is very crucial to specify the optimum level of process to process heat recovery. This level is determined by choosing an optimum value for ΔT_{min} based on the trade-off (balancing) between operating and capital costs.

3.1.1.3 Design phase

In this stage an initial HEN is constructed to meet the above defined targets. The design starts at the most constrained point which is the pinch point where ΔT_{min} is located, and then carried out below and above the pinch separately. Exchangers are placed between the streams while following the constraints of ΔT_{min} to be the minimum approach temperature. Energy balance between hot and cold streams should also be met (stream splitting might be imposed). Exchangers' placing continues until the target temperatures of each stream are met where possible otherwise, utility exchangers are to be placed to overcome the shortage of process to process heat recovery.

3.1.1.4 Optimization stage

This stage is aimed at achieving more cost effective HEN. The initial design of the previous stage is simplified an improved further using the so-called heat load loops, heat load paths and stream splitting. By doing so, the number of exchangers in the network is reduced to the minimum where the heat shifting using loops and paths reveals some inappropriate exchangers that should be removed (exposing negligible area). However, the practical temperature approach between the hot streams and cold streams must be assured.

According to Raskavic and Stoiljkovic [19], The Pinch Technology steps for the HEN design are summarized graphically as shown in Fig 3.3

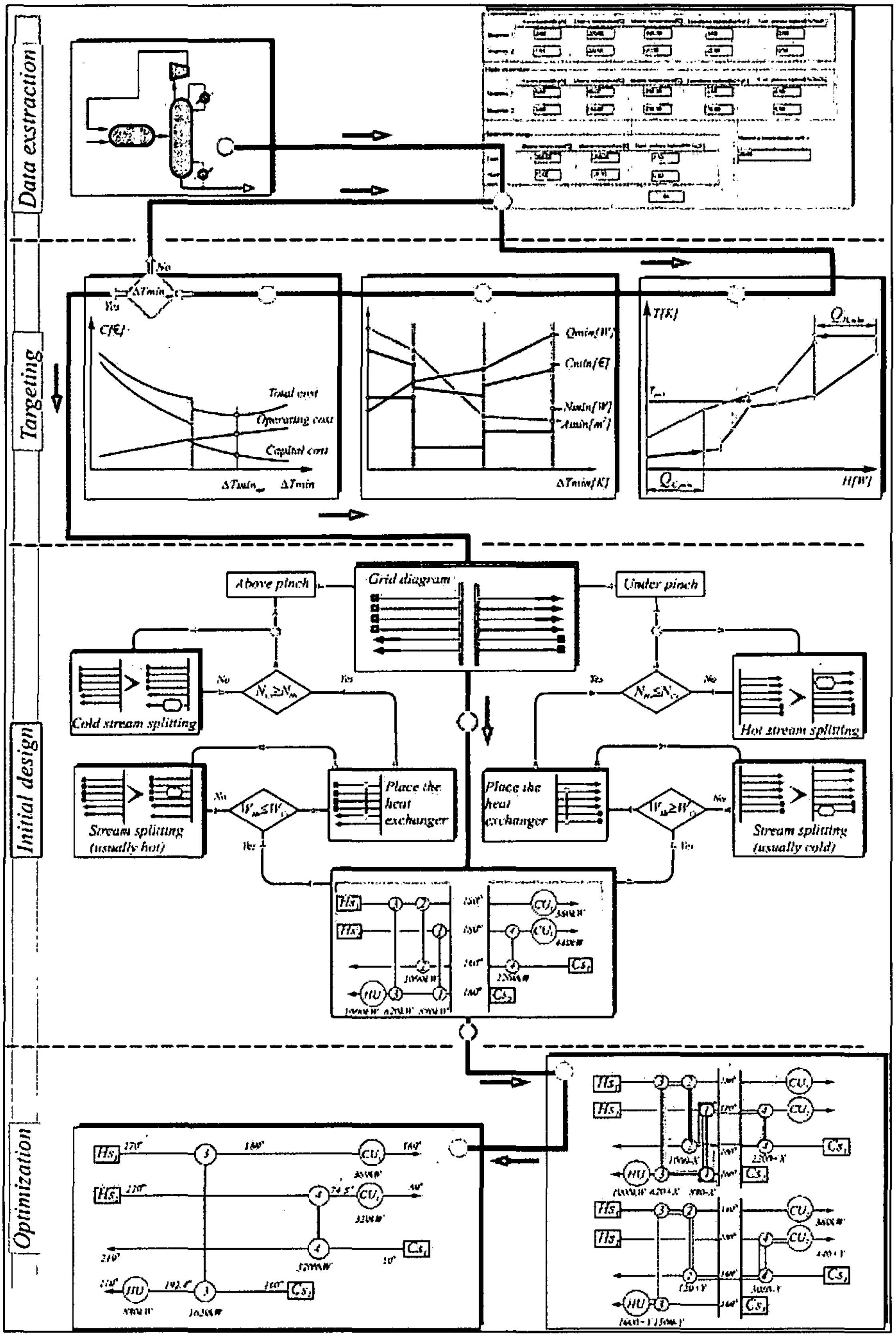

Fig 3.3: Flowchart of Pinch technology stages for HEN design
(Source: Rašković and Stoiljković, 2009)

3.2 Heat recovery enhancement in HENs using utility paths

The utility path in the HEN is defined as a connection between heater(s) and cooler(s) through definite match(es) in the HEN as stated by Shenoy [20]. A certain amount of heat load could be shifted along this path from the heat source and the heat sink within the HEN system while increasing the heat recovery. Using this path, if certain amount of heat load (x) is to be subtracted from the cooler (C) and the heater (H) in the HEN; it must be added and subtracted alternatively to and from the exchangers (E) lying on the path. Fig 3.4 explained this concept more obviously.

Later, Smith [25] added on to the path definition by allowing the load to be shifted even from a hot utility to another hot utility as shown in Fig 3.5., and likewise for the cooling utility.

Loops and paths are well established concepts used during optimizing a newly designed HEN for energy savings as well as unit reduction [25]. However, a minimum practical temperature difference must be maintained for individual matches in the HEN while undergoing the heat shifting. This understanding could be followed for the HEN retrofit to enhance the process-to-process heat recovery either with or without topological changes.

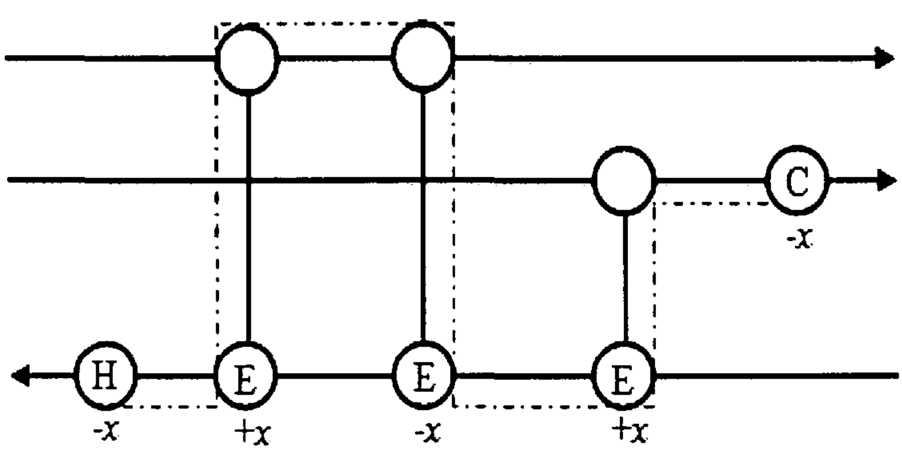

Fig 3.4: Utility path to shift heat load between heater and cooler in the HEN

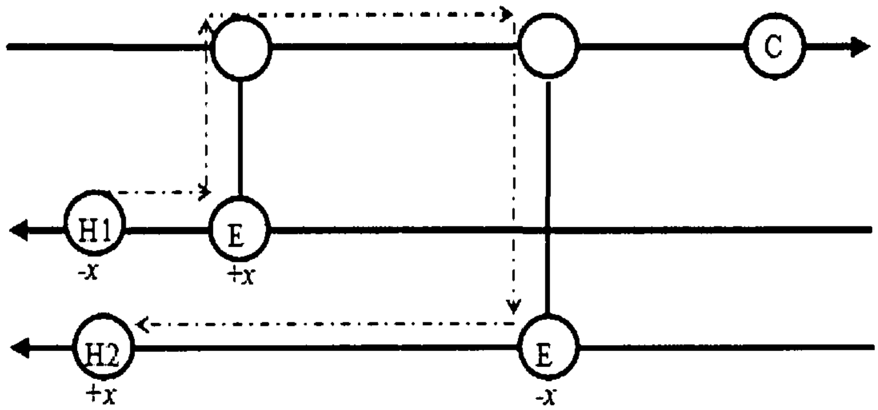

Fig 3.5: Utility path to shift heat load between two heaters in the HEN

The increase in heat load shifting through the utility path will lead to a Network Pinch taking place at some matches within the HEN where ΔT is reduced to a smaller value which finally limits the heat transfer between the heat exchange streams. The Network Pinch could be relaxed by performing topology modifications as shown by Asante and Zhu [45]. However, the Network Pinch could be avoided by maintaining a minimum practical temperature difference for the individual matches in the HEN while performing the heat load shifting. It has been shown that ΔT_{min} will no longer be a constraint to limit the heat recovery while optimizing the HEN using loops and paths [25]. However, impractical temperature driving force for individual exchangers must be avoided. Therefore, in this work the existing HRAT is maintained instead of ΔT_{min} to ensure heat transfer between the exchange streams is feasible. Meanwhile, the HRAT also becomes the constraint parameter which limits the extent of heat load shifting along the utility path in the HEN. However, HRAT could also be varied within the practical values as an optimization parameter.

3.2.1 Energy savings while maintaining the basic HEN structure

According to Zhu and Asante [43], increasing the heat recovery in a HEN could be achieved by the addition of surface area to some exchangers in the existing network without altering the HEN topology. This is possible through the exploitation of the available HEN utility paths to shift the heat load from the utility exchangers to the existing process to process exchangers. However, the heat recovery is limited to a certain amount beyond which any further addition of area will not improve heat recovery. It is obvious that there is a heat recovery limit within the HEN topology and it is independent of the area of individual exchangers in the network. It has been shown by Asante and Zhu [12] that every HEN structure has a maximum heat recovery limit and is considered as a characteristic of the network structure. This limit is caused by what is called 'pinch match' which is discussed in the following section.

3.2.1.1 Pinch matches and the Network Pinch

The pinching match point is called a Network Pinch which was first highlighted by Asante and Zhu [12], [45]. A pinching match in the HEN is defined as an exchanger match of a temperature approach that unavoidably tends towards small value which is a limit for further heat recovery in the HEN. The limitation is caused by the Exchanger Minimum Approach Temperature (EMAT) of the pinching matches which decreases as the heat recovery increases. Consequently, the area required by these pinch matches increases exponentially. Clear representation of this concept is shown by a grid diagram of a simple HEN and its corresponding process composite curves before and after undergoing maximum heat recovery as shown in Fig 3.6.

From the above discussion, the Network Pinch is considered to be a very important characteristic of HEN structures since it identifies the heat recovery bottleneck and also affects the area requirement of the network. As with the process pinch, the network pinch divides the HEN into a heat deficient (heat sink) and a heat surplus (heat source). However, the network pinch is a characteristic of both the process streams and the HEN structure, where the process pinch is a characteristic of the process streams alone.

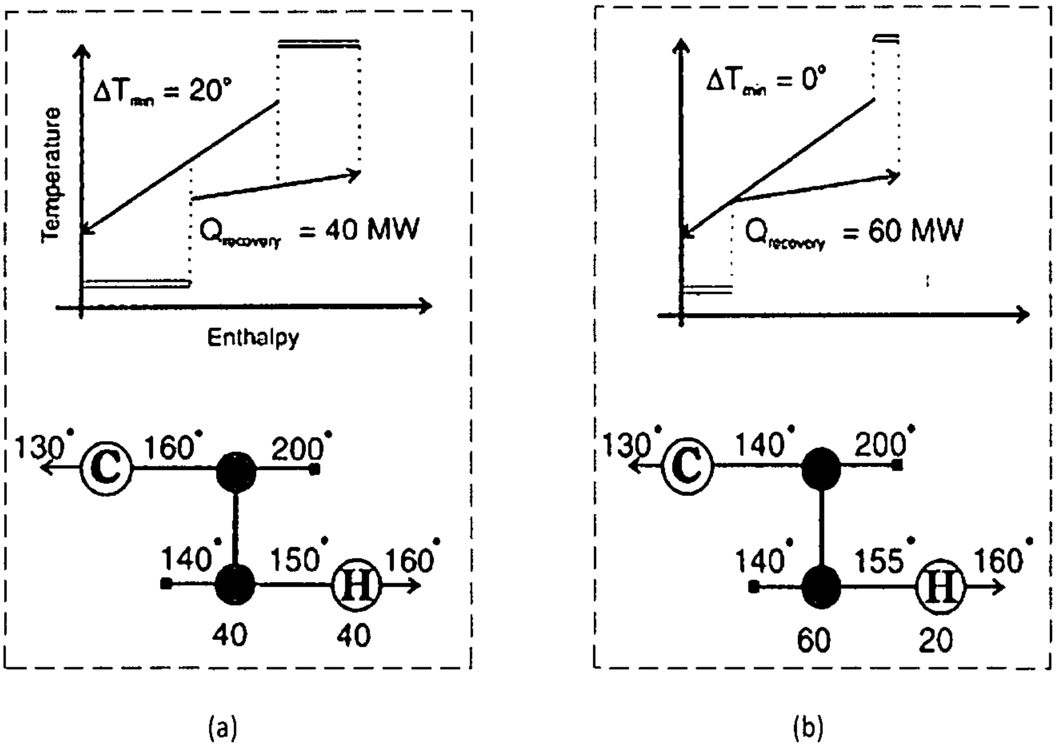

Fig 3.6: Representation of the Network Pinch
(a) Original HEN performance, (b) Maximum heat recovery

Asante and Zhu [12] have suggested three ways of topology modifications in order to overcome the Network Pinch. These include re-sequencing, adding new matches and splitting the stream. Therefore, the performance of the existing HEN could improve beyond that for the pinched condition.

- *Re-sequencing:*

It simply means moving the pinching match exchanger to a new location in the HEN within the same hot and cold streams. The utility path is then utilized to its limit to adjust and reduce the utility consumption for the network. Fig 3.7 illustrates the proposed re-sequencing.

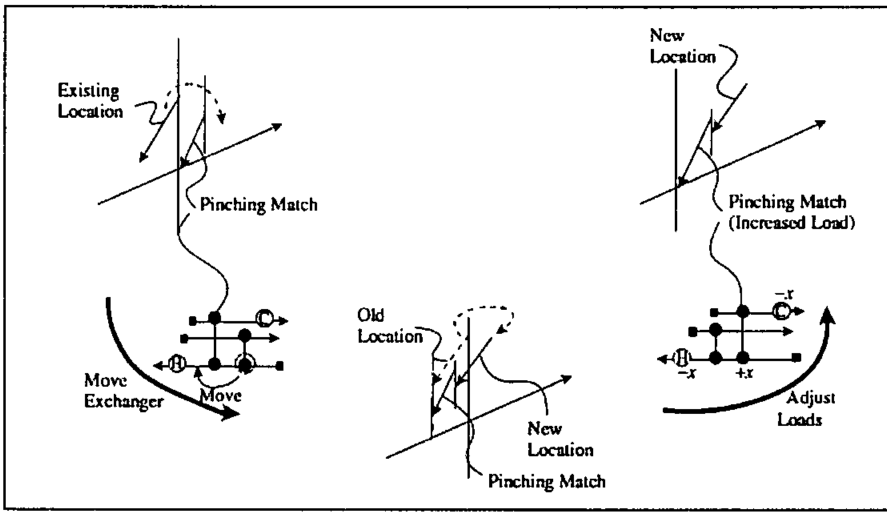

Fig 3.7: Overcoming the Network Pinch by exchanger re-sequencing

- *Inserting new exchanger:*

The position of the pinching match could be changed to be no longer pinching by decreasing the heat load of the hot stream adjacent to such a match. This is possible if a new match is inserted to replace the suggested reduction of heat load as shown in Fig 3.8. Again, a new scope of reducing the utility consumption is provided using the utility path by shifting the heat load until the network is again pinched.

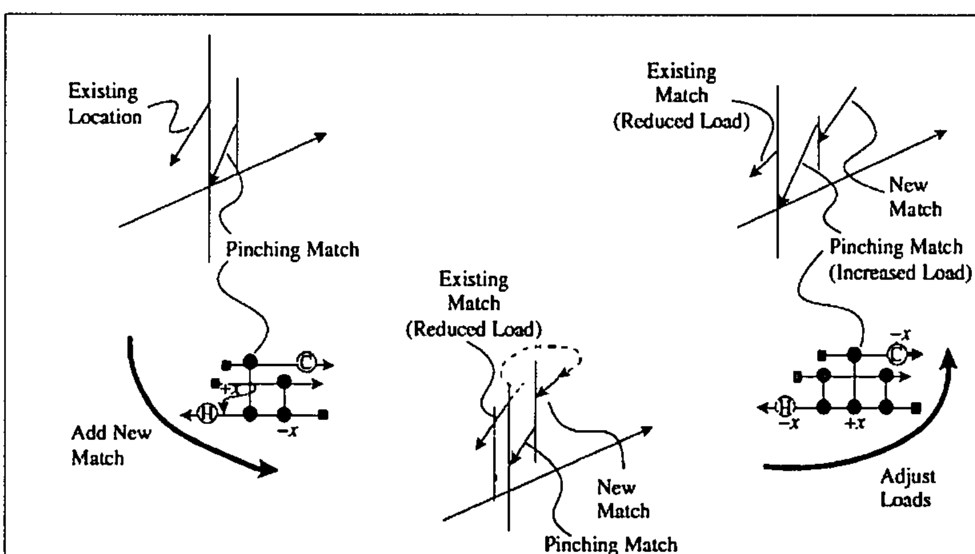

Fig 3.8: Overcoming the Network Pinch by inserting new exchanger

- *Stream splitting*

In the case where two matches are simultaneously pinched, stream splitting would be the smart solution as shown in Fig 3.9. By doing so one of the pinching matches would no longer be pinched. This provides a scope for further reducing the utility consumption using the utility path.

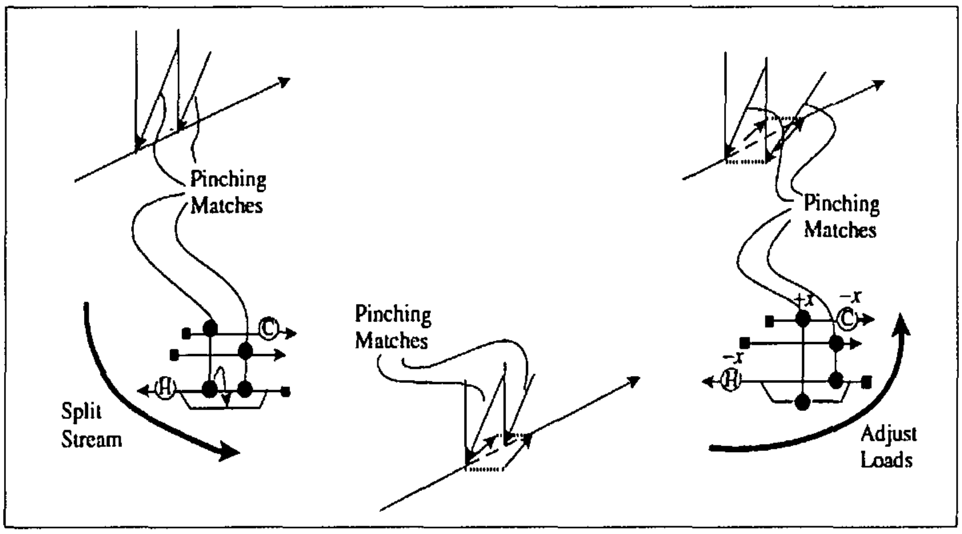

Fig 3.9: Overcoming the Network Pinch by stream splitting

3.2.2 Pressure drop and fluid velocity consideration in the HEN retrofit

The core objective of the HEN retrofit is to obtain a cost-effective heat recovery network that is capable of following the design and operation constraints. It has been mentioned that the HEN retrofit is a very complicated project compared to the new design of the HEN since the existing structure is to be maintained. Moreover, it becomes more complicated when extra care is to be taken for the pressure drop of streams and individual matches in the HEN. Therefore, more understanding is needed to handle all the flow system variables that affect the pressure drop.

The exchangers' pressure drop and streams' fluid velocity are both considered as constraints to be addressed for either the grass-root or retrofit design of the HEN. It is given that increasing the heat recovery within the HEN would typically increase the heat transfer area of the existing exchangers and thus affect the pressure drop of the system. As discussed by Polley *et al* [55], exchanger area (A), exchanger pressure drop (ΔP), and heat transfer coefficients (h) affect each other and can be correlated as described generally by the following equation:

$$\Delta P = K.A.h^{n} \qquad (3.1)$$

The streams' fluid velocity is embedded in the pressure drop correlation; where upper and lower limits must not be violated to avoid exchanger damage and fouling deposits.

As stated in the literature, pressure drop and heat transfer rate are independent parameters that affect the capital and operational cost of any heat exchanger network. In particular, the shell and tube heat transfer coefficients of the exchanger are independent variables and they are functions of pressure drop, fluid velocity and the heat transfer area (with all geometrical parameters). In the current study, the higher and lower limit of the fluid velocity are set in accordance to the guideline provided by Vieira *et al* [84] . For oily fluids it must be ranged between (1.0 - 4.0) m/s in the tube side and (0.3 - 1.0) m/s in the shell side. Violating the maximum limit of stream fluid velocity could potentially lead to damaging the heat exchanger tubes and/or shell. Whereas, fouling starts below the lower limit of such velocity. Indeed, fouling will decrease the heat transfer where it acts as a lagging material. Therefore, energy demand will increase as a result of more energy loss. Therefore, the pressure drop and streams' fluid velocities of the existing exchangers in the HEN have to be considered when calculating the heat transfer coefficients. Ignoring the pressure drop in the HEN retrofit will lead to an inoperable network as the hydraulic aspects are neglected, especially on the pumping requirement. The heat transfer coefficients are mainly calculated using equations (3.8) and (3.9) presented in section 3.4). These equations are representing the pressure drop correlations for the tube and shell side, respectively. In the current retrofit work, consideration is given to the fluid velocity in the streams through the pressure drop correlations since they are affecting each other.

3.3 Combinatorial method for utility paths' combination

The key concept for developing paths' combinations is to generate a wide range of energy savings retrofit options for an existing HEN. These options are mainly sets of combined utility paths in an existing HEN. Simply, the available utility paths in the HEN are combined using the combination law given in equation (3.2) [85]. The results of this combination are only to describe the different ways by which the utility paths could be grouped together. As mentioned previously, a single utility path could be used to shift the heat load from the HEN utilities while increasing the heat recovery within the HEN. The current method describes the idea of using combined utility paths instead of using a single utility path to shift as maximum a heat load as possible from the HEN utilities successively.

$$C(n,r) = \frac{n!}{(n-r)! \cdot r!} \tag{3.2}$$

- n, r: are non negative integers and ($r \leq n$).

For n number of paths in the HEN, several sets of combined paths could be generated in addition to the single paths. According to the combination law, if 6 paths (A, B, C, D, E, and F) are available in the existing HEN, the numbers of possible combined paths to be generated are detailed in Table 3.1.

Table 3.1: Simple demonstration for combining the available utility paths in the HEN

No. of combined paths	Combination procedure	Result of combination	Sets of combined paths
1	$C(6,1) = \frac{6!}{(6-1)! \cdot 1!}$	6 individual paths	A, B, C, D, E, F
2	$C(6,2) = \frac{6!}{(6-2)! \cdot 2!}$	15 sets of 2 combined paths	AB, AC, AD, AE, AF, BC, BD, BE, BF, CD, CE, CF, DE, DF, EF
3	$C(6,3) = \frac{6!}{(6-3)! \cdot 3!}$	20 sets of 3 combined paths	ABC, ABD, ABE, ABF, ACD, ACE, ACF, ADE, ADF, AEF, BCD, BCE, BCF, BDE, BDF, BEF, CDE, CDF, CEF, DEF
4	$C(6,4) = \frac{6!}{(6-4)! \cdot 4!}$	15 sets of 4 combined paths	ABCD, ABCE, ABCF, ABDE, ABDF, ABEF, ACDE, ACDF, ACEF, ADEF, BCDE, BCDF, BCEF, BDEF, CDEF
5	$C(6,5) = \frac{6!}{(6-5)! \cdot 5!}$	6 sets of 5 combined paths	ABCDE, ABCDF, ABCEF, ABDEF, ACDEF, BCDEF
6	$C(6,6) = \frac{6!}{(6-6)! \cdot 6!}$	1 set of 6 combined paths	ABCDEF

The summation of all the sets gives the entire options that could be considered as retrofit solutions. Therefore an equation for calculating the number of possible paths' combinations to give the retrofit options can be represented as below:

$$retrofit_{options} = \sum_{r=1}^{r=n} C(n,r) \qquad (3.3)$$

However, not all these options are feasible due to the HRAT limitation while undergoing the heat load shifting.

After the heat load shifting is done using sets of combined paths, all the generated options are then subjected to economical evaluation in order to choose the most optimum solution(s). The economic criterion is based on the amount of energy savings gained against the capital cost to be invested for increasing the heat recovery where the optimum should have a high savings and short payback period.

3.3.1 Process Condition Changes for HENs Retrofit

It is a common practice to consider process conditions as fixed parameters before the HEN is retrofitted. Nonetheless, strong interactions exist between HENs and processes. Therefore, the HEN retrofit should be considered simultaneously with process condition changes (flow rates and temperatures).

In addition to the pressure drop, the HEN retrofit would be more difficult when the operating conditions vary. Therefore, a wide knowledge of the HEN complexities would be needed for tackling the retrofit problem. In the past, most of the researches conducted under the grass-root or retrofit approach for the HEN design were constrained by fixed specified process conditions. However, process conditions are known to change such as under seasonal variation or after process modifications. It has been reported by Tjoe *et al* [37] and Floudas *et al* [86], that fixing stream conditions for the HEN while undertaking the retrofit might lead to topology changes in order to avoid excessive additional area.

In the light of the above discussion, sensible process changes should be taken positively as a means to reduce the utilities consumption in the HEN and hence increase the plant energy efficiency [87].

3.3.2 The plus-minus principle

According to the Pinch Technology approach for the HEN design, the composite curves determine the minimum energy requirements based on the mass and energy balance for a definite process. However, such energy requirements could be further reduced by changing and maneuvering the mass and energy balance of the process. It is possible to identify changes in an appropriate process parameter that would have a favorable impact on energy consumption together with applying the thermodynamic rules of the Pinch Technology. The concept of playing with process parameters called the plus-minus principle described by the Pinch Technology [88] which was first introduced by Linhoff and Parker[15].

From the Pinch Technology, the plus-minus principle has been assigned for process modifications and provides the design engineer with a definite reference for any adjustment to the process heat duties. Accordingly, it indicates which modification would be beneficial and which would be harmful.

Changing the heat and mass balance would imply changes in the composite curves of the HEN as shown in Fig 3.10. It is obvious that the process energy targets have been directly affected when altering the process parameters. From the figure, the plus-minus principles could be summarized in the following points:

- *Above the pinch point*

Increasing the hot stream(s) duty above the pinch and/or decreasing the cold stream(s) duty above the pinch would result in reducing the hot utility target.

- *Below the pinch point*

Decreasing the hot stream(s) duty below the pinch and/or increasing the cold stream(s) duty below the pinch would result in reducing the cold utility target.

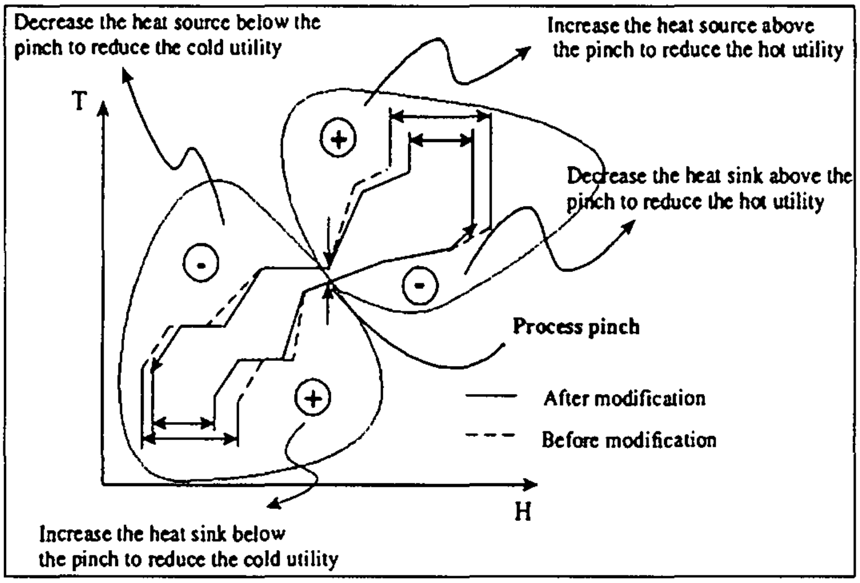

Fig 3.10: Demonstrating the plus-minus principle

Referring to the Pinch Technology approach [88], it is even possible to change temperatures rather than heat duties as shown in Fig 3.10 above so as to further reduce the heating and cooling duties. Therefore, the plus-minus principle ought to be beneficial to increase the temperature of hot streams and/or reducing the temperature of cold streams which make it easier to extract heat from them. Changing the temperature of streams in this manner would improve the driving forces in the HEN while at the same time decrease the energy targets of the process.

3.3.3 Streams' temperature flexibility in the HEN

From a practical point of view, process conditions are known to change to a certain extent for most processes. In accordance with this understanding, the plus-minus principle [15] was presented as discussed above. Later, Zhang and Zhu [17], adopted the process changes in the HEN retrofit. Based on these two ideas, the process streams temperature variation is adopted and integrated with the developed path combination approach to further enhance the heat recovery within the HEN system in this work.

Given the situation where process stream temperature could undergo slight changes, the pinch point (corresponding to the HRAT) could actually be relaxed within a certain temperature limit beyond its original value using the streams' temperature flexibility (TF) as shown in Fig 3.11. Proper maneuvering of such an effect within the HEN could result in better heat recovery as demonstrated previously by the plus-minus principle. Therefore, sensible process changes could be taken positively as a means to reduce utilities consumption and hence increase the plant energy efficiency as stated in the review given by Zhu and Vaideeswaran [87].

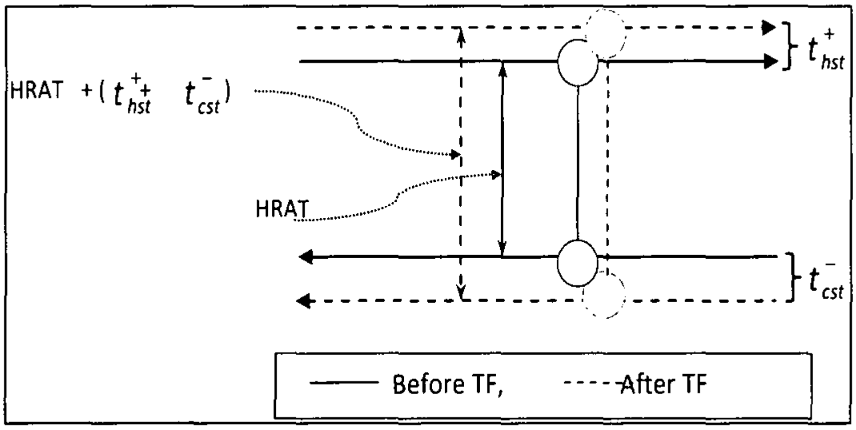

Fig 3.11: Grid representation for applying TF concept

According to the paths' combination approach, the selection of optimal solution(s) depends on how cost-effective the retrofit option would be for the studied HEN. This assessment is governed by the investment/savings ratio to determine the payback period. In addition to providing good retrofit solutions, the approach is also capable of indicating retrofit solutions that show poor economic standing but have potential to be improved further. These solutions could be improved through creating further energy saving opportunities (where applicable) which might shorten the payback period. Such saving opportunities could be achieved by relaxing the HRAT beyond the current value. The HRAT could be relaxed by making the hot streams of the HEN a bit hotter and the cold ones a bit colder according to the available temperature flexibility while keeping the utility requirements unchanged as shown in Fig 3.12 (a). Consequently, more heat load could be shifted from the HEN utilities using the paths combination approach until the HRAT is again restored to its original value as illustrated in Fig 3.12 (b). Simply adding (t^+_{hst}) °C to hot streams and/or subtracting (t^-_{cst}) °C from cold ones would result in increasing the HRAT beyond the current value. The range of the temperature added to the HRAT value is termed as the 'temperature flexibility range' which is represented by equation (3.4) below:

$$t_{hst}^{+} + t_{cst}^{-} = TF_{range} \quad (3.4)$$

For a given maximum value of (t_{hst}^{+}) and (t_{cst}^{-}), all the possible TF ranges could be identified and arranged in a simple matrix "R" of i rows and j columns. The matrix will display all the possible TF ranges that resulted from equation (3.4) above. The entries of this matrix "r_{ij}", which correspond to the TF ranges, could be determined as follows:

$$\forall \quad i,j \in \{0,1,2,3,\ldots n\},$$

$$r_{ij} = i + j \quad (3.5)$$

Therefore, if the maximum allowable (t_{hst}^{+}) and (t_{cst}^{-}) is 5°C, then the TF ranges could be represented by the following square matrix:

$$R = \begin{bmatrix} 0 & 1 & 2 & 3 & 4 & 5 \\ 1 & 2 & 3 & 4 & 5 & 6 \\ 2 & 3 & 4 & 5 & 6 & 7 \\ 3 & 4 & 5 & 6 & 7 & 8 \\ 4 & 5 & 6 & 7 & 8 & 9 \\ 5 & 6 & 7 & 8 & 9 & 10 \end{bmatrix}$$

The repeated values of the TF ranges appearing in the matrix (indicated by the diagonal arrows) would have similar energy savings in the HEN since the same value is to be added to the HRAT. However, each of the values has been obtained from different combinations of (t_{hst}^{+}) and (t_{cst}^{-}) as illustrated in the mirror representation shown in Table 3.2. Accordingly, this provides a degree of freedom for expanding the HRAT value in different manners; i.e. based on the extent of flexibility for the hot and cold streams to increase and/or decrease their temperature.

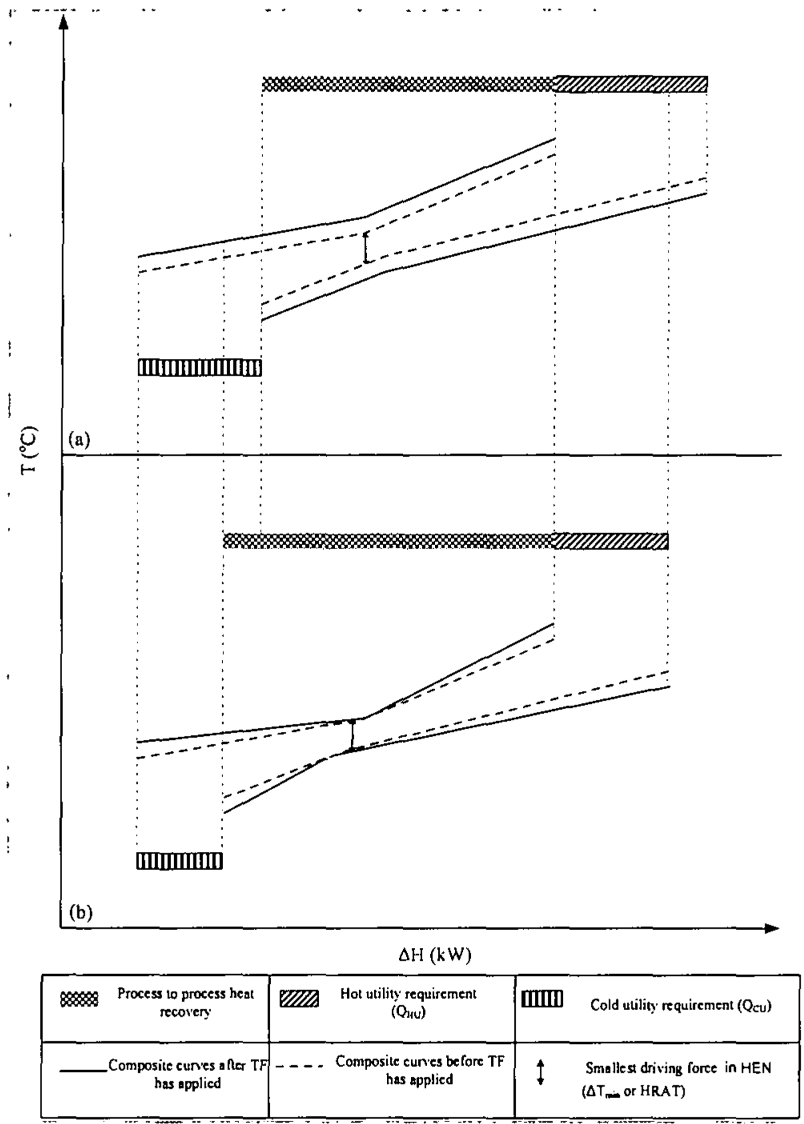

Fig 3.12: Representation for the composite curves when applying the TF concept
(a) Before shifting the heat load, (b) After shifting the heat load

For further explanation, let's suppose the TF range value of 2°C is selected from the matrix above. It shows that the value is repeated three times, and the three possible combinations for the hot and/or cold temperature changes that could lead to the TF range value being attained are;

1. Adding 2°C to the hot streams while maintaining the cold ones,
2. Adding and subtracting 1°C to and from hot and cold streams, respectively,
3. Subtracting 2°C from cold streams while maintaining the hot ones.

The entire situation of the TF concept and the way to be applied for both hot and cold streams in the HEN could be explained in more details in Table 3.2.

Table 3.2: Mirror representation of TF ranges

TF range (°C) *(Added to the HRAT)*	*0*	*1*	*2*	*3*	*4*	*5*	*6*	*7*	*8*	*9*	*10*
t^{+}_{hst} (°C) *(Added to hot streams)*	0	1 0	2 1 0	3 2 1 0	4 3 2 1 0	5 4 3 2 1 0	5 4 3 2 1	5 4 3 2	5 4 3	5 4	5
t^{-}_{cst} (°C) *(Subtracted from cold streams)*	0	0 1	0 1 2	0 1 2 3	0 1 2 3 4	0 1 2 3 4 5	1 2 3 4 5	2 3 4 5	3 4 5	4 5	5

3.4 Overall approach description

The application of the proposed *Path Combinations Approach* with Temperature Flexibility for an energy saving retrofit of the heat exchanger network is now described systematically. Firstly, the path combination approach is to be used for identifying suitable candidate for retrofit solution(s) and then to be treated with the temperature flexibility (TF) in order to exploit the most out of heat recovery. The path combination approach starts with data collection on the existing HEN which is then followed by the paths' identification. The identified paths are combined using equation (3.2) prior to generating the options for the retrofit to reduce the energy consumption using equation (3.3). Then the heat load shifting from one utility source to the other is made using single and combined paths successively. Heat balance for each exchanger shell or tube side is calculated according to equation (3.6) while upholding the existing HRAT.

$$Q = CP.(T_1 - T_2) \qquad (3.6)$$

The heat capacity flow rate (CP) shown in the above equation could also be written as a multiplication of mass flow rate (m) and heat capacity (C_P) [25].

A simple ratio between the exchanger's area and the heat load is used to roughly predict the heat transfer area that will result after the heat shifting as in equation (3.7) below:

$$\frac{A_{before}}{Q_{before}} = \frac{A_{after}}{Q_{after}} \tag{3.7}$$

The initial results of the exchanger's area after heat shifting obtained from equation (3.7) above are substituted into the pressure drop equations (3.8) for the exchanger tube side and equation (3.9) for the shell side where the existing pressure drop is used. The constant parameters involved in these equations (K_{PT1}, K_{PT2}, K_{S1}, K_{S2}, K_{S3}) are explained in detail in equations (3.10) to (3.25):

$$\Delta P_T = K_{PT1}.A.h_T^{3.5} + K_{PT2}.h_T^{2.5} \tag{3.8}$$

$$\Delta P_S = K_{S1}.h_S^{2.86} + K_{S2}.A.h_S^{4.42} + K_{S3}.A.h_S^{4.69} \tag{3.9}$$

This enables the tube and shell side heat transfer coefficients to be calculated for the different options. Therefore, the constraints of the existing pressure drop and fluid velocity are considered for both the tube and shell sides of each heat exchanger.

The constant dimensional parameters of the pressure drop equations are basically functions of the exchangers' geometrical dimensions and the physical properties of the streams' fluids. These constants for the tube side equation are explained according to the following set of equations according to Nie and Zhu [59] and Smith [25].

$$K_{PT1} = \frac{0.023.\rho^{0.8}.\mu^{0.2}.d_I^{0.8}}{F_I.d_o}.\left(\frac{1}{K_{hT}}\right)^{3.5} \tag{3.10}$$

$$F_I = \frac{\pi.d_I^2}{4}.\frac{N_T}{N_{TP}}.v \tag{3.11}$$

$$K_{PT2} = 1.25.N_{TP}.\rho.\left(\frac{1}{K_{hT}}\right)^{2.5} \tag{3.12}$$

$$N_T = \frac{\frac{\pi}{4}.D_S^2}{P_C.P_T^2} \quad (3.13)$$

$$K_{hT} = c.\left(\frac{k}{d_I}\right).\Pr^{\frac{1}{3}}.\left(\frac{d_I.\rho}{\mu}\right)^{0.8} \quad (3.14)$$

$$\Pr = \frac{C_P.\mu}{k} \quad (3.15)$$

Whereas the constants for the shell side equation are explained below:

$$K_{S1} = \frac{2.K_{PS1} - K_{PS3}}{K_{hS}^{\ 2.86}} \quad (3.16)$$

$$K_{S2} = \frac{K_{PS2}}{K_{hS}^{\ 4.42}} \quad (3.17)$$

$$K_{S3} = \frac{K_{PS4}}{K_{hS}^{\ 4.69}} \quad (3.18)$$

$$K_{PS1} = \frac{1.298.F_{Pb}.(1-B_C).D_S.\rho^{0.83}.\mu^{0.17}}{P_T.d_o^{\ 0.17}} \quad (3.19)$$

$$K_{PS2} = \frac{0.5261.F_{Pb}.F_{pL}.P_C.(1-2.B_C).(P_T - d_o).\rho^{0.83}.\mu^{0.17}}{F_o.d_o^{\ 1.17}} \quad (3.20)$$

$$K_{PS3} = \frac{2.596.F_{Pb}.F_{pL}.(1-2.B_C).D_S.\rho^{0.83}.\mu^{0.17}}{P_T.d_o^{\ 0.17}} \quad (3.21)$$

$$K_{PS4} = \frac{0.2026.F_{pL}.P_C.P_T.(P_T - d_o).\rho}{d_o.F_o}.\left(\frac{2}{D_s} + \frac{0.6.B_C}{P_T}\right) \quad (3.22)$$

$$K_{hS} = \frac{0.24.F_{hn}.F_{hw}.F_{hb}.F_{hL}.\rho^{0.64}.C_P^{\ 0.333}.k^{0.667}}{\mu^{0.307}.d_o^{\ 0.36}} \quad (3.23)$$

$$F_o = v.A_C \quad (3.24)$$

$$A_C = \left(\frac{P_T - d_o}{P_T}\right).D_S.L_B \quad (3.25)$$

For the heat exchanger, the actual heat transfer area is found from the heat exchanger design equation. It is a relationship between heat exchanger area, overall heat transfer coefficient, heat duty, LMTD and its correction factor as shown in equation (3.36) below:

$$A = \frac{Q}{U \times LMTD \times F_T} \quad (3.26)$$

In practice, the overall heat transfer coefficient U shown in the above equation depends on the streams flow arrangement. As reported by Smith [25] it is not possible to specify the flow properties in the retrofit targeting stage which is not deal with the precise area, but concern mostly about the area targeting. Therefore, the overall heat transfer coefficient must be assumed independent of the flow arrangement according to equation (3.27) below:

$$U = \frac{1}{h_T} + \frac{1}{h_S} \tag{3.27}$$

Accordingly, the relationship to calculate the exchanger heat transfer area for the retrofit is called the area targeting equation (3.28). The equation uses the film heat transfer coefficients for shell and tube sides as obtained from the pressure drop equations shown above.

$$A = \left(\frac{1}{h_T} + \frac{1}{h_S}\right) \times \frac{Q}{LMTD \times F_T} \tag{3.28}$$

The LMTD correction factor (F_T) used for the existing HEN could still be used for the retrofit work since it modifies an installed area. In the demonstration example to follow, the correction factor (F_T) was ignored and the same assumption should be followed. The LMTD is calculated as follows:

$$LMTD = \left(\frac{\Delta T1 - \Delta T2}{\ln\left(\frac{\Delta T1}{\Delta T2}\right)}\right) \qquad 3.29)$$

$$\Delta T1 = T_{H,in} - T_{C,out} \tag{3.30}$$

$$\Delta T2 = T_{H,out} - T_{C,in} \tag{3.31}$$

Energy savings, area investment and the payback period are calculated based on the following assumptions as used by Al-Riyami [89].

- Investment is considered only for the required additional area.
- No piping or other costs are considered.

- Average size of heat exchanger shell is calculated from the existing HEN area (summation of all exchangers' area) and number of shells where one shell pass is assumed.
- Existing average area per shell in the HEN is the same as for the added area.
- Material of construction is carbon steel for all exchangers.
- Fixed energy price along the payback period.

The saving cost in terms of \$/year is calculated using the set of equations (3.32) to (3.36) as follows:

$$Saving_{cost} = \sum HU_{ex.cost} - \sum HU_{new.cost} + \sum CU_{ex.cost} - \sum CU_{new.cost} \qquad (3.32)$$

$$HU_{ex.cost} = Q_{ex.H} . HU_{price} \qquad (3.33)$$

$$HU_{new.cost} = Q_{new.H} . HU_{price} \qquad (3.34)$$

$$CU_{ex.cost} = Q_{ex.C} . CU_{price} \qquad (3.35)$$

$$CU_{new.cost} = Q_{new.C} . CU_{price} \qquad (3.36)$$

The capital cost (\$) to be invested for the additional area requirement is calculated using the set of equations from (3.37) to (3.40) as shown below:

$$Investment = \Delta N \left(a + b \left(\frac{\Delta A}{\Delta N} \right)^{c} \right) \qquad (3.37)$$

$$\Delta N = \frac{\Delta A}{av_{shell}} \qquad (3.38)$$

$$av_{shell} = \frac{A_{ex.HEN}}{N_{shell}} \qquad (3.39)$$

$$\Delta A = A_{new.HEN} - A_{ex.HEN} \qquad (3.40)$$

For carbon steel exchanger, the values for the cost constants *a*, *b* and *c* shown in equation (3.37) above are 33422, 814, and 0.81, respectively.

The payback period in terms of years for refunding the invested capital is just a ratio between the investment spent and the saving cost gained which is described in equation (3.41) below.

$$Payback = \frac{Investment}{savings} \tag{3.41}$$

Once the potential options have been identified using the Paths' Combination Approach, the options are then subjected to the temperature flexibility concept. The concept is applied by increasing the temperature step wisely from 1°C to 5°C for both (t_{hst}^{+}) and (t_{cst}^{-}) with the aim to increase the HRAT value as shown in Table 3.2, and then resume the heat shifting process.

After subjecting the potential options to the temperature flexibility, the respective heat loads from the HEN utilities are shifted until the HRAT is restored back to its original value. This part of the procedure is indicated by the loop featured in the methodology flow diagram shown in Fig 3.13. It is obvious from the flowchart that the looping was applied for all the retrofit options (feasible and unfeasible) since extra saving is always preferred if applicable. Nevertheless, it is worth mentioning that the temperature flexibility is better applied for the options with long payback period to explore the extent of improvement that is possible. Regardless of the TF application, a calculation model for this procedure is presented in Appendix D to describe the computational followed from the step of heat shifting up to the economical assessment.

3.5 Heat exchanger network case study

The developed approach is demonstrated using an appropriate case of the heat exchanger network taken from Marcone *et al* [58] with all the required data. The grid representation of the case is shown in Fig 3.14. The geometrical configuration for each exchanger in the network is in accordance to the guideline provided by Philippe [90]. The heating utility for H1 is at a higher temperature and therefore more expensive than for H2. In the case of cooling, the vice versa was applied where the cooling utility for C2 is more costly than for C1.

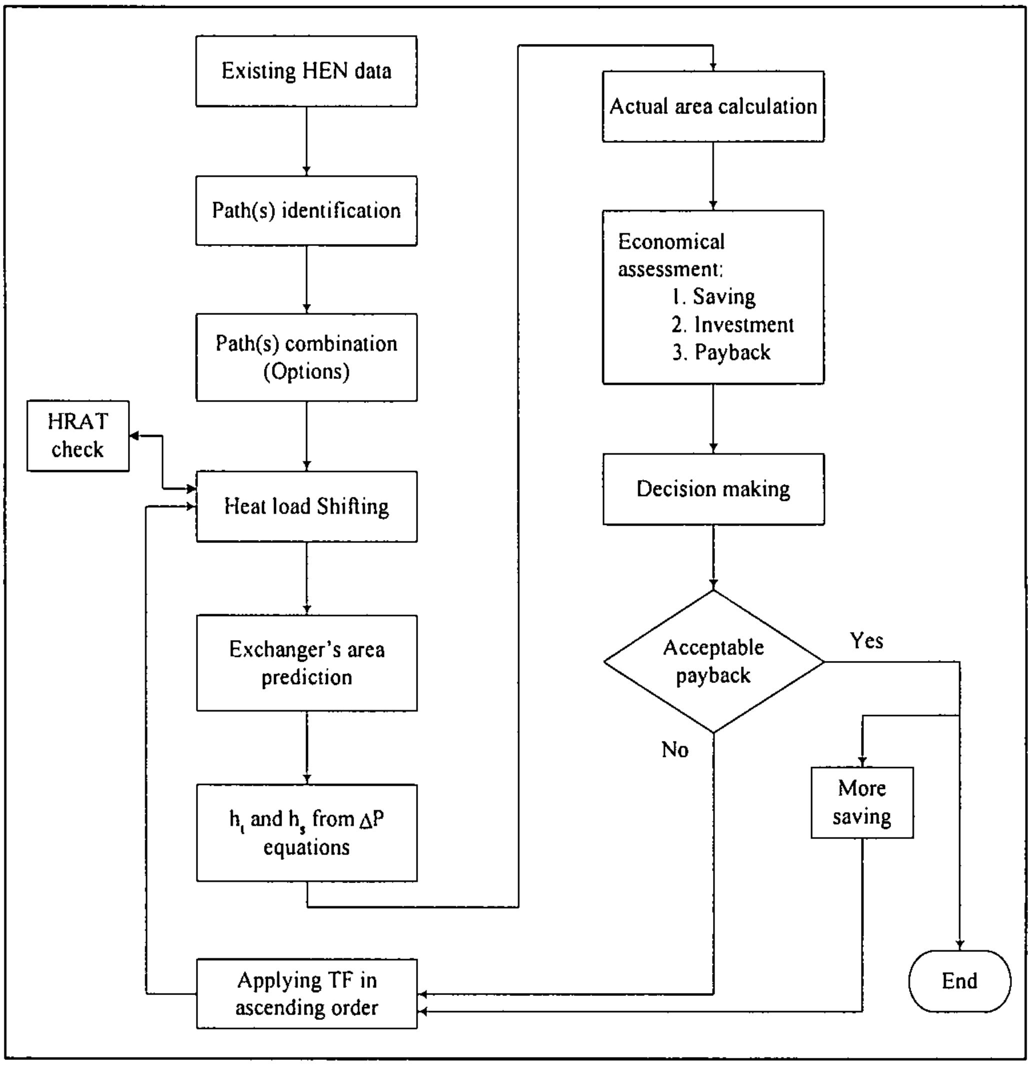

Fig 3.13: Overall methodology flow diagram

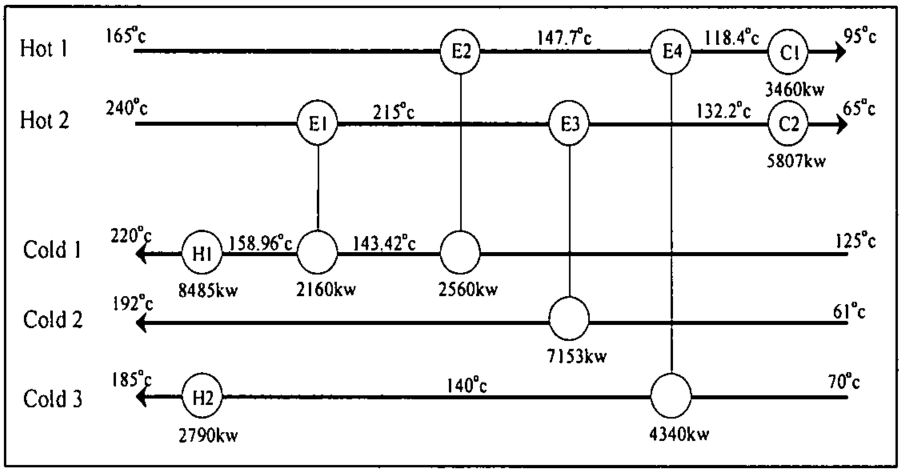

Fig 3.14: Existing heat exchanger network

Six individual utility paths were identified for this case study as shown in Fig 3.15 and namely they are:

1. Path (A): to shift heat load from C2 to C1 through E1 and E2.
2. Path (B): to shift heat load from both H1 and C1 through E2.
3. Path (C): to shift heat load from both H2 and C1 through E4.
4. Path (D) to shift heat load from both H1 and C2 through E1.
5. Path (E) to shift heat load from both H2 and C2 through E1, E2 and E4.
6. Path (F) to shift heat load from H1 to H2 through E2 and E4.

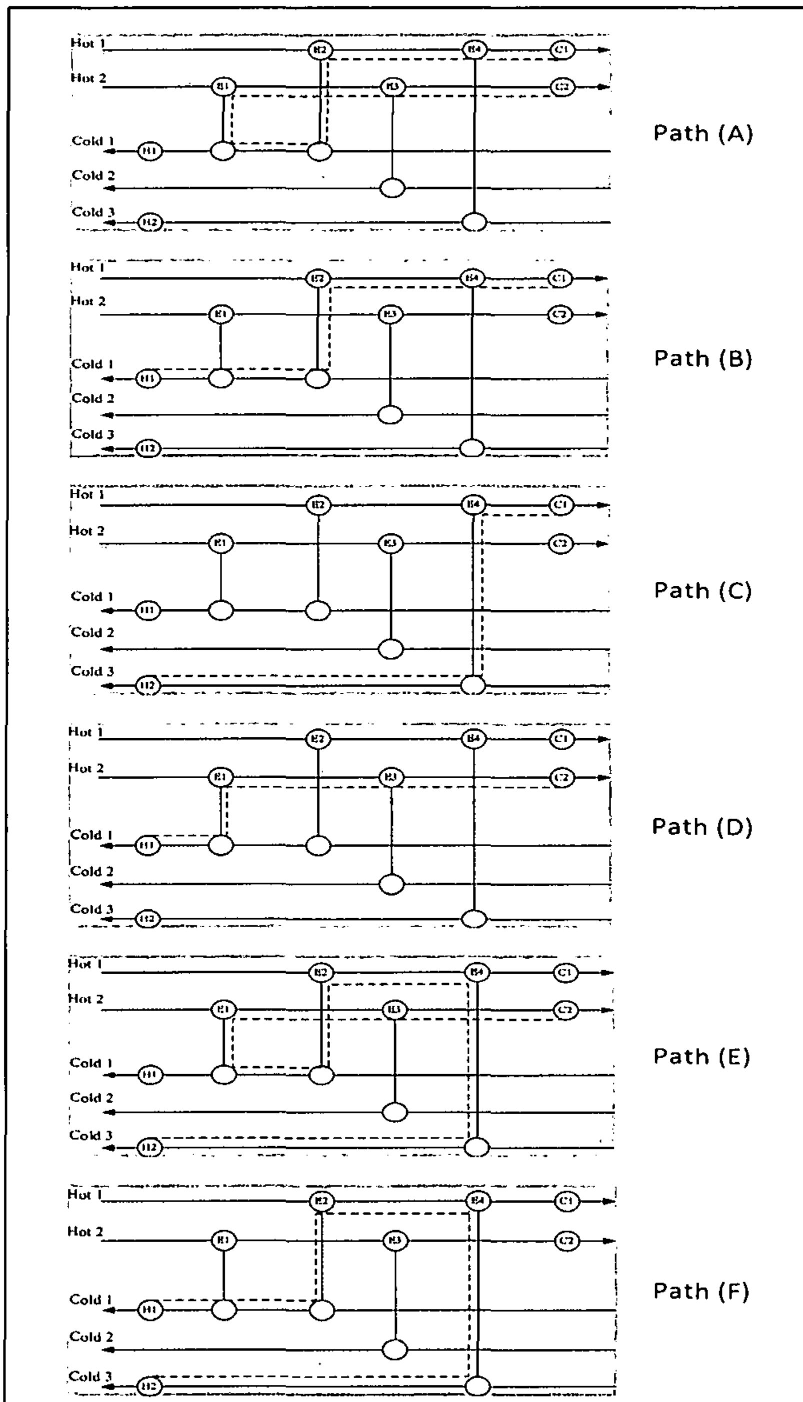

Fig 3.15: Available utility paths within the existing HEN

These paths are combined using equation (3.3) to give 63 options of heat shifting. However, only 17 options are found to be feasible for energy savings because of the HRAT control. Besides the combined paths, the single utility paths are also considered as energy saving options as shown in Table 3.3. (Grid representation of the combined utility paths is shown in Appendix B). The existing HRAT taken from the HEN is 7.7°C (i.e. the difference between the hot inlet and cold outlet of exchanger 4); but it was assumed to be 7°C since lower practical HRAT allows more heat shifting through the utility path. But it must be mentioned that the HRAT violation should be kept within a soft limit when retrofitting the HEN. On the other hand, the higher the value of HRAT, the higher additional area is required for the retrofit. By contrast, the lower the value of HRAT, the more difficult is the heat transfer between hot and cold streams in the exchanger.

3.5.1 Existing HEN comprehensive data

Beside the temperature data which is located on the grid diagram shown above, the required physical properties and the remaining stream data are tabulated in Table 3.4.

Table 3.3: Feasible path combination options

Option No.	*Corresponding path(s)*	*Option No.*	*Corresponding path(s)*
1	A	10	BF
2	B	11	CD
3	C	12	CF
4	D	13	DF
5	E	14	EF
6	F	15	ABF
7	AB	16	ACF
8	AC	17	CDF
9	AF		

Table 3.4: Existing HEN streams data

Stream	ρ *(kg/m³)*	μ *(cps)*	*k* *(W/m.°C)*	*v* *(m/s)*	*Cp* *(kJ/kg.°C)*	*CP* *(kW/°C)*	*h* *(kW/m².°C)*
Hot1	750	0.5	0.12	0.98	2.6	148	0.45
Hot2	700	0.3	0.12	0.98	2.6	86.4	0.55
Cold1	800	1	0.12	1.5	2.6	139	0.35
Cold2	750	0.4	0.12	1	2.6	54.6	0.4
Cold3	630	0.2	0.12	1	2.6	62	0.64

Exchangers' area, heat load and pressure drop for the existing network are presented in Table 3.5. The geometrical data for each exchanger in the existing HEN is presented in Table 3.6. For the utility cost, it is worth mentioning that it is changeable according to the economic situation and for the current work, it is taken as presented in the work of Al-Riyami *et al* [89]. Namely, for H1 and H2 it is 278.14$/kW and 224.4$/kW respectively, and for C1 and C2 utility cost it is 12.75$/kW and 21.04$/kW respectively; i.e. the price of hot and cold utility to produce a unit kW of heating and cooling power respectively. It must be mentioned that the cooling agent for C1 and C2 could normally be cooling water. However, different prices are shown here to indicate that the heat load could be shifted from higher to lower price cooling utility as well as for the heating utility.

Table 3.5: Exchangers' area, heat load and pressure drop for the existing HEN

Exchanger	A (m^2)	Q (kW)	ΔP_T (kPa)	ΔP_S (kPa)
E1	133	2160	1.8	21.6
E2	588	2560	5.7	20
E3	724	7153	29	117.9
E4	742	4340	141.2	25.2

Table 3.6: Geometrical configuration for each exchanger in the existing HEN

Data \ ***Exchanger***		***E1***	***E2***	***E3***	***E4***
General	P_C	1	1	1	1
	N_{TP}	2	2	8	10
	P_T (m)	$1.5d_o$	$1.5d_o$	$1.5d_o$	$1.5d_o$
Tube-side	C	0.023	0.023	0.023	0.023
	d_I (m)	0.047	0.039	0.016	0.020
	d_o (m)	0.063	0.055	0.063	0.063
Shell-side	D_s (m)	0.300	0.325	0.300	0.203
	L_B (m)	$0.2D_s$	$0.21D_s$	$0.2D_s$	$0.315D_s$
	B_C	0.2	0.2	0.2	0.3
	F_{hn}	1	1	1	1
	F_{hw}	1	1	1	1
	F_{hb}	1	1	1	1
	F_{hL}	0.8	0.8	0.8	1
	F_{Pb}	1	1	1	1
	F_{PL}	1	0.5	1	0.5

3.5.2 Exchangers' heat transfer coefficients profile with changing the area

Apart from the suggested approach, the profile of heat transfer coefficients for the tube-side (h_T) and shell-side (h_S) of each exchanger in the existing HEN is checked using equations (3.8) and (3.9) after substituting the detailed data. Unlike the conventional retrofit design, the heat transfer coefficients are found to vary with heat transfer area or the stream or exchanger pressure drop which agree well with Nie and Zhu [59]. For constant exchangers pressure drop while changing the area in the range between 0.0 m^2 to 5000 m^2, heat transfer coefficients performance are shown in Fig 3.16 for each exchanger in the network under study.

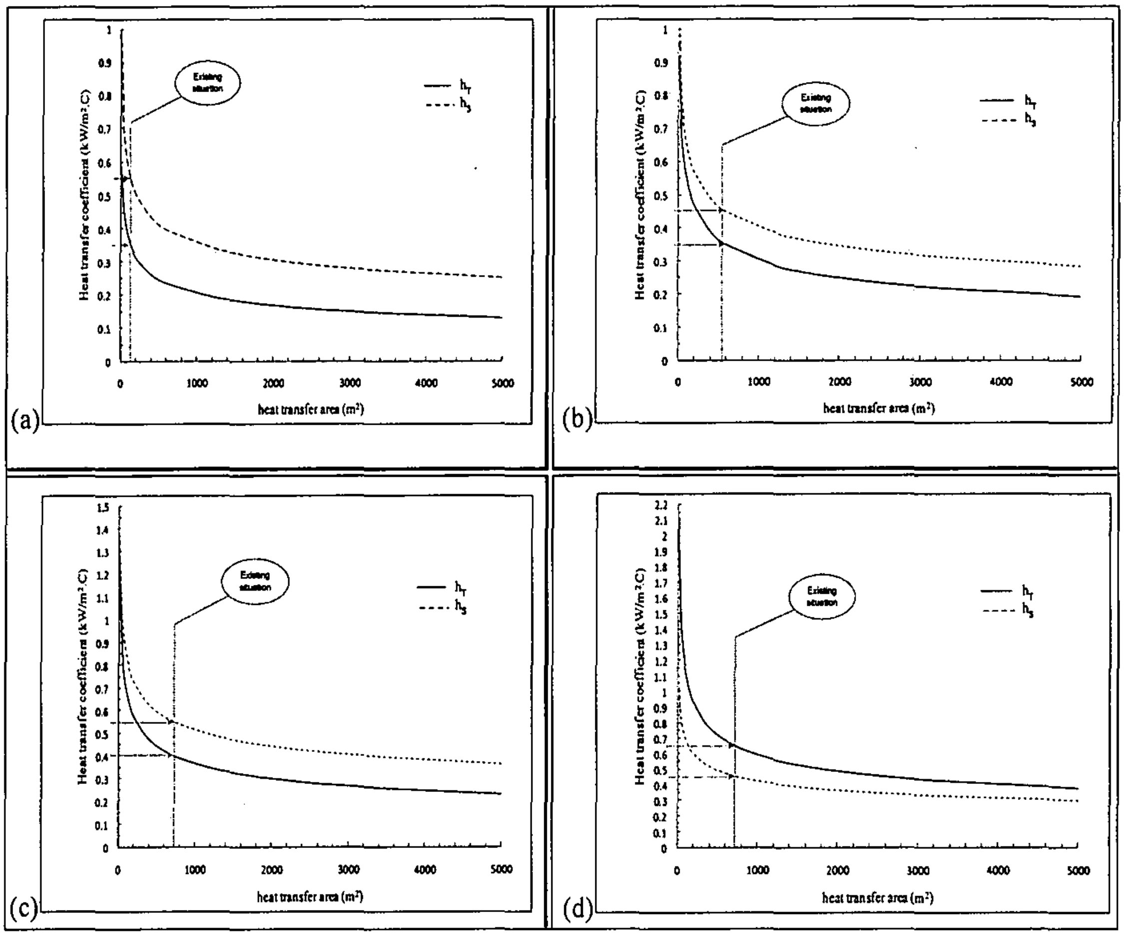

Fig 3.16: Tube and shell heat transfer coefficients profile for the existing exchangers' pressure and changeable area

(a) Exchanger 1, (b) Exchanger 2, (c) Exchanger 3, (d) Exchanger 4

The profile assured that the heat transfer coefficients are not constant parameters as was used previously. From the existing situation of each exchanger, the heat transfer coefficients are steadily reduced while increasing the exchanger heat transfer area.

Additional assumptions should also be considered since the current work is treating an integrated HEN and utility system which is extensively described in Chapter 4. These assumptions are as follows:

- In-house power generation which is required in the plant. Also, suppose that the excess power (if any) is demanded and could be sold to the external consumers.

- The HEN example discussed above uses the steam generated in the utility system as a heating media, i.e. HP steam at 41 bara in the first heater (H1) and MP steam at 15 bara for the second heater (H2)

3.6 Summary

The simple combinatorial method presented here to combine the existing utility paths in the HEN allows the generation of several energy saving candidates. Thereby, getting the most out of process-to-process heat recovery and energy savings could be addressed by shifting the heat load from the HEN utilities using sets of combined paths successively. Among the generated candidates, some options would definitely reveal poor opportunities to be promising retrofit solutions. Accordingly, the process streams' temperature flexibility could offer further chances for extra heat load shifting in order to enhance the potentials of poor solutions which could be further improved. The judgment criterion is mainly an economic based measurement to test the feasibility for each option. The approach is emphasizing the consideration of the existing exchangers' pressure drop where the geometrical configuration is of main concern. Hence, it was very difficult to get a comprehensive data for several case studies. Therefore, only one case with a detailed data is presented although the approach is logically valid for each HEN with several heaters and coolers.

CHAPTER 4

APPLICATION OF PATHS COMBINATION APPROACH ON THE UTILITY SYSTEM

In the previous chapter, the overall methodology of path combination and streams temperature flexibility for energy saving HEN retrofit has been presented. Given that the retrofit involved only addition of heat transfer area without topology changes, the invested capital is expected to be small or moderate in amount with short payback period. This is true when considering the HEN retrofit as a standalone problem without taking into account the impact on the remaining total site. However, the HEN is normally integrated with the whole total site where it derives utility from a central utility system. Therefore, the interaction between the HEN and the utility system should also be addressed in order to fully comprehend the impact of energy savings derived from the retrofit project on the utility system.

As stated by Smith [25], the site utility system must be studied in any process design project for several reasons. Among these reasons are:

1. Change in the steam and power demand on the site as a result of new process start up, process close down, process capacity change and introducing or changing the process technology.

2. The energy conservation projects to be conducted for any subsystem in the total site would at least alter the steam flow in the utility system.

4.1 Utility and steam system configuration

The main source for generating the steam required for process heating comes from the central utility system. The steam supplied at different levels of pressures and temperatures. It is commonly known in the industry that most of the processes utilize steam for heating, but several of these processes are also capable of generating steam.

Therefore, interactions exist between the process and the utility system via steam usage and generation. Simply, there is a heat recovery interaction between the processes on the site using the steam as an intermediate for the heat transfer [25]. The overall picture showing such interaction between processes and utility is adopted in Fig 4.1 which represents a typical utility system with process plants connected to it [27].

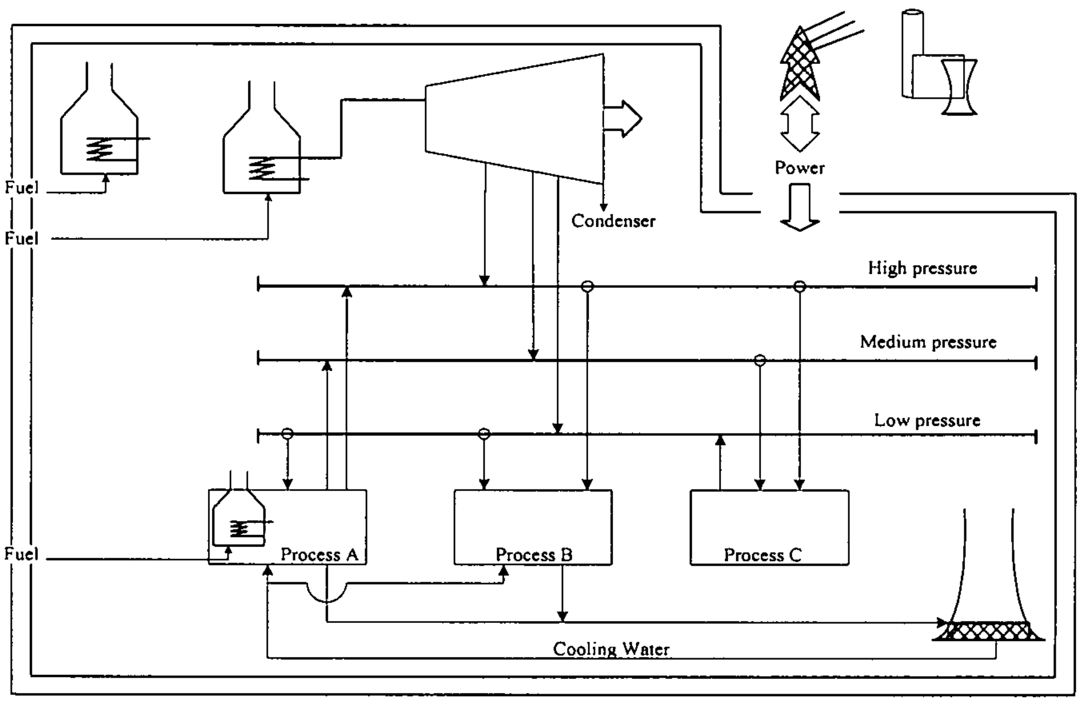

Fig 4.1: Typical utility and steam system configuration

A very high pressure steam (VHP) is generated in the boilers house. The VHP steam is expanded using steam turbine to produce power and exhausting high pressure steam (HP), medium pressure steam (MP) and low pressure steam (LP) into the steam mains accordingly. The final exhaust steam is condensed against cooling water. The power production due to steam expansion might be below or over the site processes needs. In case of power deficit in the site, the shortage must be supplemented from external resources such as the national grid. However, in case where surplus power is produced in the utility system, it can be exported to the national grid.

4.1.1 The main components of the utility system

Steam and utility system mainly consists of boiler feed water treatment unit, steam boilers, steam and gas turbines, steam distribution system (steam mains) and condensate collection. Some of these components are described here according to their relevance to the current research work.

The boiler feed water is to be treated before it is fed to the boiler for steam generation. The water treatment depends on the quality and specification of the raw water and the requirements of the water needed to generate steam in the boiler house. According to Dryden [91], there are several types of steam boilers used depending on the steam pressure and type of fuel.

Steam turbines are used to converts the energy of the steam into power while expanding steam from higher to lower pressure [92]. The higher the pressure difference across the turbine, the more power can be extracted from the steam. The amount of power production from the steam also depends on the turbine size that rate the ability of power generation which vary from 0.75kW to 100 MW and larger. Steam turbines are generally classified into back-pressure turbines and condensing turbines according to the pressure of the exhaust steam. The exhaust steam in the back-pressure turbine is higher than the atmospheric pressure, whereas for the condensing turbines the pressure of the exhaust is lower than the atmospheric. Fig 4.2 illustrates the configuration of the back-pressure and the condensing turbines. To consider the turbine flow constraints, it has been stated that there would be a minimum and maximum allowable steam flows for a given steam turbine [25]. These flow constraints are determined by the physical characteristics of individual turbines and specified by the turbine manufacturer.

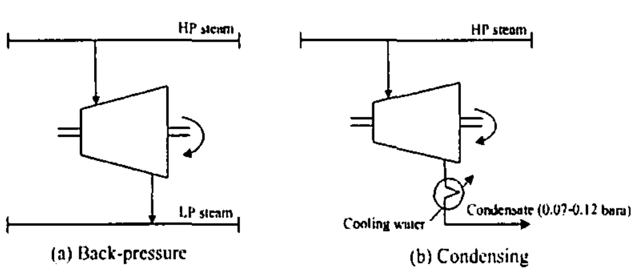

Fig 4.2: General configuration of the steam turbine

4.1.2 Power generation in the steam turbine

As a result of steam expansion in the turbine, power is produced and consumed by the processes in the site. However, not all the energy contains in the inlet steam is converted to useful power due to thermodynamic constraints, mechanical losses and kinetic losses. Moreover, the steam turbine efficiency (η_{ST}) is not a constant parameter since it is a function of the turbine power output as shown in Fig 4.3(a) [83]. And the turbine power output is a function of steam flow rate across the turbine, i.e., turbine load as shown in Fig 4.3(b).

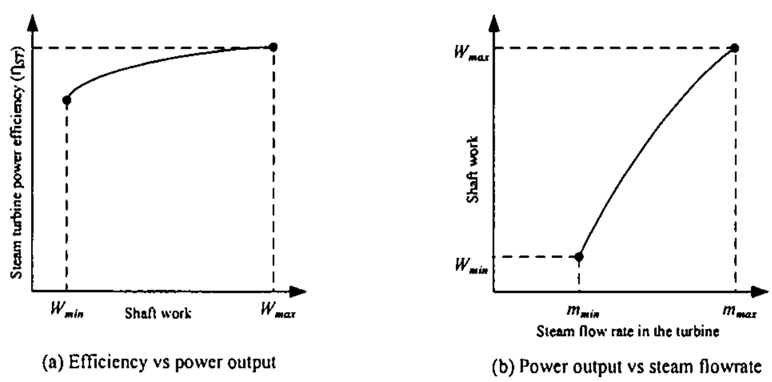

Fig 4.3: Steam turbine performance

Accordingly, the simple way to calculate the power in the steam turbines is to use the Willians' line equation as previously used by Mavromatis [81], Mavromatis and Kokossis [74]. Willians' line equation represents the relationship between the shaft power and the mass follow through the heat engine (steam turbine). Fig 4.4 below illustrates the Willians' line relationship for the steam turbine which shown to be straight line relationship [81],[79].

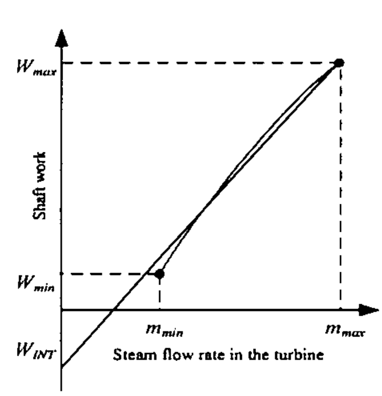

Fig 4.4: Willians' line relationship for the steam turbine

4.1.2.1 Steam turbine model for power generation

Based on the Willians' line relationship, Varbanov *et al* [79] have developed a complete model for power generation in the steam turbine as part of the modeling and optimization of the utility system. The model is used to calculate the power generation in the utility system of the current research work and could be summarized as follows:

The power produced in each steam turbine in the utility system is calculated according to the Willians' line relationship shown in Fig 4.4 above and represented by equation (4.1) below:

$$W = n.m - W_{\text{int}} \tag{4.1}$$

The slope n and the intercept W_{int} are calculated as follows:

$$n = \frac{L+1}{B} \times \left(\Delta h_{is} - \frac{A}{m_{\max}} \right) \tag{4.2}$$

$$W_{\text{int}} = \frac{L}{B} \times \left(\Delta h_{is} \times m_{\max} - A \right) \tag{4.3}$$

L is termed as the intercept ratio and its values depend on many factors, such as the pressure drop across the turbine. L values are typically ranged between 0.05 and 0.20 in most cases [79]. The particular value for L used in the current work is 0.2. The isentropic enthalpy difference (Δh_{is}) along the turbine as represented by equation (4.4) is calculated based on the pressure, temperature and the dryness fraction of the inlet steam and the exhaust steam using the steam table. The coefficients A and B used in equations (4.2) and (4.3) depend on the pressure drop across the turbine which has been represented by the equivalent saturation temperature difference [79],[83]. These coefficients are calculated from the regression relationships as shown in equations (4.5) and (4.6).

$$\Delta h_{is} = h_{T,in} - h_{T,is,out} \tag{4.4}$$

$$A = b_o + b_1.\Delta T_{sat} \tag{4.5}$$

$$B = b_2 + b_3.\Delta T_{sat} \tag{4.6}$$

In the above equations (4.5) and (4.6), the values for the regression parameters b_0, b_1, b_2 and b_3 depend on the turbine configuration and size. The values of these parameters as presented in the work of Varbanov [83] are tabulated in Table 4.1. The saturation temperature difference across the turbine (ΔT_{sat}) presents in the same equations (4.5) and (4.6) is calculated according to equation (4.7) based on the turbine inlet and outlet steam properties obtained from the steam table.

$$\Delta T_{sat} = T_{sat,in} - T_{sat,out} \tag{4.7}$$

Table 4.1: Regression parameters values for the steam turbine model

Coefficients	Back-pressure turbine		Condensing Turbine	
	$W_{max} < 2$ MW	$W_{max} > 2$ MW	$W_{max} < 2$ MW	$W_{max} > 2$ MW
b_0	0	0	0	-0.463
b_1	0.00108	0.00423	0.000662	0.00353
b_2	1.097	1.155	1.191	1.220
b_3	0.00172	0.000538	0.000759	0.000148

4.1.2.2 Material and energy balances in the utility system

The material and energy balances for the steam have to be addressed for the entire units in the utility system before exploring the interaction between the HEN and the utility system. Therefore, the steam savings derived from the HEN retrofit could be distributed regularly through the utility system devices. Fig 4.5 represents a simple demonstration for the steam flow in the utility system and site process from which material and energy balances could be explained.

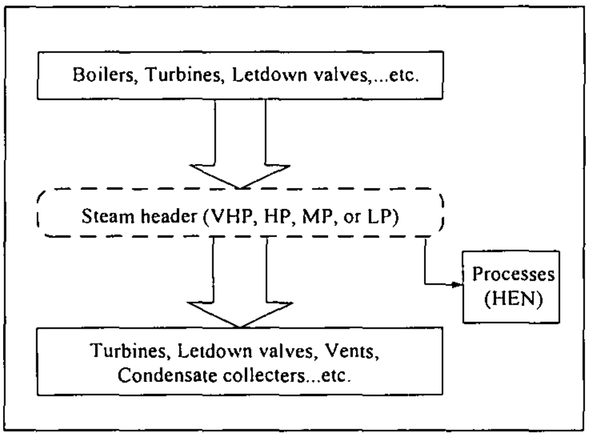

Fig 4.5: Simple representation of steam flow through site utility and processes

The steam mass flow rate to the process (m_P) could simply be found from the difference between the inlets and the outlets of the steam flow into and from the header, respectively as shown in equation (4.8) below:

$$m_P = m_{header,in} - m_{header,out} \tag{4.8}$$

The properties of the steam used for process heating are similar to those of the steam header from which it is derived. Referring to Fig 4.5 and if perfect insulation is assumed for the steam pipes, the enthalpy of the steam to heat a particular process could be found from the energy balance of the header from which the steam is derived as shown in equation (4.9). In case where two steam properties are available for the particular header, the enthalpy could be obtained directly from the steam table.

$$h_{header} = \frac{\sum \left(m_{header,in} \times h_{header,in}\right)}{\sum m_{header,in}} \tag{4.9}$$

4.1.3 Steam saving

It has been discussed earlier that the external heating required in the HEN is usually supplied from the utility system in the form of steam at a certain temperature or pressure level. For instance, heater (H) in the HEN can utilize certain amount of the HP steam flow from the HP steam header in the utility system as shown in Fig 4.6. From the figure, the amount of HP steam savings *($HP_{stm,sav}$)* derived from the HEN retrofit could be calculated from the material and energy balances across the heater (H) as described in the equations from (4.10) to (4.13).

$$HP_{stm,sav} = m_{P,HP,ex} - m_{P,HP} \tag{4.10}$$

$$m_{P,HP} = \frac{Q_H}{\Delta h_H} \tag{4.11}$$

$$\Delta h_H = h_{HP} - h_{H,out} \tag{4.12}$$

$$h_{H,out} = h_{HP} - \frac{Q_{H,ex}}{m_{P,HP,ex}} \tag{4.13}$$

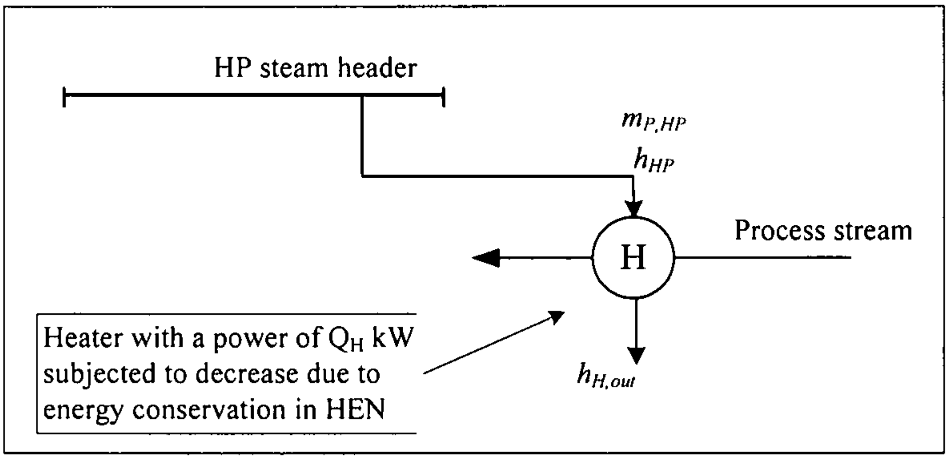

Fig 4.6: Interaction between steam saving in a process heater and HP steam header

4.1.4 Top-level and bottom-up analysis

The top-level analysis procedure was first developed by Makwana *et al* [93] to analyze the total site for retrofit operation and management. Based on the top-level analysis, Varbanov [83] presented an approach for analyzing industrial utility systems. The approach aims at estimating the true value of steam savings and hence establishing suitable improvements to the utility system. Accordingly, possible ways could be identified for retrofitting site processes to save energy. As discussed by Makwana *et al* [93], the top-level method is simple and it identifies energy saving opportunities in the HEN using only the utility system data regardless of the entire processes data.

The top-level analysis which is also shown as top-down method starts with total site analysis conducted on the utility system before moving to the process HENs. The top-level methodology adopts the concept of path analysis within the utility system which will be thoroughly discussed in the next subsections.

In contrast to the top-level analysis, the current work starts with the HEN retrofit and then investigates the impact on the utility system. The trend of this work is similar to the bottom-up analysis as in the work of Muller *et al* [73] where combination of both top-level and bottom-up analysis have been introduced. The bottom-up analysis starts with the analysis of the processes involving the HEN prior to exploring the impact of energy savings derived from process improvement on the steam distribution in the utility system.

The difference between the top-level and bottom-up methods is demonstrated in the onion diagram as shown in Fig 4.7 below:

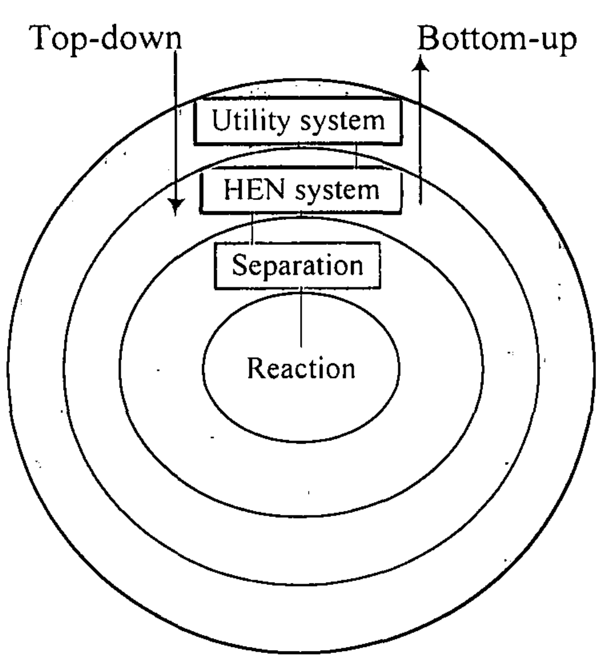

Fig 4.7: Top-down and Bottom-up methods

4.1.4.1 Path analysis in the utility system

As discussed by Zhu *et al* [87], it is very hard to improve the overall energy system in the process plant where both energy consumption and generation are fundamental features. However, the energy system improvement became straightforward in view of the established tools which provide insights to manage the heat flow in the utility system of the process plant. Path analysis in the utility system is considered to be an effective tool to analyze and manage the steam flow in the utility system as part of the top-level analysis provided by Makwana [50, 93].

It has been discussed earlier that the process retrofit projects often result in reducing the plant energy consumption which further leads to changing the steam distribution and creates surplus of steam generation in the utility system. The economic value of the retrofit projects could be realized using the top-level method where the path analysis procedure is used to adjust the steam redistribution among the utility system devices. This could be conducted by utilizing the surplus steam to generate more power in the utility system, or cutting the surplus by directly reducing the fuel firing in the boiler. There is more than one option available in adjusting the utility system by redistributing the surplus steam using the current and optional heat flow paths. The current paths are used to transfer the steam savings derived from process retrofit to the first steam header in the utility system in order to create the steam surplus. The optional paths are used to manage the surplus by either cutting the fuel firing in the boiler (power import option), or redistributing the surplus through the turbines and hence generating more power in the utility system (power generation option). The overall picture of the heat flow paths in the utility system is described in Fig 4.8.

According to the path analysis in the utility system [50, 93], each of the identified optional paths in the utility system is able to manage the surplus steam, but the most efficient must be used. The efficiency of the heat flow paths in the utility system could be found from the fuel and power prices data. The upper and lower flow limits of the boilers and turbines must be considered while redistributing the surplus steam.

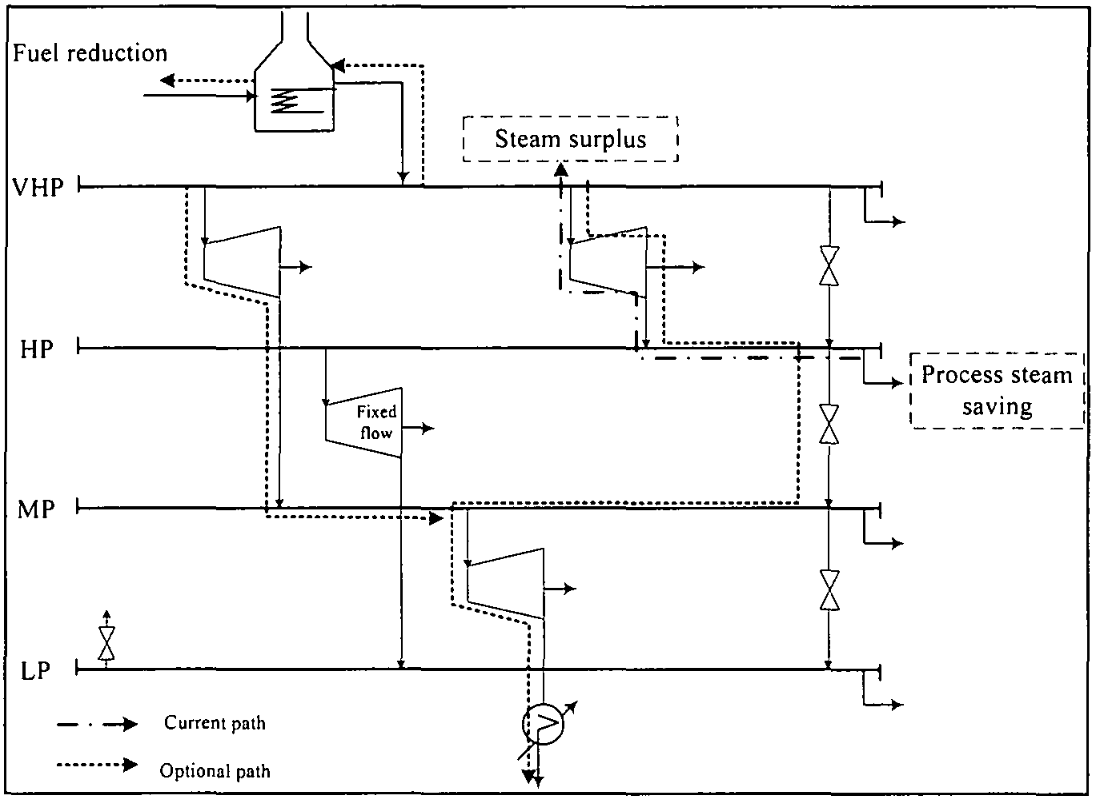

Fig 4.8: Demonstration of current and optional paths in the utility system

4.1.4.2 Heat flow path efficiency

Beside the current path(s) in the utility system, the optional paths which are either power import or power generation options must be identified as illustrated in Fig 4.8 above. Using the power import options to manage the surplus steam decreases the fuel consumption in the boiler at the expense of reducing the power generation in the utility system. Accordingly, the power deficit must be supplemented from external power source. In contrast, using the power generation options to redistribute the surplus steam leads to producing more power in the steam turbines where the excess could be exported or at least reducing the need for power import. A comparison between these options must be conducted in order to choose the proper way for redistributing the surplus steam. Accordingly, the heat flow path efficiency for all the identified paths in the utility system must be calculated based on a constant steam flow rate as a basis for comparison.

According to Makwana *et al* [93] and Smith [14], the heat flow path efficiency within the utility system is defined as follows:

- *Power import option*

The path efficiency for the power import option is the ratio of fuel price to the price of the equivalent imported power as shown in the following equation:

$$\eta_{imp} = \frac{F_{price}}{P_{price}} \tag{4.14}$$

The fuel and power import prices (F_{price} *and* P_{price}) are usually provided with the utility system data.

- *Power generation option*

On the contrary, the path efficiency for the power generation option is the ratio of change in power generation to the change in the fuel for generating the steam surplus. It is represented as a cost ratio as shown in equation (4.15) below:

$$\eta_{gen} = \frac{P_{cost,surp}}{F_{cost,surp}} \tag{4.15}$$

The cost of power produced in the turbine(s) as a result of redistributing the surplus steam ($P_{cost,\ surp}$), is found from the following equation:

$$P_{cost,surp} = P_{price} \times \sum \Delta W_T \tag{4.16}$$

The power price (P_{price}) is usually provided as power export price where the path is a power generation path. The shaft work difference before and after redistributing the surplus (ΔW_T) for any affected turbine on the path is calculated using equation (4.17). The steam turbine shaft work is calculated using the Willians' line relationship described earlier in equation (4.1).

$$\Delta W_T = W_{T,before} - W_{T,after} \tag{4.17}$$

Referring to equation (4.15) above, the fuel cost to produce surplus steam ($F_{cost,surp}$), is the cost of all types of fuel fired in the boilers and it is found using equation (4.18) below:

$$F_{cost,surp} = \left[\sum F_{price} \times \Delta h_{gen} \times \frac{1}{\eta_{boiler} - \eta_{loss}} \right] \times steam_{sav} \qquad (4.18)$$

The steam savings ($steam_{sav}$) is the amount of the steam (t/h) saved in the HEN. For instance, this savings will either be $HP_{stm,sav}$ or $MP_{stm,sav}$ which is calculated from the energy balances across the heater(s) in the HEN as described previously in section 4.1.3). The steam generation enthalpy difference (Δh_{gen}) represents the difference between the enthalpy of the boiler feed water (BFW) and the enthalpy of the produced steam in the boiler. The boilers mostly produce VHP steam and hence the (Δh_{gen}) could be found as follows:

$$\Delta h_{gen} = h_{VHP} - h_{BFW} \qquad (4.19)$$

The VHP steam enthalpy could directly be obtained from the steam table according to the provided VHP steam properties.

The enthalpy of the boiler feed water (h_{BFW}) is calculated using equation (4.20) according to its temperature (T_{BFW}) and specific heat capacity ($C_{P,W}$).

$$h_{BFW} = C_{P,W} \times (T_{BFW} - 0) \qquad (4.20)$$

4.2 Overall method to study the HEN - Utility interaction

In chapter 3, the method of paths combination and temperature flexibility for HEN retrofit which has been comprehensively discussed, was considering the HEN retrofit as standalone problem. The method has explained the economical potentials of the low-hanging-fruit solutions generated as a HEN retrofit options. As discussed earlier, the HEN and the utility system are usually interacted and consequently the energy savings derived from the HEN retrofit should be further explored to study the impact on the utility system. In this section, the HEN-Utility interaction is introduced to study the impact of savings derived from the proposed approach of paths combination for the HEN retrofit on the utility system.

From the HEN side, the derived savings from the retrofit was initially calculated and found in terms of energy savings (kW), i.e., the reduction in the amount of heat load for heating and cooling required in both heater(s) and cooler(s) of the HEN. To study the impact of energy savings on the utility system, consideration is given only to the heating demand (steam) in the HEN which affects the power generation in the utility system. The cooling requirements could simply be cooling water which is relatively cheap and would not affect the power generation in the utility system. Furthermore, the developed paths combination approach is essentially aimed at generating several retrofit options for the HEN. However, the overall saving derived for some of the retrofit options has featured decreasing the expensive hot utility demand at the expense of increasing the cheap hot utility demand in the HEN. Therefore, the HEN retrofit options that feature only reduction in the hot utility demand are carried forward to explore the impact of savings on the utility system.

The savings derived from the HEN retrofit is first prepared to cope with the steam flow in the utility system. Therefore, it is recalculated in terms of steam savings (t/hr) using the heat balances as in the equations from (4.10) to (4.13) for each heater in the HEN before and after considering the TF concept in the paths combination approach.

From the utility system side, material and energy balances are conducted for all the steam headers using equations (4.8) and (4.9). Energy balances in the steam headers are required to find the steam flow rate across each steam turbine in order to calculate the shaft power production in the utility system.

The available heat flow paths in the utility system are then identified as mentioned earlier in the top-level analysis method. The heat flow paths are classified into current paths which is used to deliver the heating steam to the process HEN, and optional paths through which the steam surplus is to be redistributed in the utility system. The optional paths are further classified into power import paths and power generation paths. In order to use the best way for managing the steam surplus, the path efficiency is calculated for each heat flow path in the utility system using equations (4.14) and (4.15) described previously. Accordingly, the most efficient optional path is carried forward to redistribute the steam surplus through the utility system devices while maintaining the boilers and turbines flow constraints. The shaft power produced in each steam turbine is then calculated using the set of equations from (4.1) to (4.7)

The calculation process to explore the HEN – Utility interaction flows in a systematic and simple manner and it has been conducted in MathCad software. The overall procedure to study the interaction between HEN and the utility system is illustrated by the flow diagram shown in Fig 4.9 below:

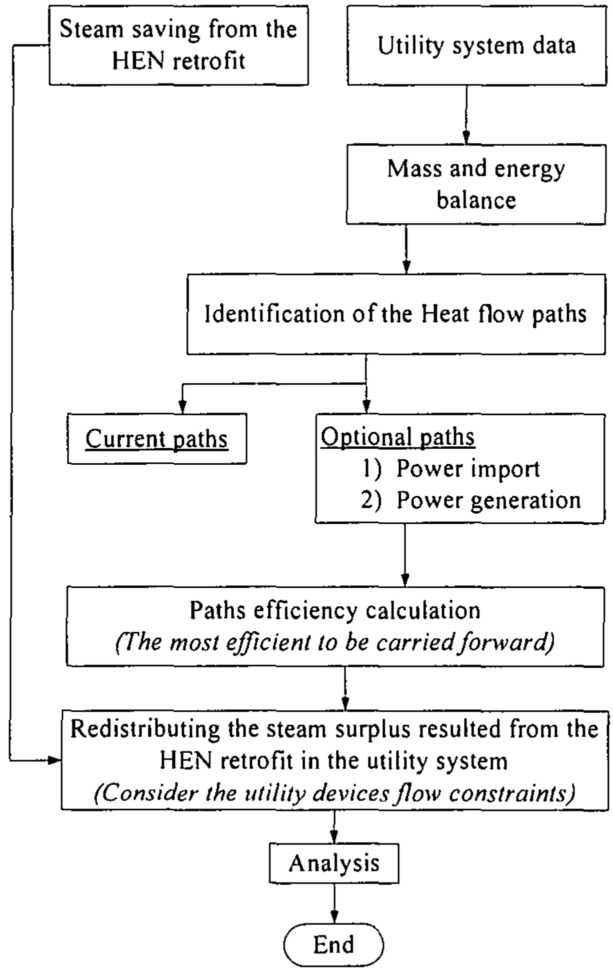

Fig 4.9: The procedure to explore the HEN – Utility interaction

4.3 Demonstration example for the utility system

In order to demonstrate the application of the proposed approach, an example involving simple utility system illustrated in Fig 4.10 is used. The process HEN was retrofitted for the purpose of energy savings using the developed paths combination approach as discussed in chapter 3. The resulted steam savings is expected to affect the steam distribution in the utility system. In the utility system example, two steam boilers with limited flow constraints are utilized to generate very high pressure steam (VHP) to fulfill the power generation and the steam heating required by the process. One of the boilers uses coal as its fuel while the other uses fuel oil. Boilers feed water (BFW) is available at 100°C with a heat capacity of 4.2kJ/kg °C. Steam generation efficiency is assumed to be 85% for each boiler with 10% distribution losses. Five steam turbines with limited flow flexibility are used to generate power by expanding the steam to lower pressure level. Turbine (T4) is shown to have a fix steam flow rate. Three letdown valves are also placed between the steam headers for the purpose of releasing the excess steam to the lower level steam header. The remaining excess steam is vented as a low value steam using the venting valve placed on the LP steam header.

The steam flow data for the various components on the utility system as well as steam properties are shown in Fig 4.10 in accordance with Makwana *et al* [50, 93] and Varbanov [83]. The required cost data to determine the paths' efficiencies is tabulated in Table 4.2 which adopted from Varbanov [83].

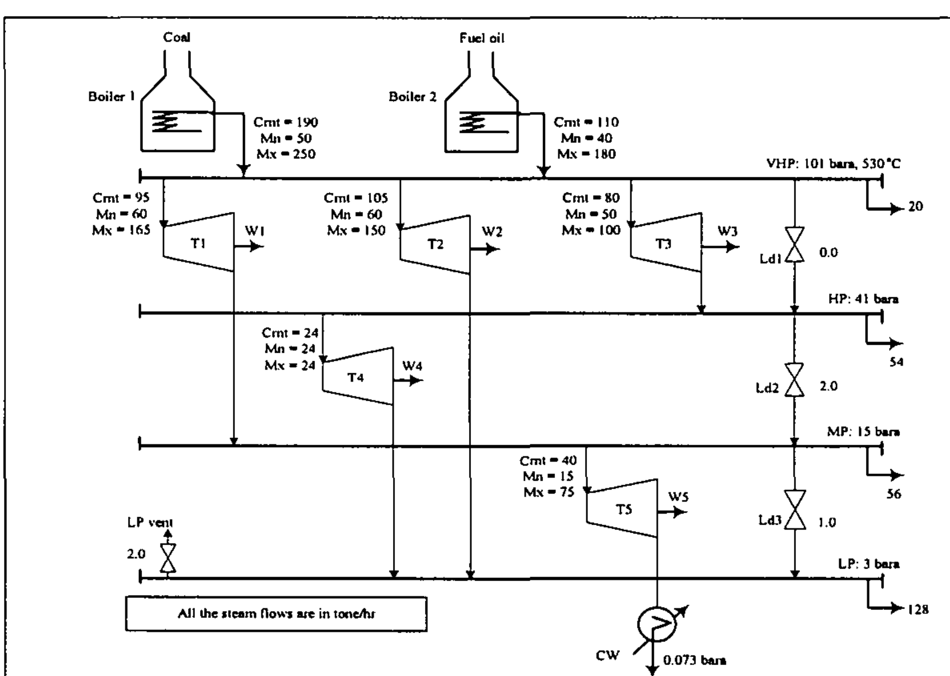

Fig 4.10: Utility system case study

Table 4.2: Power and fuel data for the utility case study

Category	***Price [$/kWh]***
Power import	0.06
Power export	0.05
Coal	0.0084
Fuel oil	0.0108

In the HEN example used to demonstrate the developed retrofit approach, two heaters of different heating media are located on the cold streams of the network as described in chapter 3. To study the interaction between the HEN and the utility system, one of the heaters in the HEN uses HP steam while the other uses MP steam as heating media which is supplied from the utility system shown in Fig 4.10 above. The HEN and the utility system case studies are assumed to be from the same plant and the overall picture to illustrate the interaction is shown in Fig 4.11 below:

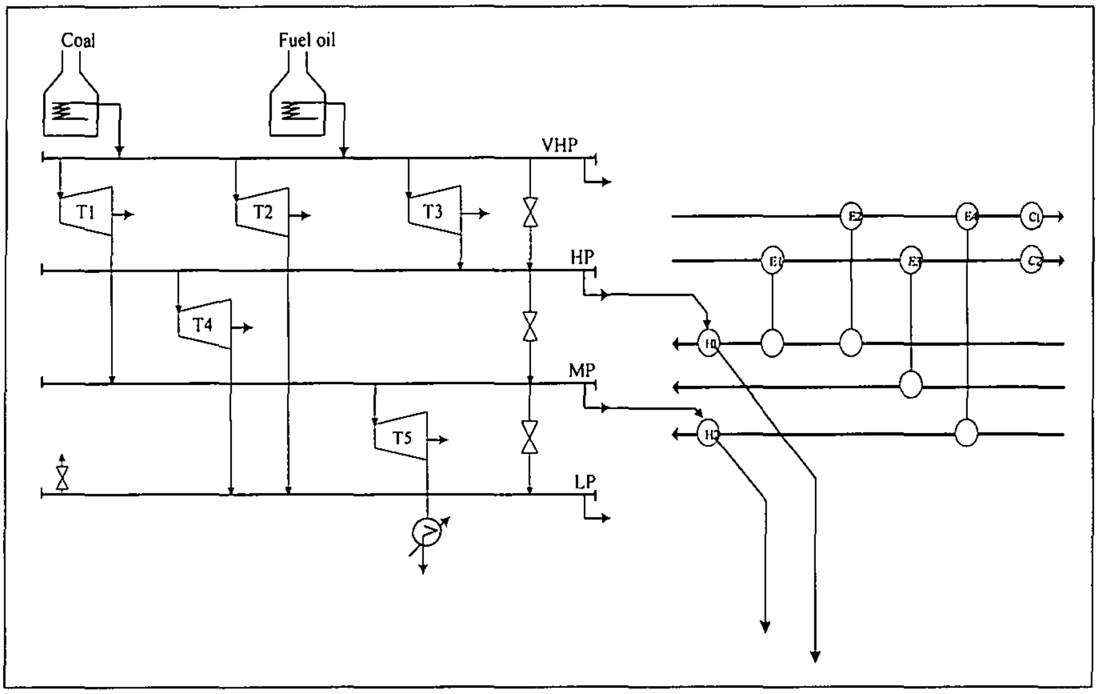

Fig 4.11: Integrated HEN and utility system

4.3.1 Heat flow paths in the utility system case study

As discussed earlier, current and optional heat flow paths could be identified in the utility system in order to manage the steam surplus derived from energy savings in the

HEN. According to the HEN retrofit approach presented in this work, only HP and/or MP steam consumption is decreased in the HEN case study. Accordingly, two current heat flow paths in the utility system could be identified as shown in Fig 4.12(a). For the HP steam savings, the current path transfers the excess HP steam from the HP steam header through turbine (T3) to create steam surplus in the VHP steam header. Meanwhile, the excess steam derived from the MP steam savings is transferred using another current path from the MP steam header through turbine (T1) to create steam surplus in the VHP steam header. The turbine flow constraints must be considered while transferring the steam from header to header.

After the surplus steam is created in the VHP steam header using the current paths, the optional paths which are either power import or power export paths are used to manage the surplus. Fig 4.12(b) shows three power generation paths that could be used to redistribute the steam surplus in the utility system. The first power generation path transfers the steam surplus from the VHP header through turbines (T1) and (T5) to the condensate. The second power generation path redistributes the surplus from the VHP header through turbine (T2) and hence generates excess of LP steam which could either be vented through the venting valve or used by other process in the plant. The third identified power generation path is used to transfer the surplus from the VHP header to the condensate through turbines (T3) and (T5). Again, the turbine flow limitations must be considered while undertaking the steam redistribution process.

The current paths and the power generation paths are similar in terms of power generation although they run in opposite directions as shown in Fig 4.12. Using the current heat flow path decreases the power production while the power generation path increases the power production in the utility system.

The power import paths are the shortest heat flow paths in the utility system which is used to cut down the fuel firing in the boilers. As shown in Fig 4.12 (c), two power import paths are identified in the utility system case study to eliminate the VHP steam surplus by reducing the fuel firing. The first path is to cut the coal fired in boiler1, while the second one is to cut the fuel oil fired in boiler2.

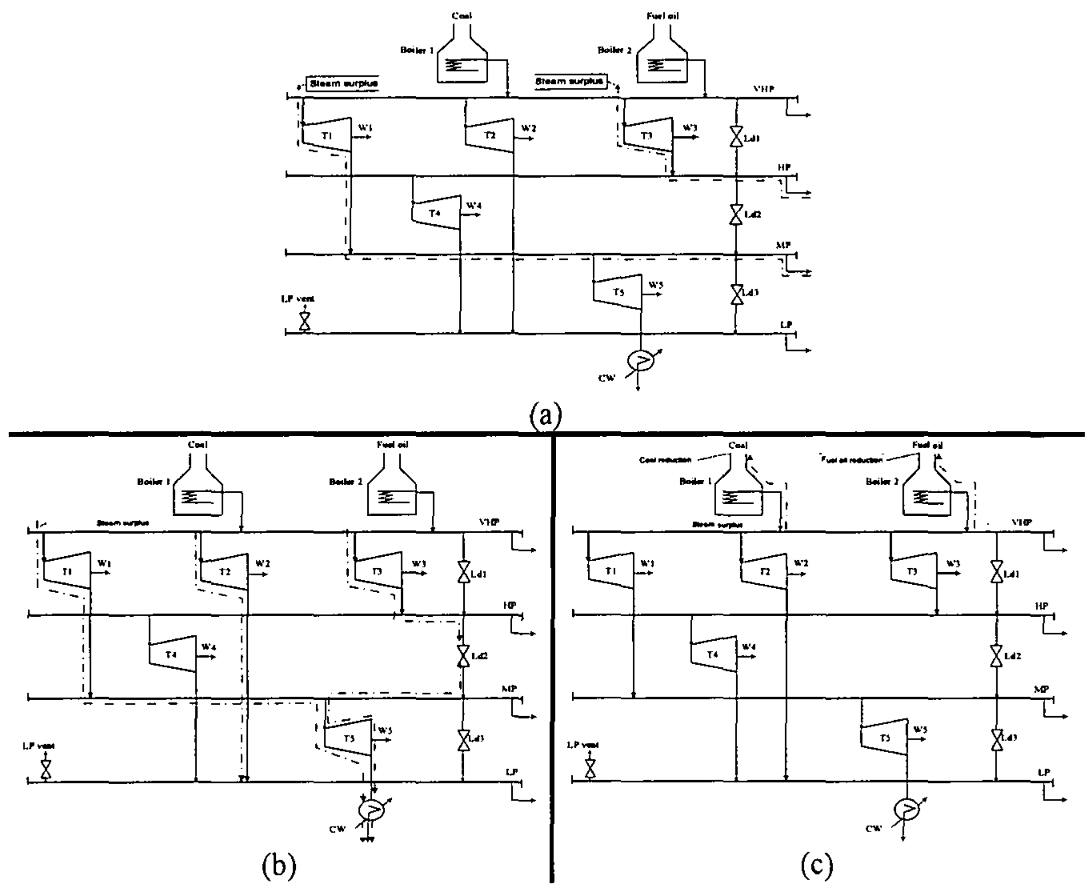

Fig 4.12: Heat flow path identification in the utility system case study
(a) Current paths, (b) power generation paths, (c) power import paths

From the various identified heat flow paths in the utility system, only the most efficient has to be carried forward for managing the surplus steam. Thereby, the efficiency for each path has to be calculated in order to pick the most efficient as described earlier.

4.3.2 Heat flow path efficiency for the utility system case study

It was discussed earlier that several HEN retrofit options have been generated using the paths combination approach. This implies that the amount of savings is different from retrofit option to another. Moreover, several heat flow paths have been identified in the utility system case study where each path features different flow constraints. To calculate the efficiency for the heat flow paths under these conditions, a constant base of comparison must be established. Therefore, a base of 25 t/h steam is assumed to flow through each path in the utility system.

4.3.2.1 Path efficiency results

The current and optional path efficiency is calculated using the fuel and power cost data provided in Table 4.2. According to the similarity between the current and power generation paths as shown in Fig 4.12, the efficiency for both could be found using the set of equations from (4.15) to (4.20) described in section (4.1.4.2) for either HP or Mp steam savings.

Based on the 25 t/h of steam flows in the path, the result of path efficiency for the current heat flow paths (η_{crnl}) is found to be 0.18 and 0.337 for the HP and MP steam savings, respectively.

Regarding the optional heat flow paths which comprise power generation and power import options, the path efficiency is also calculated to choose the best option to redistribute the surplus steam in the utility system. For the power generation option, three paths are identified in the utility system case study as shown in Fig 4.12(b). In the case of HP and/or MP steam savings, the power generation path efficiency for the three options is calculated using the same set of equations from (4.15) to (4.20). For the first power generation path which runs from the VHP steam header through turbines T1 and T5, the efficiency (η_{gen1}) is found to be 0.556 for either HP or MP steam savings. The efficiency for the second path (η_{gen2}) which links the VHP steam header with the LP steam header through turbine T2 is found to be 0.507 for either HP or MP steam savings. For the third power generation path which runs from the VHP header through turbine T3, letdown valve Ld2 and turbine T5, the efficiency (η_{gen3}) found to be 0.457 for either HP or MP steam savings.

The two identified power import paths are the shortest among the other heat flow paths in the utility system as shown in Fig 4.12. Therefore, the efficiency could simply be determined using equation (4.14) according to the provided fuel cost data in Table 4.2. For the first path which is used to cut the coal firing in boiler1, the power import efficiency (η_{imp1}) is found to be 0.14. On the other hand, the power import efficiency (η_{imp2}) for the second path which used to cut the fuel oil firing in boiler2 is determined to be 0.18.

For the sake of clear comparison, the path efficiency for all the specified heat flow paths in the utility system is shown in Fig 4.13 and Fig 4.14 for HP and MP steam savings, respectively.

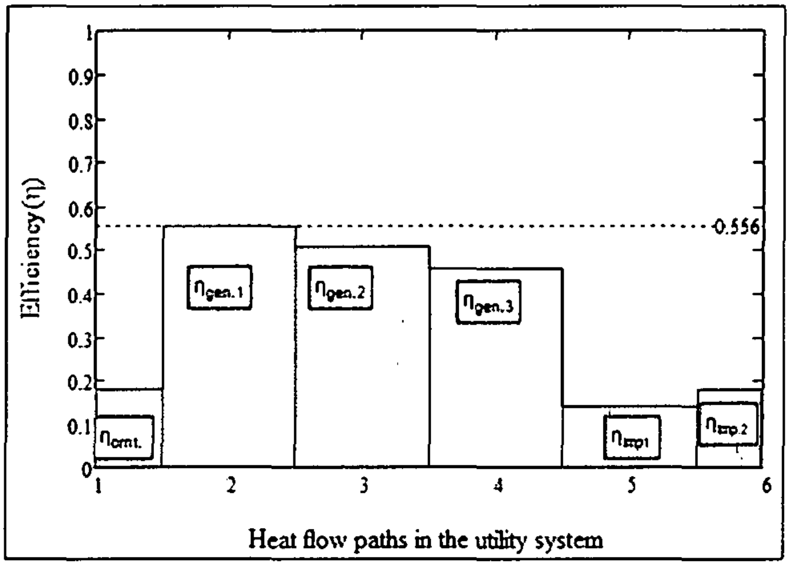

Fig 4.13: Heat flow paths' efficiency for 25 t/h of HP steam flow rate

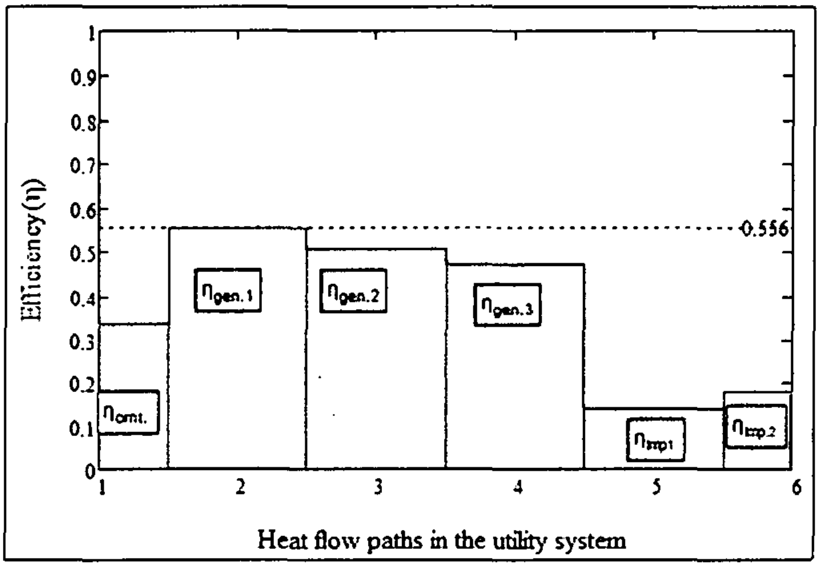

Fig 4.14: Heat flow paths' efficiency for 25 t/h of MP steam flow rate

From the figures above, it is obvious that the power generation paths are generally more efficient. Among the power generation paths, the first path is the most efficient and it is recommended for redistributing the surplus steam in the utility system while considering the turbines flow limitations.

4.4 Summary

The interaction between the HEN and the utility system is a common feature in the process plants where the utility system provides the processes with the required heat and power. The procedure to explore the HEN - Utility interaction is presented systematically in this chapter. Within the procedure, the power generation and the steam turbine model have been briefly highlighted. The energy savings derived from the HEN retrofit has been prepared in terms of steam savings (t/h) to cope with the steam flow in the utility system. The procedure to study the HEN-Utility interaction is based on the top-level analysis approach in which the path efficiency is introduced. Therefore, the impact of the derived savings from the HEN retrofit on the utility system could be properly managed. A simple example of the utility system has introduced to be integrated with the previously introduced HEN case study. The utility system has been comprehensively analyzed according to the proposed procedure. Among the specified heat flow paths, one of the power generation paths was found to be the most efficient to manage the surplus steam in the utility system, accordingly.

CHAPTER 5

RESULTS AND DISCUSSION

In chapter 3, the developed method of the *paths combination approach* for the HEN retrofit has been presented and thoroughly discussed. The essential objective of the developed method is to generate several retrofit options which involve area addition to the existing exchangers without topology changes in the HEN. Within the developed method and based on the plus/minus principle of Pinch Technology, the concept of stream temperature flexibility (TF) was also introduced to make the generated retrofit options more competitive in terms of energy savings. The application of the proposed method was demonstrated on a suitable HEN taken from the literature as shown in Fig 3.14 which was also presented and analyzed in chapter 3. According to the developed method, it was shown that 17 retrofit options could be generated for the HEN example. The initial data produced when applying the proposed method are mainly heat load and inlet/outlet temperature for the devices of HEN which were tabulated and placed in Appendix C. The results of tube side and shell side heat transfer coefficients were also placed in Appendix C.

In this chapter, the results of applying the method on the HEN example are comprehensively discussed and analyzed. The obtained results of energy consumption against the required heat transfer area before and after applying the TF concept is analyzed for all the generated retrofit options. For taking the right decision to select the best retrofit solution, the obtained results are analyzed economically in terms of investment cost, savings and payback period. The retrofit option(s) of high savings and low investment which result in a short payback period is/are considered to be promising retrofit solution(s).

The results of the HEN-Utility interaction are also analyzed in this chapter based on the path analysis in the utility system which was thoroughly discussed in chapter 4. A demonstration example for the utility system was presented as shown in Fig 4.10 to explain the impact of the HEN retrofit on the utility system. The HEN-Utility interaction results are mainly additional power production in the utility system because of HP and MP steam savings derived from the HEN retrofit.

5.1 Energy-area analysis for the entire options

Based on the HEN example which was introduced to demonstrate the proposed method, the 17 retrofit options identified have shown the heat recovery in the HEN to be increased at the expense of additional heat transfer area as shown in Fig 5.1 below:

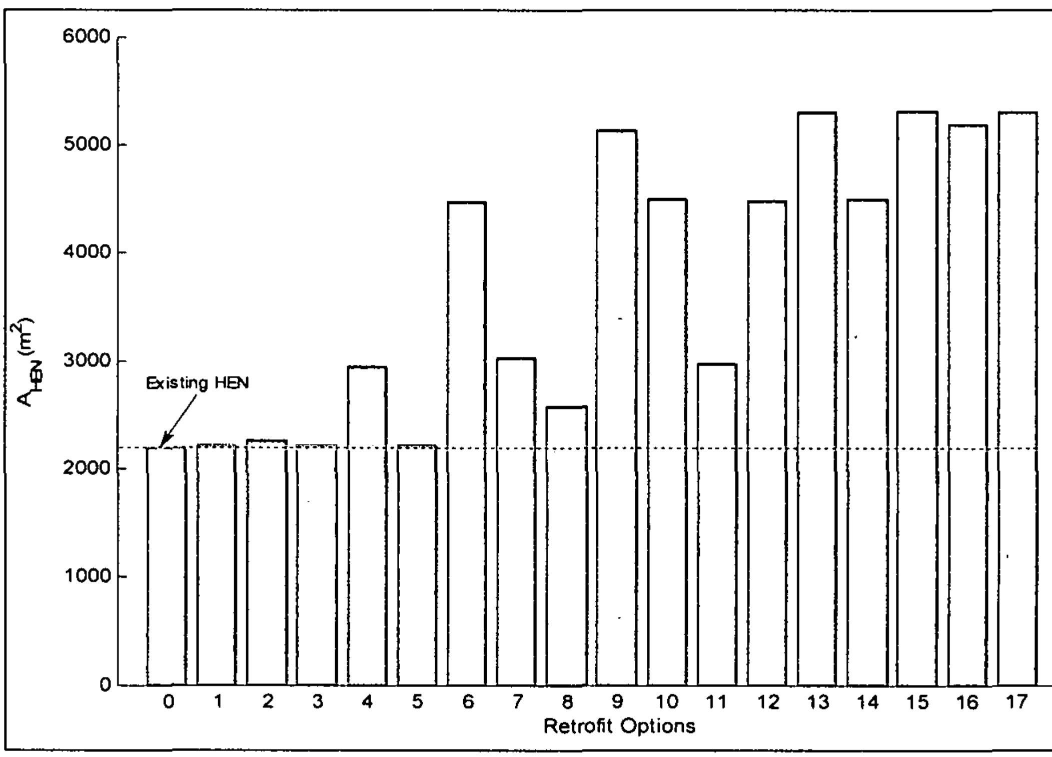

Fig 5.1: The penalty of adding new area for each retrofit option

Options 1, 2, 3 and 5, which involve only single paths, seem to be good retrofit solutions since they show only slight additional area requirement. Nevertheless, only a slight reduction in the energy consumption was attained using these options as shown in Fig 5.2 below:

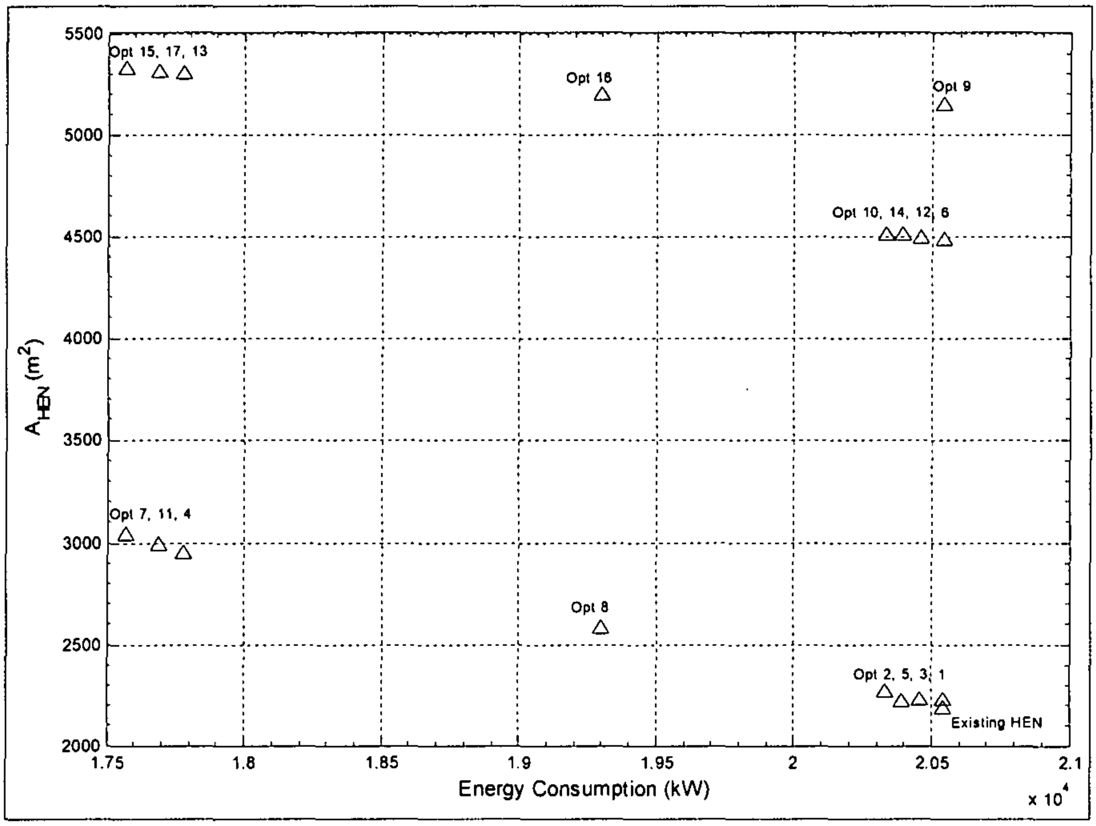

Fig 5.2: Energy consumption and area requirements for the entire retrofit options

The figure shows the required overall area for the HEN corresponding to the energy consumption for each option before applying the TF concept. The results can further change when the TF concept is applied as depicted in Fig 5.3.

5.1.1 Energy-area before applying the temperature flexibility

In the earlier discussion, 17 HEN retrofit options were identified for the demonstration example applied. When the retrofit options were plotted on the area vs. the energy consumption as shown in Fig 5.2 above, 4 groups of energy saving options and 3 individual options were located in different positions in the plot.

The existing energy consumption and HEN area is 20542kW and 2187m^2, respectively as marked in the figure. The first group which involves options 1, 2, 3 and 5 is located next to the existing HEN position. Option 1 in particular shows the same energy consumption as for the existing HEN since the heat load was shifted from cooler to cooler without increasing the heat recovery in the HEN. Although the additional HEN area required is quite small for the options of this group, it also results in minimal reduction in the energy consumption. Thus the options may not be optimal in view of the energy savings target required. The small reduction in the energy consumption is justified by the HRAT limitation which had been reached earlier while undertaking the heat load shifting from the HEN utilities as described in the proposed paths combination approach.

The second group of solutions contains options 6, 10, 12, and 14 which are located at the high energy consumption quadrant in Fig 5.2. This group shows high energy consumption similar to the previous group, but here at the expense of a higher overall area requirement which is about 4500 m^2. Option 6 from this group shows the same energy consumption as for the existing situation where the heat load was shifted from heater to heater without increasing the heat recovery in the HEN.

The third group of retrofit solutions involves options 4, 7 and 11 which are located in the lower energy consumption position in the figure. The overall energy consumption in the HEN using this group is shown to be in the range between 17500kW and 18000kW with a relatively low additional area of about 900m^2. Therefore, the retrofit solutions adopted by this group are considered to be very promising energy savings options even before assessing the amount of savings and investment costs.

The fourth group in Fig 5.2 contains options 13, 15, and 17 which are located in a position of preferably lower energy consumption similar to the third group. However, the overall area requirement is significantly higher compared to the third group. For the options involved in the fourth group, the economical assessment is needed in order to decide whether the retrofit solutions of the group are reasonable or not. The economical analysis is discussed afterwards in the present chapter.

Fig 5.2 also showed some options located at isolated points such as options 8, 9 and 16 and they are not within any of the groups discussed above. Among them, both options 8 and 16 are located in a position of relatively low energy consumption. However, option 16 shows a higher additional area requirement compared with option 8. Energy consumption for option 8 is shown to be around 19300kW with additional area of about 390m^2. Option 9 is located in the same line with option 1 and 6 where no energy consumption is featured similar to the existing HEN regardless of the additional area.

From Fig 5.2, it can be concluded that options 4, 7 and 11 which were involved in the third group are the best retrofit solutions where the energy consumption and the additional area requirements are at lower level. Option 8 is considered to be a reasonable solution where it shows a relatively low energy consumption but with small additional area.

5.1.2 Energy-area performance when introducing the temperature flexibility

In Fig 5.2 above, the retrofit options were located all over the various quadrants demonstrating the extent of the energy reduction possible with the additional area installed in the HEN. However, the effect of the HEN stream temperature flexibility (TF) was not considered. In this section, the impact of increasing and/or decreasing the hot and cold stream(s) temperature for further reduction in the HEN energy consumption is investigated. Fig 5.3 shows the profile of the energy consumption against the overall heat transfer area while applying the TF concept in the HEN for the entire retrofit options generated for the demonstrative example.

The options 1, 3, 5, and 9 shown earlier are ignored while exploring the TF concept because they are unable to undertake further reduction in the energy consumption unless some exchangers are removed from the HEN. The aim of the study is to maintain the existing HEN structure.

Fig 5.3 below shows different classification for the retrofit options to investigate the effect of the TF on the energy consumption in the HEN. The classification depends on the level of the overall heat transfer area required before applying the TF concept in order to simplify the way of comparison. The retrofit solutions that required the same range of heat transfer area are put together in one group as shown in Table 5.1. The profile of energy consumption against the A_{HEN} within the range of TF (from 0°C to 10°C) for each group of the retrofit solutions is plotted together in separate quadrants in Fig 5.3.

Table 5.1: Classification of the HEN retrofit options before applying the TF

	The retrofit options	A_{HEN} ***(m²)***
Group (1)	2, 4, 7, 8, 11	2250 - 3050
Group (2)	13, 15, 16, 17	5302 - 5322
Group (3)	6, 10, 12, 14	≈ 4500

Generally, further reduction in energy consumption is possible when applying the concept of temperature flexibility (TF) at the expense of a further slight increase in the additional area requirements as shown in Fig 5.3 below:

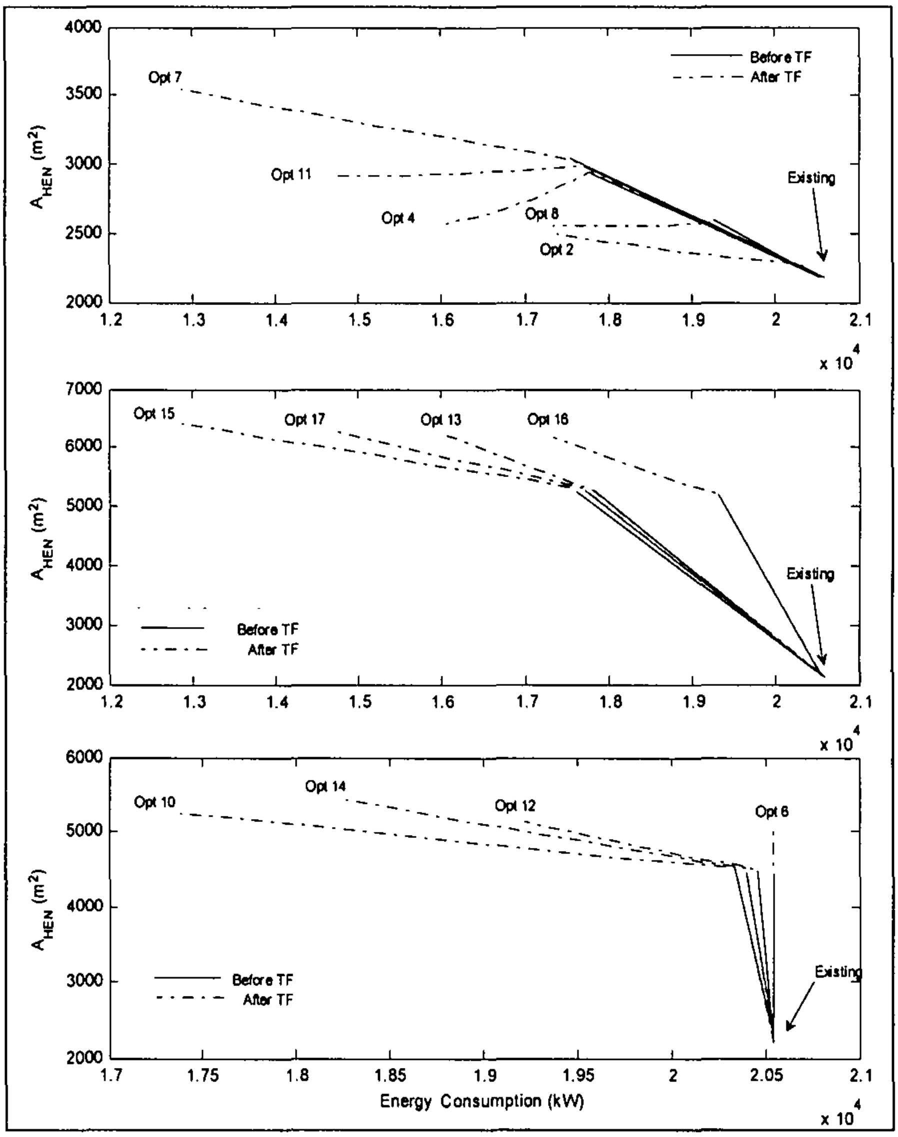

Fig 5.3: Energy - area profile under the effect of temperature flexibility for the entire retrofit options.

The detailed discussion on the TF effect for the retrofit options which are classified in groups as shown in Table 5.1 and plotted in the above figure is provided below.

The profile of energy vs. A_{HEN} with increasing the TF range for group (1) which involves options 2, 4, 7, 8 and 11 is plotted in the top quadrant of Fig 5.3. The options 2 and 7 from this group showed a similar trend when subjected to the TF where energy consumption decreased further with a slight increase in the overall HEN area. Although option 7 shows a similar trend as option 2, the reduction extent of the energy consumption was found to be higher along the TF range of 10°C. In contrast to options 2 and 7, options 4, 8, and 11 show a different trend where the A_{HEN} decreases when applying the TF to reduce the energy consumption in the HEN. This performance is considered to be attractive, especially that which is shown for options 4 and 11 where the A_{HEN} noticeably decreases along the TF range. Decreasing the A_{HEN} together with the energy consumption can be justified by rearranging the inlet and outlet temperatures of the HEN devices which lead to affecting the heat transfer area requirement for each exchanger on the HEN while applying the TF. The results of group (1) are summarized in Table 5.2 for the selected TF range values below:

Table 5.2: Energy consumption and A_{HEN} for group (1)
(referring to Fig 5.3)

Options	Before TF		After TF			
	TF range = 0 °C		TF range = 5 °C		TF range = 10 °C	
	E (kW)	A_{HEN} (m^2)	E (kW)	A_{HEN} (m^2)	E (kW)	A_{HEN} (m^2)
2	20334	2270	18854	2372	17374	2495
4	17778	**2946**	16914	**2708**	16050	**2566**
7	17570	3034	15226	3280	12882	3540
8	19298	**2580**	18316	**2554**	17334	**2549**
11	17692	**2984**	16208	**2931**	14724	**2910**

The TF effect on the area-energy performance for the retrofit options listed in group (2) as shown in Table 5.1 is plotted in the middle quadrant of Fig 5.3 as shown above. The observed trend of further reduction in the energy consumption at the expense of slight increase in the HEN area could be seen while increasing the TF range.

The performance in energy consumption by the options in group (2) is comparable to each other before the TF was applied. However, after the TF was introduced based on almost similar area addition, the reduction in energy consumption differs appreciably. Option 15 was found to be the best within this group after the TF concept was applied, followed by options 17 and 13 with option 16 being the worst retrofit solution.

The results of energy consumption and overall HEN area requirements for the retrofit options listed in group (2) are summarized in Table 5.3 for selected TF ranges as shown below:

Table 5.3: Energy consumption and A_{HEN} for group (2)
(referring to Fig 5.3)

Options	Before TF		After TF			
	TF range = 0 °C		TF range = 5 °C		TF range = 10 °C	
	E (kW)	A_{HEN} (m^2)	E (kW)	A_{HEN} (m^2)	E (kW)	A_{HEN} (m^2)
13	17778	5302	16914	5747	16050	6226
15	17570	5322	15226	5863	12882	6409
16	19298	5196	18316	5682	17334	6184
17	17692	5310	16208	5788	14724	6283

Group (3) is the last group of the retrofit solutions that could be observed. This group contains options 6, 10, 12 and 14 which are plotted in the lower quadrant of Fig 5.3. The energy consumption using these options is comparable with only a slight difference in the HEN area requirement. After subjecting the options to the TF, it was found that option 6 could not be considered further as the energy consumption stays the same as that of the existing situation in the HEN. The performance of option 6 is justified in that the heat load was shifted using this option from a heater using HP steam to another heater using MP steam in the HEN where the energy consumption is in terms of kW. Although, the right decision about option 6 could be made from the cost-wise analysis since the HP steam is more expensive than the MP steam. For the remaining options in group (3), option 10 is observed to have the best performance along the TF range for both area addition and reduction in energy consumption. The performance of area-energy along the TF range using option 14 from the group is moderate and then comes option 12 which the worst. The results of the energy consumption and overall area requirement in the HEN using the retrofit options listed in group (3) are summarized in Table 5.4 for selected TF ranges. Option 6 is crossed out since the energy consumption stays the same as with the existing HEN.

Table 5.4: Energy consumption and A_{HEN} for the group (3)
(referring to Fig 5.3)

Options	Before TF		After TF			
	TF = 0 °C		TF = 5 °C		TF = 10 °C	
	E (kW)	A_{HEN} (m^2)	E (kW)	A_{HEN} (m^2)	E (kW)	A_{HEN} (m^2)
~~6~~	~~20542~~	~~4482~~	~~20542~~	~~4757~~	~~20542~~	~~5064~~
10	20334	4502	18854	4872	17374	5246
12	20456	4490	19836	4797	19216	5121
14	20394	4508	19326	4950	18260	5420

5.1.3 Economical Analysis for the generated retrofit options

It has been stated earlier that several retrofit options were generated for the HEN demonstrative example using the developed paths combination approach. The obtained results using these options were analyzed previously in terms of energy consumption and the corresponding heat transfer area requirement in the HEN before and after applying the TF concept. In this section, the retrofit options will be analyzed economically where the investment cost ($) and the obtained savings ($/year) are considered in order to estimate the economic potentials of the obtained solutions before and after applying the TF concept. The trade-offs between the investment and the obtained savings should be made to determine the payback period for each retrofit solution. For the higher savings retrofit option(s), the shorter the payback period, the more economical the retrofit solution. The options of two years or less payback period are considered to be promising retrofit solutions by assuming a fixed energy price along the payback period. However, due to the energy market fluctuation, there might be redundant variations in the actual payback period.

5.1.3.1 Economic potential before applying the TF concept

Before applying the TF concept, the retrofit options for the HEN example which was discussed earlier, were plotted in Fig 5.2 to show the potential for reducing the overall energy consumption in the HEN at the expense of heat transfer area addition. For further analysis and assessment, the retrofit solutions provided by these options are plotted in Fig 5.4 to show the economic potential for each retrofit option before applying the TF concept.

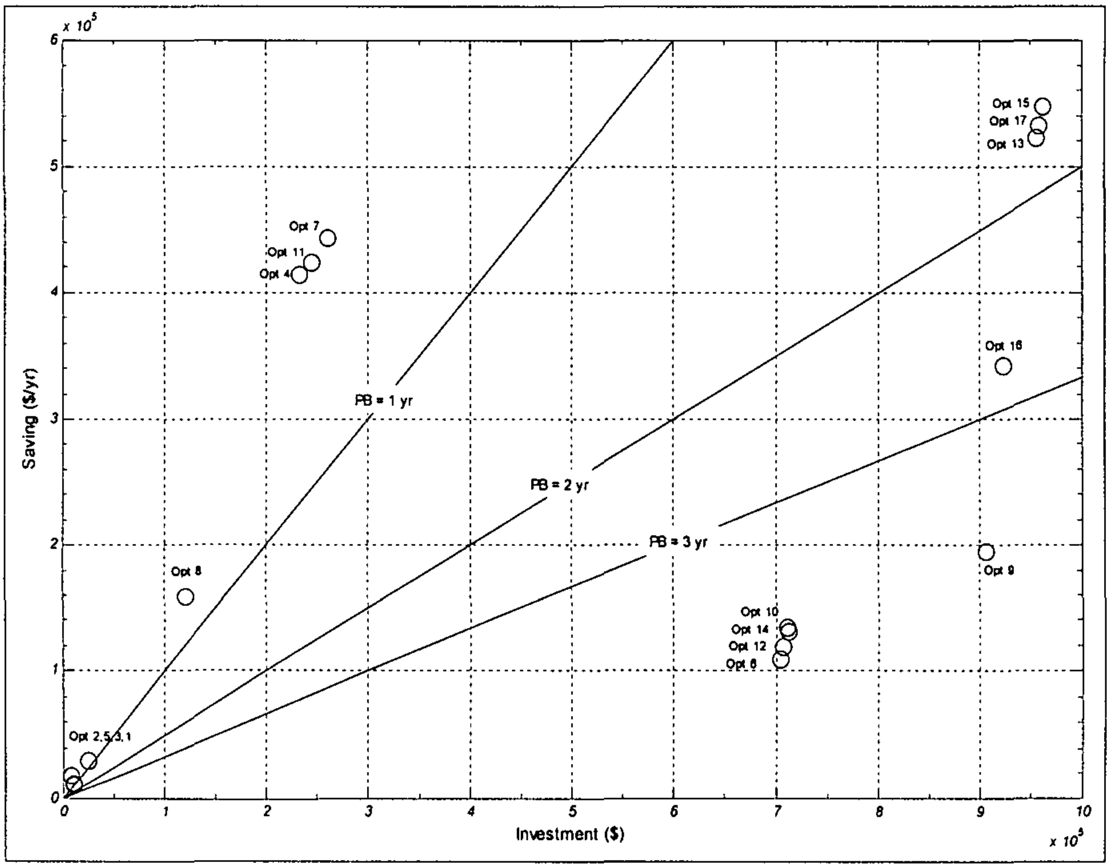

Fig 5.4: Representation of savings, investment and payback before applying the TF

The economic potential is explained here in terms of the obtained savings ($/year), the investment cost ($) and the payback period (year) for each option. The diagonal lines shown in the figure represent the payback period which are attained from the investment/savings ratio to classify the retrofit options to best, moderate and poor solutions. Accordingly, the options of high savings with less investment will be placed in the region of short payback period in the figure which is considered to be attractive.

The options 4, 7, 8 and 11 are placed in a region of less than 1 year payback period in Fig 5.4. Excluding option 8, these options are observed to be the best retrofit solutions where the savings obtained is shown to be high compared to the capital cost invested. Option 8 shows a moderate savings of 1.6×10^5\$/year which required an investment of 1.25×10^5\$.

From the figure, the highest savings obtained are shown to be for options 13, 15 and 17 which ranged between 5.2×10^5 to 5.6×10^5\$/year. However the capital to be invested is also shown to be high and it is recorded to be around 9.5×10^5 \$. On the other hand, the investment will be refunded quickly since the payback period is shown to be 1.8year. Therefore, each of these options is considered to be an attractive energy savings solution if the plant shareholders are able to invest 9.5×10^5\$ for the retrofit project.

Option 16 might be a reasonable retrofit solution if the plant shareholders would admit 2.7 years to be an acceptable payback period since the savings is relatively high. The remaining options showed a longer payback period which is more than 3 years and hence not to be considered for the retrofit.

Before applying the TF concept as shown in Fig 5.4, a decision could be taken for options 4, 7 and 11 followed by option 8 to cost-effective retrofit solutions for energy savings in the demonstrative HEN example. The additional area requirement for the HEN retrofit using these options is summarized as shown in Table 5.5 below:

Table 5.5: Retrofit Specifications Summary

Promising options	Additional area requirement [m^2]			
	E1	E2	E3	E4
4	162.995	0.0	597	0.0
7	166.569	50.376	597	32.657
8	122.514	-432.689	597	106.046
11	162.995	0.0	597	37.484

From the table, it is shown that the additional area requirement for exchanger E2 in the HEN using option 8 is negative which means subtracting area from the existing which was 588m^2. The expected configurations for the retrofitted HEN using options 4, 7, 8, and 11 are shown in Fig 5.5 below:

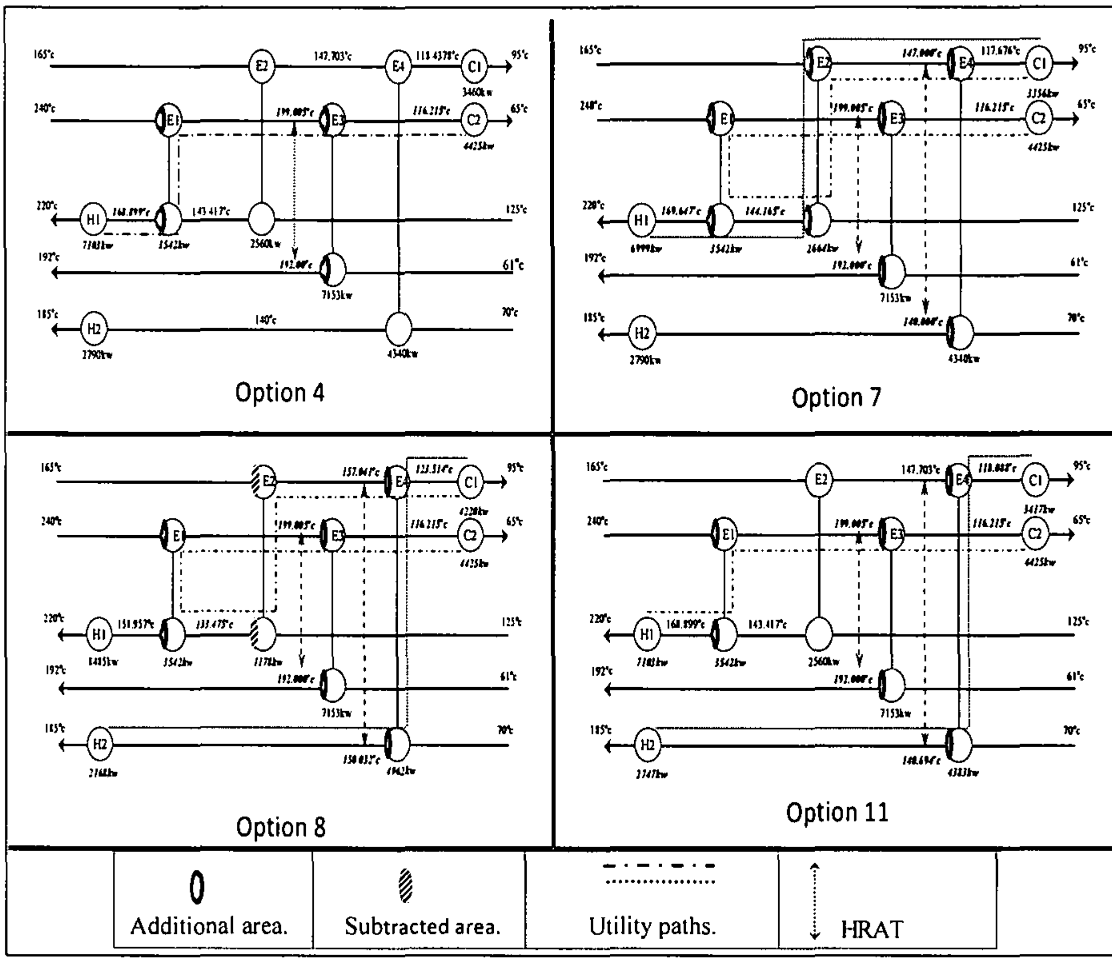

Fig 5.5: The HEN retrofits configurations using options 4, 7, 8 and 11

5.1.3.2 Economic Potential after applying the TF concept

From the above analysis before applying the TF concept, some of the retrofit solutions were economically unattractive where the saving obtained was relatively low compared to the invested capital which results in a long payback period. In particular, the options 6, 10, 12, 14 and 16 displayed a payback period of more than 3 years which might not be affordable for the plant shareholders. Subjecting these options to the TF concept had increased their potential to further reducing the energy consumption with minor heat transfer area addition as shown previously in Fig 5.3. From an economic point of view, the amount of savings could be increased with a slight increase in the capital investment for further shortening the payback period.

It was also mentioned that some options such as 1, 3, 5 and 9 are not applicable for applying the TF concept unless topology changes are introduced to the HEN.

Since additional savings is always preferred within the allowable limits, the best retrofit options selected previously (options 4, 7, 8 and 11) could also be improved by taking the advantage of the TF concept. The economic potential when applying the TF concept for the HEN retrofit options is presented graphically as a performance of savings($/year), investment($), additional A_{HEN}(m^2) and payback period (year) along the TF range. The options of a similar trend profile along the TF range are analyzed together for the sake of comparison and decision making.

It is worth mentioning that equation (3.37) for calculating the investment which was described earlier in section (3.4) is an exponential relationship and hence the profile of the investment cost with the TF range is expected to be nonlinear. However, the nonlinearity trend will not be clear for most of the retrofit options discussed here due to the scaling limits where the proposed TF range is from 0°C to 10°C. Moreover, the investment and savings are sharing the same axes (Fig 5.6, Fig 5.8-Fig 5.15, Fig 5.17 andFig 5.19) which add to the scaling limits. To clarify the nonlinearity, the investment regression correlations are presented for the HEN retrofit options that applicable for TF concept as shown in Table (5.6) below:

Table 5.6: Investment profile correlation with TF range for the HEN retrofit options

Retrofit option	***Investment regression correlation***
(2)	$inv_{opt2} = -1.6783 \cdot \underset{range}{TF}^3 + 153.25 \cdot \underset{range}{TF}^2 + 5541.1 \cdot \underset{range}{TF} + 25406$
(4)	$inv_{opt4} = -27.622 \cdot \underset{range}{TF}^3 + 1004.1 \cdot \underset{range}{TF}^2 - 18925 \cdot \underset{range}{TF} + 232741$
(6)	$inv_{opt6} = 199.53 \cdot \underset{range}{TF}^2 + 15963 \cdot \underset{range}{TF} + 703620$
(7)	$inv_{opt7} = 83.566 \cdot \underset{range}{TF}^2 + 14685 \cdot \underset{range}{TF} + 259985$
(8)	$inv_{opt8} = -0.0301 \cdot \underset{range}{TF}^5 + 1.5388 \cdot \underset{range}{TF}^4 - 28.934 \cdot \underset{range}{TF}^3 + 411.82 \cdot \underset{range}{TF}^2 - 1879.9 \cdot \underset{range}{TF} + 120636$
(10)	$inv_{opt10} = 21.678 \cdot \underset{range}{TF}^2 + 22654 \cdot \underset{range}{TF} + 710207$
(11)	$inv_{opt11} = -4.6037 \cdot \underset{range}{TF}^3 + 262.3 \cdot \underset{range}{TF}^2 - 4424.8 \cdot \underset{range}{TF} + 244564$
(12)	$inv_{opt12} = 101.05 \cdot \underset{range}{TF}^2 + 18389 \cdot \underset{range}{TF} + 706457$
(13)	$inv_{opt13} = 213.75 \cdot \underset{range}{TF}^2 + 26284 \cdot \underset{range}{TF} + 955524$
(14)	$inv_{opt14} = 172.49 \cdot \underset{range}{TF}^2 + 26350 \cdot \underset{range}{TF} + 711697$
(15)	$inv_{opt15} = 40.559 \cdot \underset{range}{TF}^2 + 32983 \cdot \underset{range}{TF} + 961917$
(16)	$inv_{opt16} = 104.08 \cdot \underset{range}{TF}^2 + 29286 \cdot \underset{range}{TF} + 923202$
(17)	$inv_{opt17} = 99.417 \cdot \underset{range}{TF}^2 + 28909 \cdot \underset{range}{TF} + 957987$

5.1.3.3 Economical potentials with TF for the HEN retrofit using options 2 and 7

The retrofit using options 2 and 7 showed a similar trend of savings, investment, additional area requirement and payback period when applying the TF concept although they had different economic potentials before the application of the TF. Fig 5.6 shows the performance of the economic potential for options 2 and 7 along the TF range of 10°C.

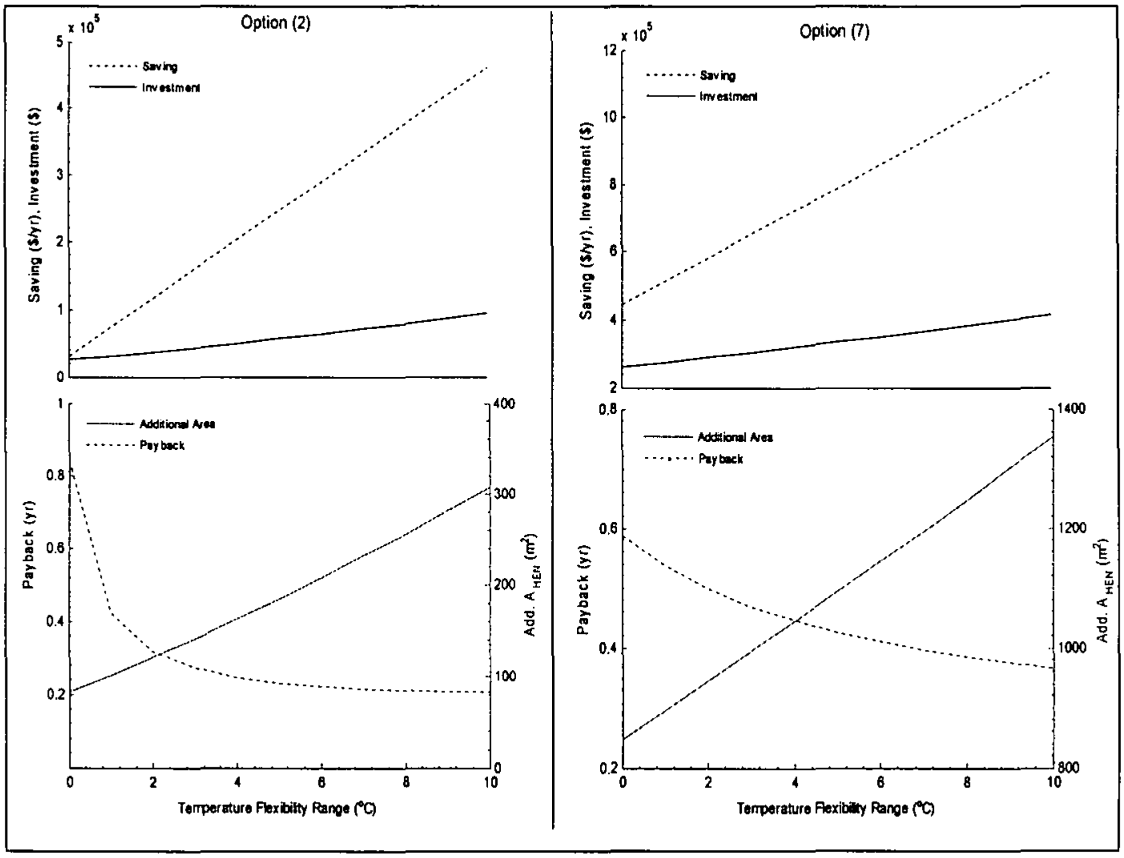

Fig 5.6: Economic profile with TF range for options 2 and 7

From the previous analysis before applying the TF concept, it was shown in Fig 5.4 that the savings obtained in the HEN using option 2 was very low regardless of the low investment required. The economical performance as illustrated in Fig 5.6 above showed the savings to increase rapidly when subjecting option 2 to the TF concept. Meanwhile, the capital investment shows a slight increase due to the small amount of additional area needed at each TF range. The additional overall HEN area has increased from about 85m^2 before TF to almost 310m^2 at the TF range of 10°C as shown in the figure. Consequently, the payback has rapidly dropped at the first two steps of TF range from 0.85 year to reach approximately a steady state of 0.2 year at only 5°C of the TF range.

For option 2, lowering the payback is not a target by itself since it was already low before the TF application, but increasing the savings as much as possible is optimistic within the TF limits. Moreover, it must be mentioned that option 2 involves only a single utility path as demonstrated earlier which implies the simplicity of the retrofit implementation where fewer exchangers will be affected.

The HEN retrofit using option 7 shows an attractive economic performance as shown in Fig 5.6. The savings obtained using this option has significantly increased along the TF range at the expense of a minor increase in the investment because of the slight increase in the required area addition. The area addition is found to be of around 500m^2 at 10°C of TF range. Therefore, the payback has steadily dropped from about 0.6 year before the application of the TF to 0.36 year at the end of the TF range.

The economic potential performance for the retrofit using options 2 and 7 for the HEN demonstrative example is summarized and compared for different TF ranges as shown in Table 5.7 below:

Table 5.7: Economic potentials summary for option 2 and 7 with TF consideration

Option	2			7		
TF range (°C)	0	5	10	0	5	10
Saving ($/yr)	30.25K	245.5K	460.8K	443.7K	788.2K	1133K
Investment ($)	25.47K	56.77K	94.51K	259.9K	335.4K	415.2K
Payback (yr)	0.842	0.231	0.205	0.586	0.426	0.366
ΔA_{HEN} (m^2)	83	185	308	847	1093	1353

Since the target is to increase the savings in the HEN by applying the TF concept for the options of a short payback period, option 2 at the TF range of 10°C looks to be better than option 7 at 0°C of the TF range. That is because; the savings achieved for option 2 at this stage is better than it is for option 7 before the TF has been applied where less area penalty is shown in the table. However, this could only be considered if the maximum range of the TF which is 10°C is applicable. Moreover, option 2 involves only a single utility path as mentioned earlier which requires less effort for the retrofit to be implemented. The expected configuration of the retrofitted HEN using option 2 at 10°C of the TF range is shown in Fig 5.7 below:

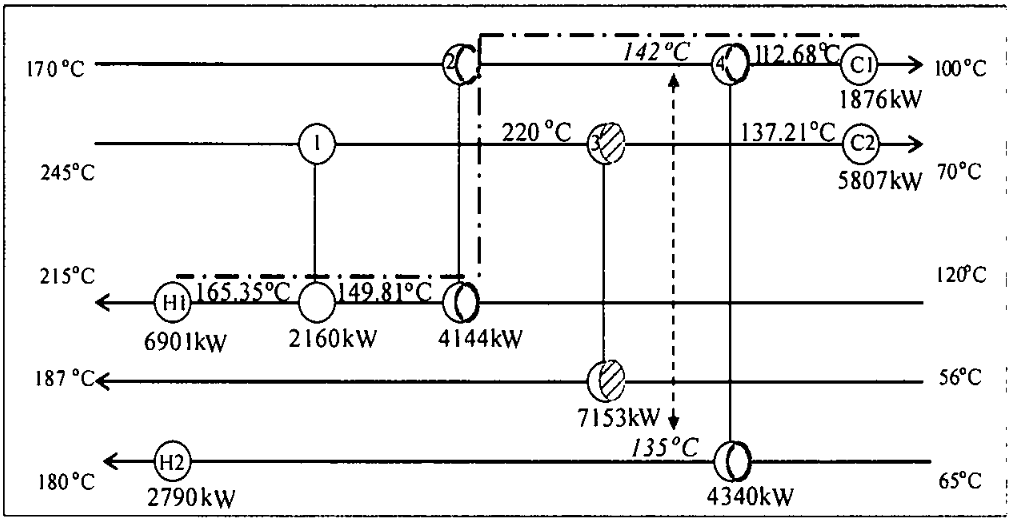

Fig 5.7: Retrofitted HEN Using Option 2 at TF range of 10°C

5.1.3.4 Economical potential with TF for the HEN retrofit using options 4, 8 and 11

As stated earlier, the retrofit for the HEN demonstrative example using options 4, 8 and 11 was considered to be economically attractive even before introducing the TF concept. However, further savings are always preferred where applicable within the provided TF ranges.

The potential for reducing the energy consumption in the HEN using options 4, 8 and 11 was previously discussed. It was shown that the reduction in the energy consumption was progressively decreased along the TF range with minor reduction in the heat transfer area as was shown earlier in Fig 5.3. The same attractive trend is featured for the economic performance of the retrofit using these options when introducing the TF concept. In general, the obtained savings is shown to increase progressively with a slight decrease in the investment while the TF range increases as shown in the Fig 5.8 to Fig 5.10 for options 4, 8 and 11. The investment decreases because of the reduction in the additional area requirements. Consequently, the payback period is rapidly dropped along the TF range as shown in the figures.

The obtained savings is found to increase by more than 200K$/year along the TF range of 10°C for the retrofit using option 4 as shown in Fig 5.8 below. The investment is decreased by approximately 100K$ along the same TF range where the additional area requirement is shown to decrease from 760m^2 before the TF is applied to reach 380m^2 at 10°C of the TF range. Consequently, the payback period is steadily dropped by 0.39 year along the TF range.

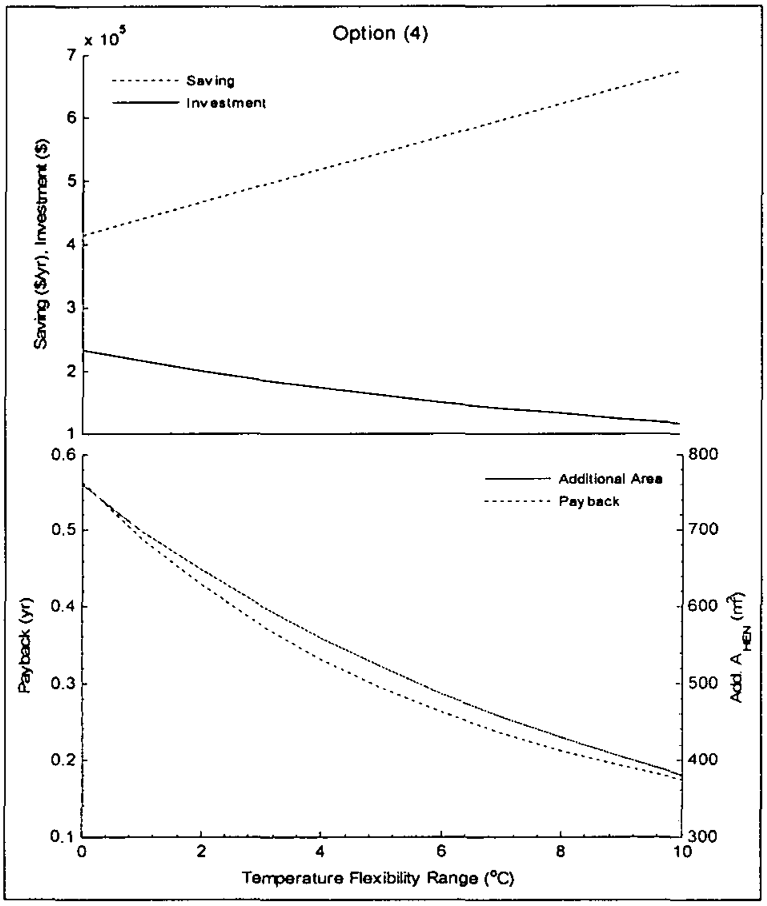

Fig 5.8: Economic performances for the HEN retrofit using option 4 with TF

The economic performances for the HEN retrofit using option 8 when applying the TF concept is shown in Fig 5.9 below. Generally along the TF range, the saving potential using option 8 performed better than it did for option 4. This is explained by the high acceleration of the saving incremental increase adopted for option 8. From 160K$/year, the saving has increased 2.5 times to reach the value of 400K$/year where the investment looks to be almost constant (ignorable decrease) along the TF range. The semi-constant trend of the investment is due to the additional area trend along the TF range as shown in the figure compared to that for option 4. Accordingly, the payback curve as shown in the figure has dropped down shortening the payback period by 0.22 year along the 10°C of the TF range.

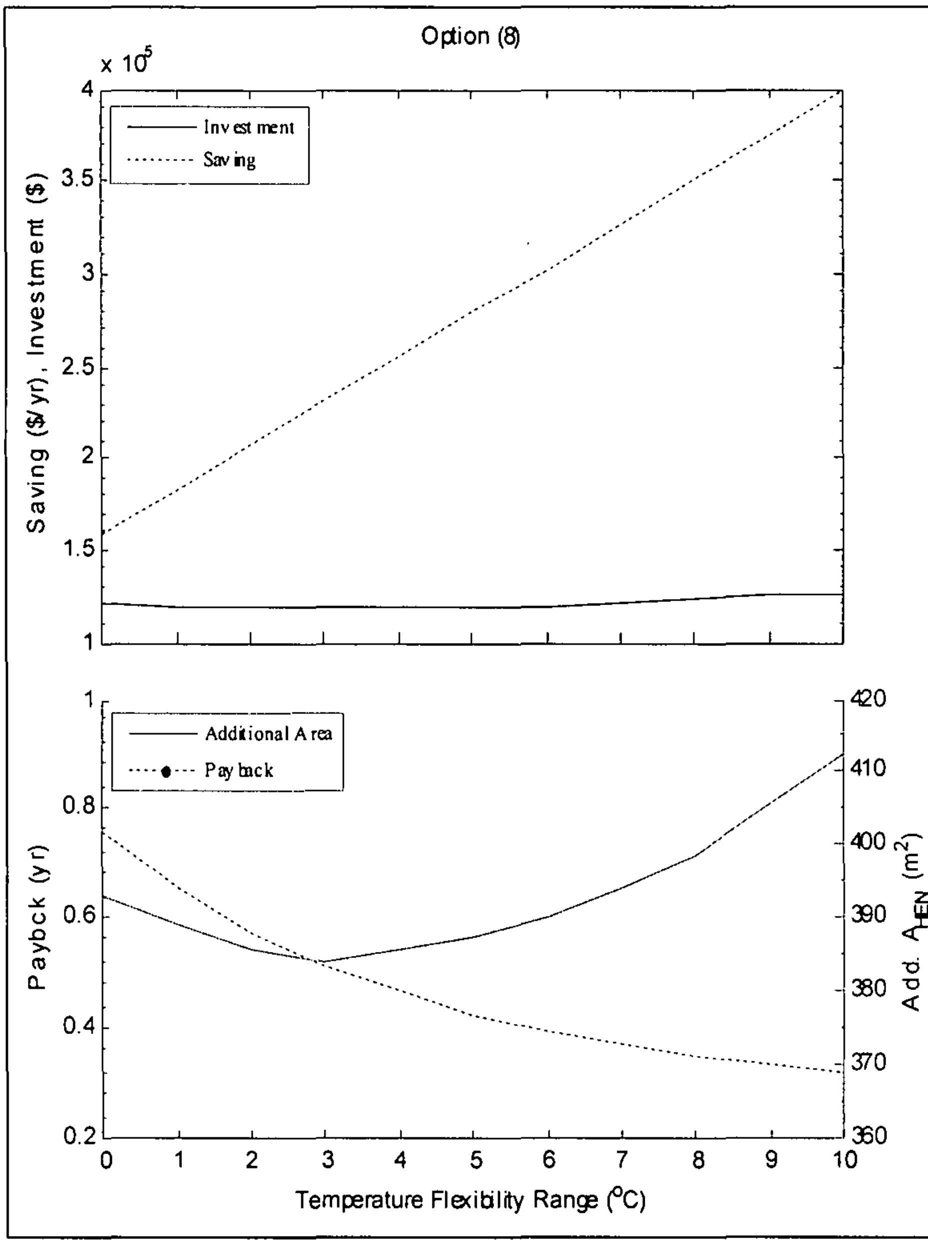

Fig 5.9: Economic performances for the HEN retrofit using option 8 with TF

Fig 5.10 below shows the economic profile for the HEN retrofit using option 11 while the TF range increases. The attractive savings which was 420K$/year before applying the TF concept has increased twice to reach the value of 820$/year at the end of the TF range. The investment has performed similar to option 8 which has slightly decreased due to the minor reduction in the additional area requirement along the TF range as shown in the figure. Consequently, the payback is shown to be reduced by 50% from 0.51 year to 0.25 year at 10°C of the TF range.

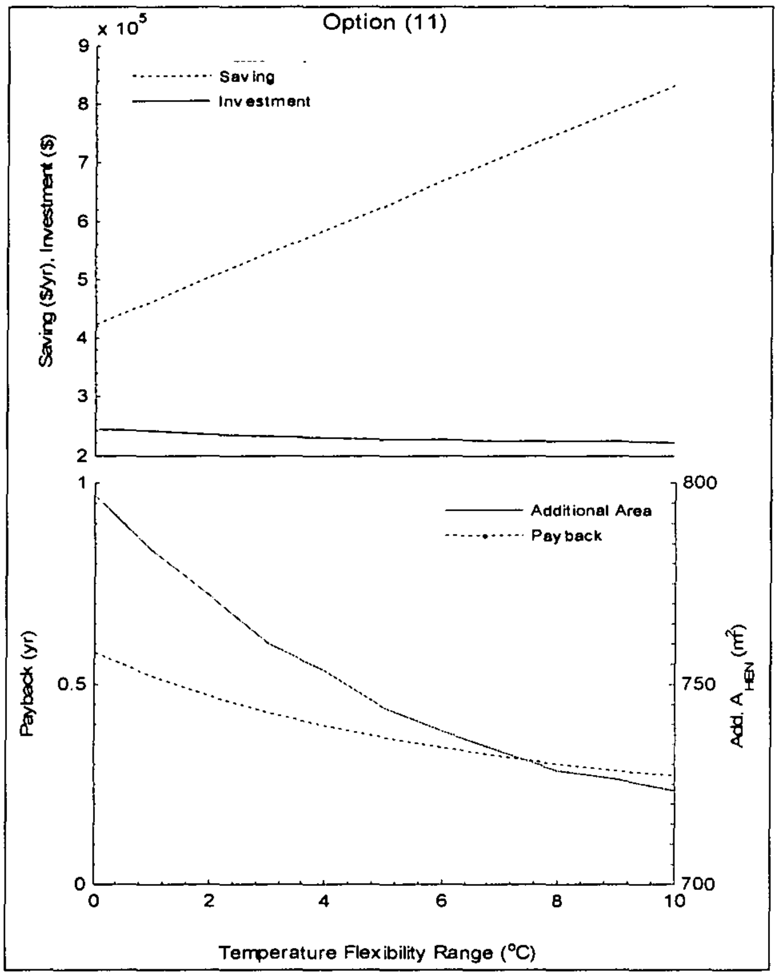

Fig 5.10: Economic performances for the HEN retrofit using option 11 with TF

For options 4, 8 and 11, it must be mentioned that the investment for each retrofit option is nearly same along the TF range while the saving is increasing dramatically resulting in a decreased payback period. The economic potential for these options when applying the TF concept is summarized in Table 5.8 for the sake of clarification and comparison.

Table 5.8: Economical potential summary for option 4, 8 and 11 with TF consideration

Option	4			8			11		
TF range (°C)	0	5	10	0	5	10	0	5	10
Saving ($/yr)	413.5K	542.7K	672K	159K	279K	399K	423.7K	626.4K	829K
Investment($)	232.9K	159.9K	116.3K	120.6K	112.6K	111.1K	244.6K	228.3K	222K
Payback (yr)	0.563	0.295	0.173	0.758	0.404	0.278	0.577	0.364	0.268
ΔA_{HEN} (m^2)	759	521	379	393	367	362	797	744	723

In general, both option 4 and 11 are shown to be better than option 8 before and after the TF is applied as detailed in the table above. The economic potential for the HEN retrofit using options 4 and 11 are found to have similar features before applying the TF concept, i.e. at TF = 0°C. When applying the TF concept, the retrofit using option 4 showed a better performance for the investment while the savings has increased with better performance for option 11 along the TF range. Although the payback is reduced along the TF range, it can be ignored here since it was less than 1year before applying the TF.

5.1.3.5 Economical potential with TF for HEN retrofit using options 13, 15 and 17

Before applying the TF concept, the options 13, 15, and 17 were placed in the same quadrant of economic results obtained for the HEN retrofit as shown in Fig 5.4 earlier. Generally, the retrofit using these options showed approximately similar performances when the TF applied as shown in the Fig 5.11 to Fig 5.13. Further energy savings is obtained along the TF range at the expense of investing more capital. The investment performance tends to increase due to the small amount of area addition at each step of the TF range. The payback period using these options is further reduced with the TF range progress although it was less than 2 years before introducing the TF concept as shown in the figures.

The economic performance using option 13 for the HEN retrofit along the TF range showed a progressive increase of both savings and the investment as illustrated in Fig 5.11 below. However, the payback period is shown to drop from 1.83 year to 1.45 year because the savings increases faster than the investment along the TF range.

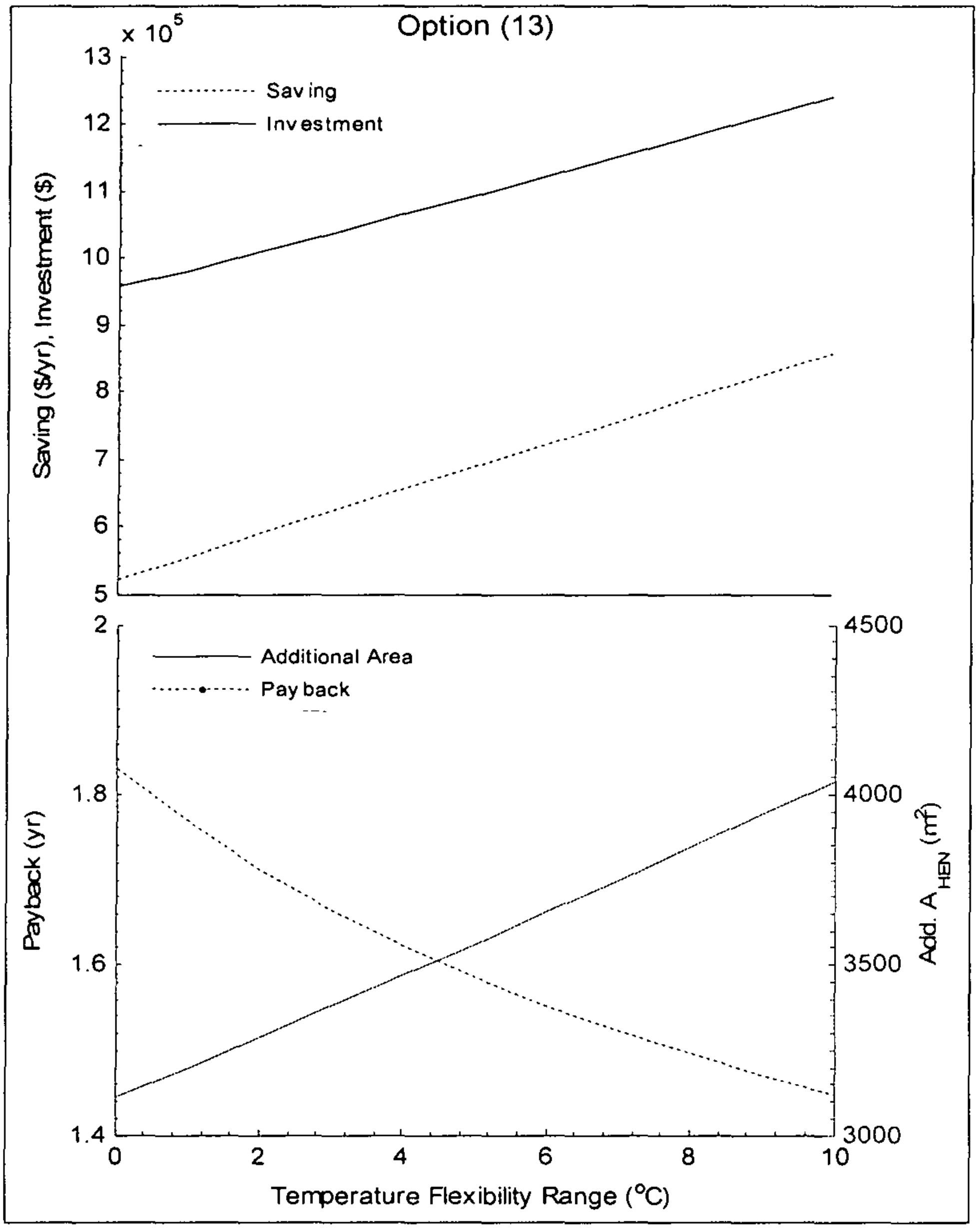

Fig 5.11: Economic performances for the HEN retrofit using option 13 with TF

From Fig 5.12 below, the HEN retrofit using option 15 shows an attractive economic performance when the TF is applied. The savings has increased progressively leading to a slight increase in the investment required along the TF range. The slight increase of the investment is justified by the minor area addition at each step of the TF range as shown in the figure. Consequently, the payback period has dropped dramatically from 1.75 year before applying the TF to reach 1.05 year at 10°C of the TF range.

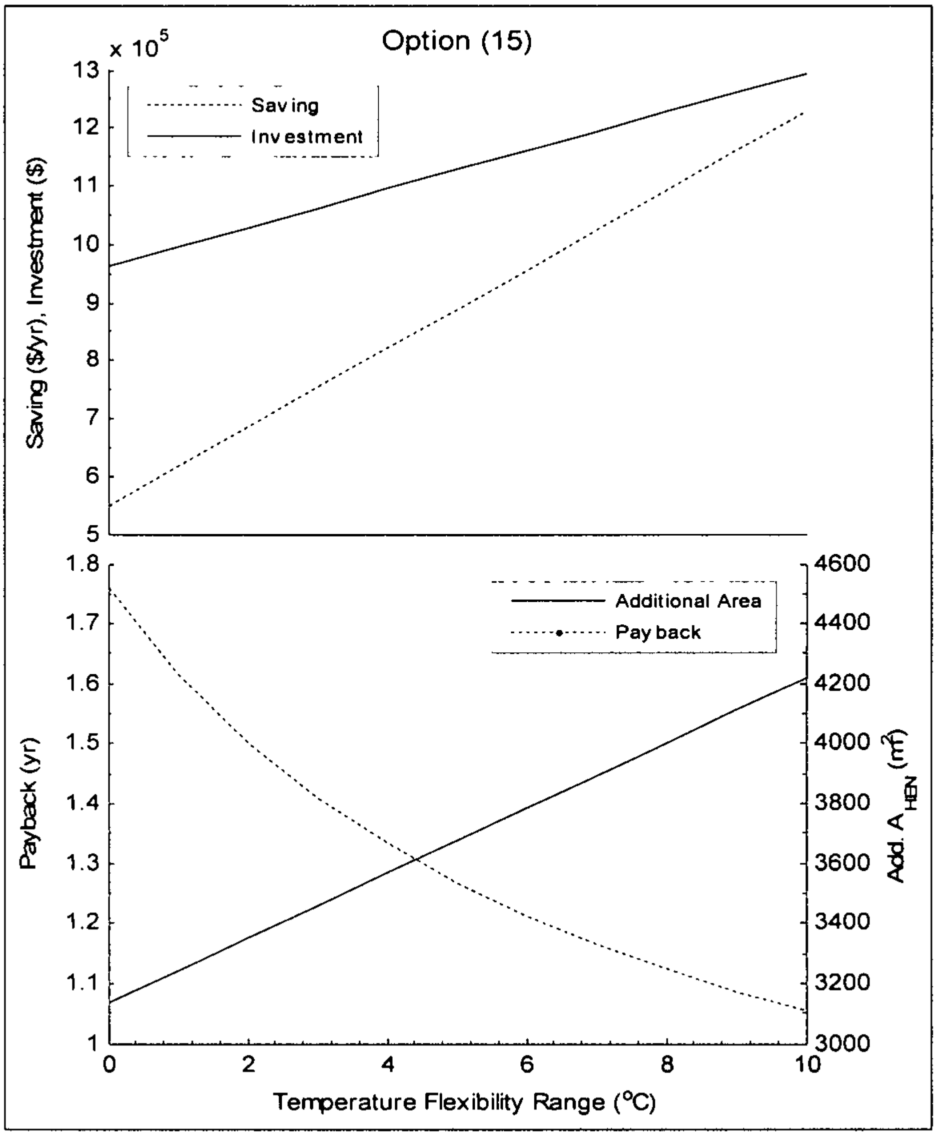

Fig 5.12: Economic performances for the HEN retrofit using option 15 with TF

Fig 5.13 below shows the economic performance of the HEN retrofit using option 17 when applying the TF concept. Similar to option 13, the savings profile along the TF range using option 17 has shown a progressive increase rate compared to the investment leading to a steep drop in the payback period due to the minor addition in the area requirement.

Although the general economic performance for the HEN retrofit using options 13, 15 and 17 with the TF range progress is almost similar, option 15 shows the best cost-effective retrofit profile.

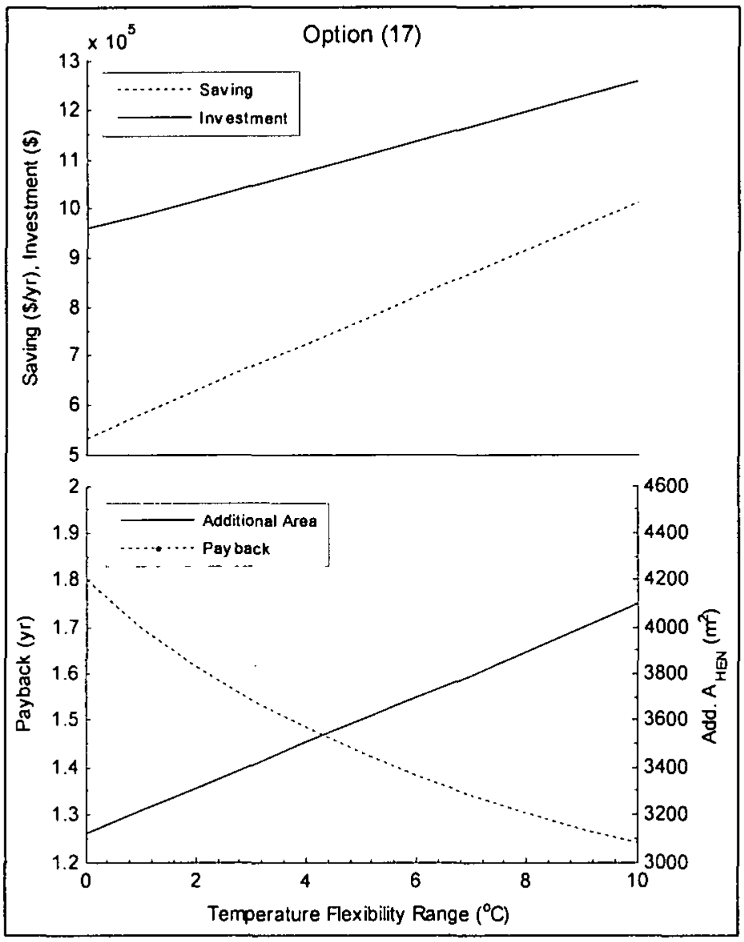

Fig 5.13: Economic performances for the HEN retrofit using option 17 with TF

For the sake of comparison and decision making, the economic performance of options 13, 15 and 17 along the TF range is summarized in Table 5.9 below:

Table 5.9: Economical potential summary for options 13, 15, and 17 with TF consideration

Option	13			15			17		
TF range(°C)	0	5	10	0	5	10	0	5	10
Saving ($/yr)	522.4K	689K	855.6K	547.1K	889.1K	1231K	532.6K	772.7K	1013K
Investment($)	955.8K	1092K	1239K	962K	1128K	1296K	958.3K	1105K	1257K
Payback (yr)	1.83	1.58	1.45	1.76	1.27	1.05	1.8	1.43	1.24
ΔA_{HEN} (m^2)	3115	3560	4039	3135	3676	4222	3123	3601	4096

As shown in the table, the economic potential using the three options have started from almost the same point before applying the TF concept (i.e. at 0°C of the TF range) which is economically feasible. Then the savings using option 15 has stepped up with relatively high acceleration compared to options 13 and 17 while the TF is progressing. Meanwhile, the investment for the three options is shown to increase slightly with a constant value along the TF range. Consequently, the payback period using option 15 is shown to have the best decreasing performance along the TF range.

5.1.3.6 Improving the economic potential for the infeasible retrofit options with the TF consideration

The previous analysis discussed the way of obtaining further savings although the HEN retrofit options were economically feasible before applying the TF concept. However, some of the obtained retrofit options using the developed paths combination approach were said to be unattractive due to the long payback period featured. For instance, the retrofit solutions adopted for options 6, 10, 12, 14 and 16 showed the payback period to be more than 3 years despite the reasonable savings obtained as shown earlier in Fig 5.4. The application of the TF concept has improved these options further towards increasing the savings and shortening the payback periods where applicable.

The HEN retrofit using option 6 was previously considered as an infeasible energy saving solution before and after the application of the TF concept when the analysis was based on the energy-area tradeoff as shown earlier in Fig 5.2 and Fig 5.3. However the energy saving solution offered by this option has improved in terms of economical potential by introducing the TF as shown in Fig 5.14. From the figure, the investment before applying the TF (at TF range =0°C) was shown to be 6.5 times the savings obtained which resulted in a long payback period of 6.5 years. Increasing the TF range has made the savings and the investment to increase in a semi-parallel trend as shown in the figure. Accordingly, the payback period has dropped slightly to 4.8 years at 10°C of the TF range which is still too long and it is yet to consider option 6 as a feasible energy saving solution.

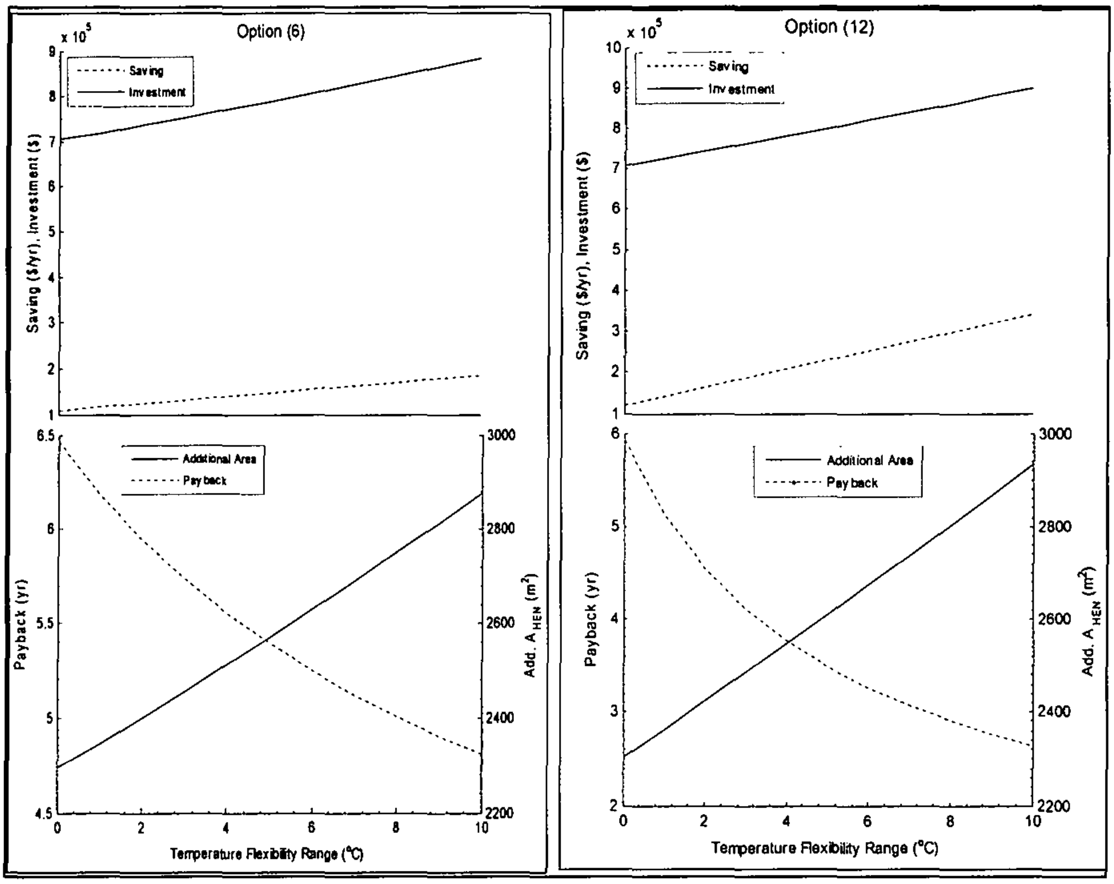

Fig 5.14: Improving the economic potential for options 6 and 12 with TF concept

The HEN retrofit using option 12 shows a similar performance as for option 6 as plotted in the same Fig 5.14 above. However, the savings profile using option 12 is shown to be more accelerated with TF range progress compared to option 6. Consequently, the payback period has dramatically fallen from 5.9 years to 2.63 years within the range of 10°C of the TF which might be acceptable for the plant shareholders.

Before introducing the TF concept, options 10, 14 and 16 for the HEN retrofit were shown earlier in Fig 5.4 to investigate their economic potential. The options showed a moderate savings at the expense of a relatively long payback period which was around 2.7 years for option 16 and more than 3 years for options 10 and 14. Accordingly, the application of the TF has made these options more competitive by improving the economic potential to be within the zone of 2 years payback period. The economic performance when applying the TF concept is shown in the Fig 5.15,Fig 5.17 andFig 5.19 for options 10, 14 and 16, respectively.

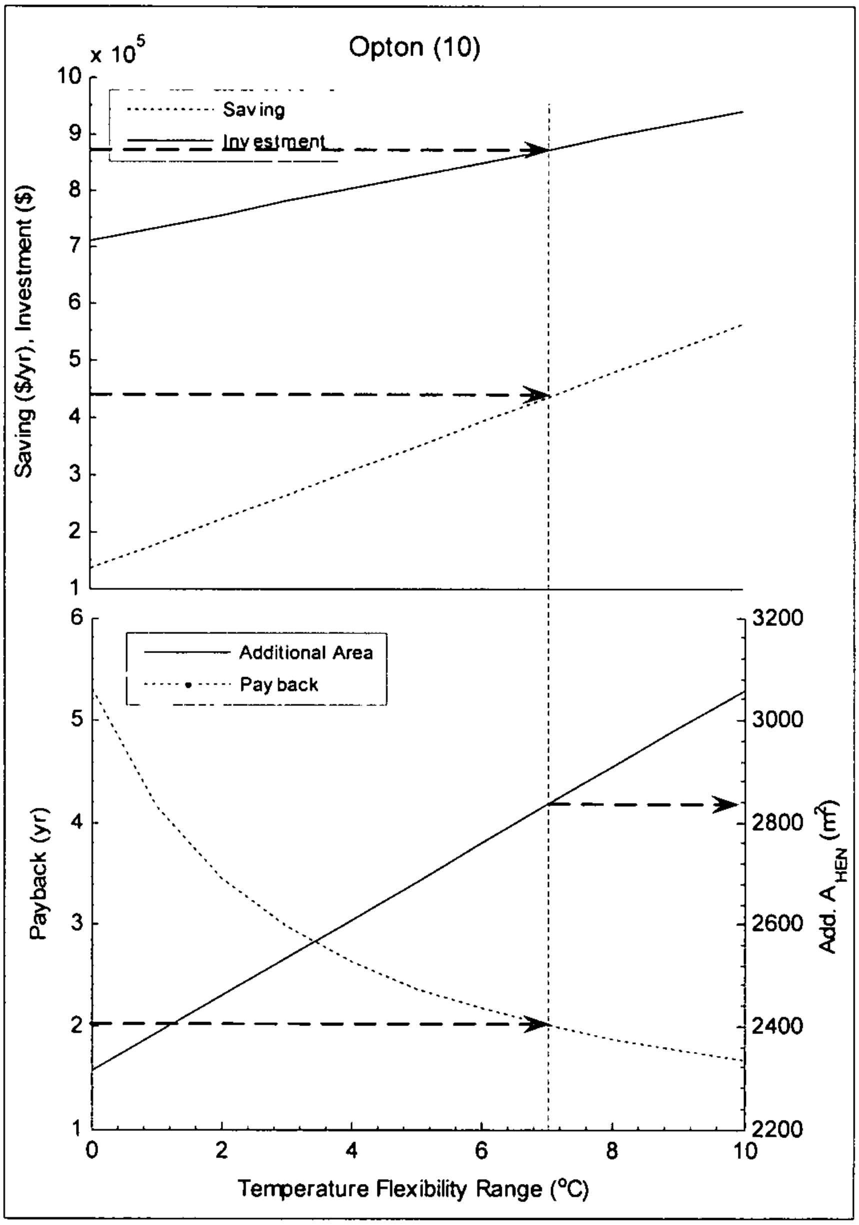

Fig 5.15: Improving the economic potential for option 10 with TF concept

As shown in Fig 5.15, using option 10 for the HEN retrofit before applying the TF (at TF range = 0°C), the savings obtained was only 135K$/year with 715K$ investment and 5.3 years payback period which is too long. When introducing the TF concept as shown in the figure, the payback period has reduced steadily to reach 2 years at 7°C of the TF range at the expense of a slight area addition. At this point, the amount of capital invested increased to 870K$ to obtain a savings of 435K$/year. The TF range of 7°C is to be applied according to the alternatives shown in Table 3.2 presented in section (3.3.3). The expected configuration of the retrofitted HEN using option 10 together with applying the TF concept is shown in Fig 5.16 below:

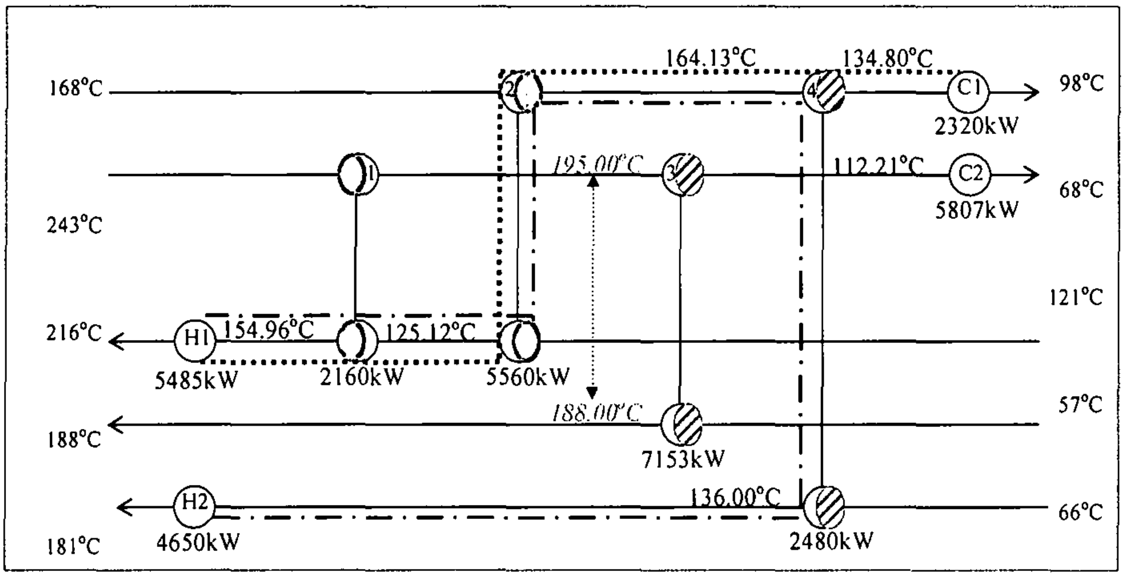

Fig 5.16: Configuration of the retrofitted HEN using option 10 at 7°C of the TF range

The economic performance of the HEN retrofit option 14 against the TF range is plotted in Fig 5.17. The economic potential without considering the TF was shown to be far from the promising zone for this option which has been further improved with the TF application as shown in the figure. The payback period has shortened to 2 years at 9°C of the TF range. From 0°C to 9°C of the TF range, the savings has increased from about 130K$/year to 510K$/year with a corresponding increase in the investment from about 720K$ to 970K$ due to the additional area of 3150m^2. The expected configuration of the retrofitted HEN using option 14 at the point of 2 years payback period is shown in Fig 5.18. The TF range of 9°C could be applied according to the TF alternatives provided in Table 3.2 presented in section (3.3.3).

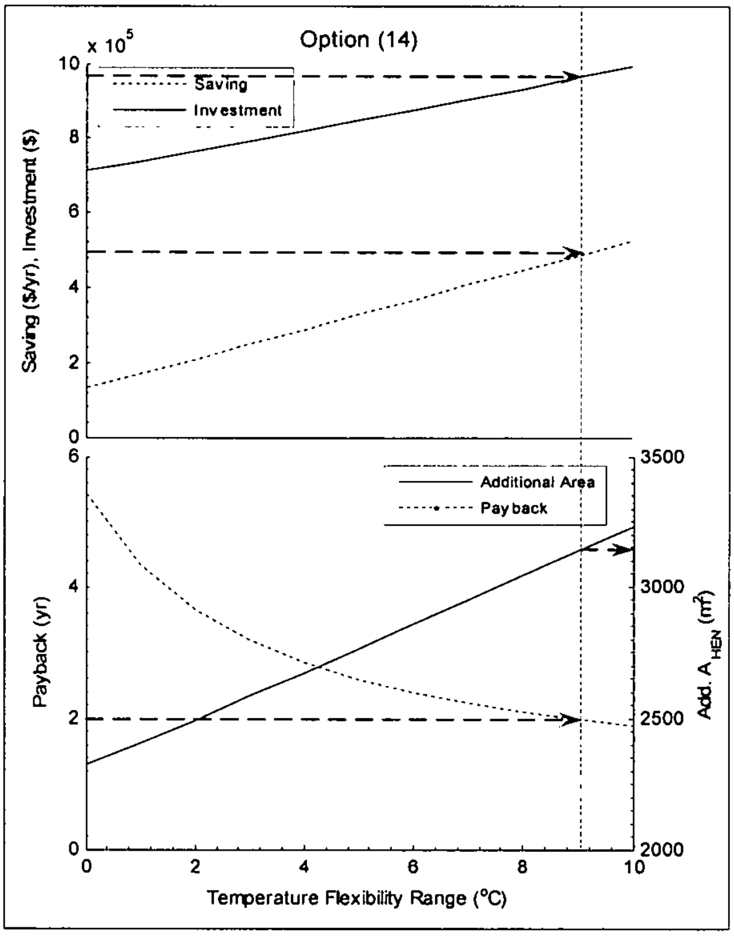

Fig 5.17: Improving the economic potential for option 14 with TF concept

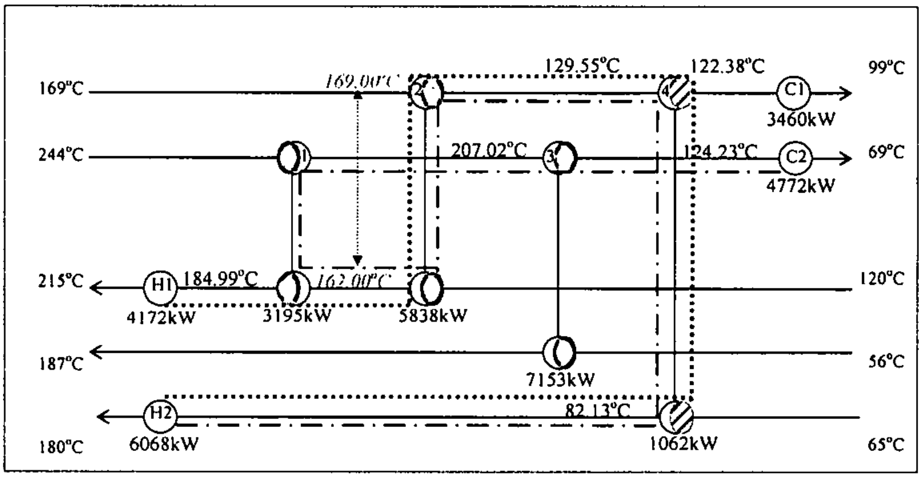

Fig 5.18: Configuration of the retrofitted HEN using options 14 at 9°C of the TF range

Before the TF was introduced, the HEN retrofit using option 16 was previously stated to show a relatively long payback period although reasonable savings were obtained. For this option to be an attractive retrofit solution, the economic potentials have been improved further by considering the TF concept as shown in Fig 5.19. For instance, the savings is shown to increase from 340K$/year at a TF range of 0°C to 560K$/year at 6°C of the TF range to shorten the payback period to 2years. The corresponding investment at this point is shown to be 1120K$ due to the 3590m^2 additional area requirements as shown in the figure. The configuration for the expected retrofitted HEN using this option at 6°C is shown in Fig 5.20. The TF range is to be managed according to the TF alternatives shown earlier in Table 3.2 where applicable.

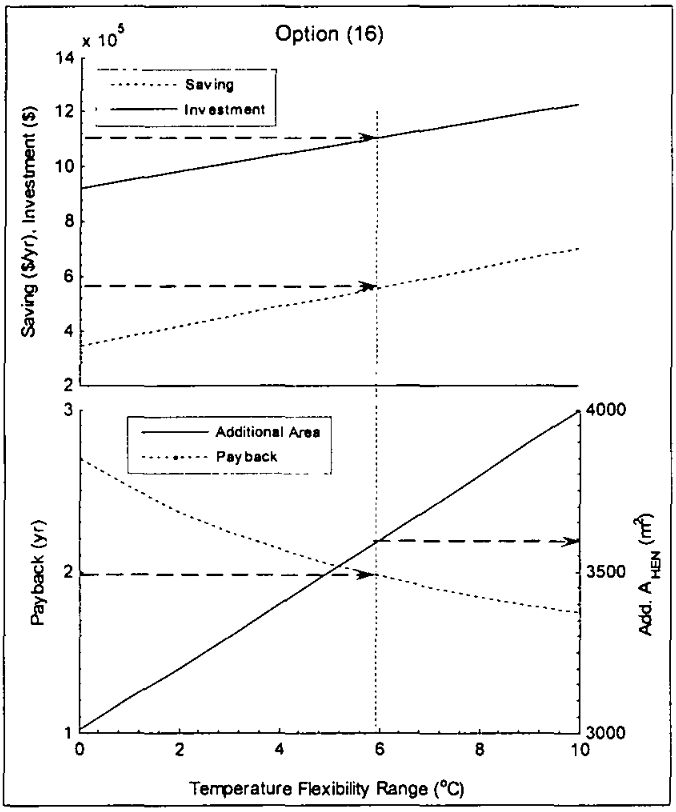

Fig 5.19: Improving the economic potential for option 16 with TF concept

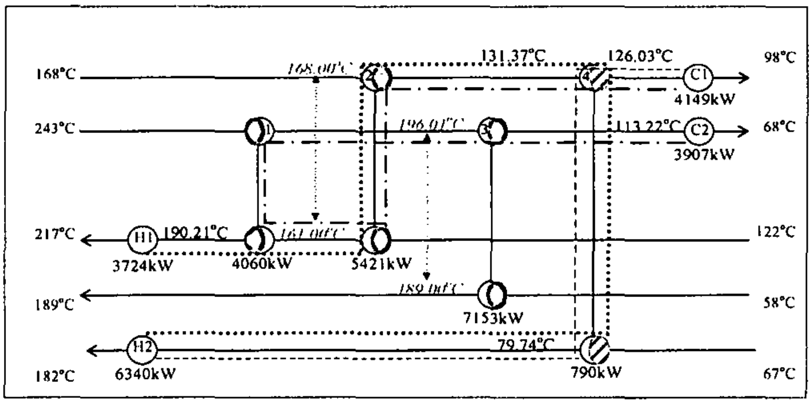

Fig 5.20: Configuration of the retrofitted HEN using option 16 at 6°C of the TF range

For more clarification and comparison, the profile of the economic potential for the HEN retrofit using options 6, 10, 12, 14 and 16 when applying the TF concept are plotted in Fig 5.21 below:

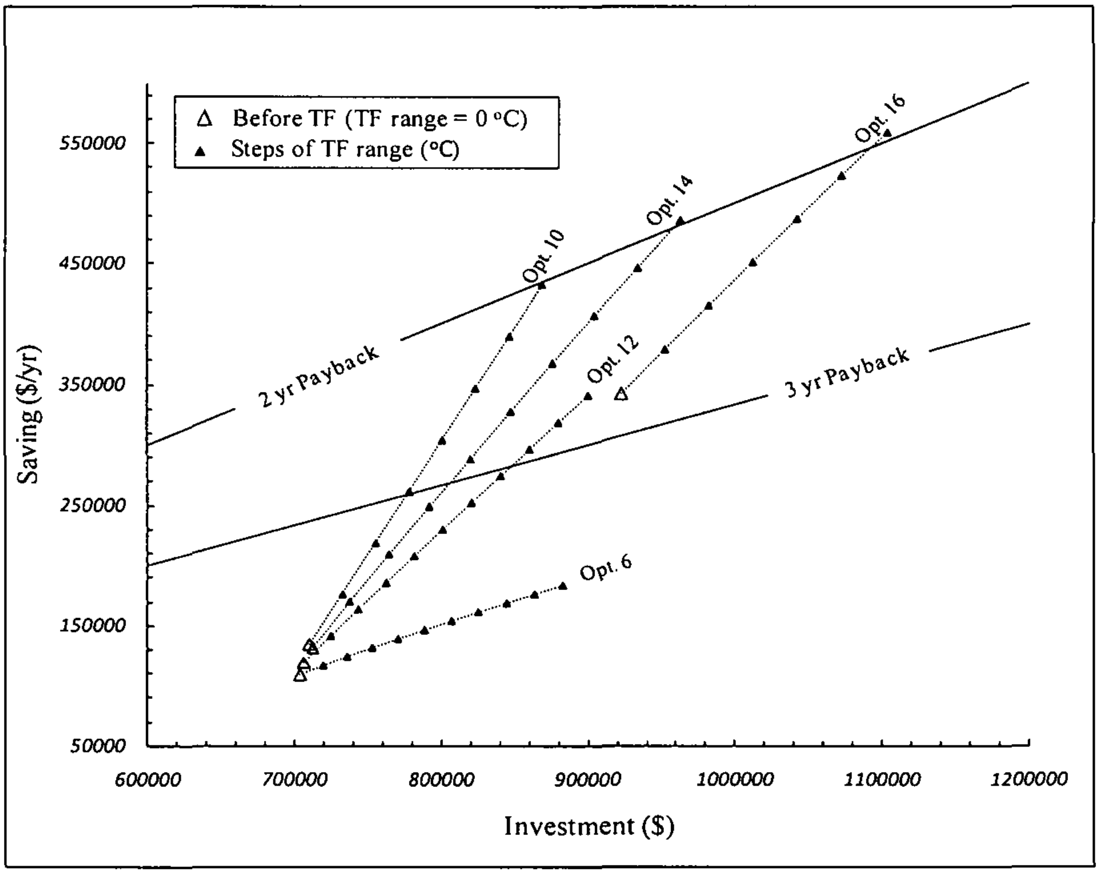

Fig 5.21: Improving the economic potential for the infeasible retrofit options by considering the TF concept.

The savings and the investment shown for options 6, 10, 12 and 14 are placed in the same quadrant of the figure before introducing the TF concept. However, different ways are shown for the options towards reducing the payback period while increasing the savings and the required investment by applying the TF concept. Option 10 has moved to the line of 2 years payback period at 7°C of the TF range. Option 14 requires 9°C of the TF range to be at the line of 2 years payback period while obtaining a bit more savings at the expense of additional investment. On the other hand, option 6 will not be a feasible solution where the trend along the TF ranges is shown to be parallel with the payback lines. Option 12 from this group might reach the 2 years payback line after the 10°C of the TF range which might not be applicable.

Option 16 requires only 6°C of the TF range to reach the 2 years payback line where higher savings will be obtained but at the expense of the highest investment among the group. The details of improving the economic potentials of the infeasible solutions by considering the TF concept are summarized in Table 5.10 below:

Table 5.10: Economic potential of HEN for the infeasible options after the TF concept

	Option 10	Option 14	Option 16	Option 6	Option 12
Savings ($/yr)	438K	485K	560K	184K	341K
Investment ($)	875K	970K	1120K	883K	900K
Payback (yr)	2	2	2	4.8	2.63
ΔA_{HEN} (m^2)	2840	3150	3590	2875	2930
TF range (°C)	7	9	6	10	10

For the existing HEN, the overall heat transfer area was 2189m^2. Improving the infeasible retrofit options using the TF concept has shown the required additional area to be very high as shown in the Table 5.10 above. This could be managed by adding new shells in parallel to the existing units of the HEN. Moreover, the feasibility of the retrofit options at 2 years payback period depends on:

- The affordability of the capital investment by the plant shareholders.
- The applicability of the TF concept to be applied on the HEN streams.

5.2 The results of the HEN-Utility interaction

Several energy saving alternatives were generated for the HEN case study using the developed paths combination approach for the HEN retrofit as discussed above. The obtained results were comprehensively discussed in terms of energy-area tradeoff and cost-wise analysis for the entire generated options before and after applying the proposed TF concept. However, the analysis was conducted for the HEN retrofit as a standalone problem without considering the utility system which supplies the HEN with the required energy. In this section, the impact of the savings derived from the

HEN retrofit on the utility system will be explored before and after the application of the TF concept.

It was mentioned earlier that one of the heaters in the HEN uses HP steam while the other uses MP steam as the heating media which is supplied from the utility system shown in Fig 4.11 presented in section (4.3). In view of the *paths combination approach* being based on shifting the heat loads from the HEN utilities, the energy savings was attained in both sides of the HEN, i.e., heater(s) and cooler(s). The HP steam was saved in all the 17 retrofit options, but sometimes at the expense of increasing the MP steam demand. In this study, the options that assigned net savings are considered, i.e. reduction in the HP, MP or a combination of the HP and MP steam. Namely, the HEN retrofit options 2, 3, 4, 5, 7, 8 and 11 will be carried forward to investigate the HEN-Utility interaction before the TF consideration. For the TF consideration, options 3 and 5 are excluded since they are not applicable to apply the TF concept as stated earlier.

The procedure to investigate the HEN-Utility interaction was previously discussed in chapter 4. Within the procedure, the energy savings (kW) derived from the HEN retrofit was prepared in terms of steam savings (t/h) in order to cope with the steam flow in the utility system. Several heat flow paths were identified in the utility system case study based on the top-level analysis. The heat flow paths were analyzed and sorted based on their efficiency to redistribute the surplus steam derived from the HEN retrofit through the utility system. One of the identified power generation paths was found to be the most efficient to manage the surplus steam in the utility system while considering the turbine flow limitations.

5.2.1 The impact of steam savings on the utility system before applying the TF

Before considering the TF concept, the energy and steam savings obtained from the HEN retrofit using the net saving options as discussed above is shown in Table 5.11 below:

Table 5.11: Energy savings data for the net saving options in the HEN without the TF consideration

Net saving option	Heaters heat loads (kW)		Corresponding savings (t/h)	
	H1	H2	HP steam	MP steam
2	8381	2790	0.662	0
3	8485	2747	0	0.863
4	7103	2790	8.796	0
5	8485	2716	0	1.485
7	6999	2790	9.457	0
8	8485	2168	0	12.485
11	7103	2747	8.796	0.863

From the table it is obvious that option 7 for the HEN retrofit features the highest HP steam savings while option 8 is the best for the MP steam savings. A combination of HP and MP steam savings is taking place using option 11 only.

All the retrofit options shown in the above table are carried forward to investigate the impact of savings on the utility system, especially before applying the TF in the HEN. As described in the HEN-Utility interaction procedure, the steam savings (t/h) was first returned to the VHP steam header through the current heat flow path in the utility system in order to generate steam surplus. To compare between the heat flow paths, the surplus steam has been redistributed using the three identified power generation paths in the utility system. Accordingly, three levels of additional power production were featured for each option of the HEN retrofit as shown in Fig 5.22 below:

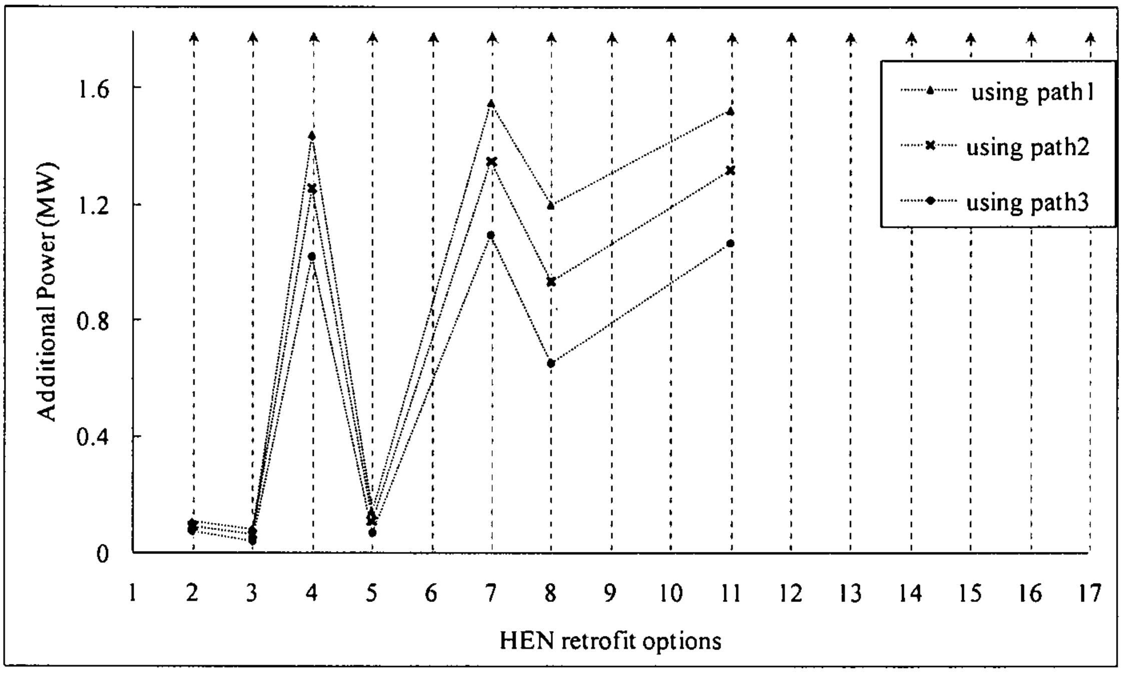

Fig 5.22: The potential of the power generation paths for redistributing the surplus steam derived from the net savings options before applying the TF
(Comparison of the available power generation paths in the utility system)

From the figure, it is confirmed that the power generation path1 is the most powerful path to redistribute the steam surplus in the utility system since it shows the highest level of additional power production.

5.2.1.1 Turbines flow rate before the TF consideration in the HEN

For the utility system case study, the surplus steam redistribution was undertaken using the power generation path1 as stated previously. The upper and lower limits of the steam flow rates for the affected turbines in the utility system were considered while redistributing the surplus steam. Using the power generation path1, the steam flow rate disturbance was adopted for the turbines T1, T3 and T5 in the utility system case study. Fig 5.23 shows the steam flow rate across these turbines as a result of steam savings derived from the HEN retrofit using options 2, 3, 4, 5, 7, 8 and 11 before applying the TF concept. For the affected turbines, the upper and lower limits of the steam flow rate are shown to be maintained as illustrated in the figure.

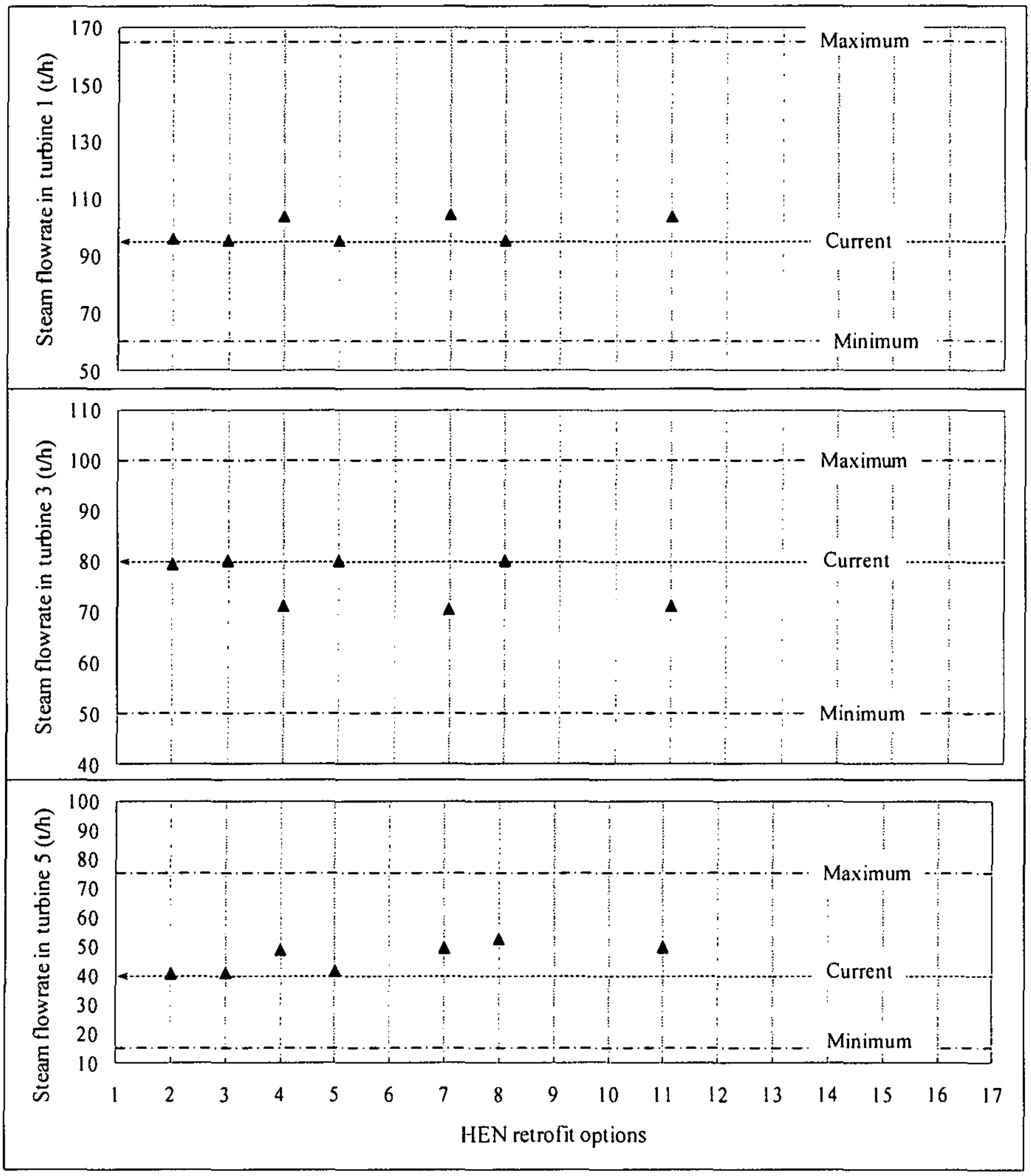

Fig 5.23: Steam flow rate through turbines 1, 3 and 5 in the utility system for selected HEN retrofit options

The steam savings derived from the HEN retrofit using options 4, 7 and 11 are shown to have noticeable impact on the affected turbines. The steam flow rate is shown to increase across the turbines T1 and T5 while it decreases for turbine T3 within the turbines' flow rate limits. The turbines T1 and T5 are shown to have an increased flow rate using these options of the HEN retrofit towards increasing the power production.

As shown earlier in Fig 4.12 presented in section (4.3.1), the turbine T3 lies on the current heat flow path which has been used to return the savings in the HP steam to the VHP steam header and it has not been used again for the redistribution task. Accordingly, the steam flow rate across this turbine has been decreased as shown in Fig 5.23 above.

The steam savings derived from the HEN retrofit using options 3, 5 and 8 shows the steam flow rate across turbines T1 and T3 to be the same as of the current flow rate. This is justified by the fact that the steam savings using these options is mainly MP steam as shown previously in Table 5.11. The MP steam was returned to the VHP header through turbine T1 in the utility system case study through the current heat flow path described earlier in Fig 4.12. However, turbine T1 also lies on the power generation path1 and hence the effect of the current path is cancelled. For the savings derived from the HEN retrofit using option 8, turbine T3 is not included in either the current or the power generation path1.

5.2.1.2 Power production in the utility system before applying the TF in the HEN

Using the power generation path1 for redistributing the surplus steam in the utility system increases the steam flow rate in the utility system turbines and hence increases the overall power production in the utility system. Fig 5.24 shows the overall power production in the utility system as a result of the steam savings derived from the HEN retrofit using options 1, 2, 3, 4, 5, 7, 8 and 11 before applying the TF concept.

The overall existing power was 38.012 MW which is shown to be increased for each HEN retrofit option except option 1 where the savings was only featured in the cooling agents of the HEN. From the figure, the options 4, 7, 8 and 11 showed high value in the power production since they previously showed high steam savings. For instance, additional power of 1.552MW (4.083%) was produced when only saving 9.457 t/h of the HP steam in the HEN using the retrofit option 7.

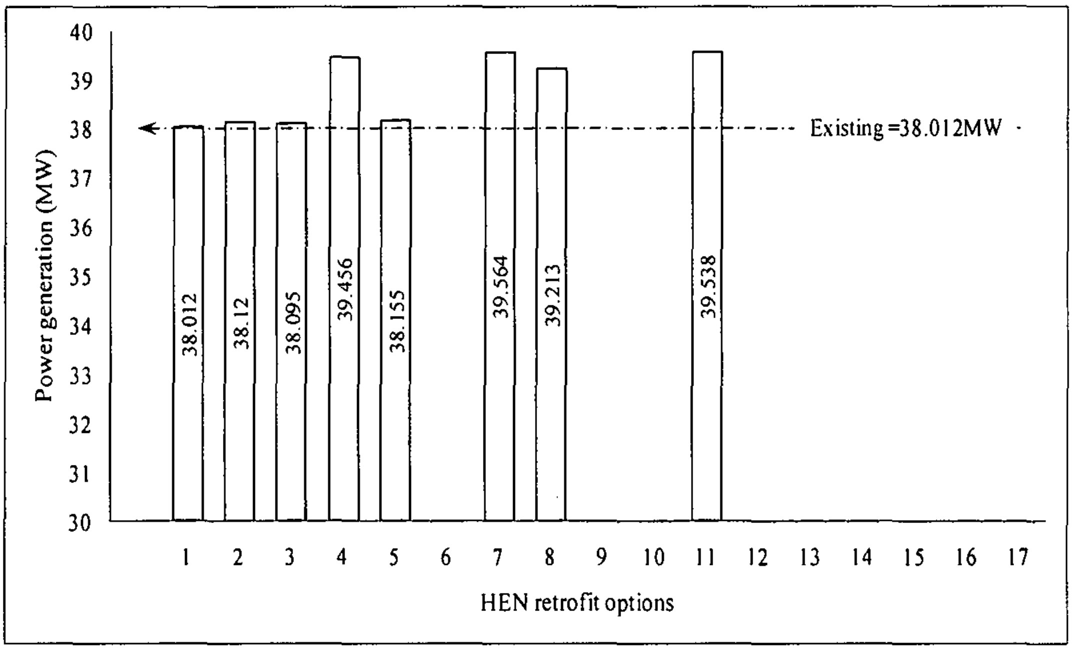

Fig 5.24: Power production potential in the utility system for selected HEN retrofit options before applying the TF

Referring to Table 5.11, although option 8 is shown to have the highest steam savings among the remaining HEN retrofit options, the power production is found to be less than it is for options 4, 7 and 11. The reason is that the savings obtained using option 8 was an MP steam savings which has less heat content compared to the HP steam.

It must be mentioned that the power production depends mainly on the fuel price fluctuation where the path efficiency in the utility system was calculated based on the fuel cost data. Accordingly, the power import path might get the priority to manage the steam surplus by just cutting down the fuel consumption in the utility system which results in a power deficit in the site.

5.2.2 HEN-Utility interaction while considering the TF in the HEN retrofit

The Application of the TF concept together with the developed path combination approach for the HEN retrofit implies reducing the required energy consumption in the HEN which means further increasing the energy savings. For the integrated HEN-Utility case, the surplus steam is further increased in the VHP steam header, accordingly.

The net savings HEN retrofit options are to be carried forward to investigate the impact of savings after the TF is applied. The options 1, 3 and 5 are excluded since they required topology changes in the HEN when considering the TF as described earlier. Therefore, only options 2, 4, 7, 8 and 11 are considered here to further investigate the impact of the TF applied for the HEN retrofit on the utility system.

The data for energy consumption in the HEN with the corresponding steam savings for the net saving options in the HEN when considering the TF concept is available in Appendix E.

Before exploring the impact of savings on the utility system, the profile of the HP and MP steam savings with the TF is shown graphically in Fig 5.25 for the net savings retrofit options.

As shown in the figure, the HP steam savings have steadily increased using options 2, 4, 7 and 11 while option 8 is showing a zero savings for the HP steam. Option 7 is shown to have the best HP steam savings profile which has steadily increased from 9.457t/h before applying the TF to reach 24.375t/h at 10°C of the TF range. The same profile of option 7 has been shown for option 2 but at a lower HP steam savings value. Options 4 and 11 are exposing an identical profile of a slight increase in the HP steam savings.

For the MP steam savings as illustrated in the figure, zero savings is still featured using options 2, 4 and 7 as with before the TF application. However, an increased MP steam savings trend is shown for both options 8 and 11. Option 8 is shown to be the best MP steam savings option before and after the TF application. Using option 8, the MP steam savings has steadily increased from 12.49t/h before applying the TF to reach 30.228t/h at 10°C of the TF range.

Similar to the case before applying the TF in the HEN, the HP and MP steam savings are returned to create steam surplus in the VHP steam header using the current heat flow paths in the utility system. The power generation path1 is then used to redistribute the surplus steam through turbines T1, T3 and T5 in the utility system case study.

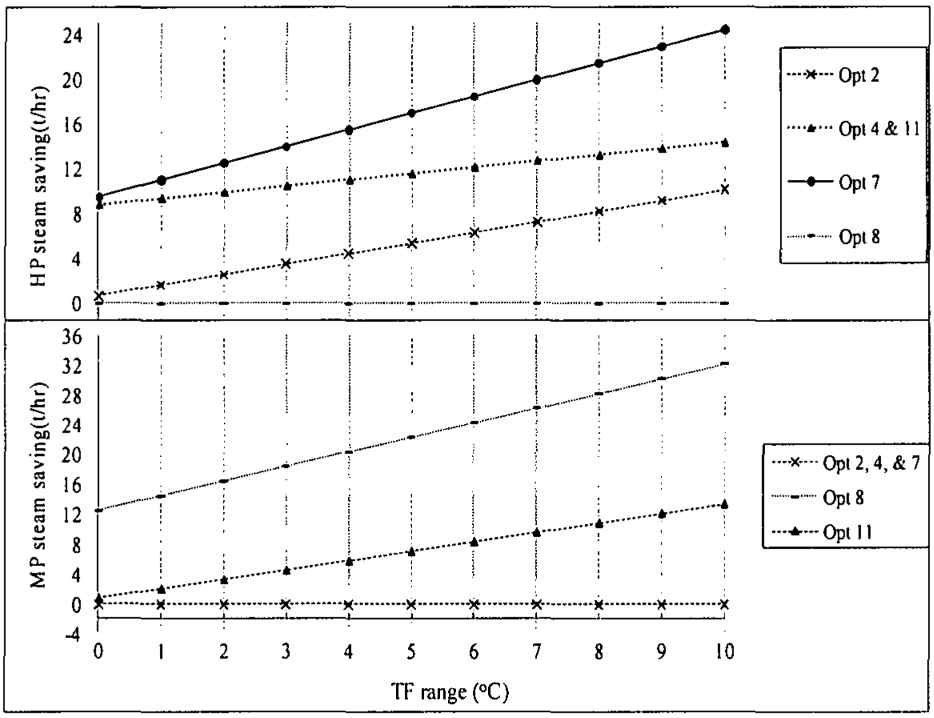

Fig 5.25: The profile of the HP and MP steam savings for selected HEN retrofit options while considering the TF in the HEN

5.2.2.1 Turbines flow rate performance while considering the TF in the HEN

For the net saving HEN retrofit options, the profile of the steam flow rate through turbines T1, T3 and T5 which lies on the power generation path1 along the TF range is shown in Fig 5.26. For turbine T1 and T5 as shown in the figure, the steam flow rate across the turbine is shown to increase steadily along the TF range for the specified HEN retrofit options except option 8 which has no effect on turbine T1. Using the same HEN retrofit options, the steam flow rate across turbine T3 is shown to decrease along the TF range except for option 8 which shows a constant trend.

The flow limits of the turbines are still maintained within the specified TF range as shown in the figure. For the HEN retrofit option 7, turbine T3 would not allow the TF range to exceed 11°C where the lower limit of the turbine flow will be violated. Meanwhile, the upper limit of the flow rate for turbine T5 will also be violated for the HEN retrofit using option 8 at 11°C of the TF range as shown in the figure.

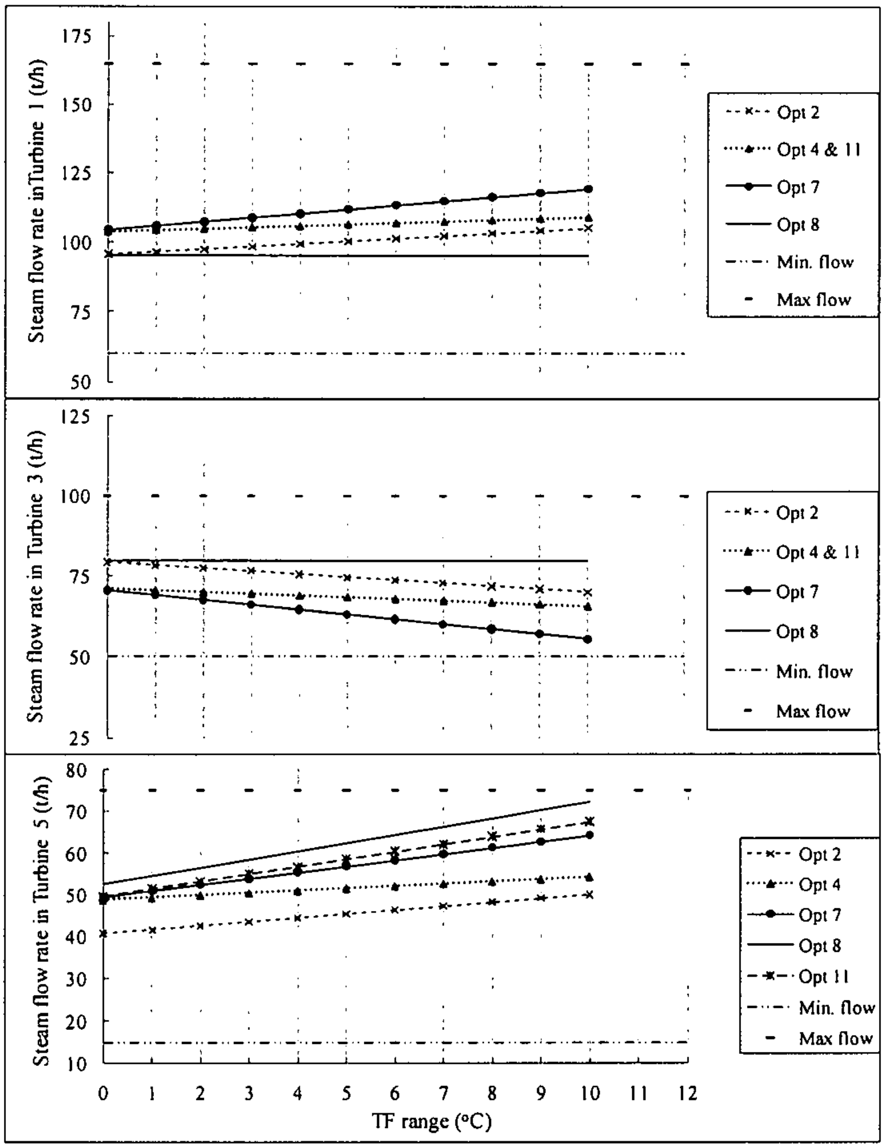

Fig 5.26: The steam flow rate across turbines T1, T3, and T5 along the TF range for the net savings HEN retrofit options

5.2.2.2 Power production profile when considering the TF in the HEN

The overall profile for the power production in the utility system using the selected HEN retrofit options while applying the TF concept is plotted in Fig 5.27. Generally, the power production in the utility system is shown to steadily increase along the TF range for the selected HEN retrofit options.

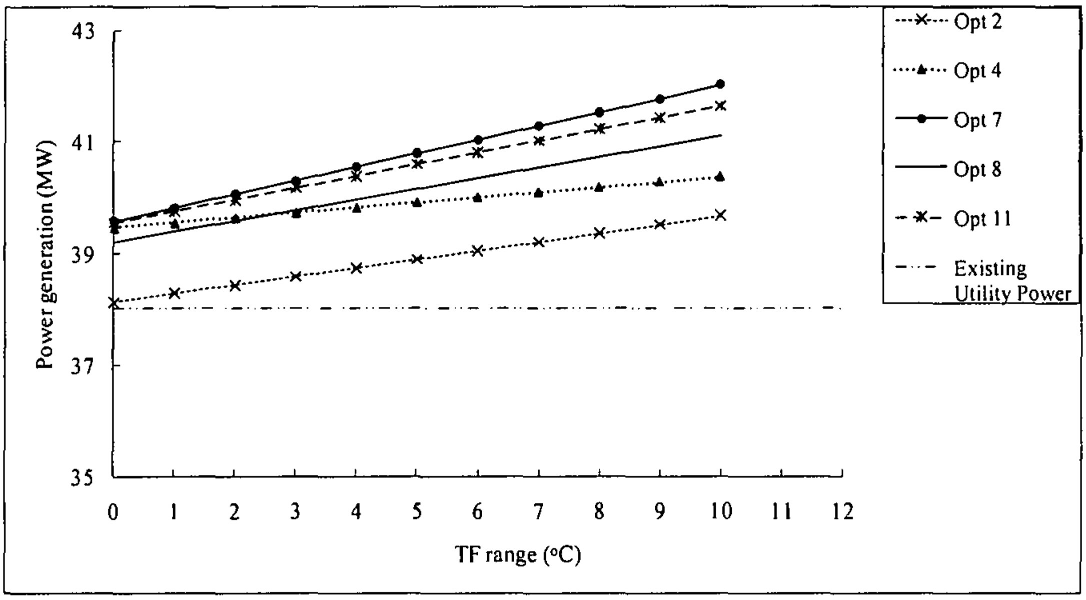

Fig 5.27: The profile of power generation in the utility system considering the TF in the HEN

As a result of the steam savings derived from the HEN retrofit using options 4, 7, and 11, the potential for additional power production in the utility system is shown to be higher even before applying the TF in the HEN as shown in the figure. When the TF is applied, options 7 and 11 have taken the advantages to perform better towards further power production while increasing the TF range.

Using the HEN retrofit option 7, the existing power production in the utility system is shown to increase from 38.012MW to 39.564MW before the application of the TF in the HEN. This amount is shown to increase proportionally with the TF range to reach 42.01MW of power production at 10°C of the TF range. Based on the existing power production, this amount is equivalent to 10.5% additional power in the utility system. Similar to option 7, the performance of power production is shown for the HEN retrofit option 11 but at a bit lower level while the TF range is increased.

The steam savings obtained from the HEN retrofit option 4 is shown to have less potential for more power production in the utility system while the TF range increases. As shown in the figure, the poor profile of option 8 towards increasing the power production was overtaken by the profile of option 8 after 2°C of the TF range.

Using option 8, the power production has increased from around 3% before the TF has been applied in the HEN to reach almost 8% at the end of TF range scale.

Option 2 is the worst among all the selected options in terms of additional power production either before or after considering the TF in the HEN.

5.3 Result summary

The developed paths combination approach for the HEN retrofit results in several energy saving options when applied for specific case study of the HEN. The obtained retrofit results were first presented for the standalone HEN without considering the utility system before and after applying the TF in the HEN. The results were also discussed and analyzed for the integrated HEN-Utility system before and after introducing the TF in the HEN. For the standalone HEN, the results were discussed in two ways:

1. The ability of the retrofit options in reducing the energy consumption while considering the required additional area in the HEN.

2. The economic potential of the retrofit options in terms of the obtained savings ($/year) and the corresponding capital investment ($).

The best energy saving options were decided to have a short payback period to refund the invested capital. Accordingly, some of the generated retrofit options were selected to be the best even before applying the TF in the HEN such as options 4, 7, 8 and 11. The unattractive options were improved further when the TF concept was introduced. For instance, options 10, 13, 14, 15, 16 and 17 were moved to the feasible zone of high savings and short payback period.

For the integrated HEN-Utility system, the impact of energy savings in the HEN was transformed into additional power production in the utility system either before or after the application of the TF in the HEN. Options 4, 7, 8 and 11 which were considered to be the best energy savings options for the HEN case study, were also shown to have the highest additional power production in the utility system. However, the result of power production is subjected to change according to the fuel price fluctuation over the time.

CHAPTER 6

CONCLUSION AND RECOMMENDATION

The overall work conducted in this research is briefly concluded in this chapter. Moreover, the extension of this work is pointed out as future research pathways which are recommended to be carried forward in the area of the heat exchanger networks and the utility system.

6.1 Accomplished work

Generally, this study is formulated to develop new HEN retrofit approach capable for generating several retrofit options and economically assessing their feasibility. A further assessment was achieved by applying the developed approach to investigate the impact of savings derived from the HEN retrofit on the utility system. Referring to the main objectives of this research together with the obtained results, the achievement and contribution of this work could be concluded in the following points:

- From the first objective, the path analysis of Pinch Technology was introduced for developing new approach called '*Paths Combination Approach for the HEN Retrofit*'. This approach was developed based on a simple combinatorial method to combine the available utility paths in the HEN for enhancing the heat recovery between the process streams. Meanwhile, the pressure drop of the existing exchangers in HEN was considered in order to avoid any additional pumping cost. Accordingly, the most-out of the energy conservation was made at the expense of adding heat transfer area to the existing HEN without subjecting the HEN to massive topology changes. The essentiality of the developed approach beyond the heat recovery improvement is to screen wider range of HEN retrofit options and allow the plant shareholders to choose according to the available capital.

- The second objective of this research has been established to further improve the obtained solutions and make use of the unfeasible ones. Particularly, it was been personalized for managing the process stream temperature flexibility based on the plus/minus principle of the Pinch Technology [15] and then applied the *paths combination approach*. It is simply by making the hot streams in the HEN slightly hotter and the cold streams slightly colder which creates what is called the temperature flexibility range (TF range). Each step of the TF range scale was produced in several alternatives providing the process engineer with wider degrees of freedom to choose according the applicability. Therefore, the heat transfer driving force in the existing HEN which is HRAT is increased beyond the existing value. This idea is found to make a platform for repeating the paths combination approach for further shifting extra heat from the HEN utilities until the existing HRAT is restored.

- From the third objective, a user friendly computer program was developed to implement the *path combination approach* with the application of streams temperature flexibility. The Programme was built based on the Java platform using the free source of Netbeans software. It was presented as user friendly interface to simplify the data input and output as shown in Appendix A. Within the availability of the HEN data, the developed programme is suitable for any HEN involving several utility paths.

- The energy conservation results of the approach were shown graphically to predict and put a base of optimum selection from the several generated solutions. The results were further analyzed economically in terms of saving amount ($) and capital investment ($/year). Savings and investment of all the retrofit options were compromised and governed by the payback period according to the Pinch Technology approach. Based on such analysis the decision could then be made for selecting the most optimum solution(s) to be implemented. From a demonstrative case study for the HEN, the obtained results for many retrofit options showed that small capital ($) is required to be invested for the retrofit. Even though, this amount could be recovered through energy savings ($/yr) within a reasonably short payback period which shown to range from 0.6 year to 2.7 years. The decision is then left to the plant management to select the most attractive solution taking into account the total cost involved. Some of the retrofit options were found to be infeasible due to the low saving and long payback period. However, the application of the proposed temperature flexibility has improved the retrofit potentials of these options towards higher savings and shorter payback at the expense of investing a bit more capital.

- The fourth objective was established to explore the impact of energy savings derived from the HEN retrofit on the utility system which provides the processes with heating, cooling and power demand. The heating demand normally extracted from the utility system in the form of steam. The potential for transforming the steam savings into other economic values in the utility system was investigated and analyzed for the HEN retrofit options. Consequently, the result showed additional power has been produced in the utility system case study which added a new value to the energy savings derived from the HEN retrofit.

6.2 Recommendations

Generally, the path analysis procedure is found to fairly manage the heat load of the HEN system devices. Accordingly, several related pathways for the HEN retrofit research could be conducted for either energy saving retrofit projects or process debottlenecking retrofit projects. The work conducted in the present study has opened other research pathways to be followed in the field of the HEN retrofit. Based on the understanding of the developed paths combination approach and the concept of temperature flexibility for the HEN retrofit, the following points could be recommended for further study:

1. Instead of putting a limit for the heat load shifting process such as HRAT, the heat shifting process of the developed approach of paths combination could be continued until a *Network Pinch* is encountered. This applies particularly when the additional area for the retrofit is very high. Then the approach of minimal topology modification for the HEN retrofit which was developed by Asante and Zhu [12, 45] could be followed to overcome the *Network Pinch*. It is worth mentioning that the pressure drop constraint is more restricted here, especially

the stream pressure drop. This is because all the options to overcome the *Network Pinch* are disturbing the stream pressure drop in addition to the existing exchangers in the HEN. Namely these options are: stream splitting, exchanger re-sequencing, re-piping and adding new exchanger(s) as stated in the literature chapter.

2. Instead of a fixed HRAT in the HEN, the promising retrofit solutions offered by the path combination approach could be optimized for different practical values of HRAT to further screen the most optimum. This idea would reflect the same targeting approach of Tjoe [7] but here it would be more improved since the pressure drop constraints were already considered in the *Paths Combination Approach*.

3. The work of Zhang and Zhu [17] could also be integrated with the path combination approach while considering the TF concept in the same manner developed in the present work. The understanding beyond this idea is that a shared foundation between the two works is already established according to the plus/minus principle of the Pinch Technology [15].

4. Beside the stream temperature flexibility in the HEN, the flow rate alteration could also be managed the same way the current work has addressed the temperature flexibility. This point is also endorsed by the plus/minus principle mentioned above. Moreover, a combination of both temperature and flow rate flexibility could also be addressed. The stream pressure drop must be taken into consideration since the flow rate alteration would hardly disturb the pressure drop and hence the pumping system.

5. For all the previous points, if the HEN retrofit to be conducted is oriented to be an energy saving scheme, the impact on the utility system could also be investigated. Moreover, the consequences on the other parts of the onion diagram must also be addressed especially when integrating the approach to the process condition changes to allow a total site improvement.

REFERENCES

[1] EIA. (2009, Integrated Energy Statistics, Office of Energy Markets and End Use. Available:

http://www.eia.doe.gov/oil_gas/petroleum/data_publications/weekly_petroleum_status_report/wpsr.html

[2] C. J. Campbell, "Oil depletion Protocol: The Rimini Protocol an Oil Depletion Protocol "Heading off Economic Chaos and Political Conflict During the Second Half of The Age of Oil"," *Energy Policy,* vol. 34, pp. 1319-1325, 2006.

[3] C. J. Campbell, and J.H. Laherrere. (March 1998) The End of Cheap Oil. *Scientific American Magazine*.

[4] OPEC, "World Oil Outlook," Vienna, Austria 978-3-200, 2007.

[5] EIA. (2009, Official energy Statistics from U.S goverment. Available: http://www.eia.doe.gov/emeu/ipsr/source2.html

[6] EIA. (2009, Official Energy Statistics from U.S goverment, Energy and the Environment. Available:

http://tonto.eia.doe.gov/energyexplained/index.cfm?page=environment_how_ghg_affect_climate

[7] T. N. Tjoe, "Retrofit of Heat Exchanger Networks," Ph.D. Thesis, Centre of Process Integration, UMIST, Manchester, U.K., 1986.

[8] B. Linnhoff and J. A. Turner, "Heat - Recovery Networks: New Insight Yield Big Saving," *Chemical Engineering,* vol. 88, pp. 56 - 70, 2 Nov. 1981.

[9] B. Linnhoff and D. R. Verdeveld, "Pinch Technology Has Come of Age," *Chemical Engineering Progress,* vol. 80, pp. 33-40, July 1984.

[10] B. Linnhoff, D. W. Townsend, D. Bland, G. F. Hewitt, B. E. A. Thomas, A. R. Guy, and R. H. Marsland, "A User Guide on Process Integration for the Efficient Use of Energy," IChemE., Rugby, U.K.1994.

[11] S. Ahmed, "Heat Exchanger Networks: Cost Trade-Offs in Energy and Capital," Ph.D. Thesis, Department of Process Integration, UMIST, Manchester, 1985.

[12] N. D. K. Asante and X. X. Zhu, "An automated and interactive approach for heat exchanger network retrofit," *Trans. IChemE,* vol. 75(A), 1997.

[13] H. F. Rong B., Andrzej K., Lars N. , "Study on the Methodology for retrofitting Chemical Processes," *Chemical Engineering Technology* vol. 23, pp. 476-484, 2000.

[14] R. Smith, "State of the Art in Process Integration," *Applied Thermal Engineering,* vol. 20, pp. 1337-1345, 2000.

[15] B. Linnhoff and S. Parker, "Heat Exchanger Networks with Process Modifications.," *IChE,* vol. Annual research meeting, 1984.

[16] B. Linnhoff and E. Kotjabasakis, "Downstream paths for operable process design," presented at the Chemical Engineering Progress, UMIST- Manchester, England, 1986.

[17] J. Zhang and X. X. Zhu, "Simultaneous Optimization Approach for Heat Exchanger Network Retrofit with Process Changes," *Ind. Eng. Chem. Res,* vol. 39, pp. 4963 - 49731, 2000.

[18] R. F. Dunn and M. M. El-Halwagi, "Process Integration Technology Review: Background and Applications in the Chemical Process Industry," *Journal of Chemical Technology and Biotechnology,* vol. 78, pp. 1011-1021, 2003.

[19] P. Rašković, Stoiljković, S., "Pinch Design Method in the Case of a Limited Number of Process Streams," *Energy,* vol. 34, pp. 593-612, May 2009.

[20] U. V. Shenoy, Heat Exchanger Network Synthesis: Process Optimization by Energy and Recourse Analysis. Houston, Texas: Gulf Publishing Company, 1995.

[21] B. Linnhoff, "Pinch Analysis: State of the Art Overview," *IChemE Research and Design,* vol. A5, pp. 503-522, 1993.

[22] J. M. Douglas, *Conceptual Design of Chemical Processes*. New York: McGraw Hill, 1988.

[23] T. Gundersen and L. Naess, "The synthesis of cost optimal heat exchanger networks: an industrial review of the state of the art," *Computers and Chemical Engineering* vol. Volume 12, pp. 503-530, June1988.

[24] K. Nagabhushan Raju, *Industrial Energy Conservation Techniques*: Atlantic Publishers & Distributors, 2007.

[25] R. Smith, *Chemical Process Design and Integration*: John Wiley & Sons Ltd, 2005.

[26] J. Klemeš, R. Smith, and J.-K. Kim, "Water and Energy Management in Food Processing," ed. Cambridge: Woodhead Publishing Limited, 2008.

[27] V. R. D. J. Klemes, K. Raissi, S.J. Perry, L. Puigjaner, "Targeting and design methodology for reduction of fuel, power and CO_2 on total sites," *Applied Thermal Engineering,* vol. 17, pp. 993–1003, 1997.

[28] E. C. Hohmann, "Optimum networks for heat exchange," Ph.D. Thesis, University of Southern California, 1971.

[29] T. Umeda, J. Itoh, and K. Shiroko., "Heat Exchange System Synthesis," *Chemical Engineering Progress,* vol. 74, pp. 70–76, 1978.

[30] B. Linnhoff and J. R. Flower, "Synthesis of heat exchanger networks. I : Systematic generation of energy optimal networks," *AIChE,* vol. 24, pp. 633–642, 1978.

[31] B. Linnhoff and J. R. Flower, "Synthesis of heat exchanger networks. II : Evolutionary generation of networks with various criteria of optimality," *AIChE,* vol. 24, pp. 642–654, 1978.

[32] B. Linnhoff and E. Hindmarsh, "The pinch design method for heat exchanger networks," *Chemical Engineering Science,* vol. 38, pp. 745–763, 1983.

[33] M. M. El-Halwagi and V. Manousiouthakis, "Synthesis of Mass Exchange Networks," *AIChE,* vol. 35, pp. 1233-1244, 1989.

[34] Y. P. Wang and R. Smith, "Wastewater Minimisation," *Chemical Engineering Science,* vol. 49, pp. 981–1006, 1994.

[35] Z. A. Manan, S. R. W. Alwi, and Z. Ujang, "Water pinch analysis for urban system: a case study on the Sultan Ismail Mosque at Universiti Teknologi Malaysia (UTM)," *Desalination,* vol. 194, pp. 52-68, 2006.

[36] C. W. Hui, "Heat Integration Between Areas of Integrity (Pinch Technology)," Ph.D. Thesis, Centre of Process Integration, UMIST, Manchester, U.K., 1991.

[37] T. N. Tjoe and B. Linnhoff, "Using Pinch Technology for Process Retrofit," *Chemical Engineering,* pp. 47-60, 1986.

[38] B. Linnhoff and T. N. Tjoe, "Pinch technology retrofit: setting targets for an existing plant," in *AIChE National Meeting*, Houston, 24-28 March1985.

[39] A. R. Ciric and C. A. Floudas, "A Retrofit Approach for Heat Exchanger Networks," *Computer and Chemical Engineering,* vol. 13, pp. 703-715, 1989.

[40] A. R. Ciric and C. A. Floudas, "A Comprehensive Optimisation Model of the HEN Retrofit Problem," *Heat Recovery System and CHP,* vol. 10, pp. 407–422, 1990.

[41] T. F. Yee and I. E. Grossmann, "A Screening and Optimisation Approach for the Retrofit of Heat Exchanger Networks," *Industrial and Engineering Chemistry Research,* vol. 30, pp. 146-162 1991.

[42] T. F. Yee and I. E. Grossmann, "Simultaneous optimization models for heat integration-II. Heat exchanger network synthesis," *Computers and Chemical Engineering,* vol. 14, pp. 1165-1184, 1990.

[43] X. X. Zhu and N. D. K. Asante, "Diagnosis and Optimization Approach for Heat Exchanger Network Retrofit," *AIChE J,* vol. 45, pp. 1488-1503, 1999.

[44] V. Briones and A. Kokossis, "A New Approach for The Optimal Retrofit of Heat Exchanger Networks," *Computer's Chemical Engineering,* vol. 20 suppl., pp. S43 - S48, 1996.

[45] N. D. K. Asante and X. X. Zhu, "An automated approach for heat exchanger network retrofit featuring minimal topology modifications," *Computer's Chemical Engineering* vol. 20, pp. S7-S12, 1996.

[46] C. B. Shokoya, " Retrofit of heat exchanger network for debottlenecking and energy saving," Ph.D. Thesis, Centre of Process Integration, UMIST, Manchester, 1992.

[47] A. Carlsson, P. Franck, and T. Berntsson, "Design Better Heat Exchanger Network Retrofits," *Chemical Engineering Progress,* vol. 89, pp. 87–96, 1993.

[48] R. Nordman and T. Berntsson, "Use of advanced composite cureves for assessing cost effective HEN retrofit, II," *Applied Thermal Engineering,* vol. 29, pp. 282-289, 2009.

[49] M. A. Gadalla, "Retrofit design of heat-integrated crude oil distillation systems," Ph.D. Thesis, Centre of Process Integration, UMIST, Manchester, U.K., 2003.

[50] Y. Makwana, "Systematic energy management of total site," Ph.D. Thesis, Centre of Process Integration, UMIST, Manchester, U.K., 1997.

[51] P. S. Varbanov and J. Klemes, "Rules of Path Construction for HENs Debottlenecking," *Applied Thermal Engineering* vol. 20, pp. 1409-1420, 2000.

[52] L. B. J. Van Reisen, G. T. Polley, and J. T. V. Peter, "The Placement of Two stream and Multi-stream Heat Exchangers in an Existing Network through Path Analysis," *Computer and Chemical Engineering* vol. 19, pp. S143-S148, 1995.

[53] L. B. J. Van Reisen, G. T. Polley, and J. T. V. Peter, "Structural Targeting for Heat Integration Retrofit," *Applied Thermal Engineering* vol. 18, pp. 283-294, 1998.

[54] S. Resat, K. Onder, and R. Marcus, "A new design approach for shell and tube heat exchanger using genetic algorithms from economic point of view," *Chemical Engineering and Processing,* vol. 45, pp. 268-275, 2006.

[55] G. T. Polley, M. H. S. Panjeh, and F. O. Jegede, "Pressure Drop Consideration in the Retrofit of Heat Exchanger Networks," *Trans. IChemE,* vol. 68, pp. 211-220, 1990.

[56] F. O. Jegede, "Power, Capital and Energy Cost Trade-Offs in Heat Exchanger Networks," Ph.D., Centre of Process Integration, UMIST, Manchester, Jan. 1990.

[57] M. H. Panjeh-Shahi, "Pressure drop consideration in process integration," Ph.D. Thesis, Centre of Process Integration, UMIST, Manchester, U.K., 1992.

[58] L. S. Marcone and J. R. Zemp, "Retrofit of Pressure Drop Constrained Heat Exchanger Network," *Applied Thermal Engineering* vol. 20, pp. 1469-1480, 2000.

[59] X. R. Nie and X. X. Zhu, "Heat Exchanger Network Retrofit Considering Pressure Drop and Heat-Transfer Enhancement," *AIChE J,* vol. 45, pp. 1239-1254, 1999.

[60] M. H. Panjeshahi and H. R. Fallahi, "Pressure drop optimization in grass root design of heat exchanger networks," in *Fourth national congress in chemical engineering*, Sharif University of Technology, Tehran, Iran, 1999, pp. 49-54.

[61] M. H. Panjeshahi and H. R. Fallahi, "Pressure drop optimization in retrofit of heat exchanger networks " *J. Faculty of Engineering, Tehran University,* vol. 33, pp. 37-53, 2000.

[62] M. H. Panjeshahi and N. Tahouni, "Pressure drop optimization in debottlenecking of heat exchanger network," *Energy,* vol. 33, pp. 942 – 951, 2008.

[63] M. A. Duran and I. E. Grossmann, "Simultaneous Optimization and Heat Integration of Chemical Process," *AIChE J,* vol. 32, pp. 123-138, 1986.

[64] Y. D. Lang, L. T. Biegler, and I. E. Grossmann, "Simultaneous Optimization and Heat Integration with Process Simulator," *Computer's Chemical Engineering,* vol. 12, pp. 311-327, 1988.

[65] A. Samanta and M. Jobson, "A New Heat Integration Model for Streams of Variable Temperature and Constraint Matches," *European Symposium on Computer Aided Process Engineering* vol. 11, pp. 511 - 516, 2001.

[66] E. Kotjabasakis and B. Linnhoff, "Sensitivity Tables for the Design of Flexible Processes: (1)-How Much Contingency in Heat Exchanger Networks is Cost Effective," *Chemical Engineering Research and Design,* vol. 64, pp. 197-211, 1986.

[67] J. Klemes and P. Stehlík, "Recent novel heat integration developments: improved operation, multi-period utilities systems, batch process scheduling, pressure consideration, retrofit, cost factors, energy price forecasts and industrial case studies," *Applied Thermal Engineering,* vol. 23, pp. 1723-1728, October 2003.

[68] A. Soršak and Z. Kravanja, "MINLP retrofit of heat exchanger networks comprising different exchanger types " *Computers and Chemical Engineering,* vol. 28, pp. 235-251, Jan. 2004.

[69] J. M. Jeżowski, H. K. Shethna, R. J. Bochenek, and F. J. L. Castillo, "On extensions of approaches for heat recovery calculations in integrated chemical process systems," *Computers and Chemistry,* vol. 24, pp. 595-601, July 2000.

[70] S. A. Papoulias and I. E. Grossmann, "A structural optimization approach in process synthesis-II : Heat recovery networks," *Computers and Chemical Engineering,* vol. 7, pp. 707-721, 1983.

[71] V. R. Dhole and B. Linnhoff, "Total site targets for fuel, cogeneration, emissions, and cooling," *Computers and Chemical Engineering,* vol. 17, pp. S101-S109, 1993.

[72] S. Bandyopadhyay, J.Varghese, and V. Bansal, " Targeting for cogeneration potential through total site integration," *Applied Thermal Engineering,* vol. 30, pp. 6-14, 2010.

[73] D. C. A. Muller, F. M. A. Marechal, T. Wolewinski, and P. J. Roux, " An energy management method for the food industry," *Applied Thermal Engineering,* vol. 27, pp. 2677-2686, 2007.

[74] S. P. Mavromatis and A. C. Kokossis, "Conceptual optimization of utility networks for operational variations-I, Target and level optimization," *Chmical Engineering Science,* vol. 53, pp. 1585-1608, 1998.

[75] S. P. Mavromatis and A. C. Kokossis, "Conceptual optimization of utility networks for operational variations-II, Network development and optimization," *Chmical Engineering Science,* vol. 53, pp. 1609-1630, 1998.

[76] S. P. Mavromatis, and A. C. Kokossis, "Hardware composites: A new conceptual tool for the analysis and optimization of steam turbine networks in chemical process industries: Part I: principles and construction procedure," *Chemical Engineering Science,* vol. 53, pp. 1405-1434, 1998.

[77] S. P. Mavromatis, and A. C. Kokossis, "Hardware composites: a new conceptual tool for the analysis and optimisation of steam turbine networks in chemical process industries: Part II: application to operation and design," *Chemical Engineering Science,* vol. 53, pp. 1435-1461, 1998.

[78] A. M. Strouvalis, S. P. Mavromatis and A. C. Kokossis "Conceptual optimization of utility networks using hardware and comprehensive hardware composites " presented at the European Symposium on Computer Aided Process Engineering -8, 1998.

[79] P. S. Varbanov, S. Doyle, and R. Smith, "Modelling and optimization of utility systems," *Chemical Engineering Research and Design,* vol. 82, pp. 561-578, 2004.

[80] K. Hirata, P. Chan, K.-Y. Cheung, H. Sakamoto, K. Ide, and C.-W. Hui, "Site-model utility system optimisation - industrial case study of KKEPC," *Applied Thermal Engineering,* vol. 27, pp. 2687-2692, 2007.

[81] S. P. Mavromatis, "Conceptual Design and Operation of Industrial Steam Turbine Networks," Ph.D.Thesis, Process Integration, UMIST, Manchester, U.K., 1996.

[82] P. S. Varbanov, S. Perry, Y. Makwana, X. X. Zhu, and R. Smith, "Top-level analysis of site utility systems," *Chemical Engineering Research and Design,* vol. 82, pp. 784-795, 2004.

[83] P. S. Varbanov, "Optimization and Synthesis of Process Utility Systems," Ph.D. Thesis, Process Integration, UMIST, Manchester. U.K., May 2004.

[84] A. J. M. Vieira, F. L. P. Pessoa, and E. M. Queiroz, "Fluid dynamical considerations on heat exchanger networks," *Brazilian Chemical Engineering,* vol. 17, 2000.

[85] W. E. Swokowski and A. J. Cole, *Precalculus*, 10th ed. Canada: Thomson Learning Academic Resource Center, 2005.

[86] C. A. Floudas, A. R. Ciric, and I. E. Grossmann, "Automated Synthesis of Optimum Heat Exchanger Network Configurations," *AIChE J.*, vol. 23, 1986.

[87] X. X. Zhu and L. Vaideeswaran, "Recent Research Development of Process Integration in Analysis and Optimization of Energy System," *Applied Thermal Engineering,* vol. 20, pp. 1381 - 1392, 2000.

[88] Linnhoff-March. (1998, Introduction to Pinch Technology. Available: http://www.linnhoffmarch.com

[89] B. A. Al-Riyami, J. Klemes, and S. Perry, "Heat Integration Retrofit Analysis of a Heat Exchanges Network of a Fluid Catalytic Cracking Plant," *Applied Thermal Engineering,* vol. 21, pp. 449-1487, 2001.

[90] W. T. Philippe and G. Louis, "Minimizing Shell and tube heat exchanger cost with genetic algorithms and considering maintenance," *International Journal of Energy Res.*, vol. 31, pp. 867-885, 2007.

[91] I. G. C. Dryden, *The Efficient Use of Energy*, 2nd ed.: Butterworth Scientific, August 1982.

[92] T. C. Elliot, Standard Handbook of Powerplant Engineering: McGraw-Hill, 1989.

[93] Y. Makwana, R. Smith, and X. X. Zhu, "A novel approach for retrofit and operations management of existing total sites," *Computers Chemical Engineering* vol. 22, pp. S793-S796, 1998.

APPENDIX A

THE DEVELOPED COMPUTER PROGRAMMING INTERFACE

For implementing the *paths combination approach* which was developed for the HEN retrofit, a user friendly Java interfacing programme has been built as a Java project based on the free source of the Netbeans software. The developed programme also allows the application of the proposed TF concept on the HEN streams. In this Appendix, the interfacing of the programme is shown step-wisely from the data entry, paths identifications, pressure drop consideration and the final results output in both graphical and table representation.

1. JAVA project startup and run

For the built Java project, the interfacing for the *startup* and *run* is illustrated as follows:

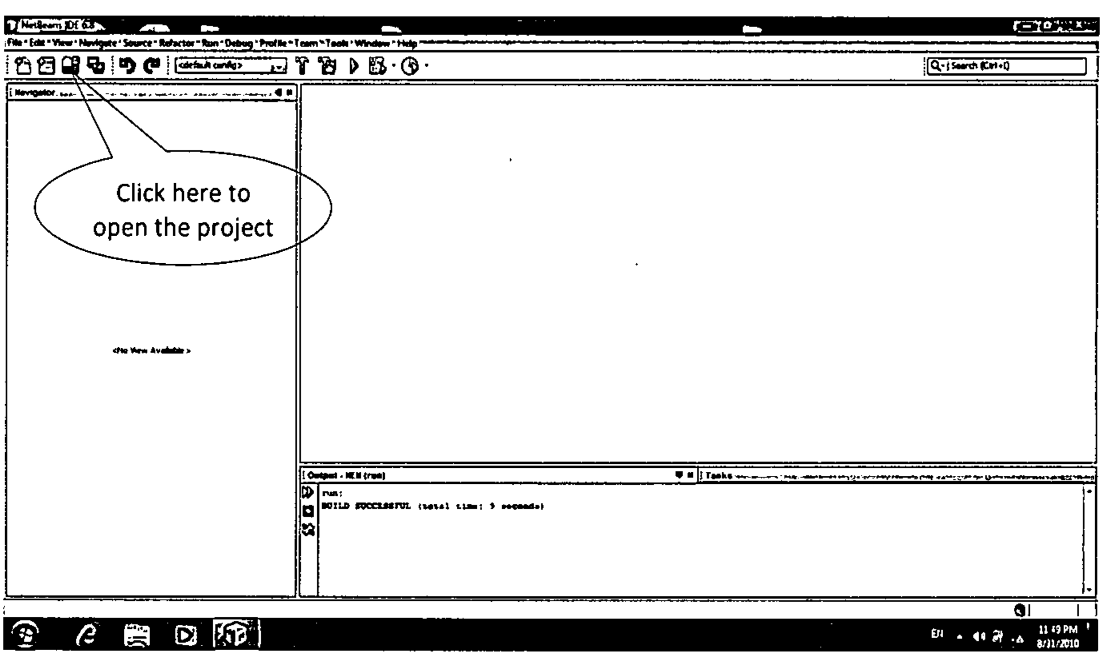

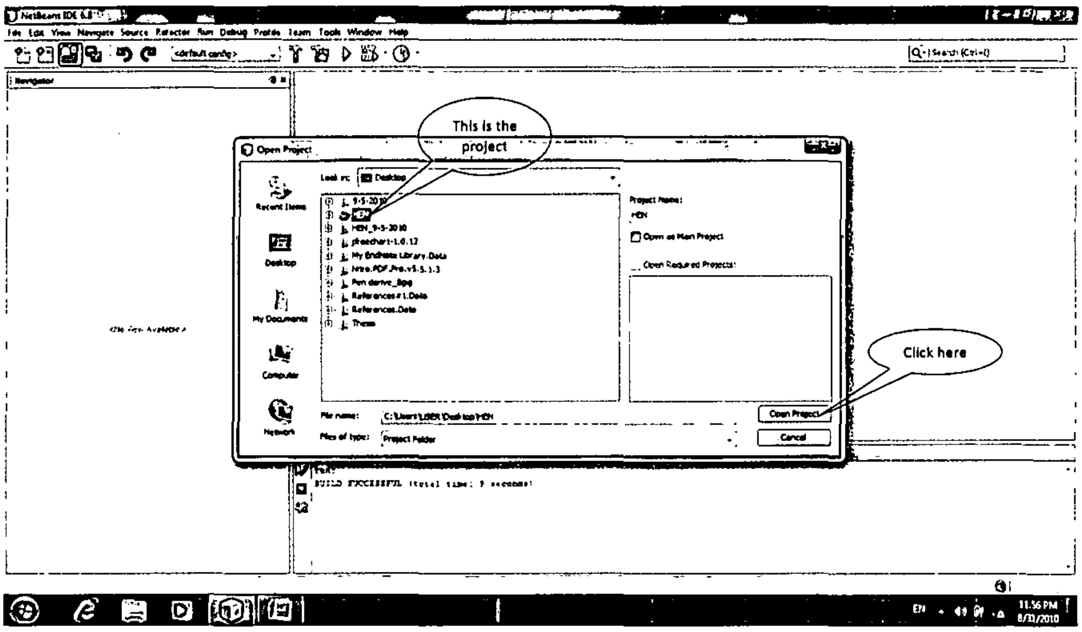
This is the project
Click here

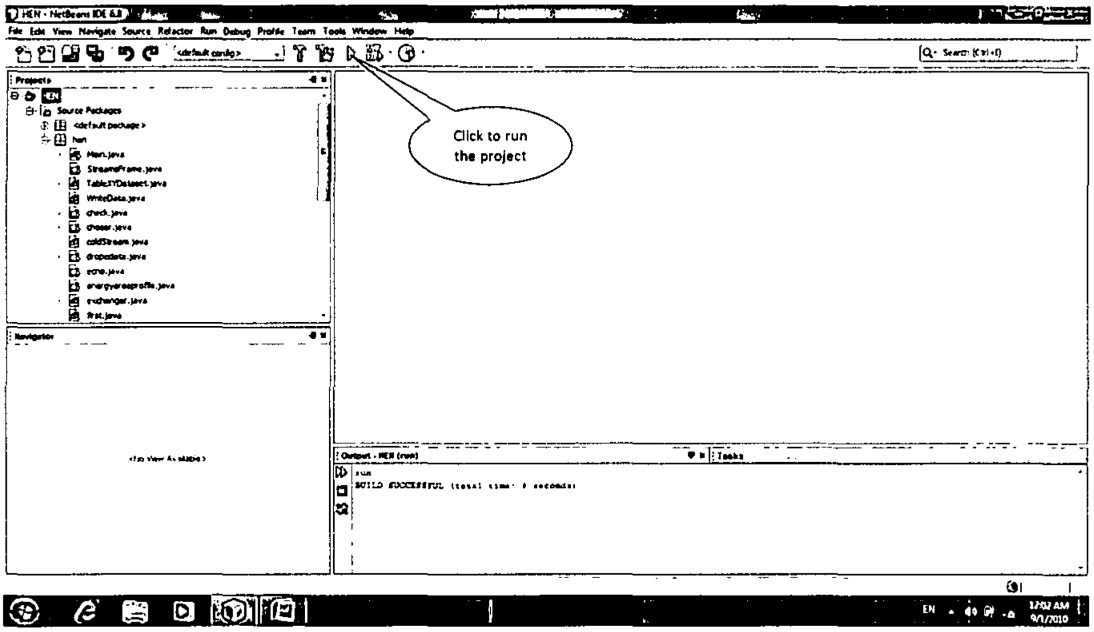
Click to run the project

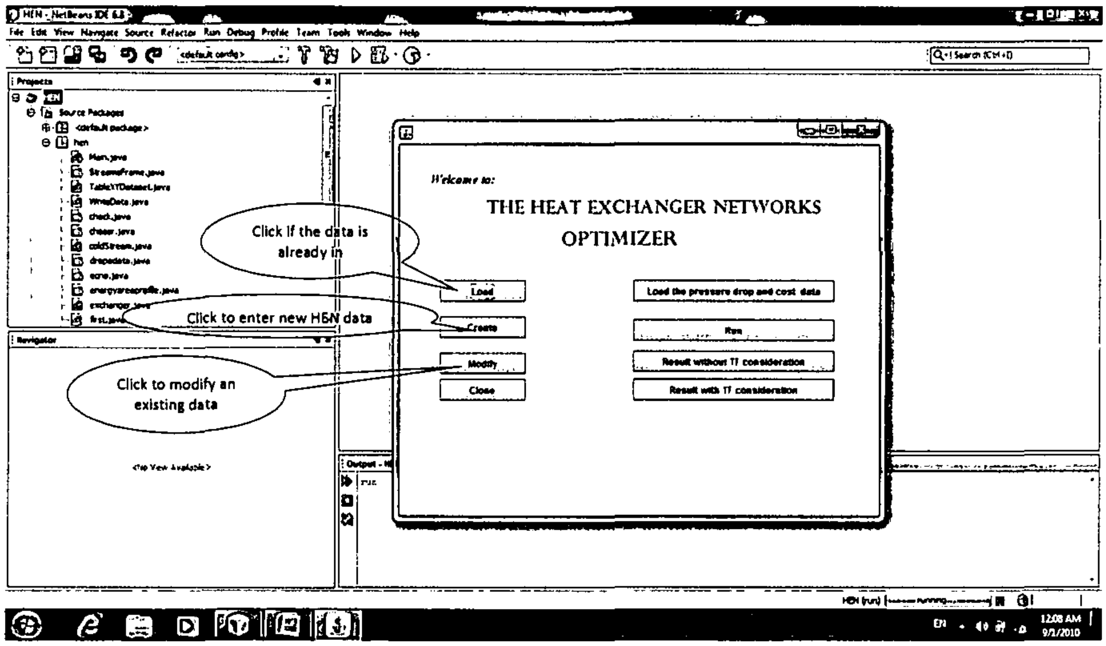

2. Initial data entry

The interfacing for introducing the HEN stream data and the exchanger's location on the streams with their heat duty and heat transfer area is illustrated in this section as shown below:

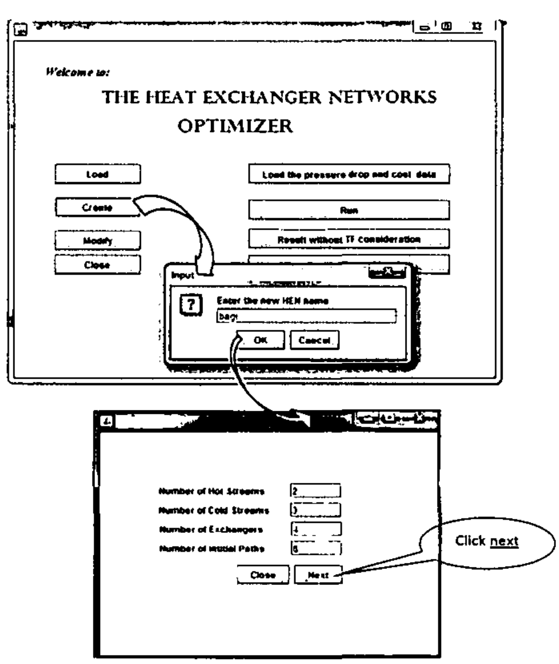

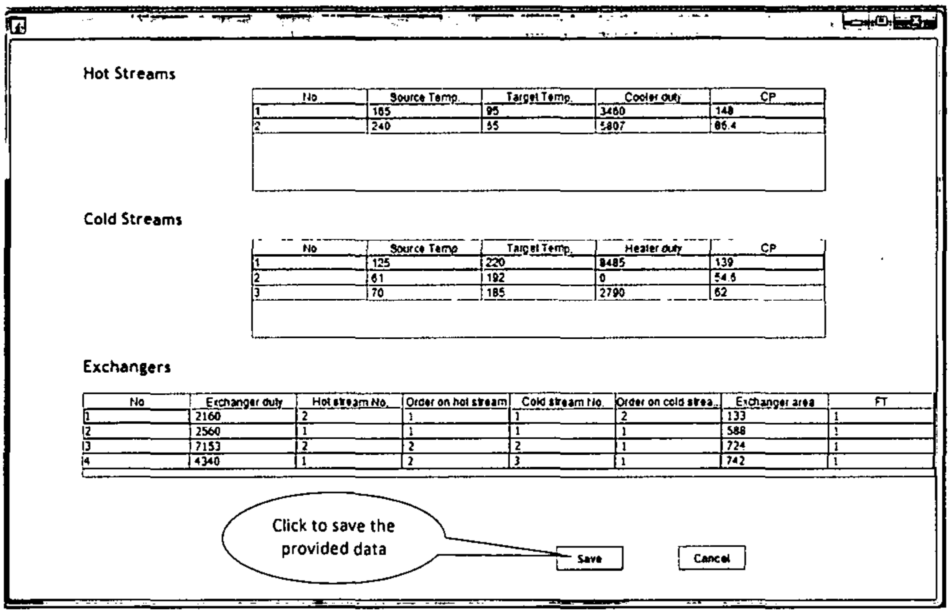

2.1. Utility paths identification

After saving the provided data as shown in the previous step, screens of paths entry will pop up where the available utility paths in the HEN are to be identified as shown below:

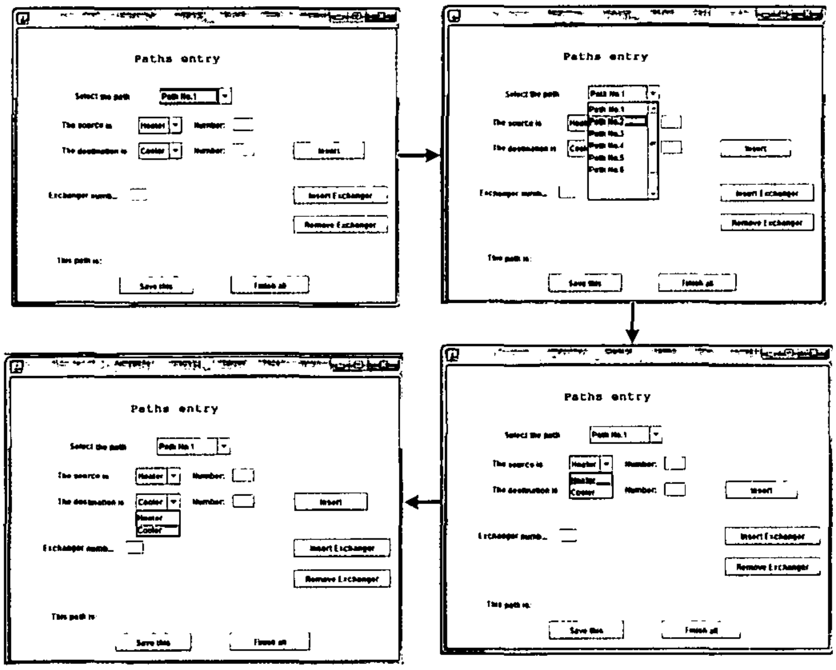

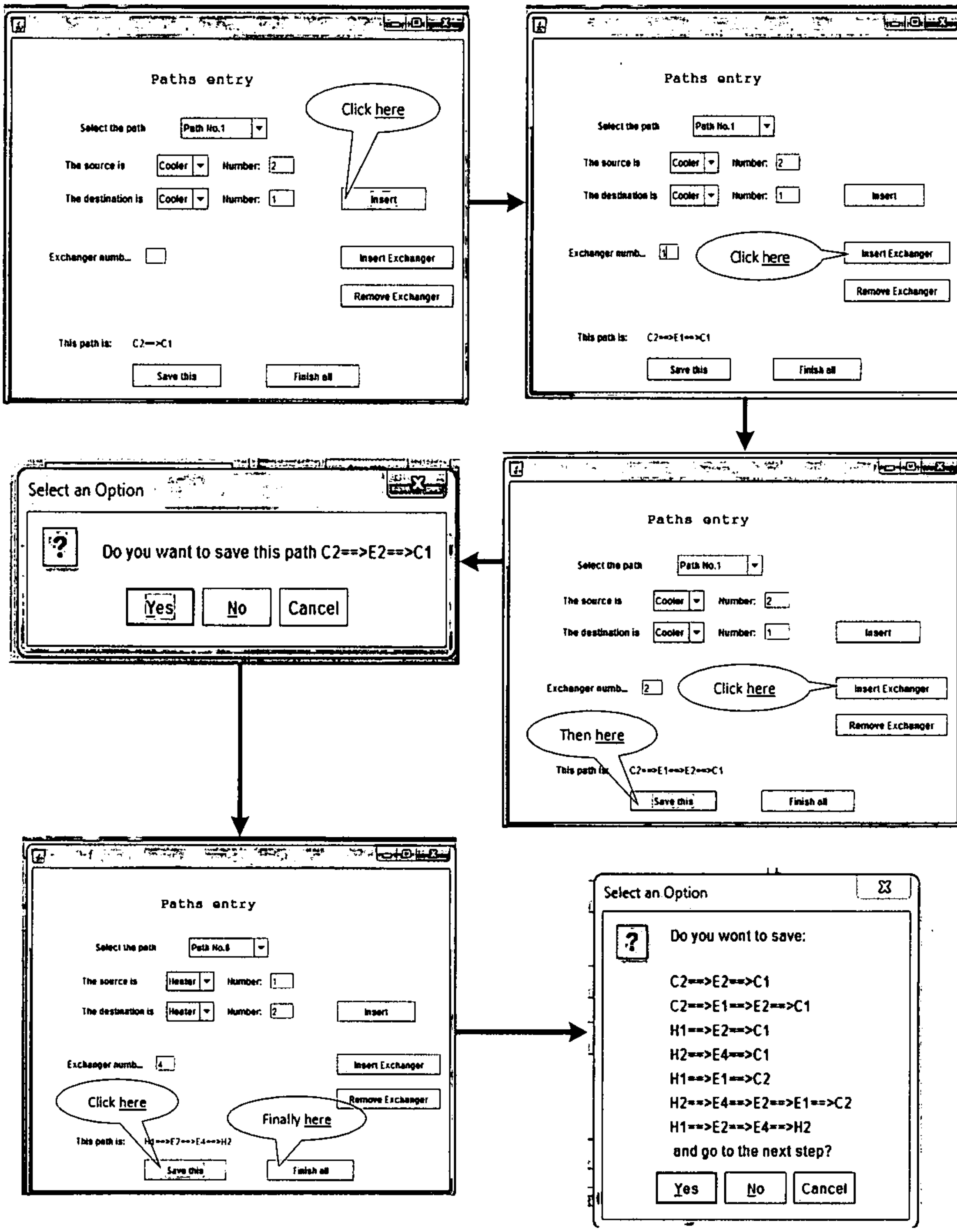

2.2. Pressure drop and utility cost data entry

The exchangers' pressure drop data for both the tube and shell sides is introduced together with the utility cost data as shown in the following interfacing:

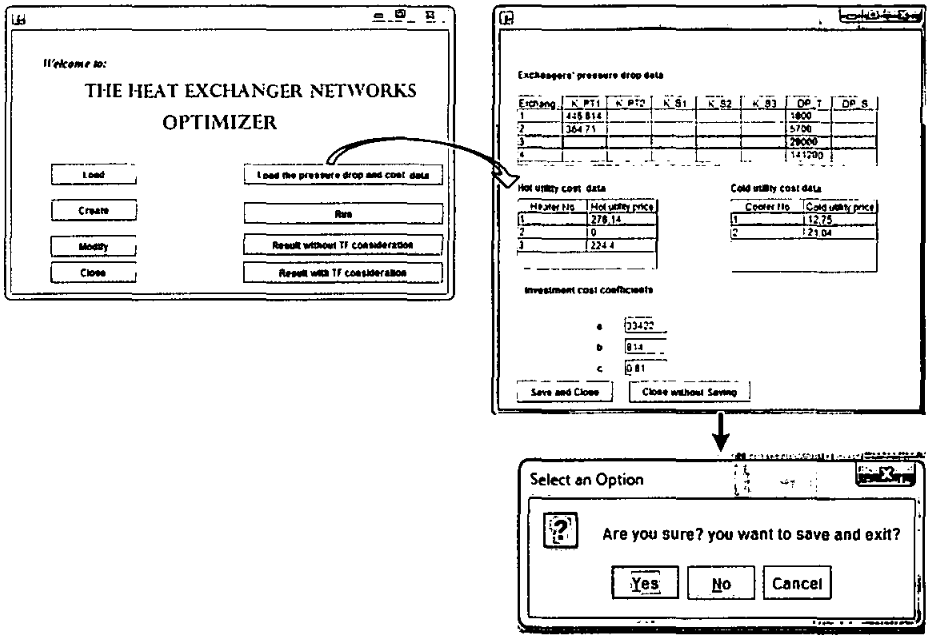

3. Data processing

The provided data is now ready for processing to get the final results as shown below:

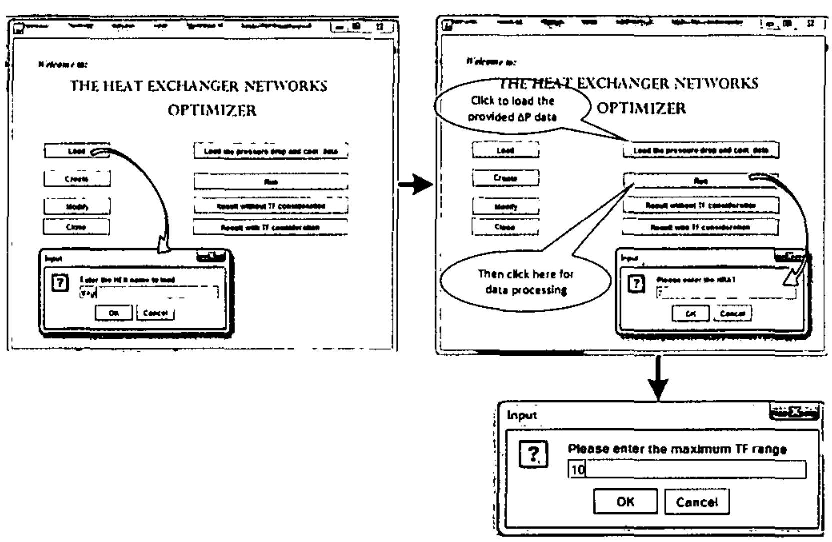

4. Results representation

The obtained results are presented graphically and in table format before and after applying the temperature flexibility (TF) on the HEN streams.

4.1. Results before the application of the TF concept

The way to pull out the results before applying the TF concept is shown in the following interfacing:

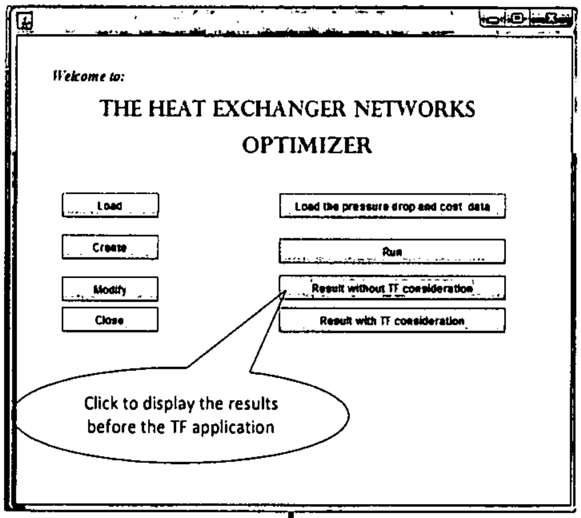

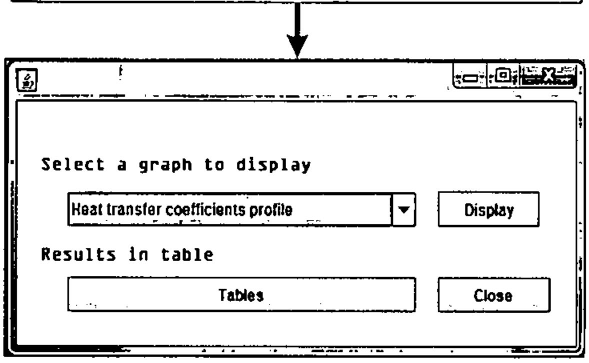

4.1.1. Graphical results

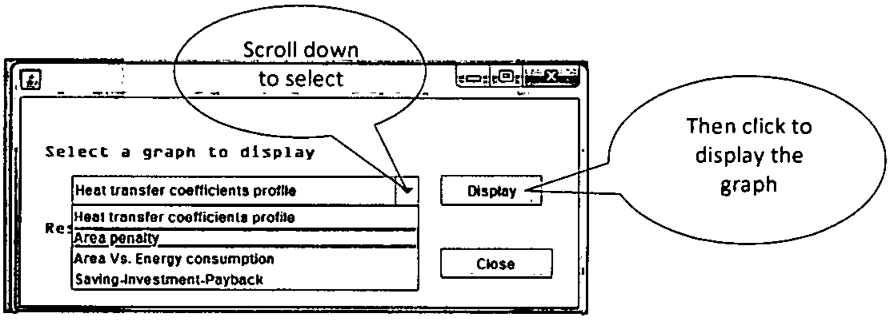

4.1.1.1. Heat transfer coefficients

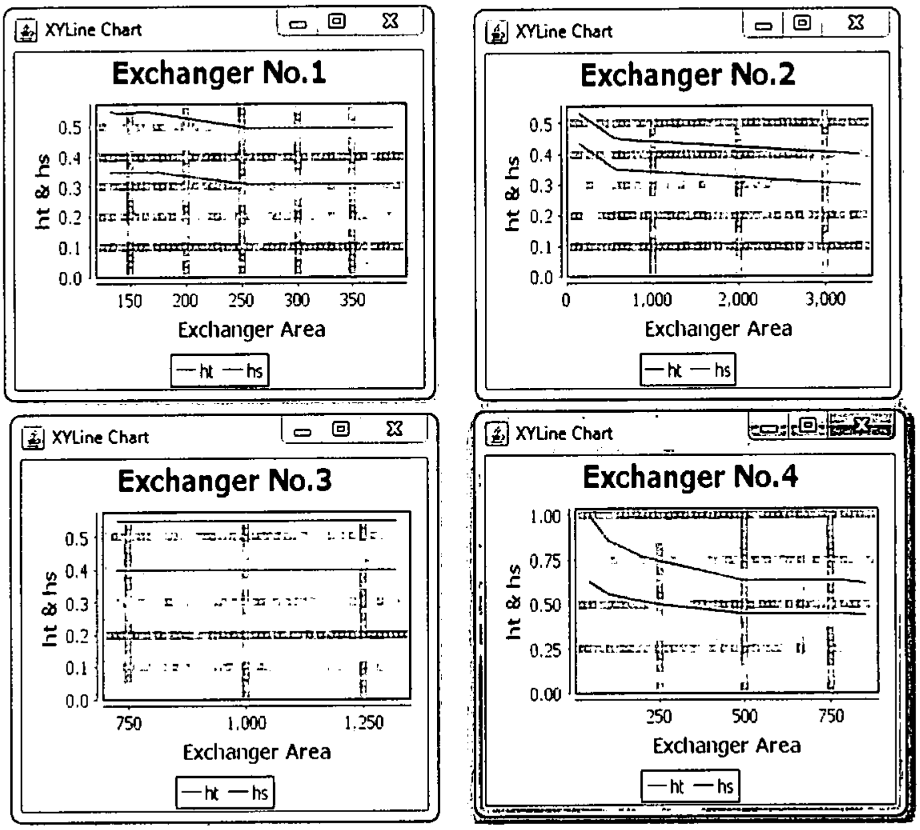

4.1.1.2. Area for each retrofit options

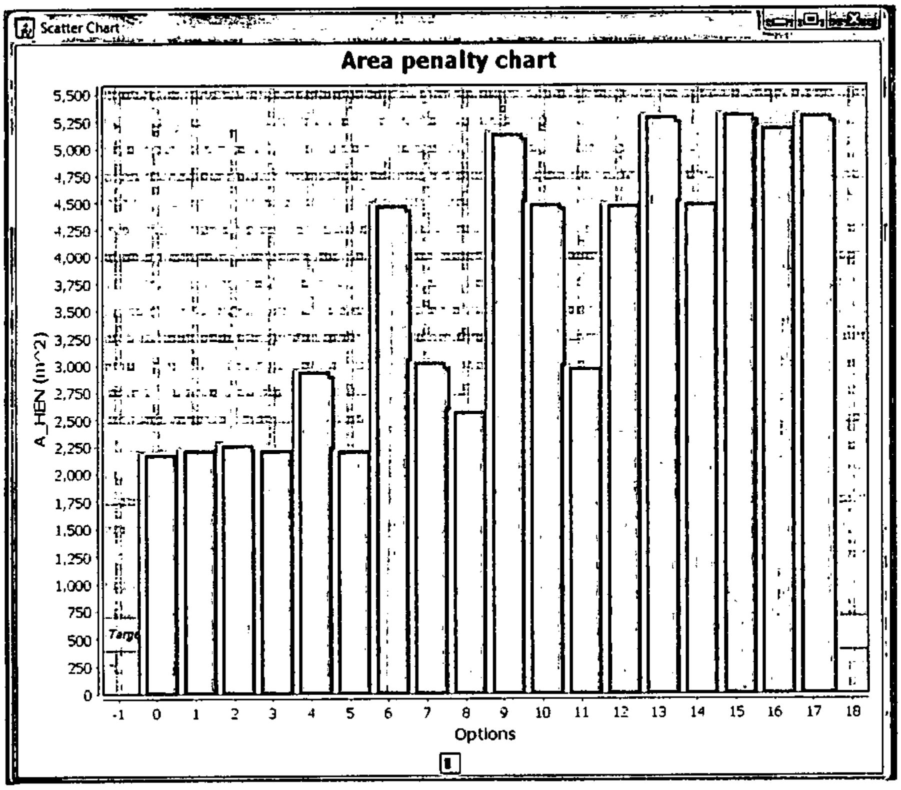

4.1.1.3. Area vs. energy consumption

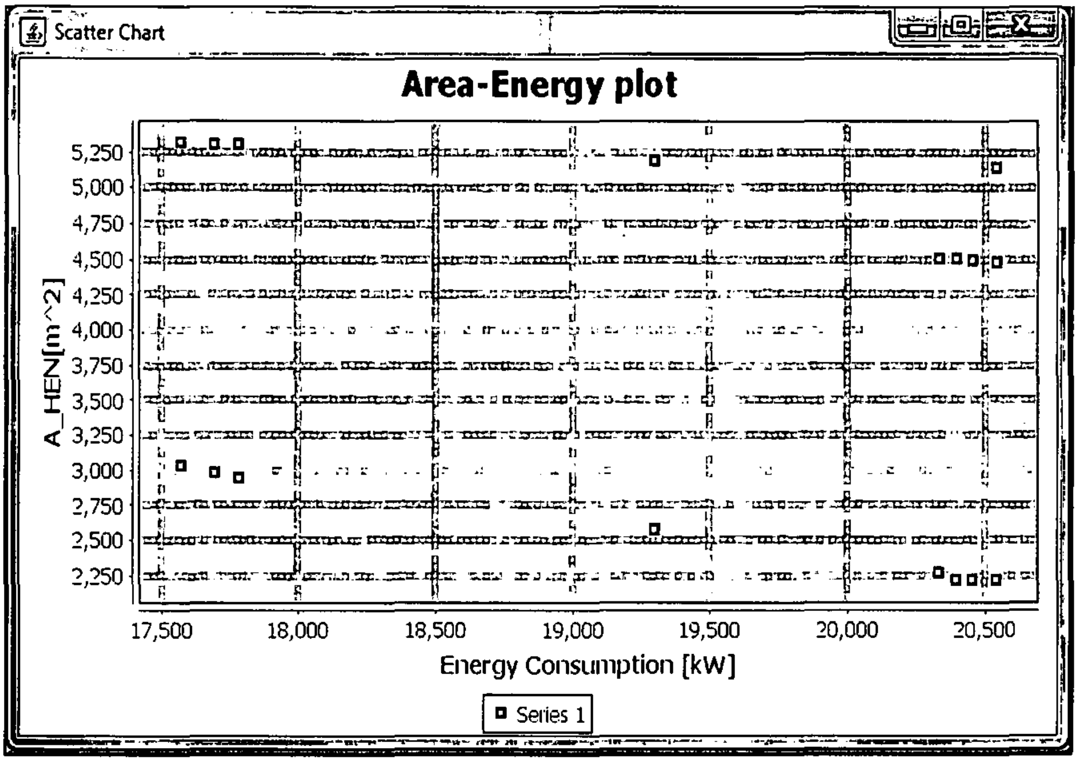

4.1.1.4. Economical results

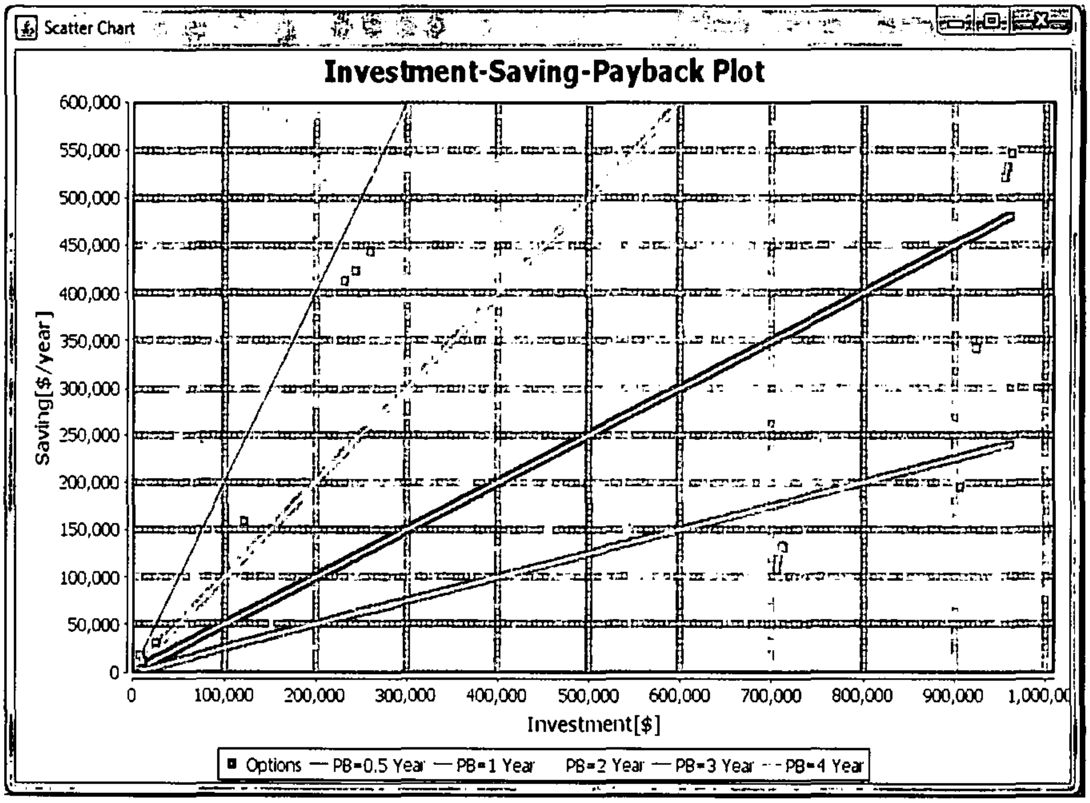

4.1.2. Results in tables

The same graphical results are also presented in table to be plotted in Excel or Matlab where the plot will be more flexible for editing and coloring. The table results are displayed as follows:

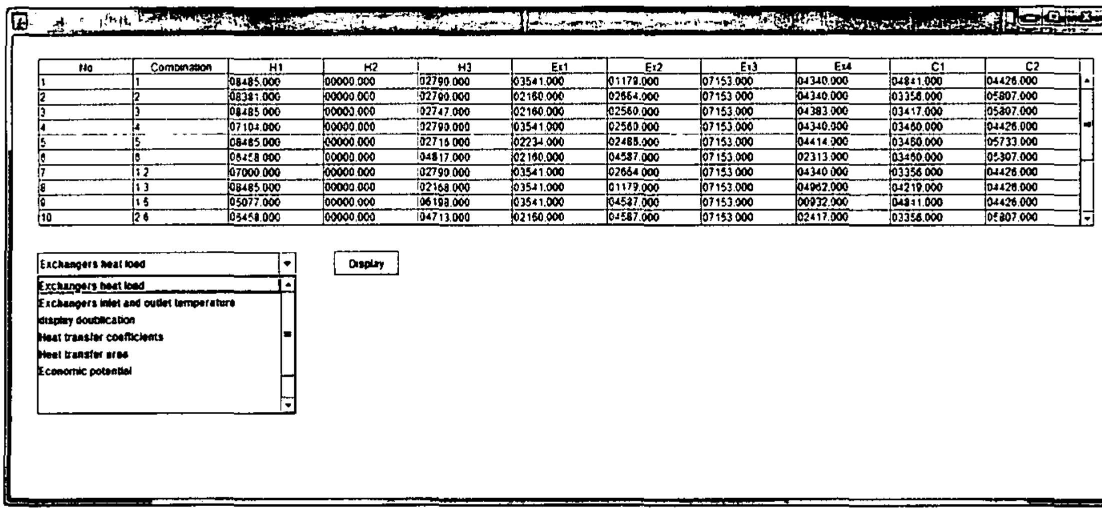

No	Combination	H1	H2	H3	Ex1	Ex2	Ex3	Ex4	C1	C2
1	1	08485.000	00000.000	02790.000	03541.000	01179.000	07153.000	04340.000	04841.000	04426.000
2	2	08381.000	00000.000	02790.000	02160.000	02664.000	07153.000	04340.000	03356.000	05807.000
3	3	08485.000	00000.000	02747.000	02160.000	02560.000	07153.000	04383.000	03417.000	05807.000
4	4	07104.000	00000.000	02790.000	03541.000	02560.000	07153.000	04340.000	03460.000	04426.000
5	5	08485.000	00000.000	02716.000	02234.000	02488.000	07153.000	04414.000	03460.000	05733.000
6	6	08458.000	00000.000	04817.000	02160.000	04587.000	07153.000	02313.000	03460.000	05307.000
7	1 2	07000.000	00000.000	02790.000	03541.000	02664.000	07153.000	04340.000	03356.000	04426.000
8	1 3	08485.000	00000.000	02168.000	03541.000	01179.000	07153.000	04962.000	04219.000	04426.000
9	1 5	05077.000	00000.000	06198.000	03541.000	04587.000	07153.000	00932.000	04841.000	04426.000
10	2 6	05458.000	00000.000	04713.000	02160.000	04587.000	07153.000	02417.000	03356.000	05807.000

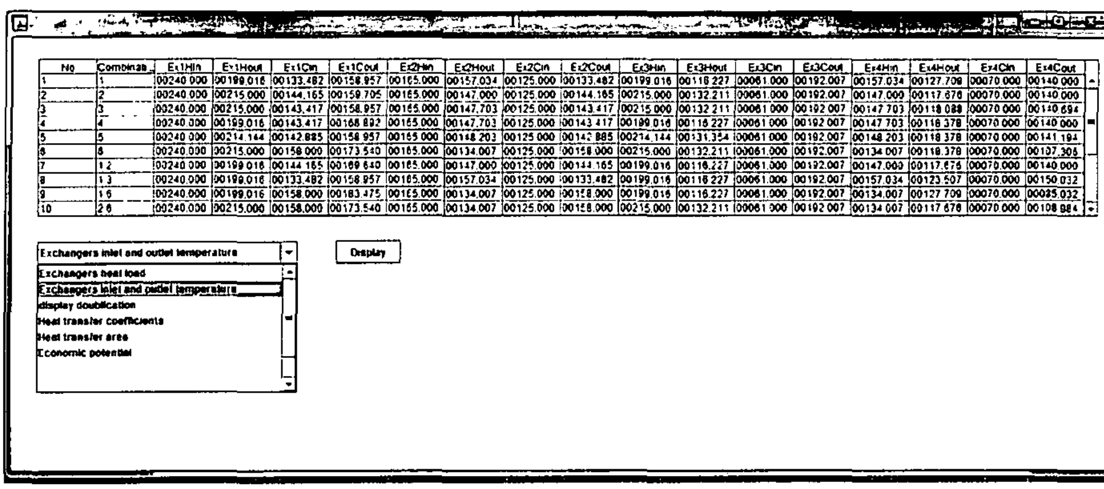

No	Combinat...	Ex1Hin	Ex1Hout	Ex1Cin	Ex1Cout	Ex2Hin	Ex2Hout	Ex2Cin	Ex2Cout	Ex3Hin	Ex3Hout	Ex3Cin	Ex3Cout	Ex4Hin	Ex4Hout	Ex4Cin	Ex4Cout
1	1	00240.000	00199.016	00133.482	00158.957	00165.000	00157.034	00125.000	00133.482	00199.016	00118.227	00061.000	00192.007	00157.034	00127.709	00070.000	00140.000
2	2	00240.000	00215.000	00144.165	00159.705	00165.000	00147.000	00125.000	00144.165	00215.000	00132.211	00061.000	00192.007	00147.000	00117.676	00070.000	00140.000
3	3	00240.000	00215.000	00143.417	00158.957	00165.000	00147.703	00125.000	00143.417	00215.000	00132.211	00061.000	00192.007	00147.703	00118.088	00070.000	00140.694
4	4	00240.000	00199.016	00143.417	00168.892	00165.000	00147.703	00125.000	00143.417	00199.016	00118.227	00061.000	00192.007	00147.703	00118.378	00070.000	00140.000
5	5	00240.000	00214.144	00142.885	00158.957	00165.000	00148.203	00125.000	00142.885	00214.144	00131.354	00061.000	00192.007	00148.203	00118.378	00070.000	00141.194
6	6	00240.000	00215.000	00158.000	00173.540	00165.000	00134.007	00125.000	00158.000	00215.000	00132.211	00061.000	00192.007	00134.007	00118.378	00070.000	00107.306
7	1 2	00240.000	00199.016	00144.165	00169.640	00165.000	00147.000	00125.000	00144.165	00199.016	00118.227	00061.000	00192.007	00147.000	00117.676	00070.000	00140.000
8	1 3	00240.000	00199.016	00133.482	00158.957	00165.000	00157.034	00125.000	00133.482	00199.016	00118.227	00061.000	00192.007	00157.034	00123.507	00070.000	00150.032
9	1 6	00240.000	00199.016	00158.000	00183.475	00165.000	00134.007	00125.000	00158.000	00199.016	00118.227	00061.000	00192.007	00134.007	00127.709	00070.000	00085.032
10	2 6	00240.000	00215.000	00158.000	00173.540	00165.000	00134.007	00125.000	00158.000	00215.000	00132.211	00061.000	00192.007	00134.007	00117.676	00070.000	00108.984

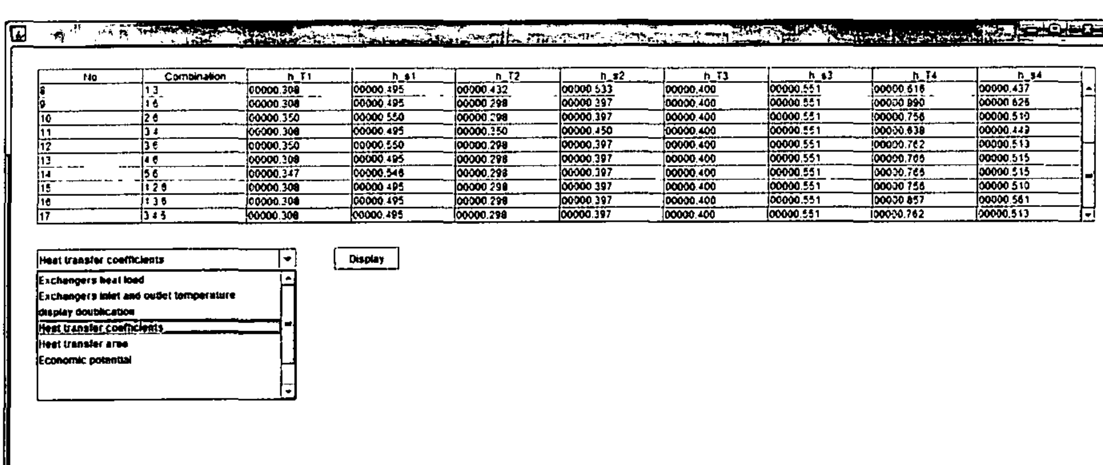

No	Combination	h_T1	h_s1	h_T2	h_s2	h_T3	h_s3	h_T4	h_s4
8	1 3	00000.308	00000.495	00000.432	00000.533	00000.400	00000.551	00000.616	00000.437
9	1 6	00000.308	00000.495	00000.298	00000.397	00000.400	00000.551	00000.990	00000.626
10	2 6	00000.350	00000.550	00000.298	00000.397	00000.400	00000.551	00000.756	00000.510
11	3 4	00000.308	00000.495	00000.350	00000.450	00000.400	00000.551	00000.638	00000.449
12	3 6	00000.350	00000.550	00000.298	00000.397	00000.400	00000.551	00000.762	00000.513
13	4 6	00000.308	00000.495	00000.298	00000.397	00000.400	00000.551	00000.765	00000.515
14	5 6	00000.347	00000.546	00000.298	00000.397	00000.400	00000.551	00000.765	00000.515
15	1 2 6	00000.308	00000.495	00000.298	00000.397	00000.400	00000.551	00000.756	00000.510
16	1 3 6	00000.308	00000.495	00000.298	00000.397	00000.400	00000.551	00000.857	00000.561
17	3 4 5	00000.308	00000.495	00000.298	00000.397	00000.400	00000.551	00000.762	00000.513

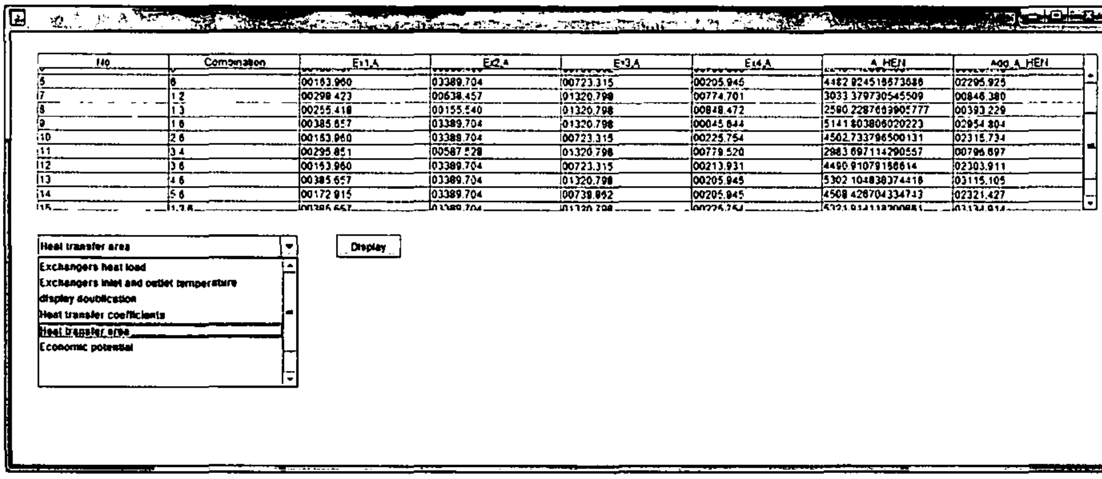

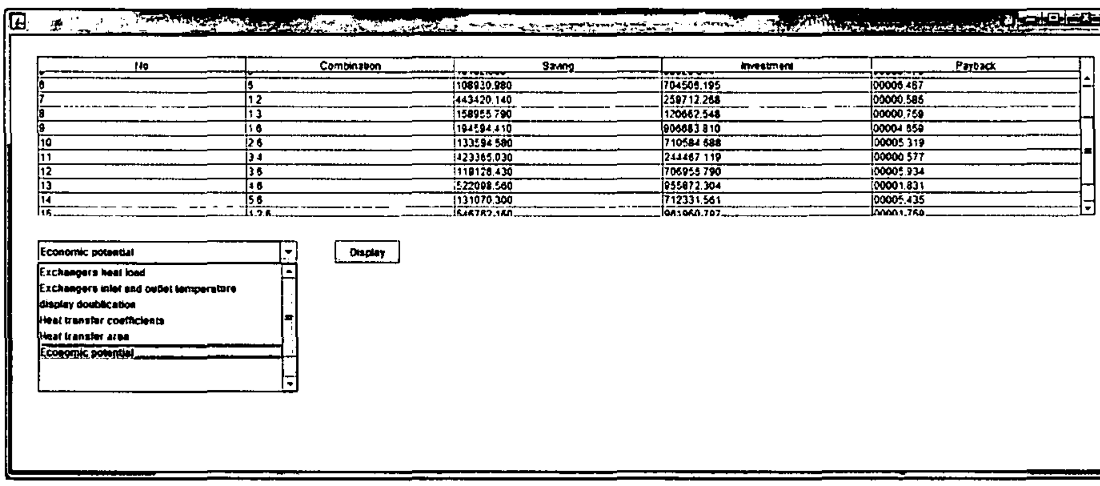

4.2. Results with the TF application

The results when applying the TF concept are mostly profile state along the TF range provided. The results are also shown graphically and in tables as for the case before the TF application. Below is the interfacing to show the way for pulling out the results after the TF application.

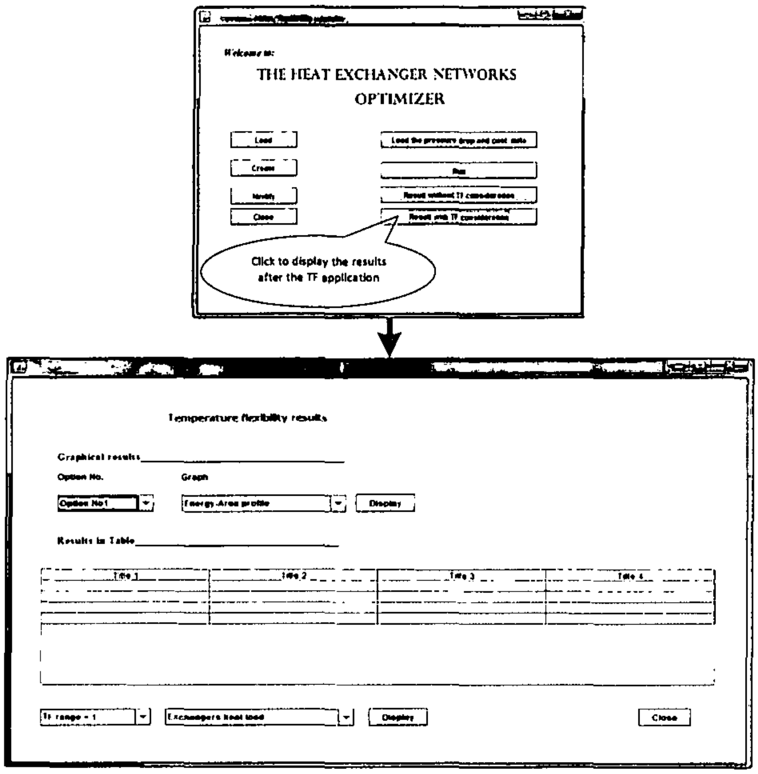

4.2.1. Graphical results

The way to display the graphical results after the TF application for each HEN retrofit option is demonstrated below:

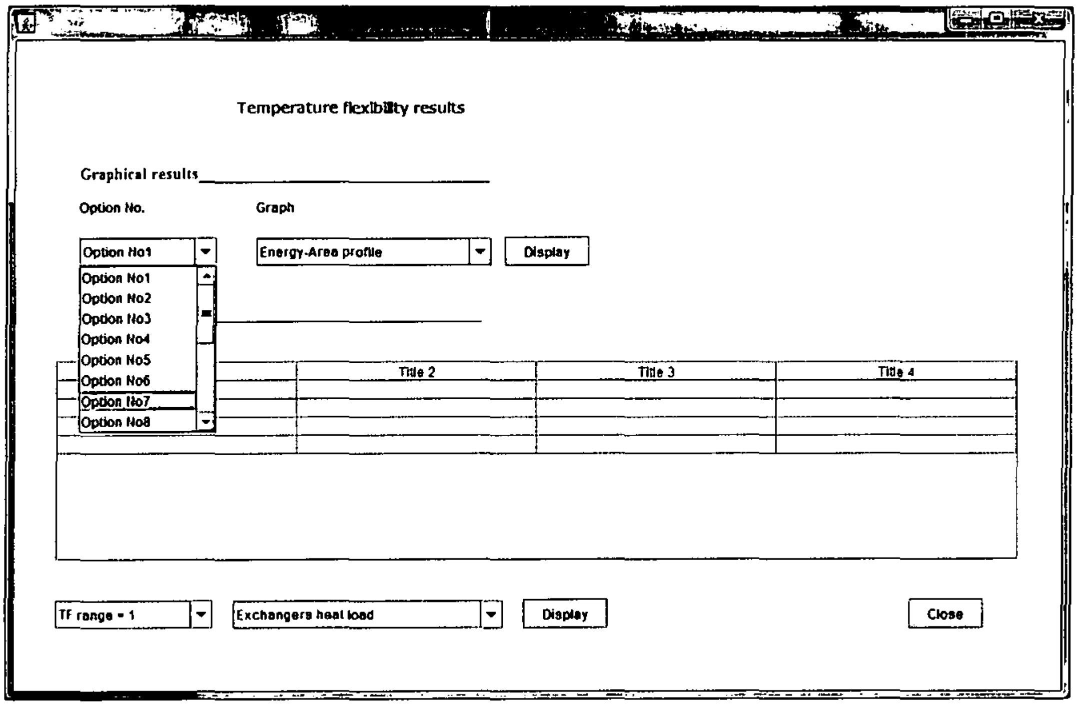

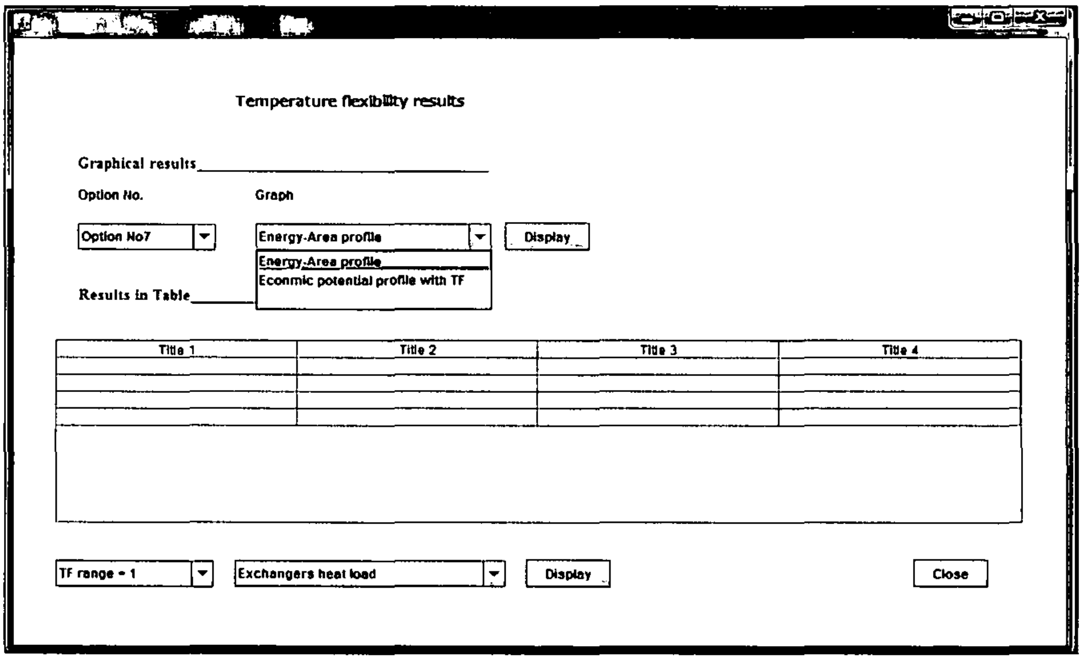
Temperature flexibility results
Graphical results
Option No.
Graph
Option No7
Energy-Area profile
Display
Energy-Area profile
Econmic potential profile with TF
Results in Table
Title 1
Title 2
Title 3
Title 4
TF range = 1
Exchangers heat load
Display
Close

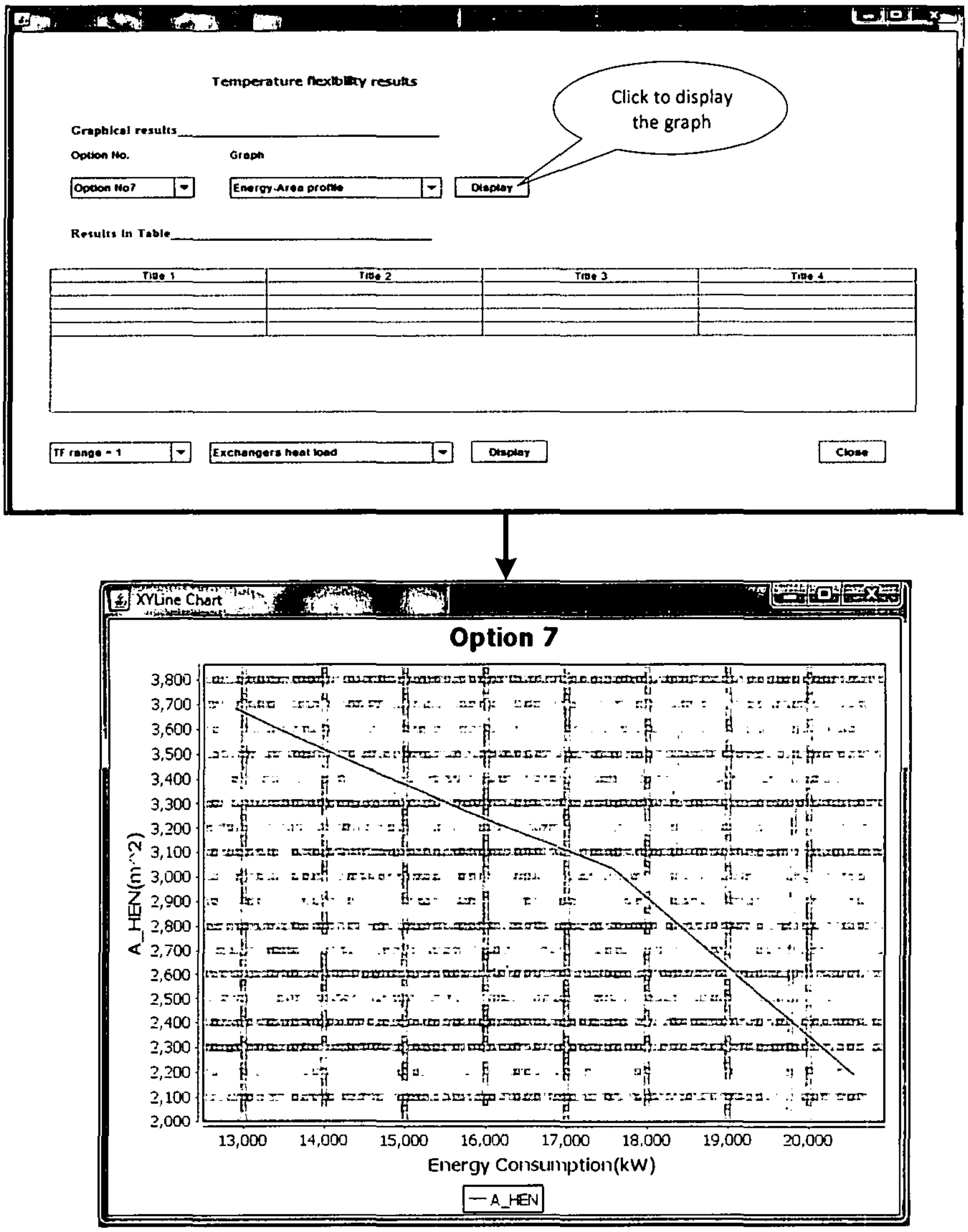
Temperature flexibility results
Click to display the graph
Graphical results
Option No.
Graph
Option No7
Energy-Area profile
Display
Results in Table
Title 1
Title 2
Title 3
Title 4
TF range = 1
Exchangers heat load
Display
Close
XYLine Chart
Option 7
A_HEN(m^2)
Energy Consumption(kW)
A_HEN

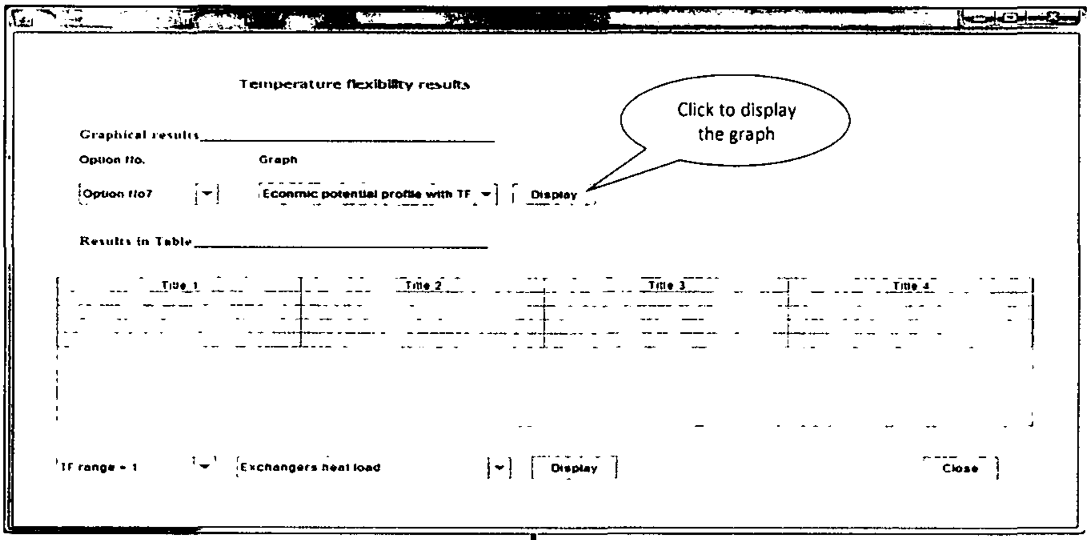
Temperature flexibility results
Click to display the graph
Graphical results
Option No.
Graph
Option No7
Econmic potential profile with TF
Display
Results in Table
Title 1
Title 2
Title 3
Title 4
TF range = 1
Exchangers heat load
Display
Close

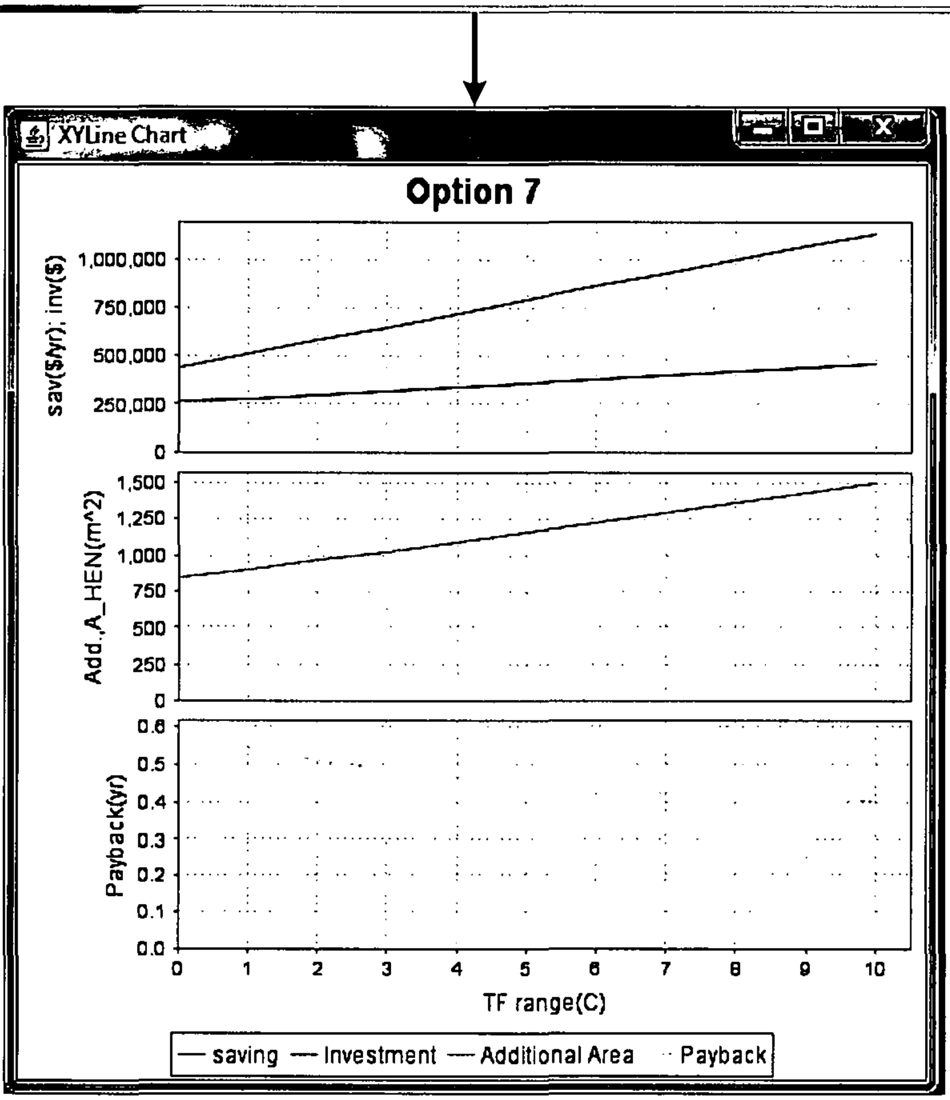
XYLine Chart
Option 7
sav($/yr); inv($)
1,000,000
750,000
500,000
250,000
0
Add.,A_HEN(m^2)
1,500
1,250
1,000
750
500
250
0
Payback(yr)
0.6
0.5
0.4
0.3
0.2
0.1
0.0
0 1 2 3 4 5 6 7 8 9 10
TF range(C)
saving
Investment
Additional Area
Payback

4.2.2. Results in tables

For the results to be shown in tables when considering the TF concept, specific TF range and the kind of the result to be displayed must be selected as shown below:

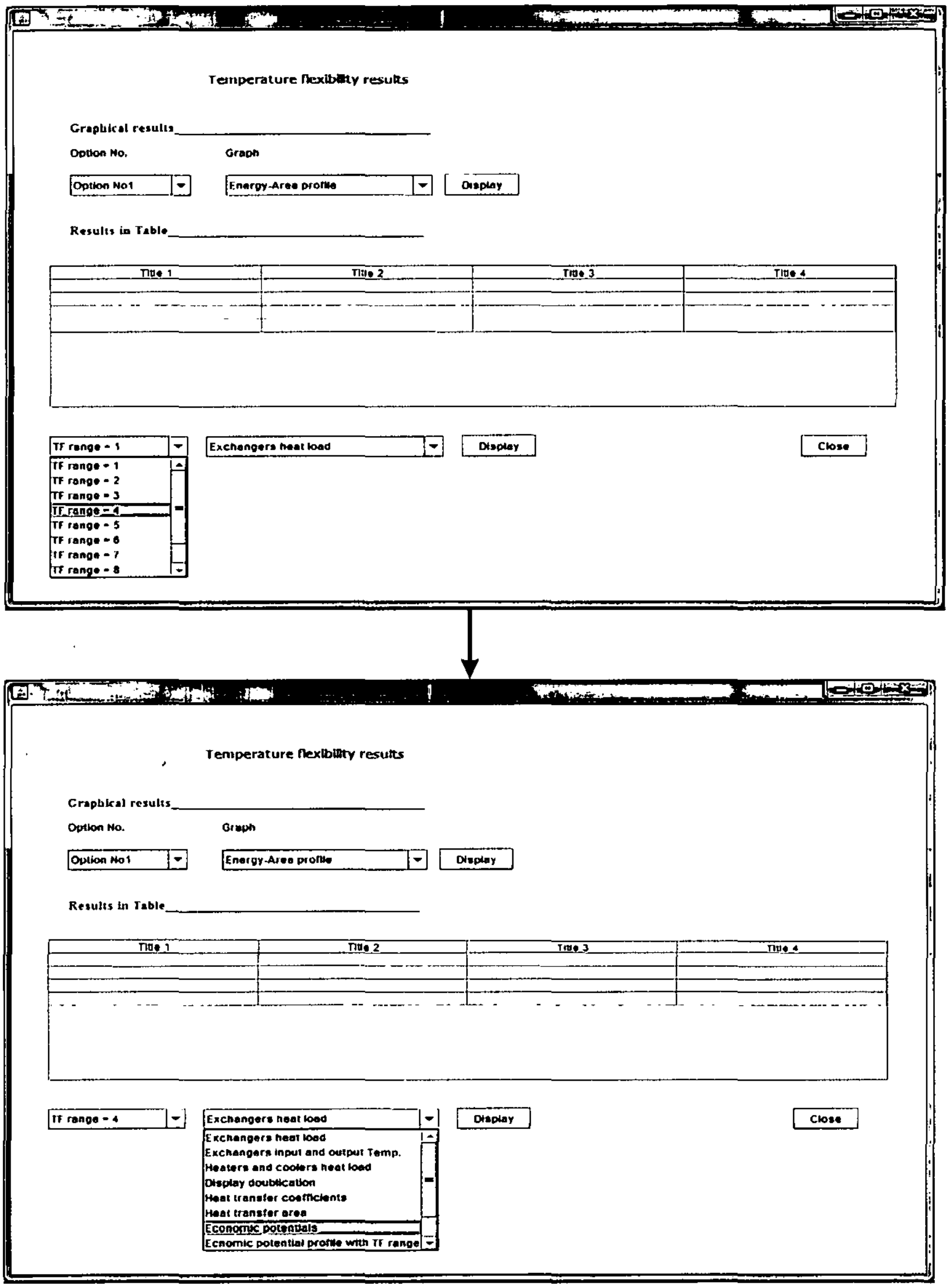

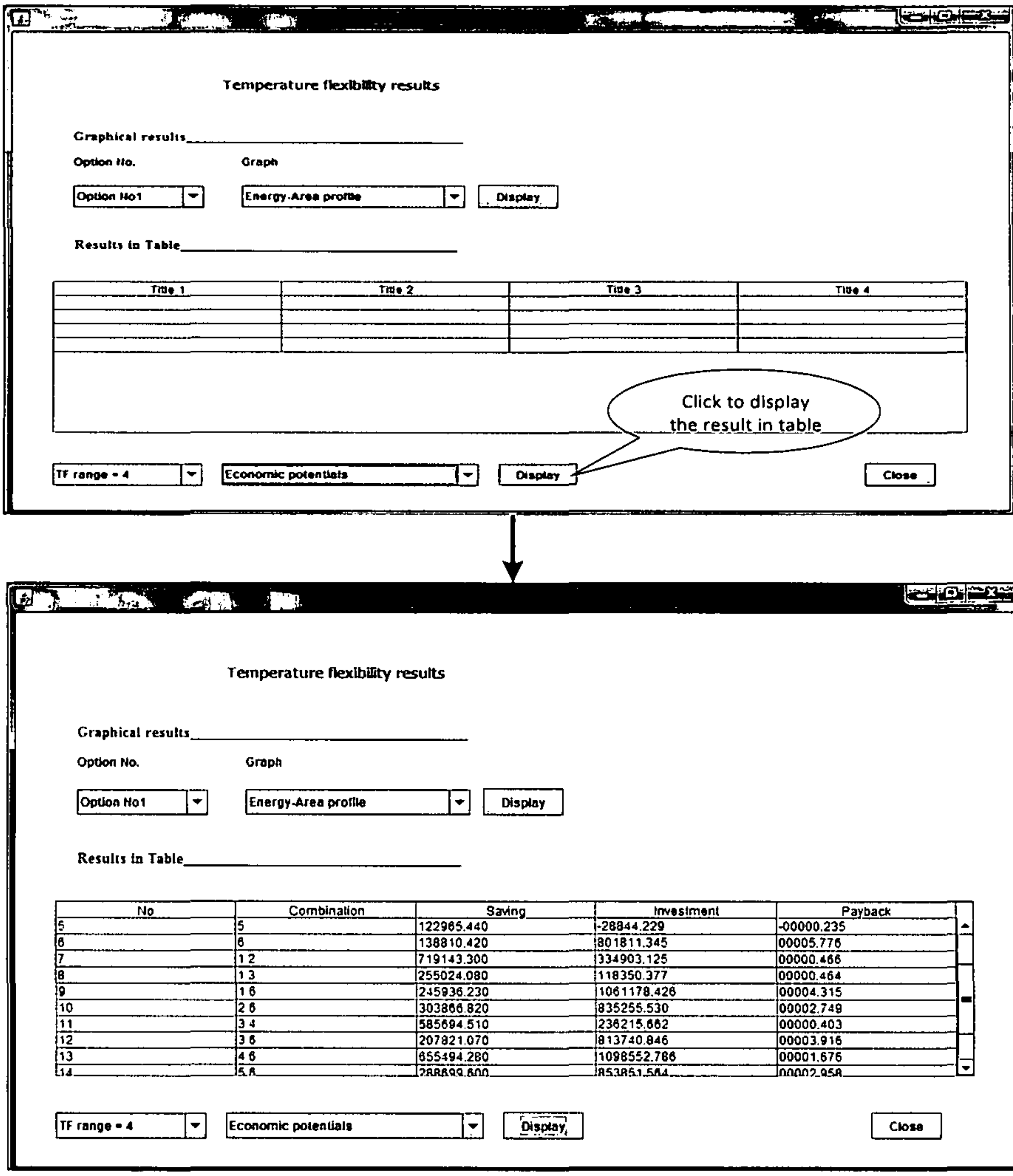

The tabulated results for the economic potentials could also be shown as a profile along the TF range for each retrofit option individually as shown below:

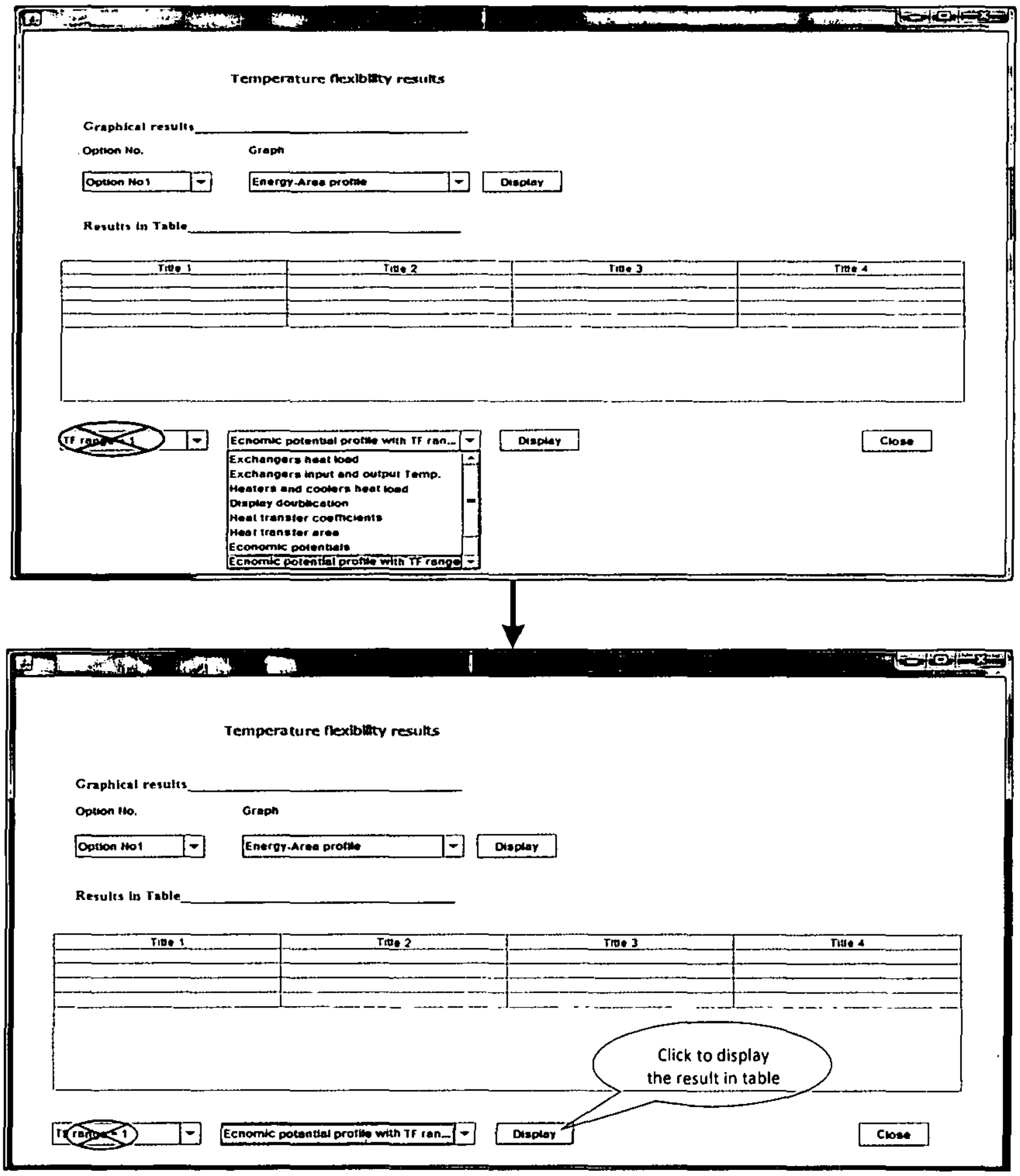
Temperature flexibility results
Graphical results
Option No.
Graph
Option No1
Energy-Area profile
Display
Results in Table
Title 1
Title 2
Title 3
Title 4
Ecnomic potential profile with TF ran...
Display
Close
Exchangers heat load
Exchangers input and output Temp.
Heaters and coolers heat load
Display doublication
Heat transfer coefficients
Heat transfer area
Economic potentials
Ecnomic potential profile with TF range
Click to display the result in table

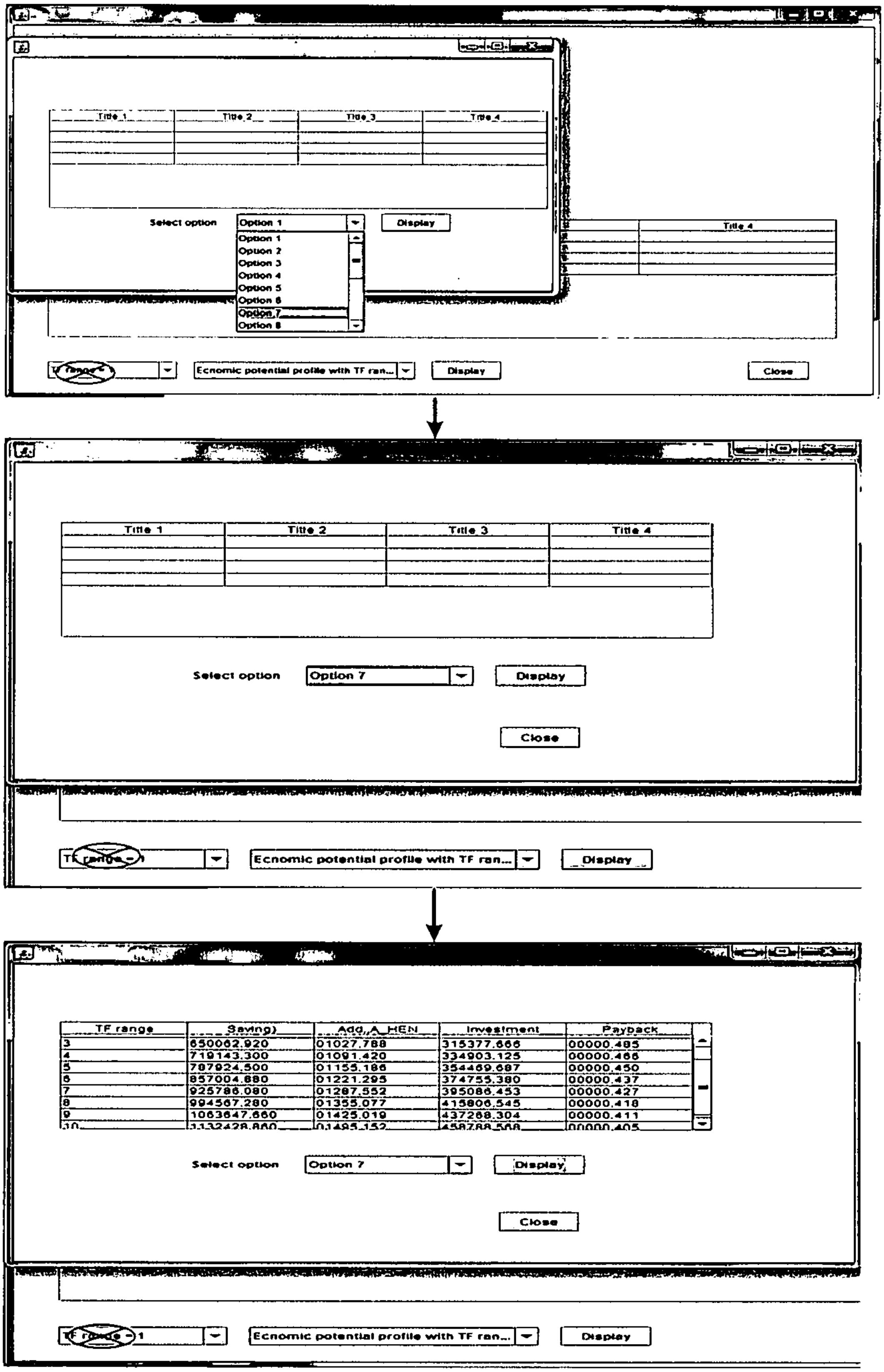
Title 1
Title 2
Title 3
Title 4
Select option
Option 1
Display
Option 2
Option 3
Option 4
Option 5
Option 6
Option 7
Option 8
Ecnomic potential profile with TF ran...
Close
TF range
Saving)
Add,,A_HEN
Investment
Payback
3
650062.920
01027.788
315377.666
00000.485
4
719143.300
01091.420
334903.125
00000.466
5
787924.500
01155.186
354469.687
00000.450
6
857004.880
01221.295
374755.380
00000.437
7
925786.080
01287.552
395086.453
00000.427
8
994567.280
01355.077
415806.545
00000.418
9
1063647.660
01425.019
437268.304
00000.411

APPENDIX B

DEMONSTRATION OF THE COMBINED PATHS ON A HEN GRID

In addition to the individual paths, combinations of them have been created in several ways according to the developed *paths combination approach* for generating the HEN retrofit options. For more understanding, these combinations are demonstrated in the grid diagram as shown in the following figures for the HEN demonstrative example.

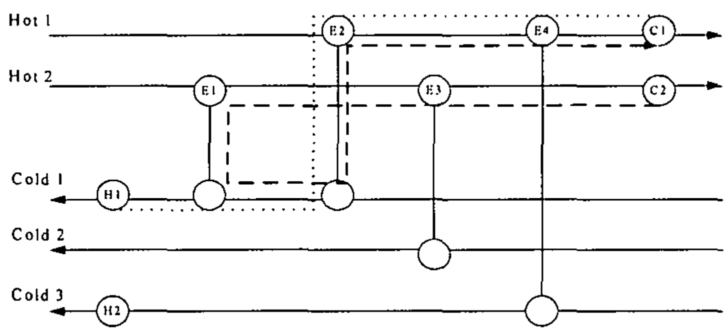

Fig. B1: Option 7

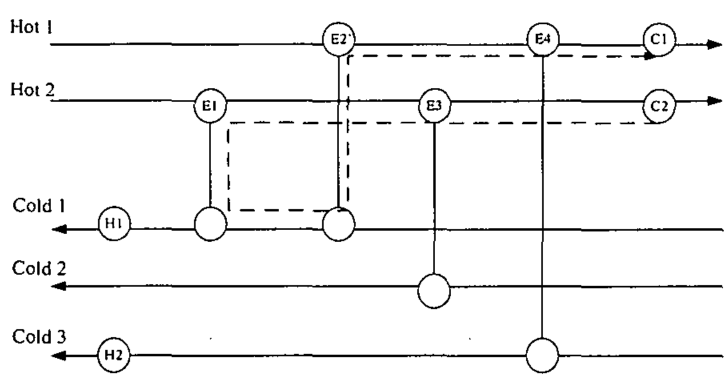

Fig. B2: Option 8

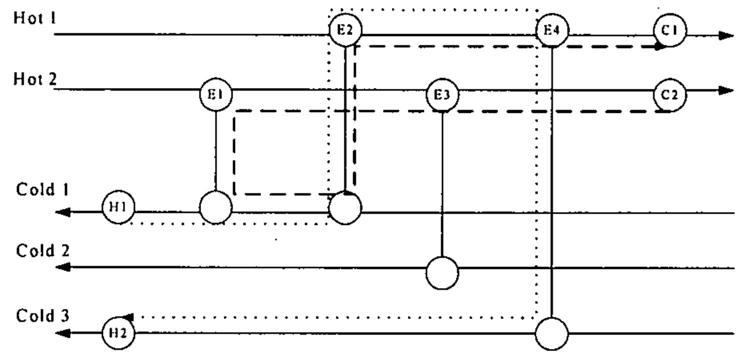

Fig. B3: Option 9

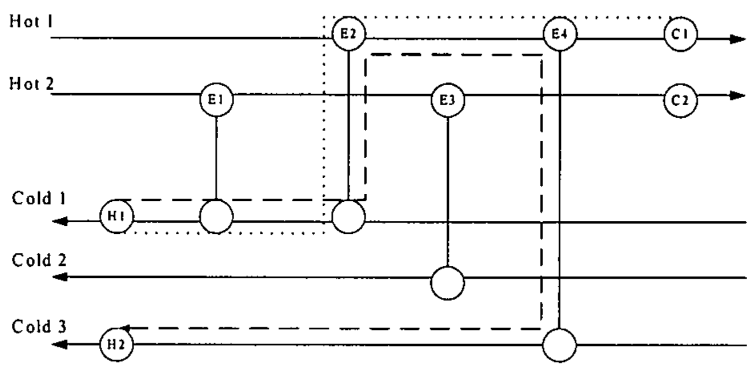

Fig. B4: Option 10

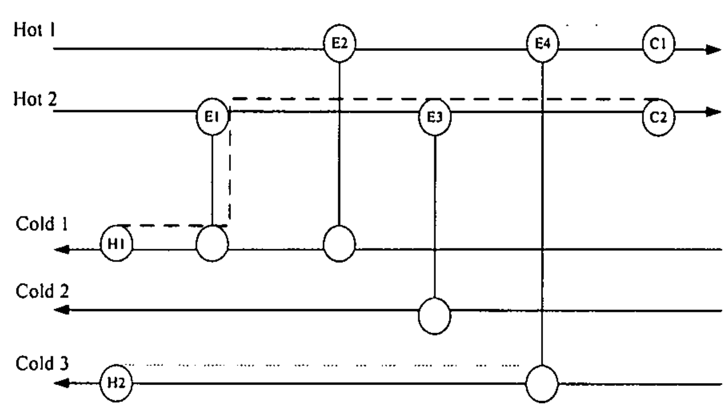

Fig. B5: Option 11

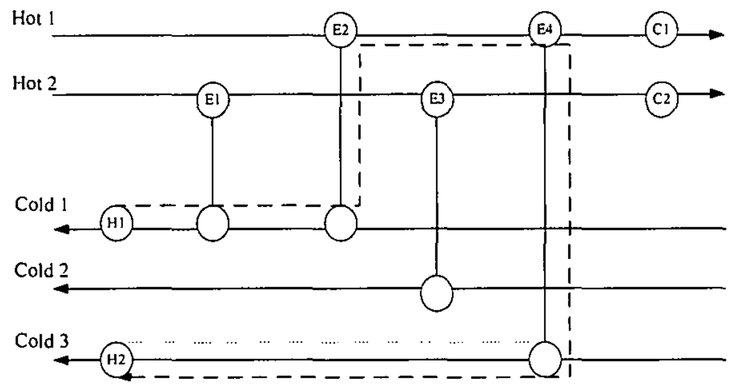

Fig. B6: Option 12

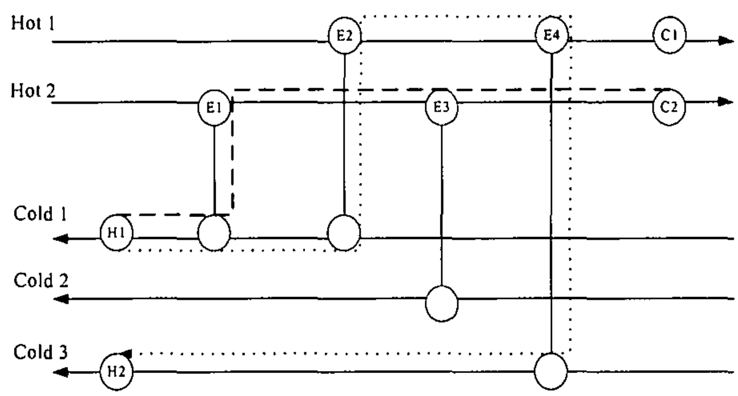

Fig. B7: Option 13

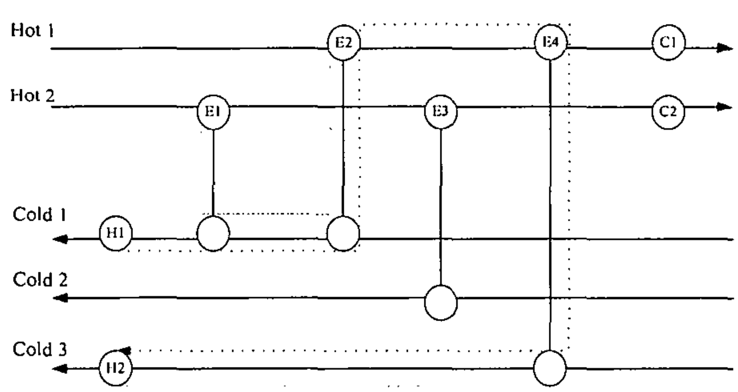

Fig. B8: Option 14

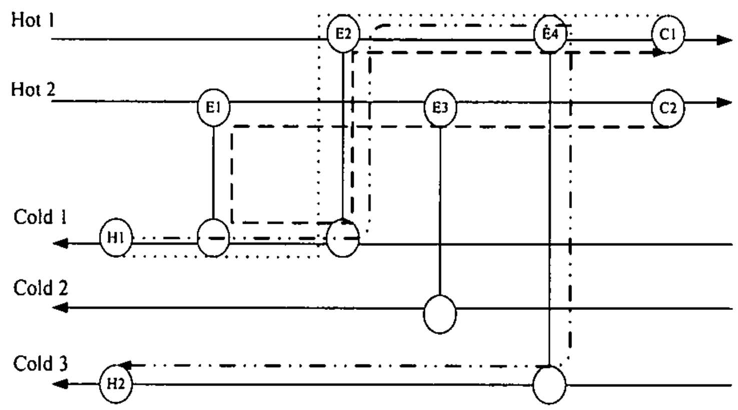

Fig. B9: Option 15

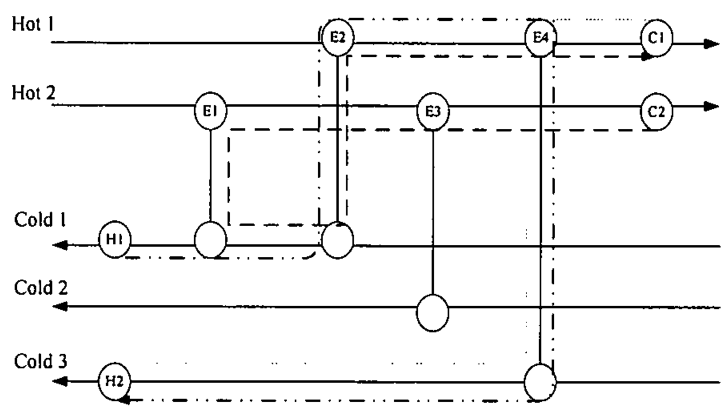

Fig. B10: Option 16

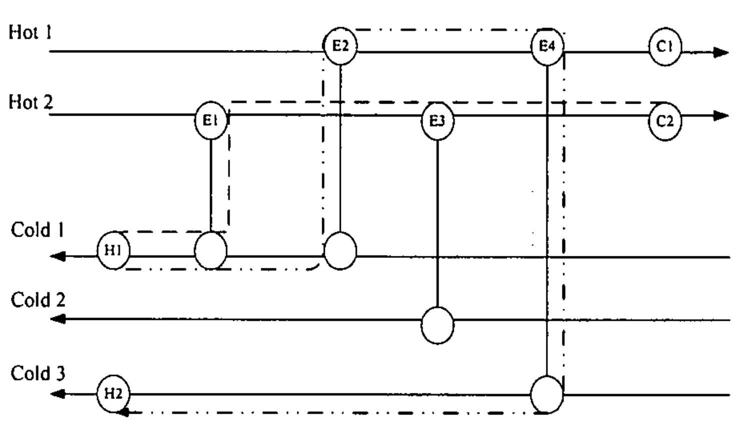

Fig. B11: Option 17

APPENDIX C

GENERATED DATA USING THE PATHS COMBINATION WITH TF CONSIDERATION

For the case study of the HEN followed in this work, the initial data resulted from the heat load shifting before and after considering the TF concept is tabulated here for heaters, exchangers, and coolers of the existing HEN. The corresponding temperature results before and after each device in the HEN is also tabulated in this Appendix. It must be mentioned that the HEN retrofit using option 9 is omitted at the TF range of 5°C onwards where one of the exchangers reveals a negative value for the heat load which is not applicable. The resulted heat transfer area and heat transfer coefficients are also tabulated here for the case before applying the TF concept.

Before the TF application

Table C1: The heat duty result before the TF application

Option	Heat load (kW)							
	Q_{H1}	Q_{H2}	Q_{E1}	Q_{E2}	Q_{E3}	Q_{E4}	Q_{C1}	Q_{C2}
1	8485	2790	3542	1178	7153	4340	4842	4425
2	8381	2790	2160	2664	7153	4340	3356	5807
3	8485	2747	2160	2560	7153	4383	3417	5807
4	7103	2790	3542	2560	7153	4340	3460	4425
5	8485	2716	2234	2486	7153	4414	3460	5733
6	6458	4817	2160	4587	7153	2313	3460	5807
7	6999	2790	3542	2664	7153	4340	3356	4425
8	8485	2168	3542	1178	7153	4962	4220	4425
9	5076	6199	3542	4587	7153	931	4842	4425
10	6458	4713	2160	4587	7153	2417	3356	5807
11	7103	2747	3542	2560	7153	4383	3417	4425
12	6458	4774	2160	4587	7153	2356	3417	5807
13	5076	4817	3542	4587	7153	2313	3460	4425
14	6384	4817	2234	4587	7153	2313	3460	5733
15	5076	4713	3542	4587	7153	2417	3356	4425
16	5076	5577	3542	4587	7153	1553	4220	4425
17	5076	4774	3542	4587	7153	2356	3417	4425

Table C2: Temperature (^oC) between the HEN devices before the TF application

Option	T_{ho2}	T_{ho4}	T_{ho1}	T_{ho3}	T_{co1}	T_{co2}	T_{co4}
1	157.041	127.716	199.005	116.215	158.957	133.475	140
2	147	117.676	215	132.211	159.705	144.165	140
3	147.703	118.088	215	132.211	158.957	143.417	140.694
4	147.703	118.378	199.005	116.215	168.899	143.417	140
5	148.203	118.378	214.144	131.354	158.957	142.885	141.194
6	134.007	118.378	215	132.211	173.54	158	107.306
7	147	117.676	199.005	116.215	169.647	144.165	140
8	157.041	123.514	199.005	116.215	158.957	133.475	150.032
9	134.007	127.716	199.005	116.215	183.482	158	85.0161
10	134.007	117.676	215	132.211	173.54	158	108.984
11	147.703	118.088	199.005	116.215	168.899	143.417	140.694
12	134.007	118.088	215	132.211	173.54	158	108
13	134.007	118.378	199.005	116.215	183.482	158	107.306
14	134.007	118.378	214.144	131.354	174.072	158	107.306
15	134.007	117.676	199.005	116.215	183.482	158	108.984
16	134.007	123.514	199.005	116.215	183.482	158	95.0484
17	134.007	118.088	199.005	116.215	183.482	158	108

Table C3: Heat transfer coefficients for the HEN exchangers before the TF application

Option	Heat transfer coefficient ($kW/m^2.^oC$)							
	E1		E2		E3		E4	
	h_T	h_S	h_T	h_S	h_T	h_S	h_T	h_S
1	0.308	0.495	0.432	0.533	0.4	0.551	0.64	0.45
2	0.35	0.55	0.346	0.446	0.4	0.551	0.64	0.45
3	0.35	0.55	0.35	0.45	0.4	0.551	0.638	0.449
4	0.308	0.495	0.35	0.45	0.4	0.551	0.64	0.45
5	0.347	0.546	0.353	0.453	0.4	0.551	0.637	0.448
6	0.35	0.55	0.298	0.397	0.4	0.551	0.766	0.515
7	0.308	0.495	0.346	0.446	0.4	0.551	0.64	0.45
8	0.308	0.495	0.432	0.533	0.4	0.551	0.616	0.437
9	0.308	0.495	0.298	0.397	0.4	0.551	0.99	0.627
10	0.35	0.55	0.298	0.397	0.4	0.551	0.756	0.51
11	0.308	0.495	0.35	0.45	0.4	0.551	0.638	0.449
12	0.35	0.55	0.298	0.397	0.4	0.551	0.762	0.513
13	0.308	0.495	0.298	0.397	0.4	0.551	0.766	0.515
14	0.347	0.546	0.298	0.397	0.4	0.551	0.766	0.515
15	0.308	0.495	0.298	0.397	0.4	0.551	0.756	0.51
16	0.308	0.495	0.298	0.397	0.4	0.551	0.857	0.561
17	0.308	0.495	0.298	0.397	0.4	0.551	0.762	0.513

Table C4: Heat transfer area for the HEN exchangers and the overall HEN before the TF application

Option	Heat transfer area (m^2)				
	A_{E1}	A_{E2}	A_{E3}	A_{E4}	A_{HEN}
1	255.514	155.311	1321	492.587	2224
2	133.851	638.376	723.231	774.657	2270
3	132.536	587.449	723.231	779.484	2223
4	295.995	587.449	1321	741.936	2946
5	138.485	553.389	739.769	783.273	2215
6	163.957	3389	723.231	205.929	4482
7	299.569	638.376	1321	774.657	3034
8	255.514	155.311	1321	848.046	2580
9	385.865	3389	1321	45.568	5141
10	163.957	3389	723.231	225.737	4502
11	295.995	587.449	1321	779.484	2984
12	163.957	3389	723.231	213.915	4490
13	385.865	3389	1321	205.929	5302
14	172.957	3389	740.176	205.929	4508
15	385.865	3389	1321	225.737	5322
16	385.865	3389	1321	99.858	5196
17	385.865	3389	1321	213.915	5310

After the TF application

Table C5: The heat duty result at the TF range of 1°C

Option	Heat load (kW)							
	Q_{H1}	Q_{H2}	Q_{E1}	Q_{E2}	Q_{E3}	Q_{E4}	Q_{C1}	Q_{C2}
1	8485	2790	3628	1092	7153	4340	4928	4339
2	8233	2790	2160	2812	7153	4340	3208	5807
3	8485	2685	2160	2560	7153	4445	3355	5807
4	7017	2790	3628	2560	7153	4340	3460	4339
5	8485	2609	2341	2379	7153	4521	3460	5626
6	6319	4956	2160	4726	7153	2174	3460	5807
7	6765	2790	3628	2812	7153	4340	3208	4339
8	8485	2070	3628	1092	7153	5060	4208	4339
9	4851	6424	3628	4726	7153	706	4928	4339
10	6319	4704	2160	4726	7153	2426	3208	5807
11	7017	2685	3628	2560	7153	4445	3355	4339
12	6319	4851	2160	4726	7153	2279	3355	5807
13	4851	4956	3628	4726	7153	2174	3460	4339
14	6138	4956	2341	4726	7153	2174	3460	5626
15	4851	4704	3628	4726	7153	2426	3208	4339
16	4851	5704	3628	4726	7153	1426	4208	4339
17	4851	4851	3628	4726	7153	2279	3355	4339

Table C6: Temperature between the HEN devices at the TF range of 1°C (increasing the hot streams' temperature by 1°C)

Option	*Ts1*	*Ts2*	*Ts3*	*Ts4*	*Ts5*	*Tt1*	*Tt2*	*Tt3*	*Tt4*	*Tt5*	*Tho2*	*Tho4*	*Tho1*	*Tho3*	*Tco1*	*Tco2*	*Tco4*
1	166.00	241.00	125.00	61.00	70.00	96.00	66.00	220.00	192.00	185.00	158.62	129.30	199.01	116.22	158.96	132.86	140.00
2	166.00	241.00	125.00	61.00	70.00	96.00	66.00	220.00	192.00	185.00	147.00	117.68	216.00	133.21	160.77	145.23	140.00
3	166.00	241.00	125.00	61.00	70.00	96.00	66.00	220.00	192.00	185.00	148.70	118.67	216.00	133.21	158.96	143.42	141.69
4	166.00	241.00	125.00	61.00	70.00	96.00	66.00	220.00	192.00	185.00	148.70	119.38	199.01	116.22	169.52	143.42	140.00
5	166.00	241.00	125.00	61.00	70.00	96.00	66.00	220.00	192.00	185.00	149.93	119.38	213.91	131.12	158.96	142.12	142.92
6	166.00	241.00	125.00	61.00	70.00	96.00	66.00	220.00	192.00	185.00	134.07	119.38	216.00	133.21	174.54	159.00	105.07
7	166.00	241.00	125.00	61.00	70.00	96.00	66.00	220.00	192.00	185.00	147.00	117.68	199.01	116.22	171.33	145.23	140.00
8	166.00	241.00	125.00	61.00	70.00	96.00	66.00	220.00	192.00	185.00	158.62	124.43	199.01	116.22	158.96	132.86	151.61
9	166.00	241.00	125.00	61.00	70.00	96.00	66.00	220.00	192.00	185.00	134.07	129.30	199.01	116.22	185.10	159.00	81.39
10	166.00	241.00	125.00	61.00	70.00	96.00	66.00	220.00	192.00	185.00	134.07	117.68	216.00	133.21	174.54	159.00	109.13
11	166.00	241.00	125.00	61.00	70.00	96.00	66.00	220.00	192.00	185.00	148.70	118.67	199.01	116.22	169.52	143.42	141.69
12	166.00	241.00	125.00	61.00	70.00	96.00	66.00	220.00	192.00	185.00	134.07	118.67	216.00	133.21	174.54	159.00	106.76
13	166.00	241.00	125.00	61.00	70.00	96.00	66.00	220.00	192.00	185.00	134.07	119.38	199.01	116.22	185.10	159.00	105.07
14	166.00	241.00	125.00	61.00	70.00	96.00	66.00	220.00	192.00	185.00	134.07	119.38	213.91	131.12	175.84	159.00	105.07
15	166.00	241.00	125.00	61.00	70.00	96.00	66.00	220.00	192.00	185.00	134.07	117.68	199.01	116.22	185.10	159.00	109.13
16	166.00	241.00	125.00	61.00	70.00	96.00	66.00	220.00	192.00	185.00	134.07	124.43	199.01	116.22	185.10	159.00	93.00
17	166.00	241.00	125.00	61.00	70.00	96.00	66.00	220.00	192.00	185.00	134.07	118.67	199.01	116.22	185.10	159.00	106.76

Table C7: The heat duty result at the TF range of 2°C

Option	Heat load (kW)							
	Q_{H1}	Q_{H2}	Q_{E1}	Q_{E2}	Q_{E3}	Q_{E4}	Q_{C1}	Q_{C2}
1	8485	2790	3715	1005	7153	4340	5015	4252
2	8085	2790	2160	2960	7153	4340	3060	5807
3	8485	2623	2160	2560	7153	4507	3293	5807
4	6930	2790	3715	2560	7153	4340	3460	4252
5	8485	2502	2448	2272	7153	4628	3460	5519
6	6180	5095	2160	4865	7153	2035	3460	5807
7	6530	2790	3715	2960	7153	4340	3060	4252
8	8485	1972	3715	1005	7153	5158	4197	4252
9	4625	6650	3715	4865	7153	480	5015	4252
10	6180	4695	2160	4865	7153	2435	3060	5807
11	6930	2623	3715	2560	7153	4507	3293	4252
12	6180	4928	2160	4865	7153	2202	3293	5807
13	4625	5095	3715	4865	7153	2035	3460	4252
14	5892	5095	2448	4865	7153	2035	3460	5519
15	4625	4695	3715	4865	7153	2435	3060	4252
16	4625	5832	3715	4865	7153	1298	4197	4252
17	4625	4928	3715	4865	7153	2202	3293	4252

Table C8: Temperature between the HEN devices at the TF range of 2°C (increasing the hot streams' temperature by 2°C)

Option	Ts1	Ts2	Ts3	Ts4	Ts5	Tt1	Tt2	Tt3	Tt4	Tt5	Tho2	Tho4	Tho1	Tho3	Tco1	Tco2	Tco4
1	167	242.00	125.00	61.00	70.00	97.00	67.00	220.00	192.00	185.00	160.21	130.89	199.00	116.21	158.96	132.23	140.00
2	167	242.00	125.00	61.00	70.00	97.00	67.00	220.00	192.00	185.00	147.00	117.68	217.00	134.21	161.84	146.30	140.00
3	167	242.00	125.00	61.00	70.00	97.00	67.00	220.00	192.00	185.00	149.70	119.25	217.00	134.21	158.96	143.42	142.69
4	167	242.00	125.00	61.00	70.00	97.00	67.00	220.00	192.00	185.00	149.70	120.38	199.00	116.21	170.14	143.42	140.00
5	167	242.00	125.00	61.00	70.00	97.00	67.00	220.00	192.00	185.00	151.65	120.38	213.67	130.88	158.96	141.35	144.65
6	167	242.00	125.00	61.00	70.00	97.00	67.00	220.00	192.00	185.00	134.13	120.38	217.00	134.21	175.54	160.00	102.82
7	167	242.00	125.00	61.00	70.00	97.00	67.00	220.00	192.00	185.00	147.00	117.68	199.00	116.21	173.02	146.30	140.00
8	167	242.00	125.00	61.00	70.00	97.00	67.00	220.00	192.00	185.00	160.21	125.36	199.00	116.21	158.96	132.23	153.19
9	167	242.00	125.00	61.00	70.00	97.00	67.00	220.00	192.00	185.00	134.13	130.89	199.00	116.21	186.73	160.00	77.74
10	167	242.00	125.00	61.00	70.00	97.00	67.00	220.00	192.00	185.00	134.13	117.68	217.00	134.21	175.54	160.00	109.27
11	167	242.00	125.00	61.00	70.00	97.00	67.00	220.00	192.00	185.00	149.70	119.25	199.00	116.21	170.14	143.42	142.69
12	167	242.00	125.00	61.00	70.00	97.00	67.00	220.00	192.00	185.00	134.13	119.25	217.00	134.21	175.54	160.00	105.52
13	167	242.00	125.00	61.00	70.00	97.00	67.00	220.00	192.00	185.00	134.13	120.38	199.00	116.21	186.73	160.00	102.82
14	167	242.00	125.00	61.00	70.00	97.00	67.00	220.00	192.00	185.00	134.13	120.38	213.67	130.88	177.61	160.00	102.82
15	167	242.00	125.00	61.00	70.00	97.00	67.00	220.00	192.00	185.00	134.13	117.68	199.00	116.21	186.73	160.00	109.27
16	167	242.00	125.00	61.00	70.00	97.00	67.00	220.00	192.00	185.00	134.13	125.36	199.00	116.21	186.73	160.00	90.94
17	167	242.00	125.00	61.00	70.00	97.00	67.00	220.00	192.00	185.00	134.13	119.25	199.00	116.21	186.73	160.00	105.52

Table C9: The heat duty result at the TF range of 3°C

Option	Heat load (kW)							
	Q_{H1}	Q_{H2}	Q_{E1}	Q_{E2}	Q_{E3}	Q_{E4}	Q_{C1}	Q_{C2}
1	8485	2790	3801	919	7153	4340	5101	4166
2	7937	2790	2160	3108	7153	4340	2912	5807
3	8485	2561	2160	2560	7153	4569	3231	5807
4	6844	2790	3801	2560	7153	4340	3460	4166
5	8485	2395	2555	2165	7153	4735	3460	5412
6	6041	5234	2160	5004	7153	1896	3460	5807
7	6296	2790	3801	3108	7153	4340	2912	4166
8	8485	1873	3801	919	7153	5257	4184	4166
9	4400	6875	3801	5004	7153	255	5101	4166
10	6041	4686	2160	5004	7153	2444	2912	5807
11	6844	2561	3801	2560	7153	4569	3231	4166
12	6041	5005	2160	5004	7153	2125	3231	5807
13	4400	5234	3801	5004	7153	1896	3460	4166
14	5646	5234	2555	5004	7153	1896	3460	5412
15	4400	4686	3801	5004	7153	2444	2912	4166
16	4400	5958	3801	5004	7153	1172	4184	4166
17	4400	5005	3801	5004	7153	2125	3231	4166

Table C10: Temperature between the HEN devices at the TF range of 3°C

(increasing the hot streams' temperature by 3°C)

Option	Ts1	Ts2	Ts3	Ts4	Ts5	Tt1	Tt2	Tt3	Tt4	Tt5	Tho2	Tho4	Tho1	Tho3	Tco1	Tco2	Tco4
1	168.00	243.00	125.00	61.00	70.00	98.00	68.00	220.00	192.00	185.00	161.79	132.47	199.01	116.22	158.96	131.61	140.00
2	168.00	243.00	125.00	61.00	70.00	98.00	68.00	220.00	192.00	185.00	147.00	117.68	218.00	135.21	162.90	147.36	140.00
3	168.00	243.00	125.00	61.00	70.00	98.00	68.00	220.00	192.00	185.00	150.70	119.83	218.00	135.21	158.96	143.42	143.69
4	168.00	243.00	125.00	61.00	70.00	98.00	68.00	220.00	192.00	185.00	150.70	121.38	199.01	116.22	170.76	143.42	140.00
5	168.00	243.00	125.00	61.00	70.00	98.00	68.00	220.00	192.00	185.00	153.37	121.38	213.43	130.64	158.96	140.58	146.37
6	168.00	243.00	125.00	61.00	70.00	98.00	68.00	220.00	192.00	185.00	134.19	121.38	218.00	135.21	176.54	161.00	100.58
7	168.00	243.00	125.00	61.00	70.00	98.00	68.00	220.00	192.00	185.00	147.00	117.68	199.01	116.22	174.71	147.36	140.00
8	168.00	243.00	125.00	61.00	70.00	98.00	68.00	220.00	192.00	185.00	161.79	126.27	199.01	116.22	158.96	131.61	154.79
9	168.00	243.00	125.00	61.00	70.00	98.00	68.00	220.00	192.00	185.00	134.19	132.47	199.01	116.22	188.35	161.00	74.11
10	168.00	243.00	125.00	61.00	70.00	98.00	68.00	220.00	192.00	185.00	134.19	117.68	218.00	135.21	176.54	161.00	109.42
11	168.00	243.00	125.00	61.00	70.00	98.00	68.00	220.00	192.00	185.00	150.70	119.83	199.01	116.22	170.76	143.42	143.69
12	168.00	243.00	125.00	61.00	70.00	98.00	68.00	220.00	192.00	185.00	134.19	119.83	218.00	135.21	176.54	161.00	104.27
13	168.00	243.00	125.00	61.00	70.00	98.00	68.00	220.00	192.00	185.00	134.19	121.38	199.01	116.22	188.35	161.00	100.58
14	168.00	243.00	125.00	61.00	70.00	98.00	68.00	220.00	192.00	185.00	134.19	121.38	213.43	130.64	179.38	161.00	100.58
15	168.00	243.00	125.00	61.00	70.00	98.00	68.00	220.00	192.00	185.00	134.19	117.68	199.01	116.22	188.35	161.00	109.42
16	168.00	243.00	125.00	61.00	70.00	98.00	68.00	220.00	192.00	185.00	134.19	126.27	199.01	116.22	188.35	161.00	88.90
17	168.00	243.00	125.00	61.00	70.00	98.00	68.00	220.00	192.00	185.00	134.19	119.83	199.01	116.22	188.35	161.00	104.27

Table C11: The heat duty result at the TF range of 4°C

Option	Heat load (kW)							
	Q_{H1}	Q_{H2}	Q_{E1}	Q_{E2}	Q_{E3}	Q_{E4}	Q_{C1}	Q_{C2}
1	8485	2790	3888	832	7153	4340	5188	4079
2	7789	2790	2160	3256	7153	4340	2764	5807
3	8485	2499	2160	2560	7153	4631	3169	5807
4	6757	2790	3888	2560	7153	4340	3460	4079
5	8485	2289	2661	2059	7153	4841	3460	5306
6	5902	5373	2160	5143	7153	1757	3460	5807
7	6061	2790	3888	3256	7153	4340	2764	4079
8	8485	1775	3888	832	7153	5355	4173	4079
9	4174	7101	3888	5143	7153	29	5188	4079
10	5902	4677	2160	5143	7153	2453	2764	5807
11	6757	2499	3888	2560	7153	4631	3169	4079
12	5902	5082	2160	5143	7153	2048	3169	5807
13	4174	5373	3888	5143	7153	1757	3460	4079
14	5401	5373	2661	5143	7153	1757	3460	5306
15	4174	4677	3888	5143	7153	2453	2764	4079
16	4174	6086	3888	5143	7153	1044	4173	4079
17	4174	5082	3888	5143	7153	2048	3169	4079

Table C12: Temperature between the HEN devices at the TF range of 4°C (increasing the hot streams' temperature by 4°C)

Option	T_{s1}	T_{s2}	T_{s3}	T_{s4}	T_{s5}	T_{t1}	T_{t2}	T_{t3}	T_{t4}	T_{t5}	T_{ho2}	T_{ho4}	T_{ho1}	T_{ho3}	T_{co1}	T_{co2}	T_{co4}
1	169.00	244.00	125.00	61.00	70.00	99.00	69.00	220.00	192.00	185.00	163.38	134.05	199.00	116.21	158.96	130.99	140.00
2	169.00	244.00	125.00	61.00	70.00	99.00	69.00	220.00	192.00	185.00	147.00	117.68	219.00	136.21	163.96	148.42	140.00
3	169.00	244.00	125.00	61.00	70.00	99.00	69.00	220.00	192.00	185.00	151.70	120.41	219.00	136.21	158.96	143.42	144.69
4	169.00	244.00	125.00	61.00	70.00	99.00	69.00	220.00	192.00	185.00	151.70	122.38	199.00	116.21	171.39	143.42	140.00
5	169.00	244.00	125.00	61.00	70.00	99.00	69.00	220.00	192.00	185.00	155.09	122.38	213.20	130.41	158.96	139.81	148.08
6	169.00	244.00	125.00	61.00	70.00	99.00	69.00	220.00	192.00	185.00	134.25	122.38	219.00	136.21	177.54	162.00	98.34
7	169.00	244.00	125.00	61.00	70.00	99.00	69.00	220.00	192.00	185.00	147.00	117.68	199.00	116.21	176.40	148.42	140.00
8	169.00	244.00	125.00	61.00	70.00	99.00	69.00	220.00	192.00	185.00	163.38	127.20	199.00	116.21	158.96	130.99	156.37
9	169.00	244.00	125.00	61.00	70.00	99.00	69.00	220.00	192.00	185.00	134.25	134.05	199.00	116.21	189.97	162.00	70.47
10	169.00	244.00	125.00	61.00	70.00	99.00	69.00	220.00	192.00	185.00	134.25	117.68	219.00	136.21	177.54	162.00	109.57
11	169.00	244.00	125.00	61.00	70.00	99.00	69.00	220.00	192.00	185.00	151.70	120.41	199.00	116.21	171.39	143.42	144.69
12	169.00	244.00	125.00	61.00	70.00	99.00	69.00	220.00	192.00	185.00	134.25	120.41	219.00	136.21	177.54	162.00	103.03
13	169.00	244.00	125.00	61.00	70.00	99.00	69.00	220.00	192.00	185.00	134.25	122.38	199.00	116.21	189.97	162.00	98.34
14	169.00	244.00	125.00	61.00	70.00	99.00	69.00	220.00	192.00	185.00	134.25	122.38	213.20	130.41	181.14	162.00	98.34
15	169.00	244.00	125.00	61.00	70.00	99.00	69.00	220.00	192.00	185.00	134.25	117.68	199.00	116.21	189.97	162.00	109.57
16	169.00	244.00	125.00	61.00	70.00	99.00	69.00	220.00	192.00	185.00	134.25	127.20	199.00	116.21	189.97	162.00	86.84
17	169.00	244.00	125.00	61.00	70.00	99.00	69.00	220.00	192.00	185.00	134.25	120.41	199.00	116.21	189.97	162.00	103.03

Table C13: The heat duty result at the TF range of 5°C

Option	Heat load (kW)							
	Q_{H1}	Q_{H2}	Q_{E1}	Q_{E2}	Q_{E3}	Q_{E4}	Q_{C1}	Q_{C2}
1	8485	2790	3974	746	7153	4340	5274	3993
2	7641	2790	2160	3404	7153	4340	2616	5807
3	8485	2437	2160	2560	7153	4693	3107	5807
4	6671	2790	3974	2560	7153	4340	3460	3993
5	8485	2182	2768	1952	7153	4948	3460	5199
6	5763	5512	2160	5282	7153	1618	3460	5807
7	5827	2790	3974	3404	7153	4340	2616	3993
8	8485	1677	3974	746	7153	5453	4161	3993
10	5763	4668	2160	5282	7153	2462	2616	5807
11	6671	2437	3974	2560	7153	4693	3107	3993
12	5763	5159	2160	5282	7153	1971	3107	5807
13	3949	5512	3974	5282	7153	1618	3460	3993
14	5155	5512	2768	5282	7153	1618	3460	5199
15	3949	4668	3974	5282	7153	2462	2616	3993
16	3949	6213	3974	5282	7153	917	4161	3993
17	3949	5159	3974	5282	7153	1971	3107	3993

Table C14: Temperature between the HEN devices at the TF range of 5°C (increasing the hot streams' temperature by 5°C)

Option	Ts1	Ts2	Ts3	Ts4	Ts5	Tt1	Tt2	Tt3	Tt4	Tt5	Tho2	Tho4	Tho1	Tho3	Tco1	Tco2	Tco4
1	170.00	245.00	125.00	61.00	70.00	100.00	70.00	220.00	192.00	185.00	164.96	135.64	199.01	116.22	158.96	130.37	140.00
2	170.00	245.00	125.00	61.00	70.00	100.00	70.00	220.00	192.00	185.00	147.00	117.68	220.00	137.21	165.03	149.49	140.00
3	170.00	245.00	125.00	61.00	70.00	100.00	70.00	220.00	192.00	185.00	152.70	120.99	220.00	137.21	158.96	143.42	145.69
4	170.00	245.00	125.00	61.00	70.00	100.00	70.00	220.00	192.00	185.00	152.70	123.38	199.01	116.22	172.01	143.42	140.00
5	170.00	245.00	125.00	61.00	70.00	100.00	70.00	220.00	192.00	185.00	156.81	123.38	212.96	130.17	158.96	139.04	149.81
6	170.00	245.00	125.00	61.00	70.00	100.00	70.00	220.00	192.00	185.00	134.31	123.38	220.00	137.21	178.54	163.00	96.10
7	170.00	245.00	125.00	61.00	70.00	100.00	70.00	220.00	192.00	185.00	147.00	117.68	199.01	116.22	178.08	149.49	140.00
8	170.00	245.00	125.00	61.00	70.00	100.00	70.00	220.00	192.00	185.00	164.96	128.12	199.01	116.22	158.96	130.37	157.95
10	170.00	245.00	125.00	61.00	70.00	100.00	70.00	220.00	192.00	185.00	134.31	117.68	220.00	137.21	178.54	163.00	109.71
11	170.00	245.00	125.00	61.00	70.00	100.00	70.00	220.00	192.00	185.00	152.70	120.99	199.01	116.22	172.01	143.42	145.69
12	170.00	245.00	125.00	61.00	70.00	100.00	70.00	220.00	192.00	185.00	134.31	120.99	220.00	137.21	178.54	163.00	101.79
13	170.00	245.00	125.00	61.00	70.00	100.00	70.00	220.00	192.00	185.00	134.31	123.38	199.01	116.22	191.59	163.00	96.10
14	170.00	245.00	125.00	61.00	70.00	100.00	70.00	220.00	192.00	185.00	134.31	123.38	212.96	130.17	182.91	163.00	96.10
15	170.00	245.00	125.00	61.00	70.00	100.00	70.00	220.00	192.00	185.00	134.31	117.68	199.01	116.22	191.59	163.00	109.71
16	170.00	245.00	125.00	61.00	70.00	100.00	70.00	220.00	192.00	185.00	134.31	128.12	199.01	116.22	191.59	163.00	84.79
17	170.00	245.00	125.00	61.00	70.00	100.00	70.00	220.00	192.00	185.00	134.31	120.99	199.01	116.22	191.59	163.00	101.79

Table C15: The heat duty result at the TF range of 6°C

Option	Heat load (kW)							
	Q_{H1}	Q_{H2}	Q_{E1}	Q_{E2}	Q_{E3}	Q_{E4}	Q_{C1}	Q_{C2}
1	8485	2790	4060	660	7153	4340	5360	3907
2	7493	2790	2160	3552	7153	4340	2468	5807
3	8485	2375	2160	2560	7153	4755	3045	5807
4	6585	2790	4060	2560	7153	4340	3460	3907
5	8485	2075	2875	1845	7153	5055	3460	5092
6	5624	5651	2160	5421	7153	1479	3460	5807
7	5593	2790	4060	3552	7153	4340	2468	3907
8	8485	1579	4060	660	7153	5551	4149	3907
10	5624	4659	2160	5421	7153	2471	2468	5807
11	6585	2375	4060	2560	7153	4755	3045	3907
12	5624	5236	2160	5421	7153	1894	3045	5807
13	3724	5651	4060	5421	7153	1479	3460	3907
14	4909	5651	2875	5421	7153	1479	3460	5092
15	3724	4659	4060	5421	7153	2471	2468	3907
16	3724	6340	4060	5421	7153	790	4149	3907
17	3724	5236	4060	5421	7153	1894	3045	3907

Table C16: Temperature between the HEN devices at the TF range of 6°C (increasing & decreasing the hot & cold streams temperature by 3°C, respectively)

Option	Ts1	Ts2	Ts3	Ts4	Ts5	Tt1	Tt2	Tt3	Tt4	Tt5	Tho2	Tho4	Tho1	Tho3	Tco1	Tco2	Tco4
1	168.00	243.00	122.00	58.00	67.00	98.00	68.00	217.00	189.00	182.00	163.54	134.22	196.01	113.22	155.96	126.75	137.00
2	168.00	243.00	122.00	58.00	67.00	98.00	68.00	217.00	189.00	182.00	144.00	114.68	218.00	135.21	163.09	147.55	137.00
3	168.00	243.00	122.00	58.00	67.00	98.00	68.00	217.00	189.00	182.00	150.70	118.57	218.00	135.21	155.96	140.42	143.69
4	168.00	243.00	122.00	58.00	67.00	98.00	68.00	217.00	189.00	182.00	150.70	121.38	196.01	113.22	169.63	140.42	137.00
5	168.00	243.00	122.00	58.00	67.00	98.00	68.00	217.00	189.00	182.00	155.53	121.38	209.73	126.94	155.96	135.27	148.53
6	168.00	243.00	122.00	58.00	67.00	98.00	68.00	217.00	189.00	182.00	131.37	121.38	218.00	135.21	176.54	161.00	90.85
7	168.00	243.00	122.00	58.00	67.00	98.00	68.00	217.00	189.00	182.00	144.00	114.68	196.01	113.22	176.76	147.55	137.00
8	168.00	243.00	122.00	58.00	67.00	98.00	68.00	217.00	189.00	182.00	163.54	126.03	196.01	113.22	155.96	126.75	156.53
10	168.00	243.00	122.00	58.00	67.00	98.00	68.00	217.00	189.00	182.00	131.37	114.68	218.00	135.21	176.54	161.00	106.86
11	168.00	243.00	122.00	58.00	67.00	98.00	68.00	217.00	189.00	182.00	150.70	118.57	196.01	113.22	169.63	140.42	143.69
12	168.00	243.00	122.00	58.00	67.00	98.00	68.00	217.00	189.00	182.00	131.37	118.57	218.00	135.21	176.54	161.00	97.55
13	168.00	243.00	122.00	58.00	67.00	98.00	68.00	217.00	189.00	182.00	131.37	121.38	196.01	113.22	190.21	161.00	90.85
14	168.00	243.00	122.00	58.00	67.00	98.00	68.00	217.00	189.00	182.00	131.37	121.38	209.73	126.94	181.68	161.00	90.85
15	168.00	243.00	122.00	58.00	67.00	98.00	68.00	217.00	189.00	182.00	131.37	114.68	196.01	113.22	190.21	161.00	106.86
16	168.00	243.00	122.00	58.00	67.00	98.00	68.00	217.00	189.00	182.00	131.37	126.03	196.01	113.22	190.21	161.00	79.74
17	168.00	243.00	122.00	58.00	67.00	98.00	68.00	217.00	189.00	182.00	131.37	118.57	196.01	113.22	190.21	161.00	97.55

Table C17: The heat duty result at the TF range of 7°C

Option	Heat load (kW)							
	Q_{H1}	Q_{H2}	Q_{E1}	Q_{E2}	Q_{E3}	Q_{E4}	Q_{C1}	Q_{C2}
1	8485	2790	4147	573	7153	4340	5447	3820
2	7345	2790	2160	3700	7153	4340	2320	5807
3	8485	2313	2160	2560	7153	4817	2983	5807
4	6498	2790	4147	2560	7153	4340	3460	3820
5	8485	1969	2981	1739	7153	5161	3460	4986
6	5485	5790	2160	5560	7153	1340	3460	5807
7	5358	2790	4147	3700	7153	4340	2320	3820
8	8485	1481	4147	573	7153	5649	4138	3820
10	5485	4650	2160	5560	7153	2480	2320	5807
11	6498	2313	4147	2560	7153	4817	2983	3820
12	5485	.5313	2160	5560	7153	1817	2983	5807
13	3498	5790	4147	5560	7153	1340	3460	3820
14	4664	5790	2981	5560	7153	1340	3460	4986
15	3498	4650	4147	5560	7153	2480	2320	3820
16	3498	6468	4147	5560	7153	662	4138	3820
17	3498	5313	4147	5560	7153	1817	2983	3820

Table C18: Temperature between the HEN devices at the TF range of 7°C (increasing & decreasing the hot & cold streams temperature by 3 & 4°C, respectively)

Option	Ts1	Ts2	Ts3	Ts4	Ts5	Tt1	Tt2	Tt3	Tt4	Tt5	Tho2	Tho4	Tho1	Tho3	Tco1	Tco2	Tco4
1	168.00	243.00	121.00	57.00	66.00	98.00	68.00	216.00	188.00	181.00	164.13	134.80	195.00	112.21	154.96	125.12	136.00
2	168.00	243.00	121.00	57.00	66.00	98.00	68.00	216.00	188.00	181.00	143.00	113.68	218.00	135.21	163.16	147.62	136.00
3	168.00	243.00	121.00	57.00	66.00	98.00	68.00	216.00	188.00	181.00	150.70	118.16	218.00	135.21	154.96	139.42	143.69
4	168.00	243.00	121.00	57.00	66.00	98.00	68.00	216.00	188.00	181.00	150.70	121.38	195.00	112.21	169.25	139.42	136.00
5	168.00	243.00	121.00	57.00	66.00	98.00	68.00	216.00	188.00	181.00	156.25	121.38	208.50	125.71	154.96	133.51	149.24
6	168.00	243.00	121.00	57.00	66.00	98.00	68.00	216.00	188.00	181.00	130.43	121.38	218.00	135.21	176.54	161.00	87.61
7	168.00	243.00	121.00	57.00	66.00	98.00	68.00	216.00	188.00	181.00	143.00	113.68	195.00	112.21	177.45	147.62	136.00
8	168.00	243.00	121.00	57.00	66.00	98.00	68.00	216.00	188.00	181.00	164.13	125.96	195.00	112.21	154.96	125.12	157.11
10	168.00	243.00	121.00	57.00	66.00	98.00	68.00	216.00	188.00	181.00	130.43	113.68	218.00	135.21	176.54	161.00	106.00
11	168.00	243.00	121.00	57.00	66.00	98.00	68.00	216.00	188.00	181.00	150.70	118.16	195.00	112.21	169.25	139.42	143.69
12	168.00	243.00	121.00	57.00	66.00	98.00	68.00	216.00	188.00	181.00	130.43	118.16	218.00	135.21	176.54	161.00	95.31
13	168.00	243.00	121.00	57.00	66.00	98.00	68.00	216.00	188.00	181.00	130.43	121.38	195.00	112.21	190.84	161.00	87.61
14	168.00	243.00	121.00	57.00	66.00	98.00	68.00	216.00	188.00	181.00	130.43	121.38	208.50	125.71	182.45	161.00	87.61
15	168.00	243.00	121.00	57.00	66.00	98.00	68.00	216.00	188.00	181.00	130.43	113.68	195.00	112.21	190.84	161.00	106.00
16	168.00	243.00	121.00	57.00	66.00	98.00	68.00	216.00	188.00	181.00	130.43	125.96	195.00	112.21	190.84	161.00	76.68
17	168.00	243.00	121.00	57.00	66.00	98.00	68.00	216.00	188.00	181.00	130.43	118.16	195.00	112.21	190.84	161.00	95.31

Table C19: The heat duty result at the TF range of 8°C

Option	Heat load (kW)							
	Q_{H1}	Q_{H2}	Q_{E1}	Q_{E2}	Q_{E3}	Q_{E4}	Q_{C1}	Q_{C2}
1	8485	2790	4233	487	7153	4340	5533	3734
2	7197	2790	2160	3848	7153	4340	2172	5807
3	8485	2251	2160	2560	7153	4879	2921	5807
4	6412	2790	4233	2560	7153	4340	3460	3734
5	8485	1862	3088	1632	7153	5268	3460	4879
6	5346	5929	2160	5699	7153	1201	3460	5807
7	5124	2790	4233	3848	7153	4340	2172	3734
8	8485	1383	4233	487	7153	5747	4126	3734
10	5346	4641	2160	5699	7153	2489	2172	5807
11	6412	2251	4233	2560	7153	4879	2921	3734
12	5346	5390	2160	5699	7153	1740	2921	5807
13	3273	5929	4233	5699	7153	1201	3460	3734
14	4418	5929	3088	5699	7153	1201	3460	4879
15	3273	4641	4233	5699	7153	2489	2172	3734
16	3273	6595	4233	5699	7153	535	4126	3734
17	3273	5390	4233	5699	7153	1740	2921	3734

Table C20: Temperature between the HEN devices at the TF range of 8°C (increasing & decreasing the hot & cold streams temperature by 4°C, respectively)

Option	Ts1	Ts2	Ts3	Ts4	Ts5	Tt1	Tt2	Tt3	Tt4	Tt5	Tho2	Tho4	Tho1	Tho3	Tco1	Tco2	Tco4
1	169.00	244.00	121.00	57.00	66.00	99.00	69.00	216.00	188.00	181.00	165.71	136.39	195.01	112.22	154.96	124.50	136.00
2	169.00	244.00	121.00	57.00	66.00	99.00	69.00	216.00	188.00	181.00	143.00	113.68	219.00	136.21	164.22	148.68	136.00
3	169.00	244.00	121.00	57.00	66.00	99.00	69.00	216.00	188.00	181.00	151.70	118.74	219.00	136.21	154.96	139.42	144.69
4	169.00	244.00	121.00	57.00	66.00	99.00	69.00	216.00	188.00	181.00	151.70	122.38	195.01	112.22	169.87	139.42	136.00
5	169.00	244.00	121.00	57.00	66.00	99.00	69.00	216.00	188.00	181.00	157.97	122.38	208.26	125.47	154.96	132.74	150.97
6	169.00	244.00	121.00	57.00	66.00	99.00	69.00	216.00	188.00	181.00	130.49	122.38	219.00	136.21	177.54	162.00	85.37
7	169.00	244.00	121.00	57.00	66.00	99.00	69.00	216.00	188.00	181.00	143.00	113.68	195.01	112.22	179.14	148.68	136.00
8	169.00	244.00	121.00	57.00	66.00	99.00	69.00	216.00	188.00	181.00	165.71	126.88	195.01	112.22	154.96	124.50	158.69
10	169.00	244.00	121.00	57.00	66.00	99.00	69.00	216.00	188.00	181.00	130.49	113.68	219.00	136.21	177.54	162.00	106.15
11	169.00	244.00	121.00	57.00	66.00	99.00	69.00	216.00	188.00	181.00	151.70	118.74	195.01	112.22	169.87	139.42	144.69
12	169.00	244.00	121.00	57.00	66.00	99.00	69.00	216.00	188.00	181.00	130.49	118.74	219.00	136.21	177.54	162.00	94.06
13	169.00	244.00	121.00	57.00	66.00	99.00	69.00	216.00	188.00	181.00	130.49	122.38	195.01	112.22	192.45	162.00	85.37
14	169.00	244.00	121.00	57.00	66.00	99.00	69.00	216.00	188.00	181.00	130.49	122.38	208.26	125.47	184.22	162.00	85.37
15	169.00	244.00	121.00	57.00	66.00	99.00	69.00	216.00	188.00	181.00	130.49	113.68	195.01	112.22	192.45	162.00	106.15
16	169.00	244.00	121.00	57.00	66.00	99.00	69.00	216.00	188.00	181.00	130.49	126.88	195.01	112.22	192.45	162.00	74.63
17	169.00	244.00	121.00	57.00	66.00	99.00	69.00	216.00	188.00	181.00	130.49	118.74	195.01	112.22	192.45	162.00	94.06

Table C21: The heat duty result at the TF range of 9 °C

Option	Heat load (kW)							
	Q_{H1}	Q_{H2}	Q_{E1}	Q_{E2}	Q_{E3}	Q_{E4}	Q_{C1}	Q_{C2}
1	8485	2790	4320	400	7153	4340	5620	3647
2	7049	2790	2160	3996	7153	4340	2024	5807
3	8485	2189	2160	2560	7153	4941	2859	5807
4	6325	2790	4320	2560	7153	4340	3460	3647
5	8485	1755	3195	1525	7153	5375	3460	4772
6	5207	6068	2160	5838	7153	1062	3460	5807
7	4889	2790	4320	3996	7153	4340	2024	3647
8	8485	1284	4320	400	7153	5846	4114	3647
10	5207	4632	2160	5838	7153	2498	2024	5807
11	6325	2189	4320	2560	7153	4941	2859	3647
12	5207	5467	2160	5838	7153	1663	2859	5807
13	3047	6068	4320	5838	7153	1062	3460	3647
14	4172	6068	3195	5838	7153	1062	3460	4772
15	3047	4632	4320	5838	7153	2498	2024	3647
16	3047	6722	4320	5838	7153	408	4114	3647
17	3047	5467	4320	5838	7153	1663	2859	3647

Table C22: Temperature between the HEN devices at the TF range of 9°C (increasing & decreasing he hot & cold streams temperature by 4 & 5°C, respectively)

Option	Ts1	Ts2	Ts3	Ts4	Ts5	Tt1	Tt2	Tt3	Tt4	Tt5	Tho2	Tho4	Tho1	Tho3	Tco1	Tco2	Tco4
1	169.00	244.00	120.00	56.00	65.00	99.00	69.00	215.00	187.00	180.00	166.30	136.97	194.00	111.21	153.96	122.88	135.00
2	169.00	244.00	120.00	56.00	65.00	99.00	69.00	215.00	187.00	180.00	142.00	112.68	219.00	136.21	164.29	148.75	135.00
3	169.00	244.00	120.00	56.00	65.00	99.00	69.00	215.00	187.00	180.00	151.70	118.32	219.00	136.21	153.96	138.42	144.69
4	169.00	244.00	120.00	56.00	65.00	99.00	69.00	215.00	187.00	180.00	151.70	122.38	194.00	111.21	169.50	138.42	135.00
5	169.00	244.00	120.00	56.00	65.00	99.00	69.00	215.00	187.00	180.00	158.70	122.38	207.02	124.23	153.96	130.97	151.69
6	169.00	244.00	120.00	56.00	65.00	99.00	69.00	215.00	187.00	180.00	129.55	122.38	219.00	136.21	177.54	162.00	82.13
7	169.00	244.00	120.00	56.00	65.00	99.00	69.00	215.00	187.00	180.00	142.00	112.68	194.00	111.21	179.83	148.75	135.00
8	169.00	244.00	120.00	56.00	65.00	99.00	69.00	215.00	187.00	180.00	166.30	126.80	194.00	111.21	153.96	122.88	159.29
10	169.00	244.00	120.00	56.00	65.00	99.00	69.00	215.00	187.00	180.00	129.55	112.68	219.00	136.21	177.54	162.00	105.29
11	169.00	244.00	120.00	56.00	65.00	99.00	69.00	215.00	187.00	180.00	151.70	118.32	194.00	111.21	169.50	138.42	144.69
12	169.00	244.00	120.00	56.00	65.00	99.00	69.00	215.00	187.00	180.00	129.55	118.32	219.00	136.21	177.54	162.00	91.82
13	169.00	244.00	120.00	56.00	65.00	99.00	69.00	215.00	187.00	180.00	129.55	122.38	194.00	111.21	193.08	162.00	82.13
14	169.00	244.00	120.00	56.00	65.00	99.00	69.00	215.00	187.00	180.00	129.55	122.38	207.02	124.23	184.99	162.00	82.13
15	169.00	244.00	120.00	56.00	65.00	99.00	69.00	215.00	187.00	180.00	129.55	112.68	194.00	111.21	193.08	162.00	105.29
16	169.00	244.00	120.00	56.00	65.00	99.00	69.00	215.00	187.00	180.00	129.55	126.80	194.00	111.21	193.08	162.00	71.58
17	169.00	244.00	120.00	56.00	65.00	99.00	69.00	215.00	187.00	180.00	129.55	118.32	194.00	111.21	193.08	162.00	91.82

Table C23: The heat duty result at the TF range of 10°C

Option	Heat load (kW)							
	Q_{H1}	Q_{H2}	Q_{E1}	Q_{E2}	Q_{E3}	Q_{E4}	Q_{C1}	Q_{C2}
1	8485	2790	4406	314	7153	4340	5706	3561
2	6901	2790	2160	4144	7153	4340	1876	5807
3	8485	2127	2160	2560	7153	5003	2797	5807
4	6239	2790	4406	2560	7153	4340	3460	3561
5	8485	1649	3301	1419	7153	5481	3460	4666
6	5068	6207	2160	5977	7153	923	3460	5807
7	4655	2790	4406	4144	7153	4340	1876	3561
8	8485	1186	4406	314	7153	5944	4102	3561
10	5068	4623	2160	5977	7153	2507	1876	5807
11	6239	2127	4406	2560	7153	5003	2797	3561
12	5068	5544	2160	5977	7153	1586	2797	5807
13	2822	6207	4406	5977	7153	923	3460	3561
14	3927	6207	3301	5977	7153	923	3460	4666
15	2822	4623	4406	5977	7153	2507	1876	3561
16	2822	6849	4406	5977	7153	281	4102	3561
17	2822	5544	4406	5977	7153	1586	2797	3561

Table C24: Temperature between the HEN devices at the TF range of 10°C
(increasing & decreasing the hot & cold streams temperature by 5°C, respectively)

Option	Ts1	Ts2	Ts3	Ts4	Ts5	Tt1	Tt2	Tt3	Tt4	Tt5	Tho2	Tho4	Tho1	Tho3	Tco1	Tco2	Tco4
1	170.00	245.00	120.00	56.00	65.00	100.00	70.00	215.00	187.00	180.00	167.88	138.55	194.01	111.22	153.96	122.26	135.00
2	170.00	245.00	120.00	56.00	65.00	100.00	70.00	215.00	187.00	180.00	142.00	112.68	220.00	137.21	165.35	149.81	135.00
3	170.00	245.00	120.00	56.00	65.00	100.00	70.00	215.00	187.00	180.00	152.70	118.90	220.00	137.21	153.96	138.42	145.69
4	170.00	245.00	120.00	56.00	65.00	100.00	70.00	215.00	187.00	180.00	152.70	123.38	194.01	111.22	170.12	138.42	135.00
5	170.00	245.00	120.00	56.00	65.00	100.00	70.00	215.00	187.00	180.00	160.41	123.38	206.79	124.01	153.96	130.21	153.40
6	170.00	245.00	120.00	56.00	65.00	100.00	70.00	215.00	187.00	180.00	129.62	123.38	220.00	137.21	178.54	163.00	79.89
7	170.00	245.00	120.00	56.00	65.00	100.00	70.00	215.00	187.00	180.00	142.00	112.68	194.01	111.22	181.51	149.81	135.00
8	170.00	245.00	120.00	56.00	65.00	100.00	70.00	215.00	187.00	180.00	167.88	127.72	194.01	111.22	153.96	122.26	160.87
10	170.00	245.00	120.00	56.00	65.00	100.00	70.00	215.00	187.00	180.00	129.62	112.68	220.00	137.21	178.54	163.00	105.44
11	170.00	245.00	120.00	56.00	65.00	100.00	70.00	215.00	187.00	180.00	152.70	118.90	194.01	111.22	170.12	138.42	145.69
12	170.00	245.00	120.00	56.00	65.00	100.00	70.00	215.00	187.00	180.00	129.62	118.90	220.00	137.21	178.54	163.00	90.58
13	170.00	245.00	120.00	56.00	65.00	100.00	70.00	215.00	187.00	180.00	129.62	123.38	194.01	111.22	194.70	163.00	79.89
14	170.00	245.00	120.00	56.00	65.00	100.00	70.00	215.00	187.00	180.00	129.62	123.38	206.79	124.01	186.75	163.00	79.89
15	170.00	245.00	120.00	56.00	65.00	100.00	70.00	215.00	187.00	180.00	129.62	112.68	194.01	111.22	194.70	163.00	105.44
16	170.00	245.00	120.00	56.00	65.00	100.00	70.00	215.00	187.00	180.00	129.62	127.72	194.01	111.22	194.70	163.00	69.53
17	170.00	245.00	120.00	56.00	65.00	100.00	70.00	215.00	187.00	180.00	129.62	118.90	194.01	111.22	194.70	163.00	90.58

APPENDIX D

MODEL CALCULATION

In this section, a calculation example is presented to show the way of the computation followed in the procedure adopted for the HEN retrofit in this study. From the HEN retrofit options offered by the developed *Paths Combination Approach,* option 11 is taken as a model to show the overall calculation procedure (step-by-step) and the corresponding results. The existing HEN with the heat duty and temperature data is shown in Fig. D1 below:

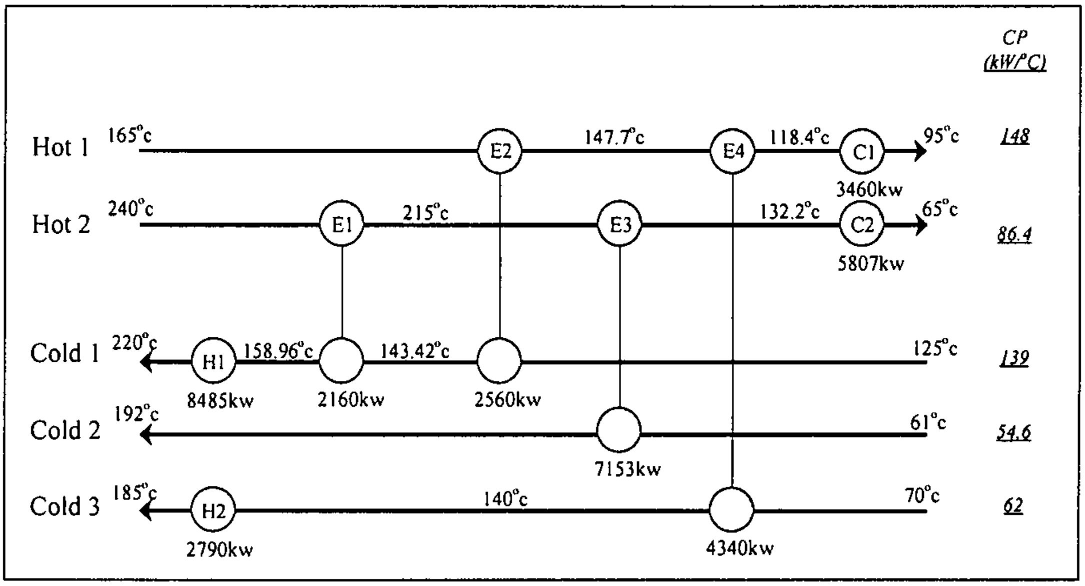

Fig. D1: Existing HEN

1. Exchangers' duty and temperature

The exchangers heat duty and inlet/outlet temperature after the heat shifting process using the HEN retrofit option 11 is shown in the HEN grid representation in Fig. D2. The heat shifting is done using two utility paths for this option while maintaining the HRAT value to be 7°C as shown in the figure and also maintaining the heat balance across each exchanger in the HEN using the following equation:

$$Q = CP.(T_1 - T_2) \quad \text{(D.1)}$$

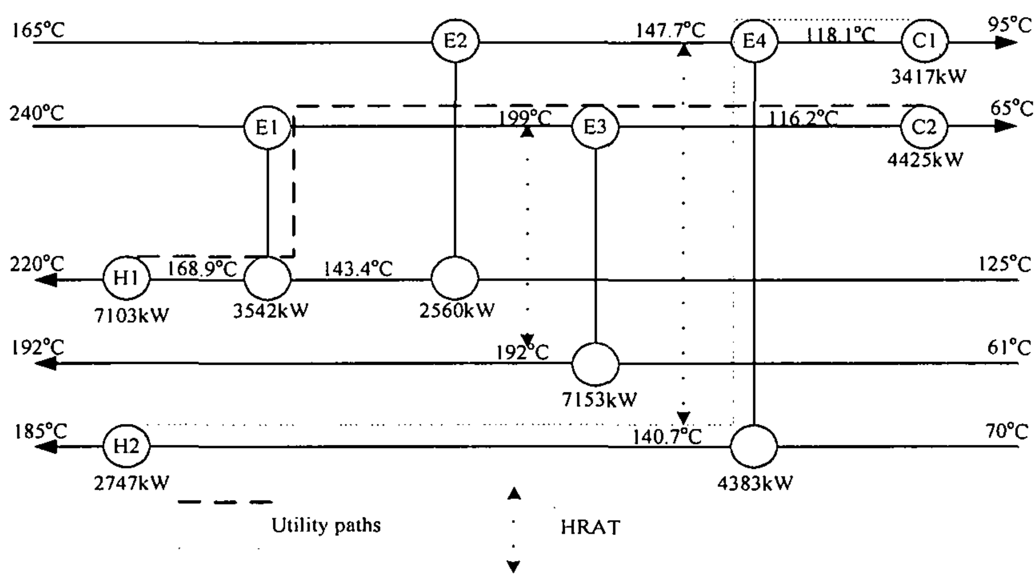

Fig. D2: HEN after heat load shifting using option 11

The heat duty of the exchangers in the HEN is found directly by alternatively subtracting and adding 1kW from and to the exchangers lied on the utility path starting with heater or cooler. This is called the heat shifting process which is continued until HRAT is equal to 7°C. Equation D.1 shown above is used to calculate the inlet and outlet temperature of each exchanger in the HEN. The starting point would be the utility exchangers (H1, H2, C1 and C2) where the outlet temperature is known. For H1:

$$7103 = 139.(220 - T_2)$$

Therefore, T_2 for exchange H1 will be <u>168.9°C</u> as shown in the figure which is the outlet temperature from exchanger E1 for the cold side. Accordingly, for exchanger E1, the inlet temperature will be calculated as:

$$3542 = 139.(168.9 - T_2)$$

Therefore, T_2 for exchanger E1 will be <u>143.4°C</u> as shown in the figure and it is the outlet temperature for the cold side of exchanger E2. The same procedure is followed to calculate the outlet and/or inlet temperature for all the exchangers in both hot and cold sides.

2. Exchangers heat transfer area prediction

The heat transfer area for each exchanger in the HEN is first predicted to calculate the heat film transfer coefficients h_T and h_S. The simple ratio for the area before and after the heat shifting which is presented in equation D.2 is used to initially predict the heat transfer area.

$$\frac{A_{before}}{Q_{before}} = \frac{A_{after}}{Q_{after}} \qquad \text{(D.2)}$$

For exchanger E1, A_{before} was 133m^2 and the heat duty for the existing situation Q_{before} was 2160kW. Using option 11 for the HEN retrofit, the heat duty has changed to Q_{after} which is 3542kW as shown in Fig. D2. From the above equation A_{after} will be found as follows:

$$\frac{133}{2160} = \frac{A_{after}}{3542}$$

Accordingly, the predicted area for E1which is A_{after} is found to be 218.1m^2. The predicted area for the remaining exchangers in the HEN is calculated using the same procedure.

3. The film heat transfer coefficient

The exchanger pressure drop correlations (D.3 and D.4) for the tube and shell sides are used to calculate the film heat transfer coefficients h_T and h_S based on the predicted area found above.

$$\Delta P_T = K_{PT1}.A.h_T^{\ 3.5} + K_{PT2}.h_T^{\ 2.5} \qquad \text{(D.3)}$$

$$\Delta P_S = K_{S1}.h_S^{2.86} + K_{S2}.A.h_S^{4.42} + K_{S3}.A.h_S^{4.69} \qquad \text{(D.4)}$$

The constants K_{PT1}, K_{PT2}, K_{S1}, K_{S2}, K_{S3} are dependent of the fluid physical properties and exchanger geometrical configurations and they are found according to the equations from (3.10) to (3.25) explained in section (3.4). The required physical properties and geometrical data are shown in Tables (3.4) and (3.6) which are presented in section (3.5.1) of the thesis. For exchanger E1, these constants were found to be:

$$K_{PT1} = \underline{446.614}$$

$$K_{PT2} = \underline{4125}$$

$$K_{S1} = \underline{60.344}$$

$$K_{S2} = \underline{592.348}$$

$$K_{S3} = \underline{1974}$$

And the pressure drop for exchanger E1 was given to be 1800Pa and 21600Pa in the tube and shell side, respectively. The film heat transfer coefficients could be found by substituting the constant values, the predicted heat transfer area and the pressure drop in equations D.3 and D.4 as follows:

$$1800 = 446.614 \times 218.1 \times h_T^{3.5} + 4125 \times h_T^{2.5}$$

$$21600 = 60.344 \times h_S^{2.86} + 592.348 \times 218.1 \times h_S^{4.42} + 1974 \times 218.1 \times h_S^{4.69}$$

It is very difficult to solve the above polynomials manually where h_T and h_S are raised to fractional power. Accordingly, the computer programming developed for this study has solved the difficulty associated in solving the pressure drop equations. Therefore, for exchanger E1 using option 11 from the HEN retrofit options, h_T and h_S are found to be $\underline{0.308 kW/m^2.^oC}$ and $\underline{0.495 kW/m^2.^oC}$, respectively. The same procedure is followed to calculate the film heat transfer coefficients for the remaining exchangers in the HEN.

4. The actual heat transfer area of the exchanger

The actual heat transfer area is calculated using equation D.5 shown below:

$$A = \left(\frac{1}{h_T} + \frac{1}{h_S}\right) \times \frac{Q}{LMTD \times F_T} \quad \text{(D.5)}$$

For exchanger E1, h_T and h_S are calculated as shown above. Q is shown in Fig. D2 which is 3542kW and the F_T is ignored as for the base case of the existing HEN.

$$LMTD = \left(\frac{\Delta T1 - \Delta T2}{\ln\left(\frac{\Delta T1}{\Delta T2}\right)} \right) \quad \text{(D.6)}$$

Referring to the inlet and outlet temperatures in the hot and cold sides of E1 as shown in Fig. D2, the *LMTD* is found as follows:

$$LMTD = \left(\frac{(240-168.9)-(199-143.4)}{\ln\left(\frac{(240-168.9)}{(199-143.4)}\right)} \right) = 63.03^{\circ}C$$

Therefore, the actual heat transfer area for E1 using the HEN retrofit option 11 is found as follows:

$$A = \left(\frac{1}{0.308} + \frac{1}{0.495} \right) \times \frac{3542}{63.03 \times 1} = 296\text{m}^2$$

The actual heat transfer area for the remaining exchangers in the HEN is calculated the same way. The area for the four exchangers in HEN using option 11are summed to give the overall heat transfer area for the entire HEN (A_{HEN}) which is found to be 2984m^2 where for the existing HEN it was 2187m^2 and the difference (ΔA) is 797m^2.

5. Economical assessment

In this section, the calculation of savings, investment cost and payback is presented. The obtained savings is calculated based on the utility prices data from the following equation:

$$Saving_{cost} = \sum HU_{ex.cost} - \sum HU_{new.cost} + \sum CU_{ex.cost} - \sum CU_{new.cost} \quad \text{(D.7)}$$

The hot utility price (HU_{price}) for H1 and H2 in the HEN are given to be 278.14\$/kW and 224.4\$/kW, respectively. Also the cold utility price (CU_{price}) for C1 and C2 is given to be 12.75$/kW and 21.04$/kW, respectively. Referring to the utility exchangers' heat duties, i.e., before and after the heat shifting as shown in Figs. D1 and D2, the hot and cold utility cost for hot and cold utilities is found as follows:

$$HU_{ex.cost} = Q_{ex.H} . HU_{price} \tag{D.8}$$

$$HU_{new.cost} = Q_{new.H} . HU_{price} \tag{D.9}$$

$$CU_{ex.cost} = Q_{ex.C} . CU_{price} \tag{D.10}$$

$$CU_{new.cost} = Q_{new.C} . CU_{price} \tag{D.11}$$

The *hot* utility cost *before* the heat shifting:

For H1

$$HU_{ex.cost} = 8485 \times 278.14 = 2360018\$ / yr$$

For H2:

$$HU_{ex.cost} = 2790 \times 224.4 = 626076\$ / yr$$

The *cold* utility cost *before* the heat shifting:

For C1:

$$CU_{ex.cost} = 3460 \times 12.75 = 44115\$ / yr$$

For C2:

$$CU_{ex.cost} = 5807 \times 21.04 = 122179.3\$ / yr$$

The *hot* utility cost *after* the heat shifting:

For H1:

$$HU_{new.cost} = 7103 \times 278.14 = 1975628.42\$ / yr$$

For H2:

$$HU_{new.cost} = 2747 \times 224.4 = 616426.8\$ / yr$$

The *cold* utility cost *after* the heat shifting:

For C1:

$$CU_{new.cost} = 3417 \times 12.75 = 43566.75\$ / yr$$

For C2:

$$CU_{new.cost} = 4425 \times 21.04 = 93102\$ / yr$$

Using equation D.7 shown above, the obtained savings using option 11 for HEN retrofit is found as follows:

$$Saving_{cost} = (2360018 + 626076) - (1975628.42 + 616426.8) + (44115 + 122179.3) - (43566.75 + 93102)$$

$$Saving_{cost} = 423664.33\$ / yr$$

The investment cost is calculated according to the following equations:

$$Investment = \Delta N \left(a + b \left(\frac{\Delta A}{\Delta N} \right)^{C} \right) \quad \text{(D.12)}$$

$$\Delta N = \frac{\Delta A}{av_{shell}} \quad \text{(D.13)}$$

$$av_{shell} = \frac{A_{ex.HEN}}{N_{shell}} \quad \text{(D.14)}$$

The cost constants *a*, *b* and *c* were given to be 33422, 814, and 0.81, respectively. ΔA was calculated previously and found to be 797m^2. The number of shells N_{shell} is same as the number of the exchangers in HEN which is 4. The existing HEN area is given to be 2187m^2. Therefore, the average size of the exchanger shell av_{shell} could be calculated as follows:

$$av_{shell} = \frac{2187}{4} = 546.75m^2$$

The required additional shells ΔN is found as follows:

$$\Delta N = \frac{797}{546.75} \approx 1.5$$

Therefore, the investment cost required for the retrofit using option 11is found as follows:

$$Investment = 1.5 \times \left(33422 + 814 \times \left(\frac{797}{1.5} \right)^{0.81} \right) = 247000\$$$

The payback is found from a simple ratio between the investment and the savings as follows:

$$payback = \frac{investment}{savings} \tag{D.15}$$

Therefore, the payback period for HEN retrofit using option 11 is:

$$payback = \frac{247000\$}{423664.33\$/yr} = 0.583yr$$

APPENDIX E

HOT UTILITIES HEAT DUTY AND ITS CORRESPONDING SAVINGS WITH TF CONSIDERATION

The heat duty for the heaters H1 and H2 with the corresponding HP and MP steam saving, respectively for the HEN case study are tabulated here along the suggested TF range steps for the net savings HEN retrofit options.

Table E1: The heat duty and the corresponding HP and MP steam saving for selected HEN retrofit options (*TF range = 1°C to 5°C*)

TF range (°C)	Heaters heat load and corresponding saving		HEN retrofit options				
			2	4	7	8	11
1	Heat load (KW)	H1	8233	7017	6765	8485	7017
		H2	2790	2790	2790	2070	2685
	saving (t/h)	HP steam	1.604	9.343	10.946	0	9.343
		MP steam	0	0	0	14.452	2.108
2	Heat load (KW)	H1	8085	6930	6530	8485	6930
		H2	2790	2790	2790	1972	2623
	saving (t/h)	HP steam	2.546	9.896	12.442	0	9.896
		MP steam	0	0	0	16.419	3.352
3	Heat load (KW)	H1	7937	6844	6296	8485	6844
		H2	2790	2790	2790	1873	2561
	saving (t/h)	HP steam	3.488	10.444	13.931	0	10.444
		MP steam	0	0	0	18.406	4.596
4	Heat load (KW)	H1	7789	6757	6061	8485	6757
		H2	2790	2790	2790	1775	2499
	saving (t/h)	HP steam	4.429	10.997	15.427	0	10.997
		MP steam	0	0	0	20.373	5.841
5	Heat load (KW)	H1	7641	6671	5827	8485	6671
		H2	2790	2790	2790	1677	2437
	saving (t/h)	HP steam	5.371	11.545	16.916	0	11.545
		MP steam	0	0	0	22.34	7.085

Table E2: The heat duty and the corresponding HP and MP steam saving for selected HEN retrofit options (*TF range = 6°C to 10°C*)

TF range (°C)	Heaters heat load and corresponding saving		HEN retrofit options				
			2	4	7	8	11
6	Heat load (KW)	H1	7493	6585	5593	8485	6585
		H2	2790	2790	2790	1579	2375
	saving (t/h)	HP steam	6.313	12.092	18.405	0	12.092
		MP steam	0	0	0	24.307	8.33
7	Heat load (KW)	H1	7345	6498	5358	8485	6498
		H2	2790	2790	2790	1481	2313
	saving (t/h)	HP steam	7.255	12.646	19.901	0	12.646
		MP steam	0	0	0	26.274	9.574
8	Heat load (KW)	H1	7197	6412	5124	8485	6412
		H2	2790	2790	2790	1383	2251
	saving (t/h)	HP steam	8.197	13.193	21.39	0	13.193
		MP steam	0	0	0	28.241	10.819
9	Heat load (KW)	H1	7049	6325	4889	8485	6325
		H2	2790	2790	2790	1284	2189
	saving (t/h)	HP steam	9.139	13.747	22.886	0	13.747
		MP steam	0	0	0	30.228	12.063
10	Heat load (KW)	H1	6901	6239	4655	8485	6239
		H2	2790	2790	2790	1186	2127
	saving (t/h)	HP steam	10.081	14.294	24.375	0	14.294
		MP steam	0	0	0	32.195	13.308

PUBLICATIONS LIST

Journal papers

1. Osman, A., Abdul Mutalib, M. I., Shuhaimi, M. and Amminudin, K. A. "Paths Combination for HENs Retrofit." Appllied Thermal Engineering 29(15-14): 3103-3109. (2009).

2. Osman, A., Abdul Mutalib, M. I. and Shuhaimi, M. "Integrating the Process Streams' Temperature Flexibility with the Approach of Paths Combination for HENs Retrofit." KIChE, *(Accepted, 2010).*

Conference papers

1. Osman, A., Abdul Mutalib, M. I. and Shuhaimi, M. "Path Analysis and Temperature Flexibility for the Retrofit of Heat Exchanger Networks" NPC, University Teknology Petronas, Malaysia, (March 2008).

2. Osman, A., Abdul Mutalib, M. I. and Shuhaimi, M. "Process Streams' Temperature Flexibility for Energy Savings in HENs" APCChE, Taipie, Taiwan, (Oct. 2010).